AN ABSTRACT OF THE THESIS OF

<u>Julraht Konsil</u> for the degree of <u>Doctor of Philosophy</u> in <u>Pharmacy</u> presented <u>on June 9,</u>

<u>1997.</u> Title: <u>Formulation and Pharmacokinetics of Melatonin.</u>

Abstract approved: _____Redacted for Privacy_____

Keith A. Parrott

Abstract approved: _____Redacted for Privacy_____

James W. Ayres

Pharmacokinetics following oral melatonin (MT) were evaluated in human subjects. Blood and urine samples were collected for measurement of plasma MT and urinary 6-sulphatoxymelatonin (6STMT), respectively. Pharmacokinetics of immediate release (IR) MT given at a high dose of 50 mg and a sustained release (SR) MT formulation given at three low doses of 0.2, 0.4, and 0.8 mg were studied in 7 young and 7 old healthy volunteers. SR MT formulation contained 10% IR MT and 90% SR MT (20% Aquacoat® coated beads). No significant effect of age nor gender was found in MT pharmacokinetics. MT pharmacokinetics were found to be generally linear within the dose range of 0.2-0.8 mg.

MT pharmacokinetics were further studied in young healthy subjects (7 females and 5 males). A solution of MT and two SR MT formulations containing either 10% Aquacoat® coated beads or 9% Eudragit® L 30D coated on 20% Aquacoat® coated beads were orally given to the subjects (all dosed at 0.75 mg). There was no significant effect of gender on MT pharmacokinetics. MT plasma concentrations were largely

variable among individuals. Urinary 6STMT excretion rate-time profiles supported use of 20% Aquacoat® rather than 10% Aquacoat® coating to sustain drug release rate over duration of 6-8 hours. Following administration of an enteric coating to SR MT beads, a delay in absorption onset time of about 2 hours was found in 3 subjects.

Analysis of relative change in MT bioavailability with change in dose suggested the possibility of dose-dependent bioavailability. Bioavailability generally decreased with decrease in dose. Dose dependent bioavailability, and differences in first pass metabolism could cause large intersubject variation in MT plasma concentrations. Special techniques were developed to assist in predicting *in vivo* performance of a formulation based on *in vitro* dissolution tests and deconvolution/convolution technique.

A transdermal delivery system for MT was also developed and evaluated *in vitro*. A patch was developed as a membrane moderated system consisting of 4 layers with MT dissolved in a liquid reservoir compartment. The best release rate was obtained from 40% (v/v) propylene glycol solvent system with drug release through a 28% vinyl acetate membrane.

Formulation And Pharmacokinetics Of Melatonin

by

Julraht Konsil

A THESIS

submitted to

Oregon State University

in partial fulfillment of
the requirements for the
degree of

Doctor of Philosophy

Presented June 9,1997
Commencement June 1998

Doctor of Philosophy thesis of Julraht Konsil presented on June 9, 1997.

APPROVED:

Redacted for Privacy

Co-Major Professor, representing Pharmacy

Redacted for Privacy

Co-Major Professor, representing Pharmacy

Redacted for Privacy

Dean of College of Pharmacy

Redacted for Privacy

Dean of Graduate School

I understand that my thesis will become part of the permanent collection of Oregon State University libraries. My signature below authorizes release of my thesis to any reader upon request.

Redacted for Privacy

Julraht Konsil, Author

ACKNOWLEDGMENTS

"Education's purpose is to replace an empty mind with an open one."
— Malcolm S. Forbes

TABLE OF CONTENTS

TABLE OF CONTENTS (continued)

TABLE OF CONTENTS (continued)

TABLE OF CONTENTS (continued)

FORMULATION AND PHARMACOKINETICS OF MELATONIN

INTRODUCTION

Melatonin (MT) is an indole neurohormone secreted by the pineal gland in a circadian rhythm. MT has been tried to improve conditions where rhythm abnormalities are associated with lack of well being and/or poor performance such as jet lag, insomnia, and other disorders resulting from delay of sleep. It is also being studied in depressive disorders, and in large doses for its contraceptive activity. There are several studies suggesting benefits of exogenous MT administered in physiological quantities to the circadian rhythm sleep disorders including jet lag, shift work syndrome, and seasonal affective diseases. MT is safe, and well tolerated. MT is currently available over the counter as supplementary nutrient in conventional/sublingual tablet, containing about 2-3 mg of MT, and MT spray, containing 2 ounce spray (49 applications at 3 mg each). Due to MT short plasma half-life, controlled delivery of exogenous MT is essential for imitation of its physiological pattern. An oral sustained release (SR) formulation of MT have been developed in our laboratory and evaluated previously in 6 human subjects. Additional pharmacokinetic studies of MT following oral administration are important for optimization of the SR formulation. The objectives of this research are to study pharmacokinetics of MT orally administered as immediate release (IR) and SR MT in humans subjects as well as to develop a transdermal delivery system for MT.

Chapter 1 reports pharmacokinetic study in 7 old and 7 young healthy volunteers receiving IR MT at a supra-physiologic dose of 50 mg and three low doses of SR MT formulation given at 0.2, 0.4, and 0.8 mg. Blood and urine samples were collected for measurement of plasma MT and urinary 6-sulphathoxymelatonin (chief MT metabolite, 6STMT). This work was designed to investigate influence of age and gender on MT pharmacokinetics as well as dose proportionality of SR MT given at the low doses. The large difference between doses of IR MT and SR MT formulation used in the study was based on doses of MT used in clinical studies.

In chapter 2, difference in MT pharmacokinetics between gender were studied in 7 young female and 5 young male healthy subjects. MT was given at a low dose of 0.75 mg as a solution, and two different MT SR formulations. Blood and urine samples were collected following administration of the solution not only for pharmacokinetic comparison between gender but also for investigation of relationship between plasma MT and urinary 6STMT. *In vivo* performances of the two SR formulations were examined using tracking urinary 6STMT data collected over 24 hours.

Chapter 3 describes two techniques developed to obtain high *in vitro / in vivo* correlation for optimization of a SR MT formulation. The data from pilot study of MT SR formulation was employed as an initial correlation to predict *in vivo* performance of SR formulation with different drug release rate.

Chapter 4 adds special approach to assist in prediction of individual MT plasma profile as well as to investigate possibility of saturable first pass metabolism of

MT. The analysis performed in chapter 4 was an attempt to improve prediction of MT plasma profile, which is highly variable among subjects and possibly dose dependent following administration of SR MT, delivered at doses/low release rate. Oral bioavailability of MT generally decrease with reduction in drug release rate. Mathematical equation describing theoretical saturable first pass effect was applied to predict change in bioavailability with change in drug release rate.

In chapter 5, two mathematical techniques were proposed to predict MT plasma profile using tracking urinary 6STMT data. Data from previous biostudies of MT given orally and transdermally was employed to validate the proposed methods.

Chapter 6 describes the manufacture and *in vitro* characterization, by *in vitro* diffusion study of a transdermal delivery system for MT. A transdermal delivery system may provide another option to deliver exogenous MT similarly to the physiological pattern.

CHAPTER 1

PHARMACOKINETICS AND DOSE PROPORTIONALITY OF MELATONIN ORALLY GIVEN AT HIGH AND LOW DOSES IN HEALTHY YOUNG AND ELDERLY VOLUNTEERS

ABSTRACT

The use of melatonin (MT) as a sleep promoting factor have been investigated by several investigators. Its application for sleep in the elderly were supported by previous studies. This study aimed to determine pharmacokinetics and dose proportionality of MT in the old and young healthy volunteers orally given a single high dose of immediate release (IR) MT (50 mg) and three single low doses of a sustained release (SR) MT formulation (0.2, 0.4, and 0.8 mg). The SR MT formulation, contained 10% IR MT and 90% SR MT, was developed and evaluated earlier in six human subjects. In this study, fourteen healthy volunteers, following an overnight fast, each received MT dosage forms in double blind, randomized, crossover fashion with space of one week apart. Venous blood and urine samples were taken over 12 hour period and analyzed for measurement of plasma MT concentrations and its urinary chief metabolite, 6-sulphatoxymelatonin (6STMT), using GC/MS assay and radioimmunoassay, respectively. Statistical comparisons were made using analysis of variance and Duncan's multiple range test following a log-transformation. Following 50 mg IR MT, there was no significant difference in MT pharmacokinetics between the elderly and the youngsters. Urinary 6STMT (0-12 hours) of females were significantly lower than that of males. Geometric means of peak plasma concentration (Cmax), time

to Cmax (Tmax), the area under the plasma concentration versus time curve (AUC), the apparent half life ($t_{1/2}$), the oral clearance (CL/F), and the terminal volume of distribution (Vd/F), calculated using noncompartmental method were 66.2 ng/ml, 1.3 hour, 204.0 ng h/ml, 1.4 hour, 245.3 L/h, and 485.2 L, respectively. Approximate linearity of MT pharmacokinetics following administration of SR MT formulation was found between the dose range of 0.2-0.8 mg. Geometric means of Cmax were 113.8 pg/ml, 262 pg/ml, and 501.6 pg/ml following 0.2, 0.4, and 0.8 mg dose, respectively. Geometric means of AUC(0-12 hours) were 542 pg h/ml, 1364 pg h/ml, and 2691 pg h/ml following 0.2, 0.4, and 0.8 mg dose, respectively. The dose normalized plasma concentrations in young males were lower than those of the other groups. Similarly, the dose normalized Cmax, and AUC were significant lower in young males than in the other groups. MT plasma concentrations were highly variable following administration of the four doses. Since the study evaluated MT pharmacokinetics only in a limited population, firm conclusion on differences in MT pharmacokinetics of young males from the other age-gender groups, found after administration of the three low doses of SR MT formulation, cannot be made.

INTRODUCTION

Many elderly people are dissatisfied with their sleep. The frequent nocturnal awakenings, loss of slow wave sleep, increased daytime sleepiness and phase advance of the sleep/wake cycle are all features of sleep disturbances in the elderly, and can be viewed as circadian rhythm disturbances (1,2). Melatonin (MT), a pineal

neurohormone normally secreted at night in the dark (3,4), has attracted attention as a sleep promoting factor (5, 6). Its effect on sleep in the elderly has been evaluated by several investigators (7, 8, 9, 10, 11). Exogenous MT administration in physiological quantities could also help treat various disorders including certain sleep disorders (12), jet lag (13), shift work syndrome (14), and seasonal affective diseases (15). Administration of MT in insomnia has been studied by many researchers with administered doses varied from less than 1 mg to more than 50 mg given as an oral bolus (5, 6, 8, 9, 10, 11, 16, 17, 18, 19). Generally, the results support application of MT given at high doses to improve sleep (8, 11, 16, 17). However, low doses of MT (less than 5 mg) have shown inconsistent effect on sleep improvement (6, 9, 10, 18, 19). Hypnotic effects of MT may be associated with dose-related differences. Due to MT short plasma half life, immediate release (IR) dosage forms of MT cannot maintain MT plasma concentrations at or above the normal physiological concentrations over 6-8 hours, unless they are given at high doses. Nighttime production by the pineal gland sustaining the plasma concentrations between about 25 to 120 pg/ml for over 6 to 8 hours (20). In our laboratory, an oral sustained release (SR) product has been formulated to mimic the normal MT physiological pattern (21, 22). The preliminary pharmacokinetic evaluation of the SR product in humans was reported previously (22).

MT given orally undergoes extensive first pass metabolism (23, 24). MT is mainly metabolized in the liver and subsequently excreted in urine as inactive metabolites. MT is hydroxylated to 6-hydroxymelatonin following by sulfate or glucoronide conjugation which is renally excreted (23, 25). About 1% of intact MT

was found in urine (26). MT is also passively secreted into saliva which reflects closely the changes in serum MT i.e. Tmax and terminal half life are similar (27). However, MT saliva concentration is about 55% of its serum concentration. The clearance of MT from blood showed a biexponential decay following administration of iv bolus, iv infusion, and oral administration of low dose (2 mg) with half lives of about 2-5 minutes and 45 minutes, respectively (23, 28, 29, 30). Systemic clearance (CLss) and apparent volume of distribution at steady-state (Vss) were estimated to be about 38 L/h (28) to 58 L/h (29), and 35 L (28) to 63 L (29), respectively. However, following oral administration of MT at high dose of 80 mg and 100 mg, changes in MT plasma concentrations were best described by a biexponential equation with absorption half life of 24 minutes and elimination half life of 45 minutes (27, 31). In this case, the absorption was slower than distribution and the resultant MT plasma concentration-time profile was best described by assuming a one-compartment model behavior. Peak plasma concentration following oral administration was generally reached at about 1-2 h after dosing with very large interindividual variation of more than 25-37 folds (23, 30, 31). The high variation following oral administration could be due to variation in first pass metabolism and absorption (23). Binding of MT to hemoglobin was found to be rapid, saturable, and reversible (32). Hemoglobin may serve as a carrier protein for MT in blood and discharge it in the target sites including brain, retina, pituitary, and many peripheral tissues (32, 23).

Although MT has been administered to a number of human subjects at either physiological or pharmacological concentrations, its pharmacokinetics in the elderly are

limited. Drug absorption, hepatic and renal drug elimination are changed with age (33, 34, 35). Oxidative metabolism, hepatic blood flow and liver volume decline with aging (36, 37), so MT may have a longer half life in the elderly. Absorption and first-pass hepatic clearance may also be different, so that dose-plasma concentration relationships for MT established in younger subjects may not be valid in the elderly.

The objective of the study is to investigate pharmacokinetics of MT orally given at a high-dose (50 mg IR) and low-doses (0.2, 04, and 0.8 mg SR) in elderly and youthful subjects. Both supra-physiologic and physiologic doses were selected in this study based on doses of MT applied in clinical studies. Both high dose IR MT and low dose SR MT could provide MT plasma concentrations above or at the physiological concentrations for a certain period of time. The prolongation of MT plasma concentrations at or above the physiological concentrations was believed to be related to pharmacological effects of exogenous MT (5). Pharmacokinetics of MT given at low doses of slow release formulations are essential for development of MT SR formulations. Large variation in MT oral bioavailability could extensively affect extent of absorption of MT released from the SR formulations. Therefore, the assessment of its pharmacokinetics and dose-proportionality following oral administration of MT given at three low doses of SR formulation (0.2, 0.4, and 0.8 mg) were also carried out in the old and young subjects.

Structure of MT and 6STMT are shown in Figure 1.1.

A. Melatonin [N-acetyl-5-methoxytryptamine, MW = 232, mp 116-118°, uv max 223, 278 nm (Budavari et al., eds, The Merck Index 12th ed. Merck & Co., Inc, 1996)]

$$CH_3O \quad\quad NHCOCH_3 \quad CH_2CH_2 \quad N\text{-}H$$
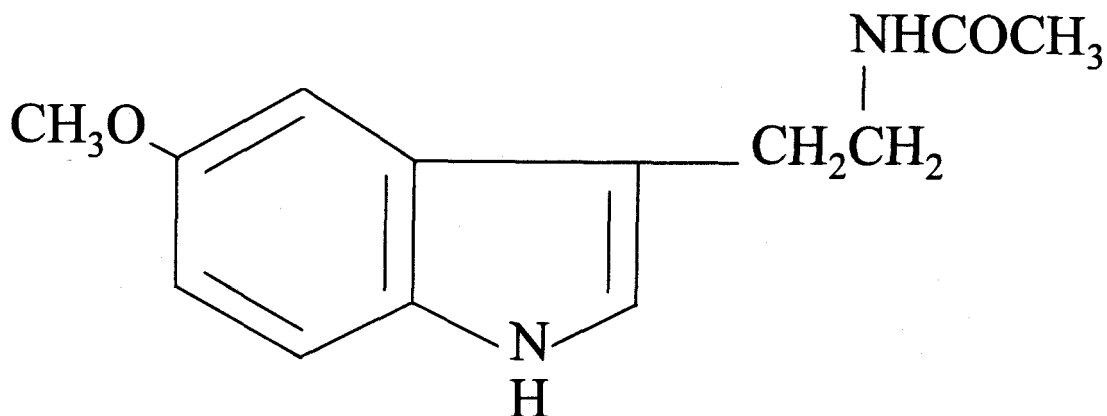
B. 6-Sulphatoxymelatonin (6-Hydroxymelatonin sulphate, MW = 328)

$$CH_3O \quad HSO4 \quad NHCOCH_3 \quad CH_2CH_2 \quad N\text{-}H$$
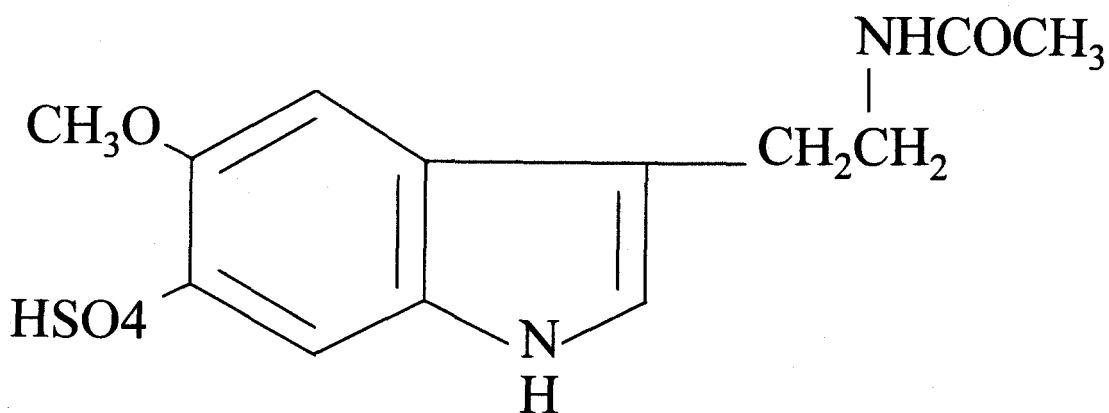
Figure 1.1: Structure of melatonin (A) and 6-sulphatoxymelatonin (B), melatonin chief metabolite in humans.

MATERIALS AND METHODS

Materials

MT was purchased from Regis Chemical Co. (Morton Grove, IL). Core sugar spheres (USP/NF) were purchased from Paulaur Co. (Robbinsville, NJ, USA). Aquacoat ® (aqueous polymeric ethylcellulose suspension, Type ECD-30) was provided courtesy of FMC Corp. (Philadelphia, USA). All other chemicals used were reagent grade and were used without further purification.

Preparation of dosage form

The SR formulation, developed previously (21, 22), consisting of MT loaded sugar beads coated with 20% Aquacoat ®. Gelatin capsules containing MT dispersed in lactose powder were used as an IR formulation.

Study Protocol

Seven healthy subjects (4 females and 3 males) over age seventy and seven healthy subjects (5 females and 2 males) under age thirty, were recruited from the community. Subject weights were within ± 20% of their ideal body weights. All subjects were taking no medications known to affect hepatic, renal, or cognitive function. Subjects were admitted to the Clinical Research Center at Oregon Health Sciences University on four occasions. In double-blind, single-dose, four period, randomized crossover study, they received oral administration of MT in an IR dose of

50 mg, and in total doses of 0.2 mg (0.02 mg IR plus 0.18 mg SR MT), 0.4 mg (0.04 mg IR plus 0.36 mg SR MT), and 0.8 mg (0.08 mg IR plus 0.72 mg SR MT) based on randomization schedule with treatments spaced one week apart. Subjects fasted over night and for twelve hours after dosing. Caloric and fluid replacement with fruit juice and corn starch supplements were given orally ad lib. During the study, subjects were in a brightly lit room to ensure that endogenous MT production was totally inhibited. Blood samples were collected at 0.5 hour prior to the dosing to provide baseline values and at 0.5, 1, 1.5, 2, 2.5, 3, 3.5, 4, 4.5, 5, 5.5, 6, 7, 8, 9, 10, 11, and 12 hour post dosing. Urine samples were collected over the 12 hour study periods.

Plasma MT concentrations were determined by a highly sensitive and specific GC/MS assay (38). Urinary 6STMT concentrations were determined by radioimmunoassay (39).

Pharmacokinetic and statistical analysis

Pharmacokinetic analysis

Individual endogenous MT plasma concentrations received at 0.5 hour predosing was used as baseline MT plasma concentration. Both of the plasma concentrations with and without baseline adjustment were analyzed using the empirical, model-independent (SHAM) method (40). Thus, peak plasma concentration (Cmax) and time to Cmax (Tmax) were taken directly from the observed data. The area under the plasma concentration versus time curve (AUC$_T$) truncated at the last

measurable plasma concentration at time T (C_T) was calculated using linear trapezoidal rule for incremental trapezoids and log-trapezoidal rule for decremental trapezoids (41). Equations used in calculation of AUC_T are shown below.

For incremental trapezoids:

$$[AUC]_{t_{i-1}}^{t_i} = \int_{t_{i-1}}^{t_i} y\, dt = \frac{1}{2} h_i (y_i + y_{i-1})$$

For log-trapezoidal rule for decremental trapezoids:

$$[AUC]_{t_{i-1}}^{t_i} = h_i (y_i - y_{i-1}) / \ln(y_i / y_{i-1})$$

where

$h_i = t_i - t_{i-1}$

y = plasma concentration

t = time

The cumulative amount of 6STMT in urine was calculated from urine concentration and urine volume data collected over the 12 hour study period.

Following the supra-physiologic dose of 50 mg IR MT, the terminal-phase elimination rate constant (λz) was estimated by a log-linear regression of the last three to six observed plasma concentrations, and the terminal-phase disposition half life ($t_{1/2}$) was calculated as $t_{1/2} = \ln2/\lambda z$. Total AUC was then estimated by AUC = AUC_T + $C_T/\lambda z$. The oral dose mean residence time (MRT $_{oral}$) was estimated using the statistical moment approach. In pharmacokinetics, MRT $_{oral}$ is the sum of the intrinsic mean residence time (MRT) and mean absorption time (MAT), and is estimated by MRT $_{oral}$ = MRT + MAT = AUMC/AUC, where AUMC is the area under the first moment curve. AUMC is calculated as AUMC = $\int t \cdot C\, dt$ = $AUMC_T$ + ($T \cdot C_T/\lambda z$) +

($C_T/\lambda z^2$). Either a mono- or bi-exponential pharmacokinetic equation with a first-order input (see below) was applied to best fit individual MT plasma data using RSTRIP® (41).

$$C = A_2 e^{-\lambda 1t} - A_2 e^{-kat}$$

$$C = A_1 e^{-\lambda 1t} + A_2 e^{-\lambda 2t} - (A_1+A_2) e^{-kat}$$

The plasma data was also fitted to one compartment open model using P-PHARM (43) to investigate effect of covariates; age and gender, on the oral clearance (CL/F), the terminal volume of distribution (Vd/F), the apparent absorption rate constant (ka), and the apparent elimination rate constant (k). A lag time was also included in the model to satisfactorily fit data.

Following administration of the SR formulation of MT given at 0.2, 0.4, and 0.8 mg, dose proportionality of MT AUC_T with respect to the lowest (0.2 mg) dose was estimated by the following equation.

$$R = \frac{AUC_{T\ 0.2,\ 0.4,\ or\ 0.8\ mg}}{AUC_{T\ 0.2\ mg}}$$

R is dose proportionality ratio. If dose proportionality is linear, the ratios for the three doses should not be statistically different from 1.0 : 2.0 : 4.0. In addition, a power function relationship (44) was used to describe the relationship between AUC_T and dose.

$$AUC_T = a \cdot (DOSE)^b$$

In the above equation, a represents the coefficient, and b represents the exponent of the power function regression. If AUC_T exhibits linear dose proportionality, then b should be equal to unity. The parameters a and b were estimated by linear least square regression following a log-transformation as follows:

$$\ln(AUC_T) = \ln(a) + b \cdot \ln(DOSE)$$

A similar power function relationship was also established for Cmax, and total excreted urinary 6STMT collected over 12 hour postdosing. Linearity was indicated if 95% confidence interval for the exponent included the value of 1 (44).

Statistical analysis

Statistical analysis of MT pharmacokinetic parameters obtained from the studies of IR MT (50 mg) and SR MT (0.2, 0.4, and 0.8 mg) was performed separately due to differences in type of dosage form and dose range.

Following supra-physiologic MT dose of 50 mg, comparison between the elderly and youngsters with respect to the mean pharmacokinetic parameters were made by using analysis of variance; ANOVA (45). Pairwise comparisons among gender/age groups were made using Duncan's multiple range test at a significant level of $\alpha = 0.05$. Duncan's multiple range test is a test used after an ANOVA to determine which sample means differ significantly from one another. The test allows one to protect the results from Type I errors for a small number of comparisons. It is more powerful than Tukey's Honestly Significant Differences (HSD). However, unlike Tukey's HSD, it does not control the experiment-wide error rate. For a small number of comparisons, it

is a good compromise between the least significant differences and Tukey's HSD methods (46).

Following administration of MT SR formulation at three different doses, statistical comparisons of mean plasma concentrations at each sampling time and estimates of the pharmacokinetic parameters among the three doses were made using ANOVA. Pairwise comparisons among the three doses were made using Duncan's multiple range test at a significant level of $\alpha = 0.05$. Prior to statistical comparisons, all plasma concentrations and all dose-dependent pharmacokinetic parameters (Cmax, AUC_T, and urinary 6STMT) were normalized to those of 0.2 mg MT dose, assuming linearity.

If an assessment of pharmacokinetic linearity by the power function relationship and ANOVA appeared to be linear, effect of age-gender on pharmacokinetics parameters would be simultaneously investigated to increase power of analysis i.e. treating the parameters obtained from the three different doses like they were from the same dose administration. Dose-independent pharmacokinetic parameters (MRT, and Tmax) were directly applied in the statistical comparison whereas all plasma concentrations and all dose-dependent pharmacokinetic parameters (Cmax, AUC_T, and urinary 6STMT) were normalized to those of 0.2 mg dose prior to statistical comparison. Pairwise comparisons among age-gender groups were made using Duncan's multiple range test at a significant level of $\alpha = 0.05$.

STATGRAPHICS Plus (version 2.1) was used for statistical analysis (46).

RESULTS AND DISCUSSION

Total 14 subjects were recruited for the study with 11 subjects completed the four treatments. Subject GL (elderly male) and RC (young female) finished only the three treatments (SR MT formulation given at 0.2, 0.4, and 0.8 mg). Subject JB (young female) completed only the study of IR MT given at 50 mg. No discomfort or toxicity was reported during the time of the study. The subjects withdrew from the study due to personal reasons. Demographic variables of individual subjects are presented in Table 1.1. The subjects included in the study were 21 to 95 years of age. Average age of the elderly and youngsters was 81 ± 9 years and 25 ± 2 years, respectively. There were nine females (mean age of 50 ± 30 years) and five males (mean age of 57 ± 32 years) included in the study. Endogenous MT during the day time (the time of the study) was found to be low and had no significant effect on statistical data analysis. Analysis results were similar for data set with and without baseline correction. Therefore, data without baseline correction were presented herein.

MT pharmacokinetics following the oral single supra-physiologic dose

Individual pharmacokinetic parameters estimated using noncompartmental method, RSTRIP, and P-PHARM are presented in Table 1.2, and Table 1.3, respectively. Pharmacokinetic parameters of subject JB was excluded from statistical analysis. As seen in Table 1.2, parameters such as λz, $t_{1/2}$, and MRT of subject JB deviate from mean more than $\pm 3 \cdot SD$ (n=11). As a result there is more than 3 to 1

Table 1.1: Demographic characteristics

Subject	Age	Gender
AK	87	female
AO	75	female
AT	80	female
HF	86	female
GL	69	male
LA	75	male
SK	95	male
CB	28	female
KT	23	female
RC	24	female
SL	21	male
SN	26	female
VB	26	male
JB	25	female

Table 1.2: Pharmacokinetic parameters (noncompartmental method) in healthy young and old subjects receiving 50 mg IR MT. (EM = Elderly males, EF = Elderly females, YM = young males, and YF = young females)

Subject	Cmax (ng/ml)	Tmax (h)	AUC_T (ng h/ml)	AUC (ng h/ml)	λz (h^{-1})	$t_{1/2}$ (h)	MRT_{oral} (h)	CL/F (L/h)	Vd/F (L/h)	6STMT (0-12h, mg)
SK (EM)	53.5	1.5	201	204	0.37	1.9	3.1	245.7	672.3	25.3
HF (EF)	101.4	2	341	345	0.42	1.7	3.7	144.8	346.8	19.1
AT (EF)	90.0	2	312	314	0.67	1.0	2.9	159.2	237.7	10.6
AO (EF)	65.2	1.5	186	187	0.76	0.9	2.5	267.6	354.2	13.7
AK (EF)	208.6	1	388	399	0.54	1.3	2.8	125.5	230.3	17.2
LA (EM)	89.0	1	246	248	0.66	1.1	3.0	201.6	307.8	21.1
CB (YF)	41.1	1	129	129	0.43	1.6	2.5	387.0	898.8	21.7
SL (YM)	36.6	1	72	74	0.66	1.0	2.3	679.2	1025.1	22.3
VB (YM)	45.2	1.5	150	150	0.57	1.2	2.8	333.0	586.0	NA
SN (YF)	100.0	1	465	466	0.78	0.9	3.4	107.3	137.0	NA
KT (YF)	81.2	1	166	166	0.46	1.5	2.1	301.0	656.9	11.8
JB (YF)	21.6	2	90	114	0.17	4.0	6.5	438.2	2515.9	NA
Mean[#]	54.3	1.25	179	183	0.51	1.7	3.3	374.3	970.0	18.6
(SE)	(48.0)	(0.4)	(121.1)	(122.6)	(0.1)	(0.3)	(0.5)	(163.3)	(291.7)	(5.1)
%CV	57.9	30.7	50.1	50.3	24.7	27.0	16.7	60.8	58.9	28.2
Geometric mean	66.2	1.3	198	204	0.51	1.4	3.0	245.3	485.2	17.4

NA: not available

[#] Mean (SE) calculated from 11 subjects excluding JB.

Table 1.3: Individual pharmacokinetic parameters in healthy young and old subjects receiving 50 mg IR MT. Parameters are estimated using either a monoexponential equation (RSTRIP®) or one compartment open model (P-PHARM). (EM = Elderly males, EF = Elderly females, YM = young males, and YF = young females).

	Calculation using RSTRIP®			**Calculation using P-PHARM**				
Subject	**ka** (h^{-1})	λ_1 (h^{-1})	**Lag time** **(h)**	**ka** (h^{-1})	**k** (h^{-1})	**Lag time** **(h)**	**CL/F** **(L/h)**	**Vd/F** **(L)**
AK (EF)	0.79	0.52	0	4.72	0.44	0.38	114.8	261.3
AO (EF)	1.11	0.65	0	2.91	0.53	0.34	264.6	501.9
AT (EF)	0.99	0.35	0.06	0.99	0.61	0.39	153.4	252.1
HF (EF)	0.74	0.46	0.16	0.79	0.52	0.39	142.8	273.1
LA (EM)	1.34	0.43	0.03	2.50	0.49	0.38	205.4	420.3
SK (EM)	0.76	0.57	0.02	2.09	0.46	0.33	245.4	532.6
CB (YF)	1.21	0.58	0	3.16	0.55	0.34	381.9	695.0
KT (YF)	1.10	0.98	0.06	2.25	0.74	0.41	285.6	384.4
SL (YM)	1.31	0.70	0.02	3.03	0.59	0.36	661.8	1125.8
SN (YF)	0.87	0.51	0.05	0.94	0.48	0.35	106.4	222.0
VB (YM)	1.27	0.73	0	1.26	0.59	0.38	322.9	550.8
JB (YF)	0.55	0.43	0.08	0.33	0.55	0.38	465.1	850.8
Mean[#]	1.04	0.59	0.04	2.24	0.54	0.37	262.26	474.49
(SE)	(0.23)	(0.17)	(0.05)	(1.20)	(0.09)	(0.03)	(159.35)	(263.27)

[#] Mean (SE) was calculated from 11 subjects excluded JB.

difference between the smallest standard deviation and the largest among subjects groups. The difference still exists even after transformation of the data. The large difference among group standard deviation violate assumption of ANOVA in that the standard deviation are all equal and the data come from normal distribution. Additionally, the small value of λz also affect the calculation of AUC. AUC extrapolated (AUCext = AUC - AUC_T) of subject JB (27%) is 5 times higher than those of the others which were less than 5%. Therefore, ANOVA of age and gender was performed on data from 11 subjects excluding JB. Group pharmacokinetic parameters and result of ANOVA of log-transformed data is presented in Table 1.4. Statistical comparison of MT plasma concentrations is reported in Table 1.5. Supportive Figure 1.2A and 1.2B present individual MT plasma concentration-time profiles in healthy subjects following a single oral dose of 50 mg. Figure 1.3 shows the mean plasma concentration versus time plots for each group of subjects.

MT plasma concentration-time profiles, following IR MT 50 mg, were characterized by a rapid absorption phase with maximum observed plasma concentrations occurring between 1- 2 hour postdosing. In general, elderly female, young female, and elderly male subjects showed higher MT plasma concentrations than did young males. No difference between age groups was noted. Statistically significant difference was found in urinary 6STMT (0-12h) when males were compared with females. It appeared that amount of urinary 6STMT in females (16.4 ± 14.4 mg) was lower than that of males (25.4 ± 26.1 mg). Plasma concentration at 11 and 12 hour following the drug administration in the elderly were higher than those in

Table 1.4: Pharmacokinetic parameters of MT given at 50 mg (noncompartmental method). Data are presented as mean (SE).

	Cmax (ng/ml)	Tmax (h)	AUC_T (ng h/ml)	AUC (ng h/ml)	λz (h^{-1})	$t_{1/2}$ (h)	MRT_{oral} (h)	CL/F (L/h)	Vd/F (L/h)	6STMT (0-12h, mg)
Elderly males										
Mean[#]	71.3	1.3	224	226	0.52	1.5	3.1	223.7	490.1	23.2
SE	(25.1)	(0.4)	(32)	(31)	(0.21)	(0.6)	(0.1)	(31.2)	(257.7)	(3.0)
Elderly females										
Mean[#]	116.3	1.6	307	311	0.60	1.2	3.0	174.3	292.3	15.2
SE	(63.4)	(0.5)	(86)	(90)	(0.15)	(0.4)	(0.5)	(63.7)	(67.4)	(3.8)
Young males										
Mean[#]	40.9	1.3	111	112	0.62	1.1	2.6	506.1	805.6	22.3
SE	(6.1)	(0.4)	(55)	(54)	(0.06)	(0.1)	(0.4)	(244.8)	(310.5	(-[$])
Young females										
Mean[#]	74.1	1.0	253	254	0.56	1.3	2.7	265.1	564.2	16.8
SE	(30.1)	(0)	(184)	(185)	(0.19)	(0.4)	(0.7)	(143.3)	(389.3)	(7.0)
p-value from ANOVA[#]										
Age	0.099	0.131	0.114	0.114	0.861	0.861	0.171	0.114	0.229	0.847
Gender	0.098	0.854	0.122	0.122	0.880	0.880	0.943	0.122	0.190	0.023
Age_Gender	0.174	0.257	0.170	0.170	0.858	0.858	0.580	0.170	0.381	0.109

[$] Impossible to calculate standard error due to missing data.

[#] Mean (SE) and ANOVA of log-transformed data was performed on data received from 11 subjects excluding JB.

Table 1.5: Statistical comparison of MT plasma concentrations in healthy volunteers receiving a single dose of MT 50 mg.

MT plasma concentrations (ng/ml)

	0 h	0.5 h	1 h	1.5 h	2 h	2.5 h	3 h	3.5 h	4 h	4.5 h	5 h	5.5 h	6 h	7 h	8 h	9 h	10 h	11 h	12 h
Elderly males																			
Mean[#]	0	30.8	66.9	62.9	51.6	43.6	43.4	33.3	25.0	17.7	12.1	12.5	21.5	4.6	3.1	2.3	1.5	1.2	1.0
SE	(0)	(4.4)	(31.2)	(13.3)	(2.1)	(4.8)	(2.0)	(6.3)	(5.9)	(8.6)	(1.0)	(4.6)	(15.6)	(0.9)	(1.4)	(1.6)	(-)	(-)	(-)
Elderly females																			
Mean[#]	0	37.3	92.2	94.1	79.4	61.0	57.8	47.8	38.9	23.9	22.4	14.5	10.1	6.3	4.0	2.2	2.9	4.4	3.7
SE	(0)	(26.5)	(80.4)	(43.3)	(24.7)	(25.1)	(21.5)	(18.8)	(20.7)	(9.1)	(11.7)	(8.0)	(5.2)	(5.0)	(3.5)	(2.2)	(-)	(4.7)	(2.7)
Young males																			
Mean[#]	0	12.5	39.5	33.2	28.7	24.0	21.3	30.6	14.2	8.9	7.0	4.2	3.5	1.4	-	-	0.4	0.3	0.2
SE	(0)	(2.3)	(4.2)	(17.1)	(13.7)	(17.7)	(12.9)	(-)	(9.9)	(6.4)	(3.8)	(2.8)	(2.5)	(0.6)	(-)	(-)	(-)	(-)	(-)
Young females																			
Mean[#]	0	27.6	74.1	65.4	66.9	58.8	46.1	35.4	29.3	21.5	27.2	16.9	12.8	9.1	4.1	3.5	0.9	0.4	0.2
SE	(0)	(7.9)	(30.1)	(31.0)	(33.3)	(37.0)	(46.9)	(37.2)	(26.6)	(23.2)	(30.5)	(24.3)	(19.2)	(11.7)	(5.5)	(3.3)	(1.0)	(0.3)	(0.1)

p-value from ANOVA[#]

	0 h	0.5 h	1 h	1.5 h	2 h	2.5 h	3 h	3.5 h	4 h	4.5 h	5 h	5.5 h	6 h	7 h	8 h	9 h	10 h	11 h	12 h
Age	-[§]	0.230	0.638	0.081	0.174	0.306	0.130	0.306	0.228	0.206	0.472	0.181	0.125	0.313	0.604	0.569	0.169	0.035	0.024
Gender	-[§]	0.305	0.424	0.083	0.056	0.113	0.365	0.793	0.294	0.294	0.212	0.581	0.785	0.439	0.938	0.786	0.590	0.571	0.525
Age* Gender	-[§]	0.282	0.746	0.123	0.128	0.225	0.366	0.713	0.456	0.426	0.526	0.509	0.410	0.521	0.857	0.833	0.617	0.210	0.116

[§] No statistical analysis was performed.
[#] Mean (SE) and ANOVA of log transformed data was performed on data of 11 subjects excluding JB.

22

SK   HF   AT   AO   AK   LA

⋯O⋯ Observed plasma concentration-time profile
●   Concentration used in the calculation of terminal slope
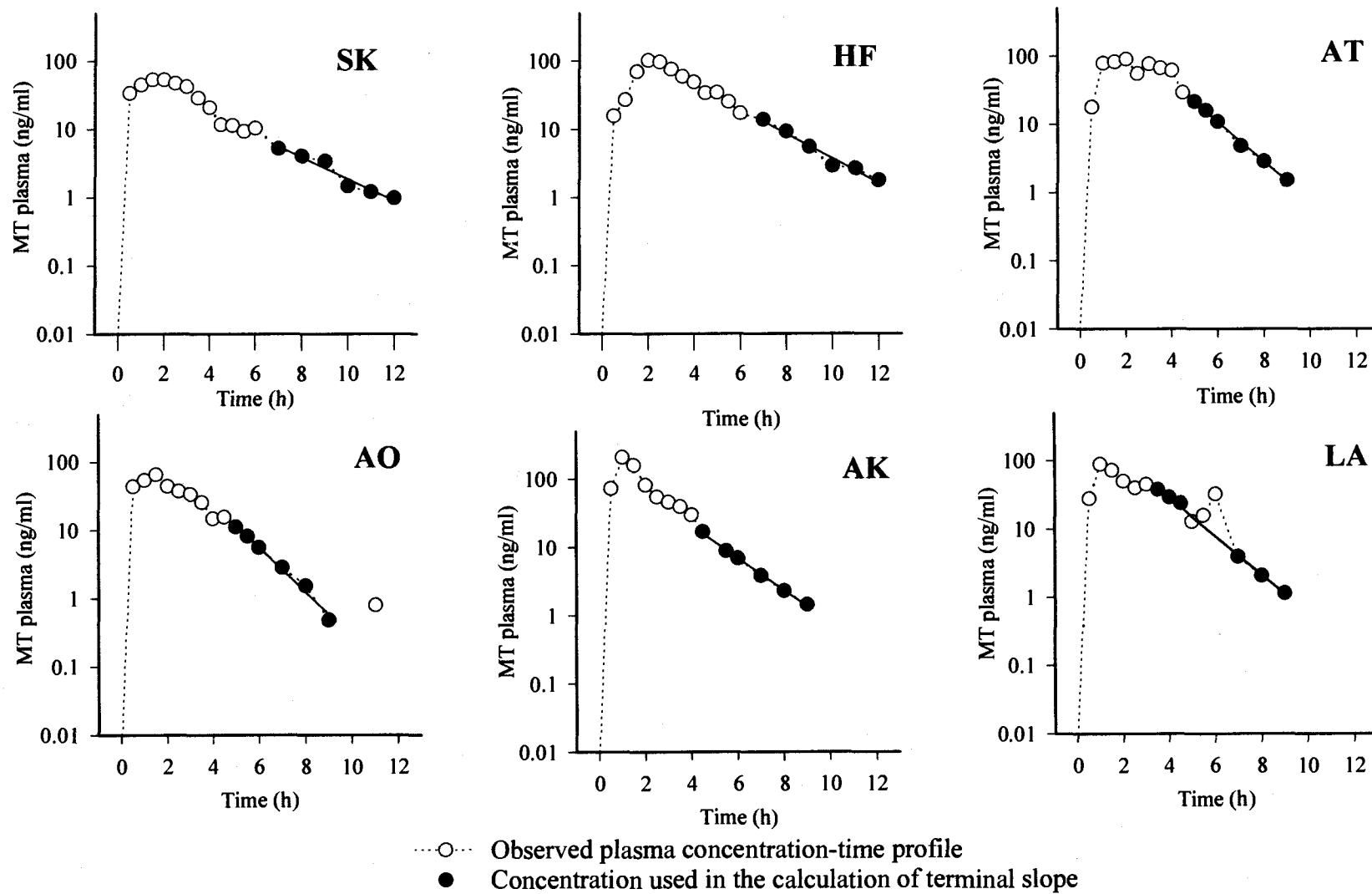
Figure 1.2A: MT plasma concentration time profiles following oral administration of IR MT 50 mg.
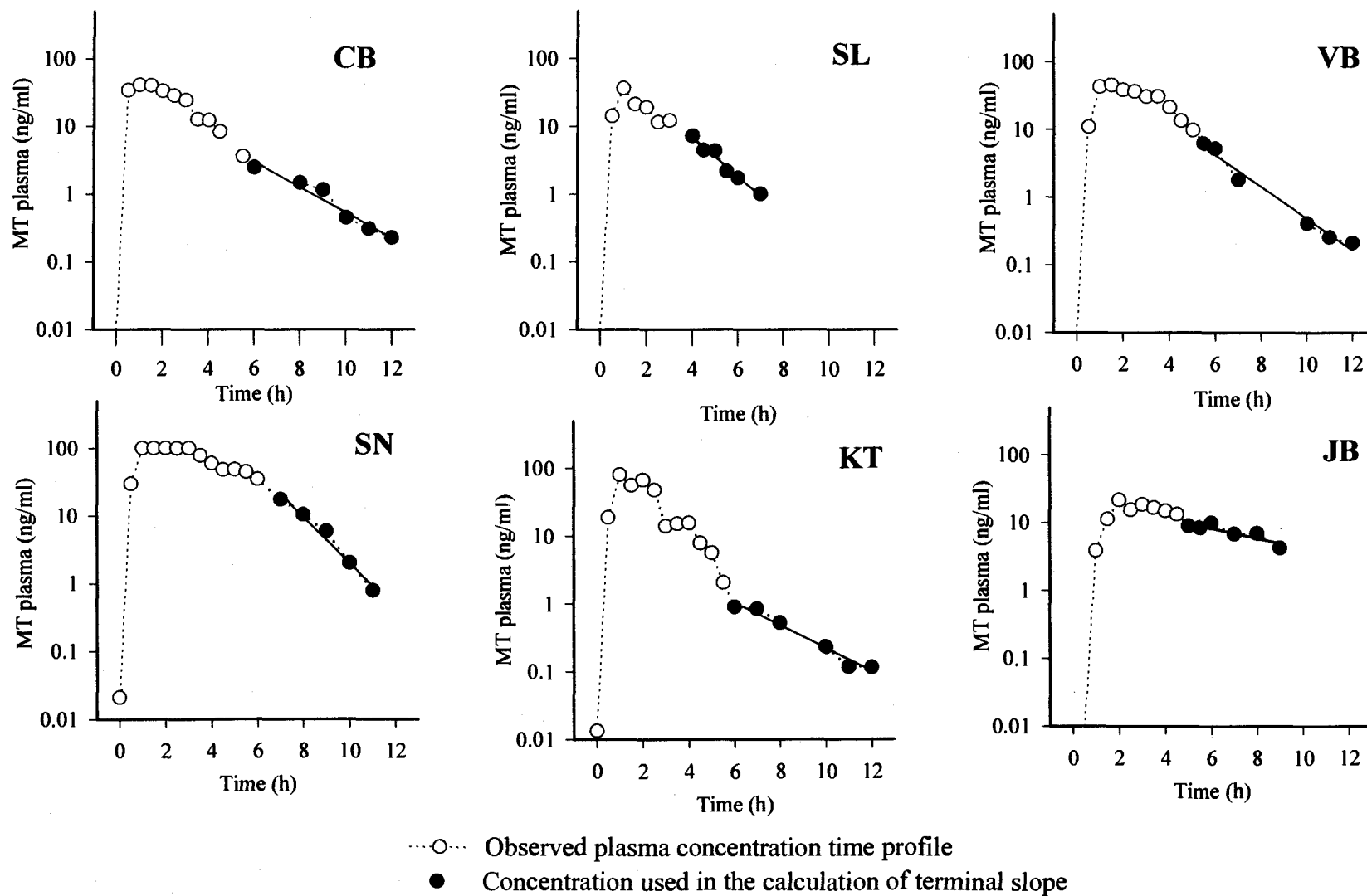
Figure 1.2B: MT plasma concentration time profiles following oral administration of IR MT 50 mg.
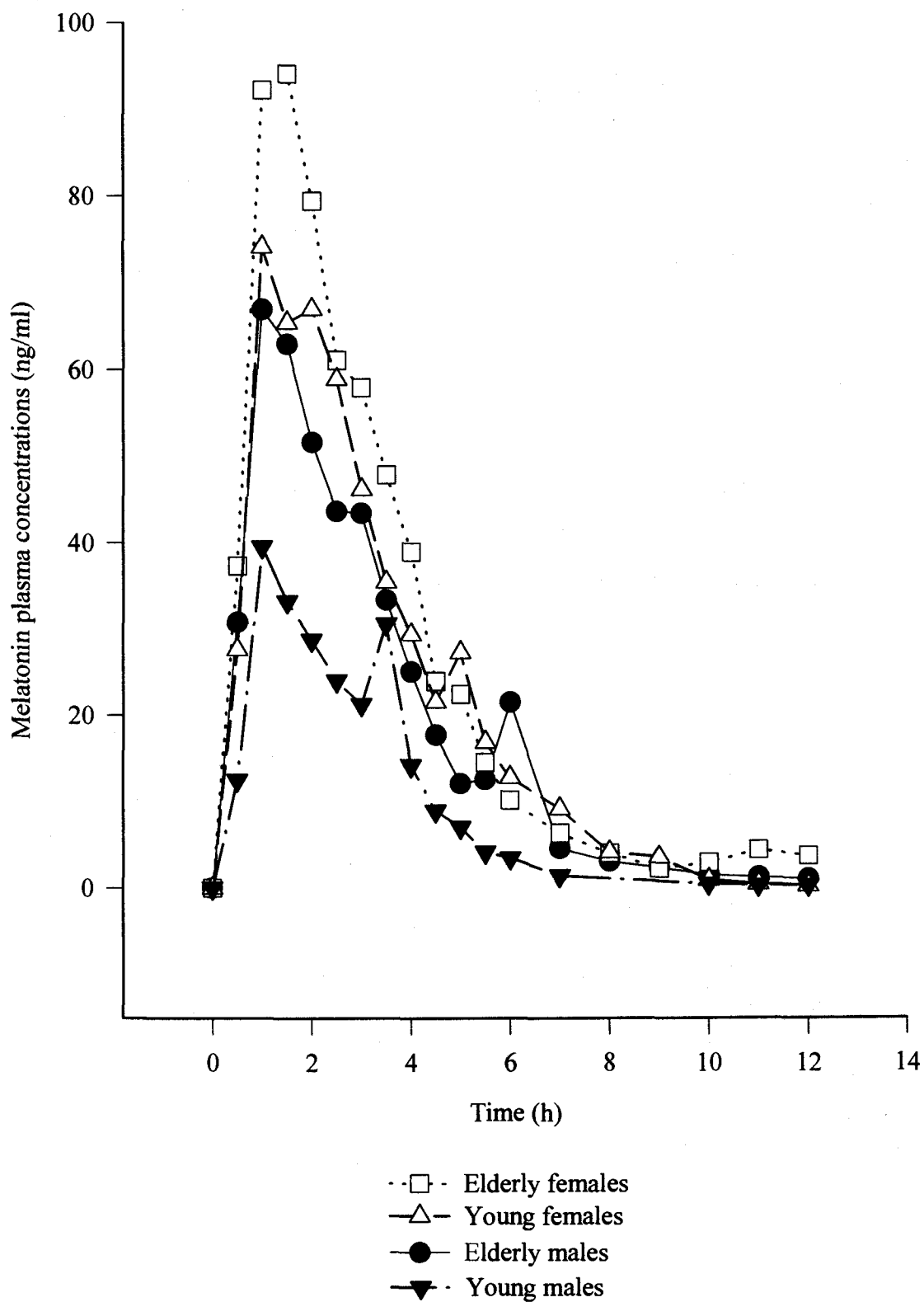
Figure 1.3: Mean MT plasma concentrations following a single dose of IR MT 50 mg in four age-gender groups.

the youngsters. Analysis of covariates using P-PHARM showed neither age nor gender had significant effect on MT pharmacokinetics. High variation among individual pharmacokinetic parameters especially in Cmax, AUC_T, AUC, CL/F, and Vd/F were also noted.

Graphical comparison of the fitted profiles using P-PHARM were generally better than those using RSTRIP®. Estimation of the monoexponential equation parameters by RSTRIP® is based on a striping method whereas estimation of pharmacokinetic parameters by P-PHARM can be done using either the stripping method or a simplex method. When a few data points are collected in the absorption phase, the stripping method (RSTRIP) tends to be less efficient or fail to fit the data (i.e. in P-PHARM if one chooses stripping method, data could not be fitted.) In this case, the simplex method fits data fairly well.

To predict whether there is a possibility of MT plasma concentration remaining above the normal physiological concentration during the day time after administration of the supra-physiologic dose (50 mg) at bed time (9 p.m.), MT population pharmacokinetic parameters received from P-PHARM are further applied to simulate MT plasma concentration profile. Simulation result of MT plasma concentration-time profile following administration of 50 mg at bed time is shown in Figure 1.4. Result shows that not only MT plasma concentration could peak at many times (about 400 times) higher than the MT normal nighttime concentration (about 25 to 120 pg/ml) but also could remain at these concentrations until noon of the next morning. If hypnotic effect of MT involving MT concentration being at or above its normal nighttime
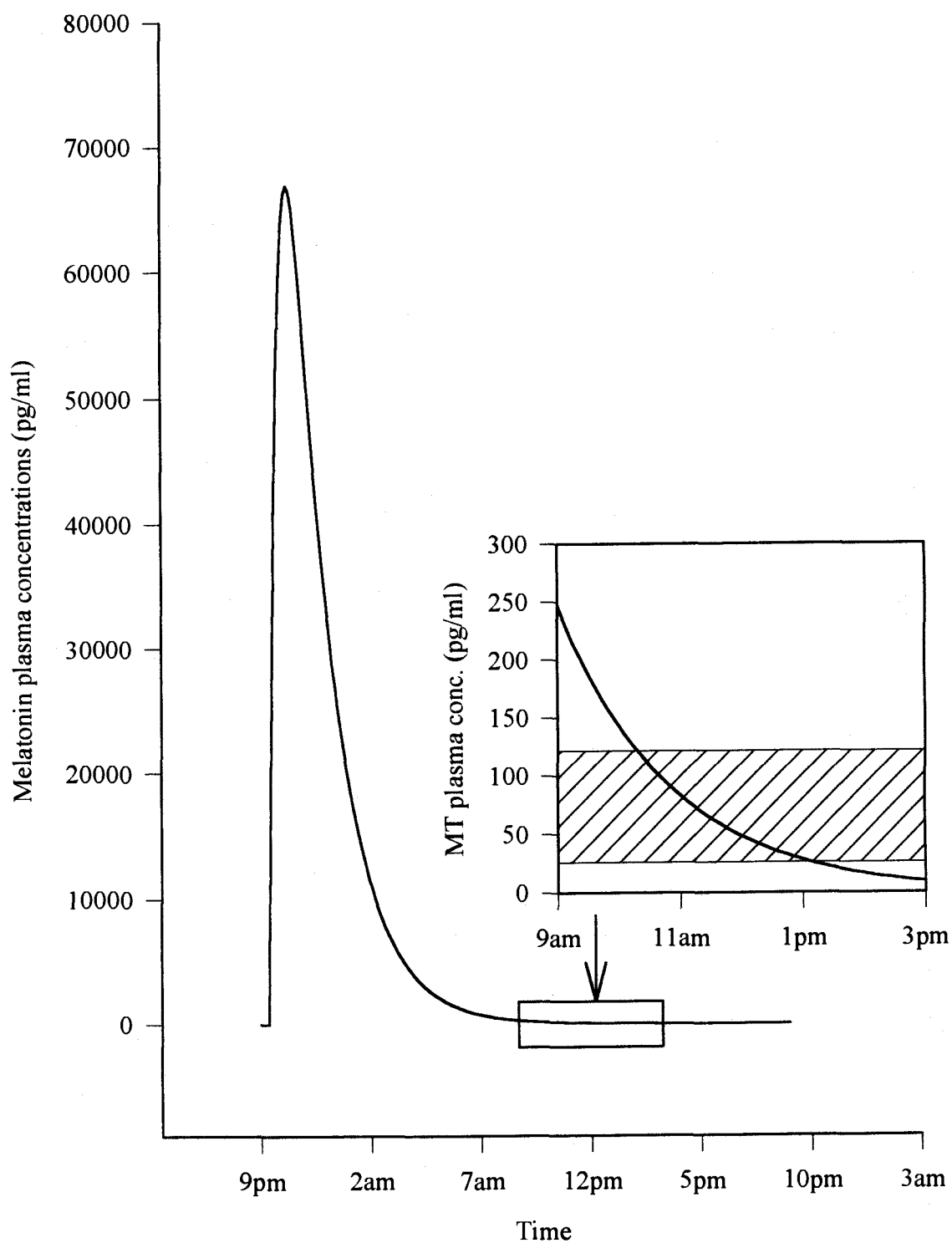
Figure 1.4: Simulation of MT plasma concentration time profile following a single dose 50 mg IR MT at bed time (9 pm). MT plasma concentration during day time (9 am to 3 pm) is magnified in the small figure. The shadow area represents the normal nighttime MT plasma concentrations.

concentrations, the supra-physiologic dose of 50 mg at bed time may cause undesired effect during the daytime.

MT pharmacokinetics and dose proportionality following the oral single physiologic doses

Individual MT plasma concentration-time profiles following oral administration of SR MT formulation at 0.2, 0.4, and 0.8 mg are presented in Figure 1.5A, 1.5B, 1.6A, 1.6B, 1.7A, and 1.7B, respectively. Individual pharmacokinetic parameters obtained from noncompartmental method in the volunteers receiving 0.2, 0.4, and 0.8 mg are reported in Table 1.6, 1.7, and 1.8, respectively. The concentration-time profiles, following the three regimens, were characterized by a rapid absorption phase with maximum observed plasma concentrations occurring between 0.5 to 3.5 hours postdosing. MT plasma concentrations were generally maintained above the nighttime physiological concentrations following 0.4 and 0.8 mg doses for more than 6 hours.

Figure 1.8, 1.9, and 1.10 compare the individual AUC_T, Cmax, and total 6STMT following administration of 0.2, 0.4, and 0.8 mg dose, respectively. The relationship between AUC_T versus dose, Cmax versus dose, and total 6STMT versus dose, using the power model, are also presented in Figure 1.8, 1.9, and 1.10, respectively. Summary of statistical comparison between dose, and age-gender group effects of pharmacokinetic parameters following the three doses is shown in Table 1.9. Dose-dependent parameters such as AUC_T, Cmax, total 6STMT were dose-normalized to those of 0.2 mg dose prior to the comparison. Effect of dose and age-gender groups were included in ANOVA
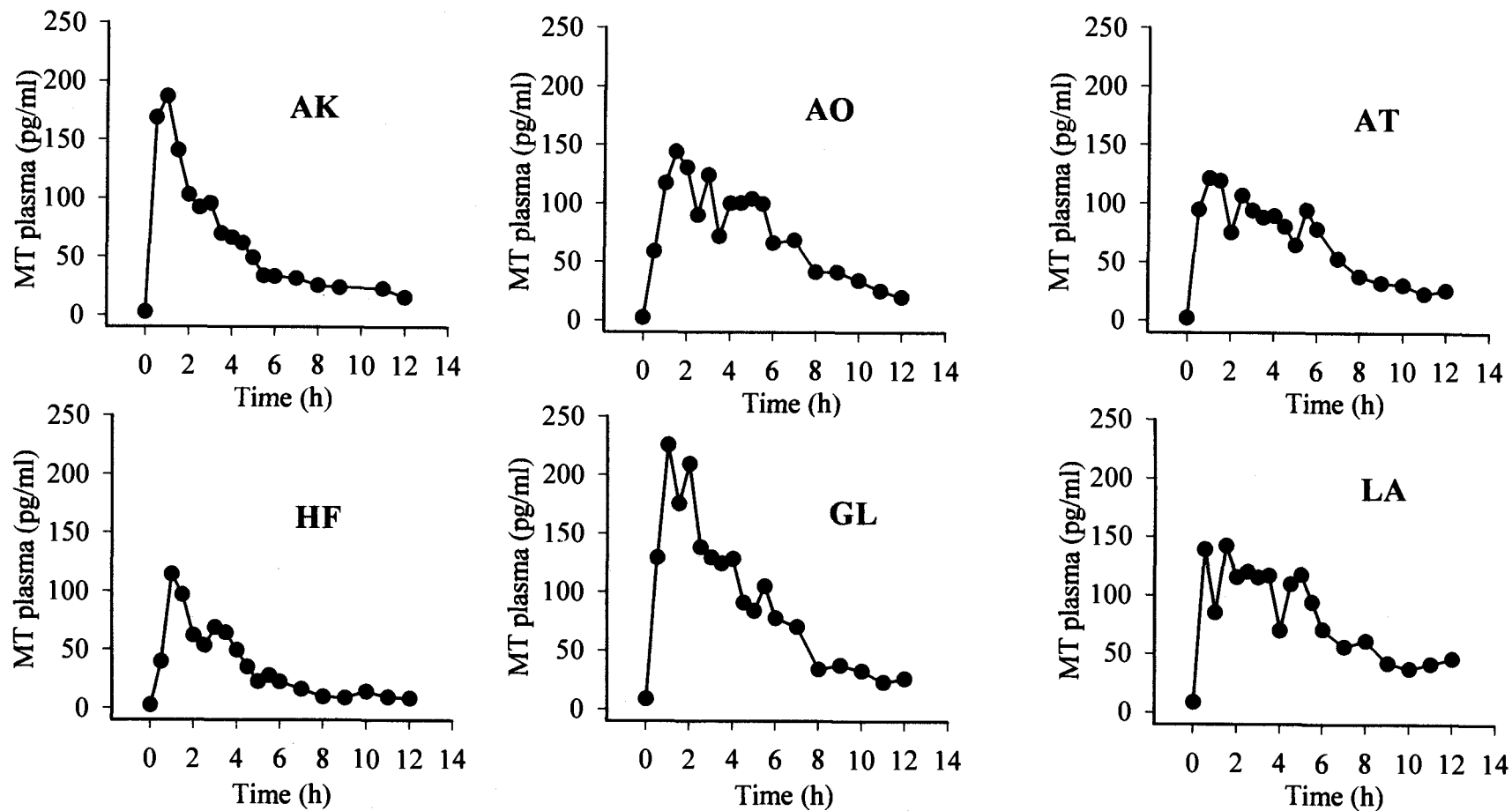
Figure 1.5A: MT plasma concentration time profiles following oral administration of SR MT 0.2 mg.
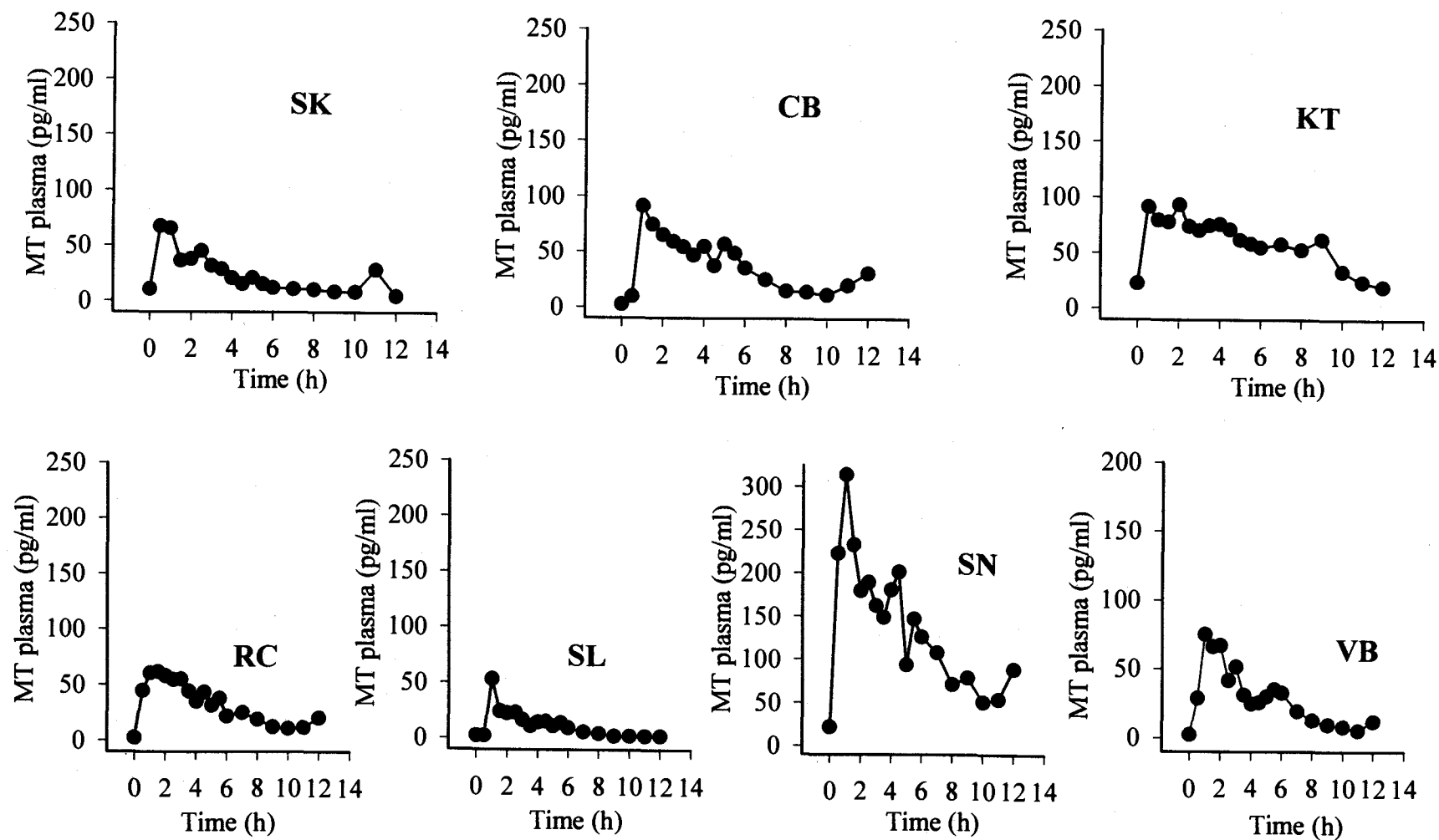
Figure 1.5B: MT plasma concentration time profiles following oral administration of SR MT 0.2 mg.
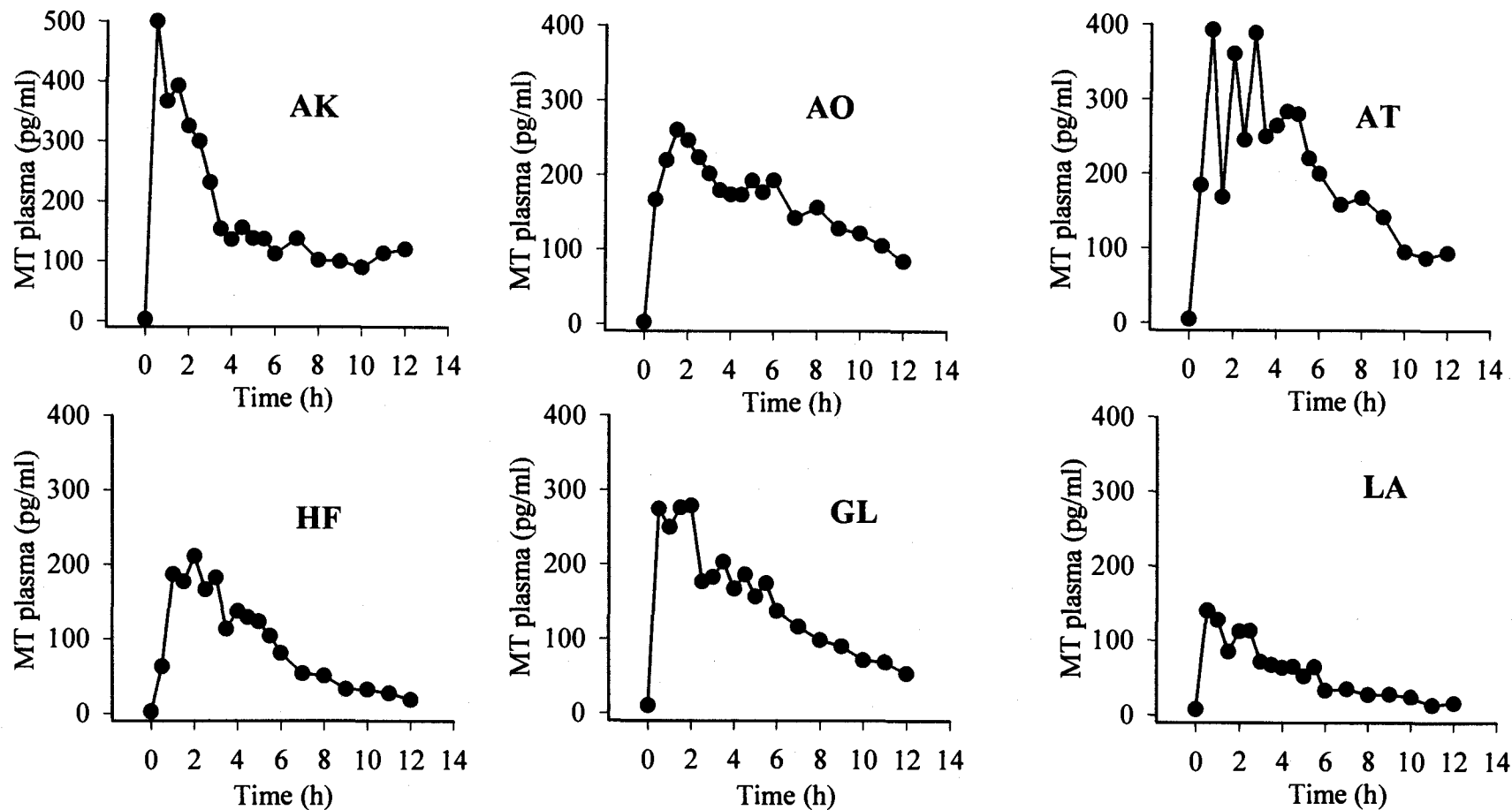
Figure 1.6A: MT plasma concentration time profiles following oral administration of SR MT 0.4 mg.
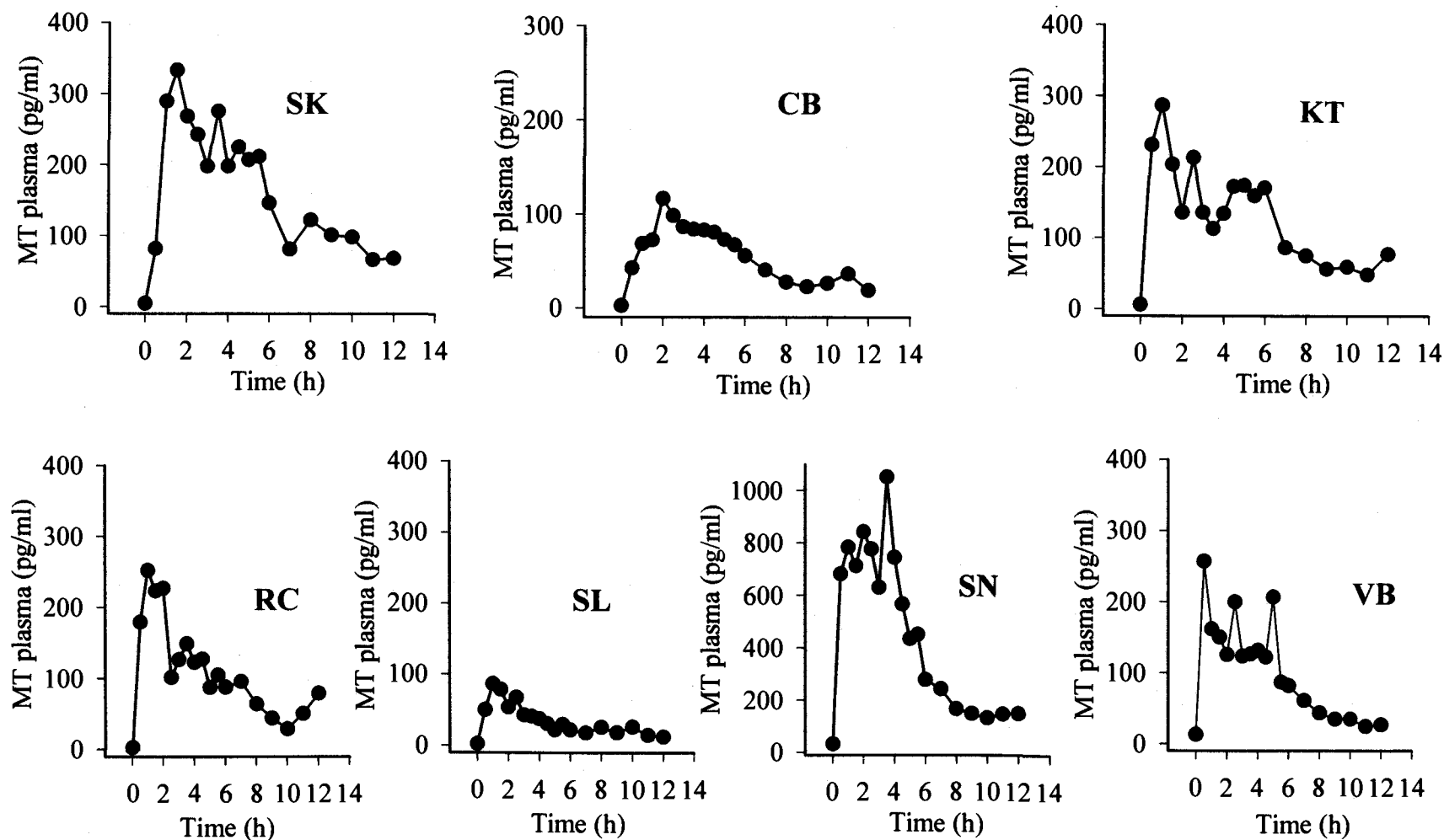
Figure 1.6B: MT plasma concentration time profiles following oral administration of SR MT 0.4 mg.
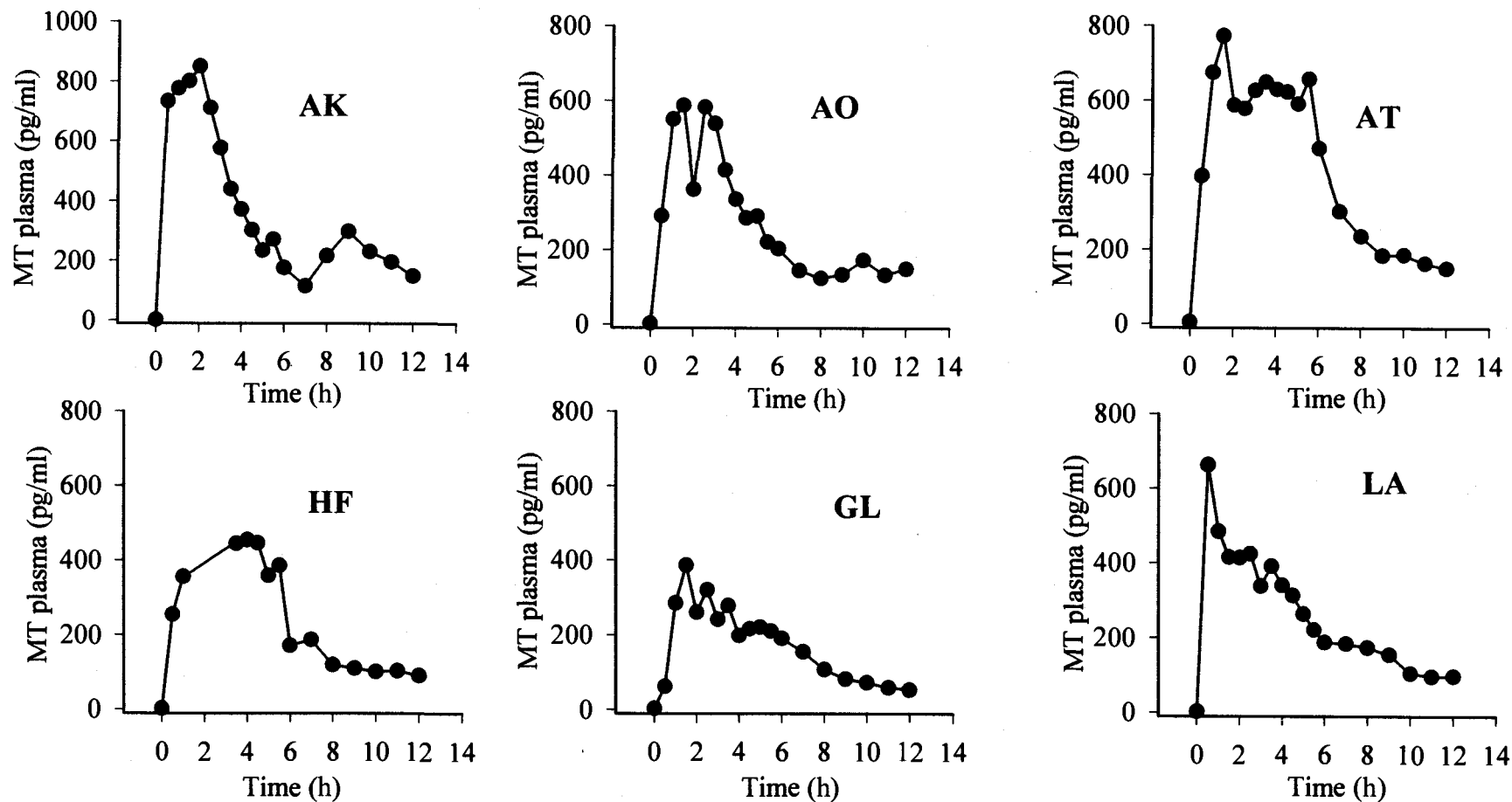
Figure 1.7A: MT plasma concentration time profiles following oral administration of SR MT 0.8 mg.
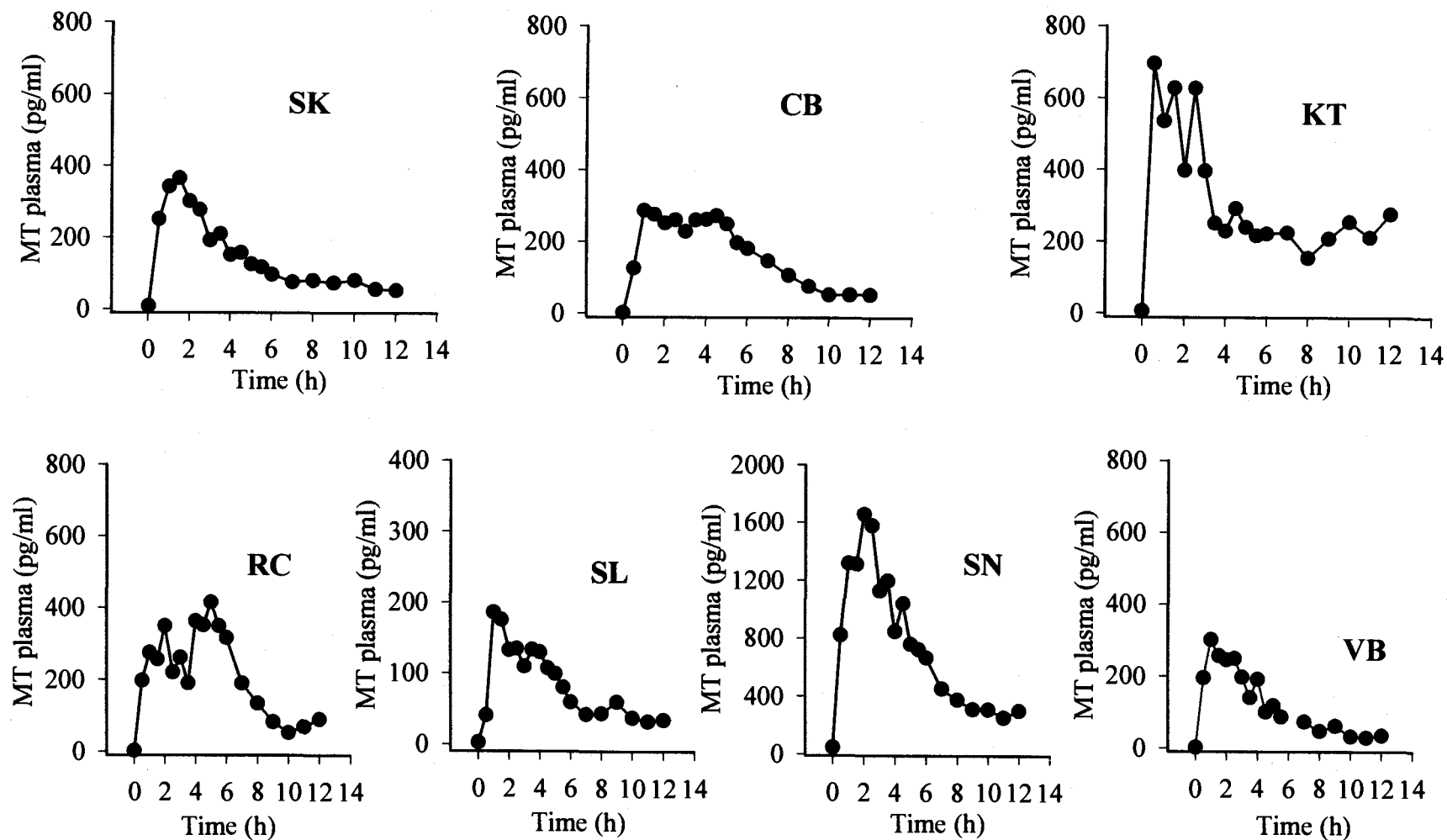
Figure 1.7B: MT plasma concentration time profiles following oral administration of SR MT 0.8 mg.

Table 1.6: Individual pharmacokinetic parameters (noncompartmental method) in healthy young and old subjects receiving 0.2 mg SR MT formulation. (EM = Elderly males, EF = Elderly females, YM = young males, and YF = young females).

Subjects	Cmax (pg/ml)	Tmax (h)	AUC$_T$ (0-12h, pg h/ml)	6STMT (μg)	MRT (0-12 h)
AK (EF)	144.0	1.5	692.8	46.3	3.5
AO (EF)	186.7	0.5	843.1	50.3	4.7
AT (EF)	121.8	1.0	766.1	42.4	3.7
HF (EF)	114.3	1.0	397.6	NA	3.7
GL (EM)	225.7	1.0	1041	63.2	4.1
LA (EM)	142.0	1.0	929.54	32.3	4.8
SK (EM)	67.4	1.5	272.6	67.6	4.2
CB (YF)	91.1	1.0	427.9	71.9	4.6
KT (YF)	93.6	2.0	701.2	NA	5.0
RC (YF)	61.7	1.0	369.2	68.6	4.4
SL (YM)	53.3	2.0	133	50.2	3.7
SN (YF)	314.2	1.0	1542.9	87.5	4.5
VB (YM)	75.2	1.0	326.2	104.2	4.0
Mean	130.1	1.2	649.5	62.2	4.2
SE	74.9	0.4	386.2	21.0	0.5
%CV	58	36	59	34	12
Geometric mean	113.8	1.1	542.0	59.1	4.2

NA: Data was not available.

Table 1.7: Individual pharmacokinetic parameters (noncompartmental method) in healthy young and old subjects receiving 0.4 mg SR MT formulation. (EM = Elderly males, EF = Elderly females, YM = young males, and YF = young females).

Subjects	Cmax (pg/ml)	Tmax (h)	AUC_T (0-12h, pg h/ml)	6STMT (μg)	MRT (0-12 h)
AK (EF)	500.0	2.0	2104.0	93.6	4.4
AO (EF)	260.3	3.5	1947.0	58.6	5.3
AT (EF)	393.3	1.0	2371.3	100.0	4.9
HF (EF)	210.8	1.0	1061.8	131.2	4.2
GL (EM)	278.6	0.5	1737.9	102.5	4.6
LA (EM)	332.9	1.0	1875.2	139.3	4.8
SK (EM)	140.2	1.5	644.8	131.7	4.0
CB (YF)	116.7	0.5	641.9	158.1	4.8
KT (YF)	286.7	1.0	1470.7	164.6	4.6
RC (YF)	252.0	2.0	1240.4	145.3	4.4
SL (YM)	86.8	2.0	399.2	118.6	4.5
SN (YF)	1051.2	1.5	4961.2	133.8	4.1
VB (YM)	257.0	0.5	1123.1	152.4	4.1
Mean	320.5	1.4	1659.9	125.4	4.5
SE	246.2	0.8	1163.7	30.0	0.4
%CV	77	61	70	24	8
Geometric mean	262.2	1.2	1363.8	121.4	4.5

Table 1.8: Individual pharmacokinetic parameters (noncompartmental method) in healthy young and old subjects receiving 0.8 mg SR MT formulation. (EM = Elderly males, EF = Elderly females, YM = young males, and YF = young females).

Subjects	Cmax (pg/ml)	Tmax (h)	AUC$_T$ (0-12h, pg h/ml)	6STMT (µg)	MRT (0-12 h)
AK (EF)	850.4	5.0	4298.8	179.8	4.3
AO (EF)	588.0	0.5	3169.2	190.5	4.5
AT (EF)	772.9	1.0	4893.5	204.5	4.6
HF (EF)	454.0	2.0	2948.5	267.0	4.6
GL (EM)	387.0	1.0	1993.3	257.4	4.6
LA (EM)	663.3	1.0	3042.7	275.9	4.3
SK (EM)	365.1	1.5	1711.5	226.3	4.2
CB (YF)	287.9	2.0	1950.8	386.2	4.6
KT (YF)	697.2	1.5	3632.2	165.0	4.9
RC (YF)	415.3	4.0	2426.9	151.8	4.8
SL (YM)	185.7	1.5	942.2	248.6	4.6
SN (YF)	1657.0	0.5	8553.0	NA	4.3
VB (YM)	302.0	1.5	1374.2	242.6	3.9
Mean	586.6	1.8	3149.0	233.0	4.5
SE	380.2	1.3	1984.0	63.3	0.3
%CV	65	74	63	27	6
Geometric mean	501.6	1.4	2691.3	225.8	4.5

NA: Data was not available.
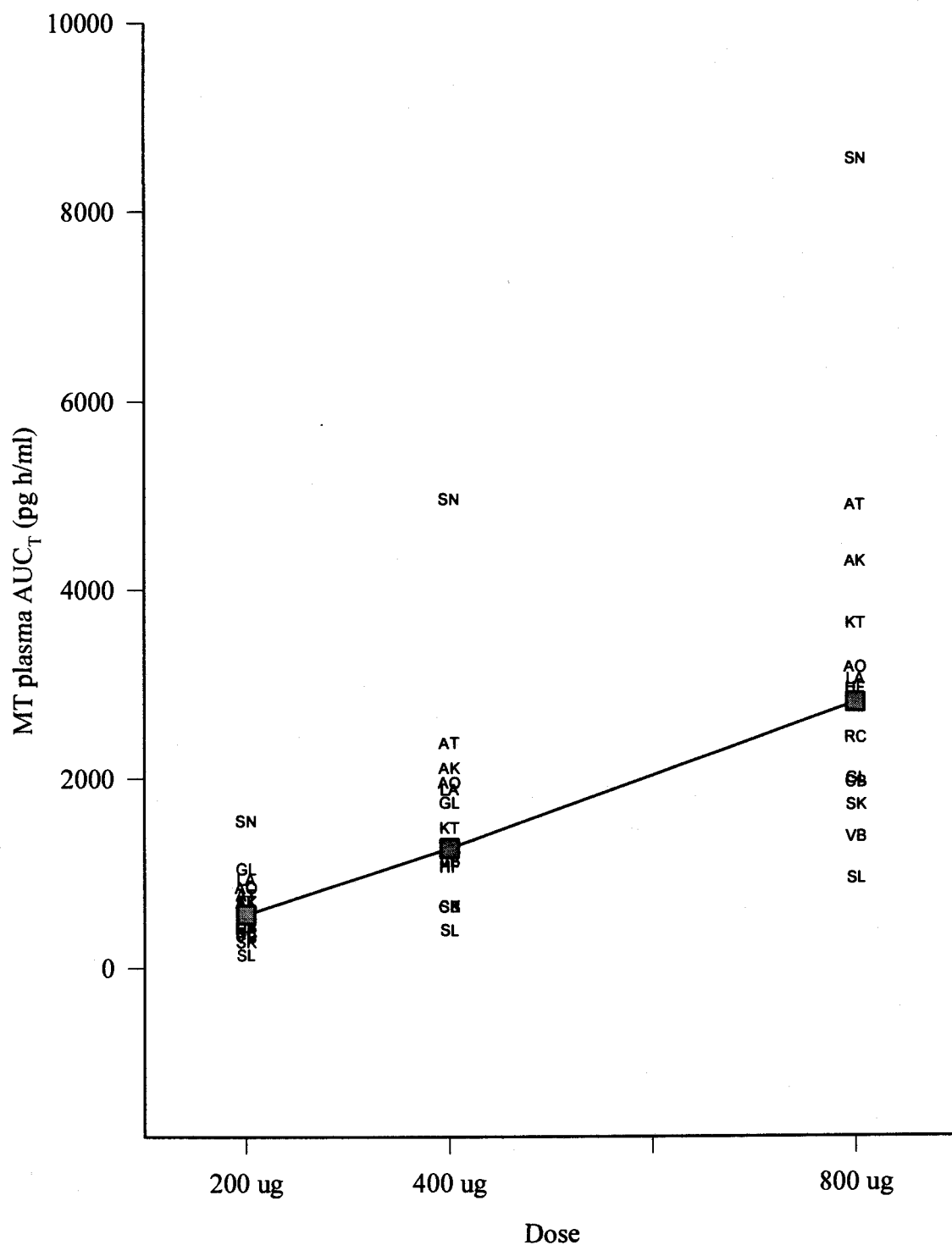
Figure 1.8: MT plasma AUC_T versus dose following single dose administration of 0.2, 0.4, and 0.8 mg oral SR MT with fitted power function.

$$AUC_T = 1.23462 \ Dose^{1.15602}$$
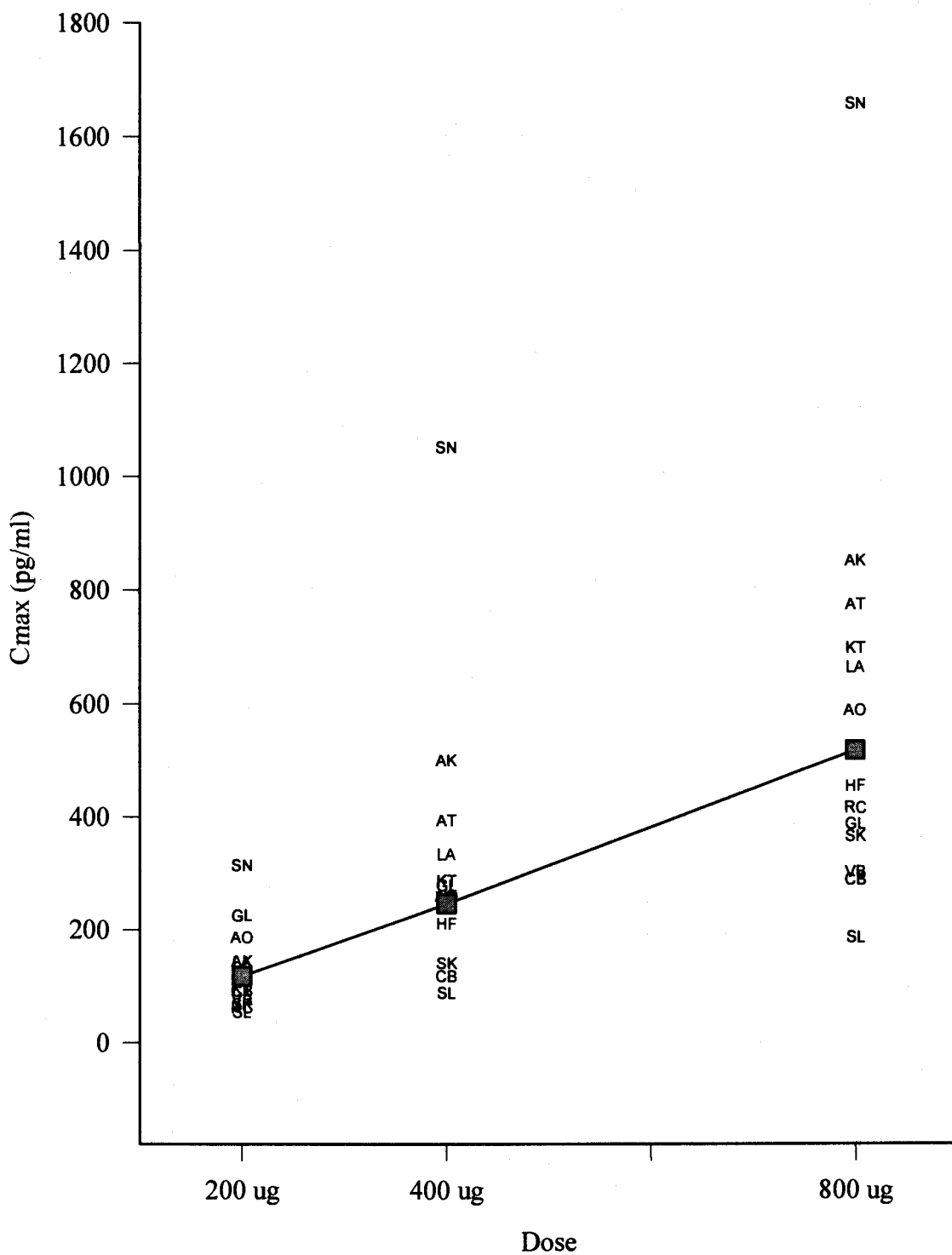
Figure 1.9: MT plasma Cmax versus dose following single dose administration of 0.2, 0.4, and 0.8 mg oral SR MT with fitted power function.

$$Cmax = 0.404578 \ Dose^{1.0702}$$
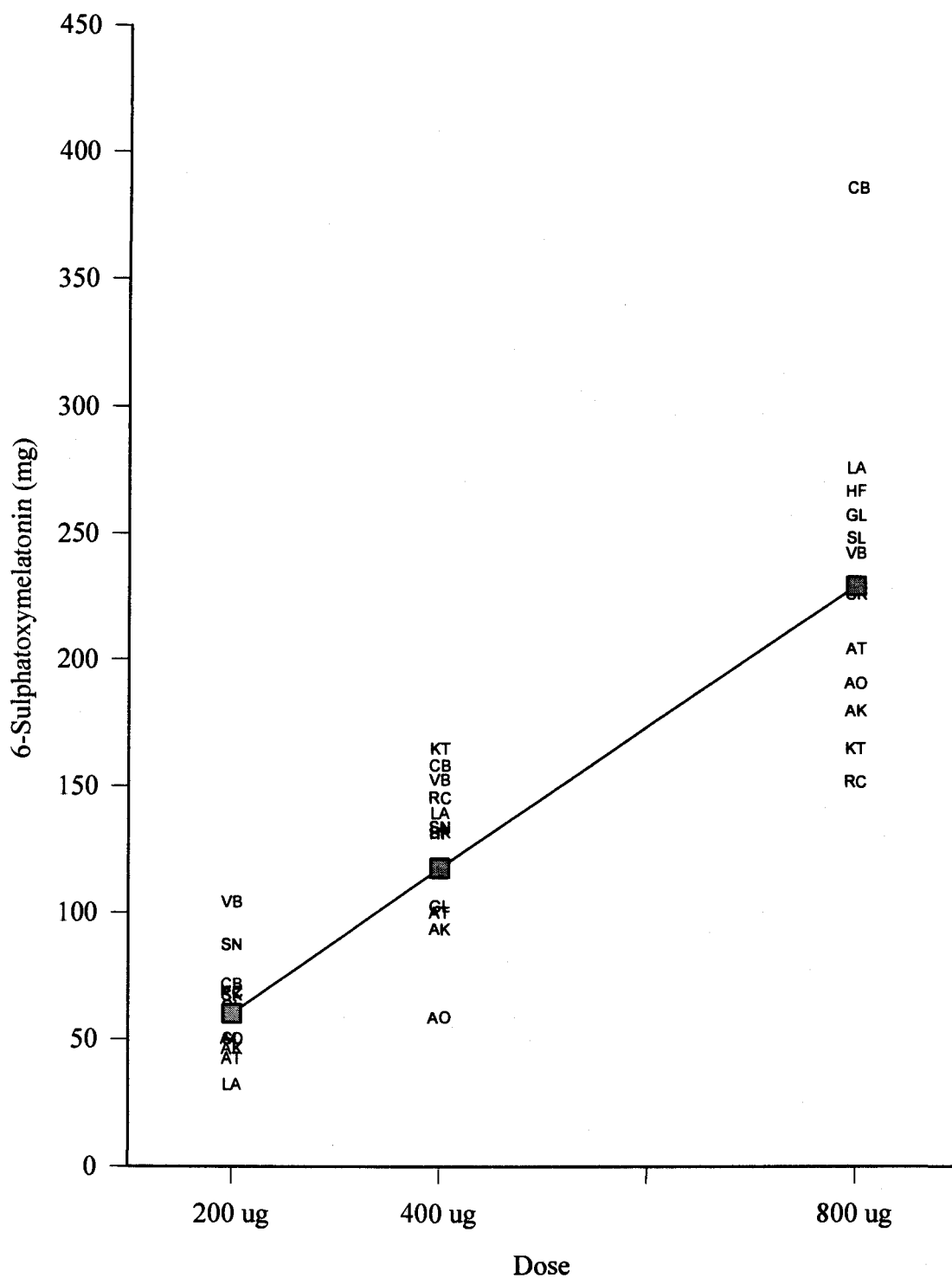
Figure 1.10: MT plasma 6STMT versus dose following single dose administration of 0.2, 0.4 , and 0.8 mg oral SR MT with fitted power function.

$$6STMT = 0.361276 \ Dose^{0.9656}$$

Table 1.9: Pharmacokinetic parameters of MT given at 0.2, 0.4, 0.8 mg SR formulation. Data are presented as mean (SE). (EM = Elderly males, EF = Elderly females, YM = young males, and YF = young females).

	Cmax [S] (pg/ml)	Tmax (h)	AUC$_T$ [S] (0-12h, pg h/ml)	6STMT [S] (μg)	MRT (0-12 h)
Elderly males					
Mean	129.4	1.1	673.2	60.0	4.4
SE	(52.6)	(0.3)	(293.9)	(12.0)	(0.3)
Elderly females					
Mean	159.6	1.7	855.8	49.2	4.4
SE	(46.7)	(1.3)	(254.5)	(10.3)	(0.5)
Young males					
Mean	70.4	1.4	299.9	68.8	4.1
SE	(31.7)	(0.6)	(150.4)	(19.3)	(0.3)
Young females					
Mean	181.5	1.5	944.9	70.5	4.6
SE	(153.2)	(1.0)	(717.4)	(18.6)	(0.3)
p-value from ANOVA of log-transformed data					
Dose	0.779	0.543	0.46	0.849	0.093[@]
Age_gender	0.018	0.847	0.001	0.028	0.097[@]

Duncan's multiple comparison test at a 0.05 level of significant

Age_gender	YM<EM=YF=EF		YM<EM=YF=EF	EF<YM=YF	

[S] Dose-dependent parameter was dose-normalized to that of 0.2 mg dose prior to statistical analysis including calculation of mean (SE), and ANOVA.
[@] ANOVA was performed on untransformed data.

model. MT plasma concentration data for each age-gender group and statistical comparisons following the three SR MT low doses are shown in Table 1.10. Plots of MT plasma profiles corresponding to each age-gender group were presented in Figure 1.11.

Approximate linear dose proportional increases were noted in mean AUC_T, Cmax, and total 6STMT which was supported by lack of statistically significant deviation from linearity in the dose normalized AUC_T, Cmax, or total 6STMT. Likewise, there was no significant differences in a dose independent pharmacokinetic parameters (MRT). Additionally, with the power model the exponent of dose for AUC_T [$1.235 \cdot DOSE^{1.156}$], Cmax [$0.405 \cdot DOSE^{1.070}$], and total 6STMT (0-12h) [$0.3613 \cdot DOSE^{0.966}$] were not significantly different from unity (p< 0.386, p<0.696, and p<0.668, respectively) and 95% confident interval of these exponents included 1; AUC_T (0.796, 1.516), Cmax (0.741, 1.399), and total 6STMT (0.788, 1.143). The geometric-mean proportionality ratios of 1.0 : 2.5 : 4.9 for AUC_T, 1.0 : 2.3 : 4.4 for Cmax, and 1.0 : 2.1 : 3.8 for STMT were not statistically different from the expected ratio of 1.0 : 2.0 : 4.0. Statistical comparison of dose-normalized plasma concentrations was also not significantly different following the three doses.

Differences in age-gender groups of pharmacokinetic parameters showed that young males had lower values of Cmax, AUC, and plasma concentrations. However, no firm conclusion can be made on difference in age-gender groups due to large intersubject variability and small sample size.

Table 1.10: Statistical comparison of MT plasma concentrations after dose-normalization to those of the lowest dose (0.2 mg) in healthy volunteers receiving a single dose of SR MT formulation at 0.2, 0.4, and 0.8 mg.

	0 h	0.5 h	1 h	1.5 h	2 h	2.5 h	3 h	3.5 h	4 h	4.5 h	5 h	5.5 h	6 h	7 h	8 h	9 h	10 h	11 h	12 h
Elderly males																			
Mean	9.4	57.8	68.1	66.7	65.4	55.6	48.6	51.3	41.1	42.0	40.5	40.2	29.9	24.6	21.1	18.0	15.9	15.9	13.8
SE	4.9	48.4	63.9	57.2	62.8	44.1	43.9	43.3	38.4	36.9	37.8	37.1	27.5	23.3	18.6	14.4	12.8	13.3	14.4
Elderly females																			
Mean	3.2	58.0	81.6	80.5	69.9	63.0	67.5	49.2	49.6	47.2	43.0	42.6	34.2	28.3	23.1	21.1	18.8	16.8	15.3
SE	1.4	47.9	48.4	40.8	30.7	24.5	30.7	21.3	25.8	25.7	26.1	28.0	22.1	19.2	13.9	12.4	9.9	8.5	8.6
Young males																			
Mean	4.3	20.5	36.8	29.2	26.5	26.0	21.6	17.0	17.0	15.5	18.8	14.9	12.0	8.7	6.8	5.5	5.1	3.6	4.8
SE	4.4	23.5	24.3	20.3	21.5	16.3	16.9	11.3	9.8	10.5	18.6	11.9	12.4	6.8	4.2	3.0	3.1	1.8	4.0
Young females																			
Mean	14.8	52.1	72.5	62.7	60.6	57.8	49.2	50.7	49.0	49.5	37.0	40.2	33.3	28.1	20.7	20.3	14.9	15.2	20.5
SE	18.3	61.0	82.2	60.7	51.3	52.1	43.8	47.9	49.4	52.8	26.0	38.2	32.6	28.8	20.6	24.3	14.3	14.0	23.1

p-value from ANOVA of log-transformed data

	0 h	0.5 h	1 h	1.5 h	2 h	2.5 h	3 h	3.5 h	4 h	4.5 h	5 h	5.5 h	6 h	7 h	8 h	9 h	10 h	11 h	12 h
Dose	0.817	0.548	0.977	0.602	0.493	0.278	0.65	0.39	0.375	0.326	0.301	0.591	0.555	0.64	0.184	0.239	0.217	0.325	0.445
*Age_ Gender	0.008	0.036	0.027	0.009	0.005	0.012	0.001	0.003	0.002	0.001	0.008	0.002	0.007	0.001	0.001	0.005	0.001	0.0001	0.001

* Duncan's multiple comparison test at a 0.05 level of significant show differences between age-gender groups as young males < elderly males = young females = elderly females for postdosing MT plasma concentrations.
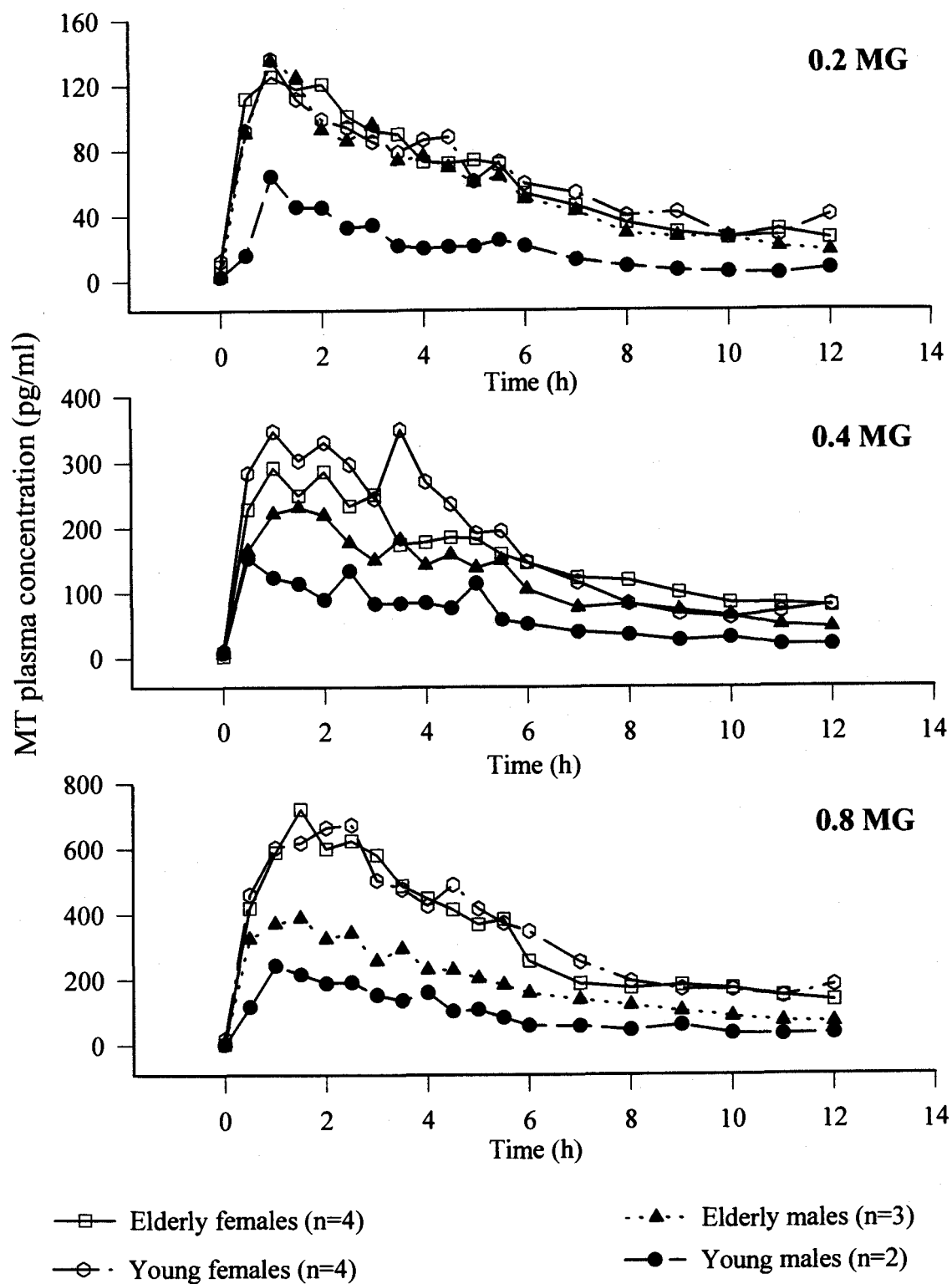
Figure 1.11: MT plasma concentration time profiles following oral administraion of

0.2, 0.4, and 0.8 mg of SR MT formulation in each subject age-group.

The large intersubject variability and small size sample size highly effect power of statistical hypothesis test. The power of the test is the probability that the test does reject the null hypothesis when it is false (47, 48). The power of the comparison of four age-gender groups is directly dependent on variability and number of observation in each groups as well as the desired degree of detectable differences among means. Though, herein ANOVA of age-gender group was performed on combined data from the three doses (based on linearity assumption confirmed earlier by the power model and ANOVA as described above) to increase the power of the analysis. Firm conclusion should not be made due to the small sample size of young males and large variability between subjects. The results suggests the need of additional study of larger sample size in each age-gender group to confirm their effects. Due to MT large therapeutic range and safety record, it is unlikely that differences in its pharmacokinetics would greatly impact on its clinical use. However, the information obtained from the study is valuable, specially for development of SR MT products.

CONCLUSION

The results showed that pharmacokinetics of MT given at the supra-physiologic dose of 50 mg IR MT were similar in the old and young subjects as well as in males and females. Following oral administration of SR MT formulation given at physiologic doses of 0.2, 0.4, and 0.8 mg, approximate linearity in pharmacokinetics of MT was found. However, MT plasma profiles in young males were statistically lower than those of elderly males, young females, and elderly females. Firm conclusion of age-gender effect cannot be made due to intersubject large variability and small sample size. Additionally, effect of age-gender seemed to fade away when given at the supra-physiologic dose of 50 mg. Cmax and AUC were varied up to 12 times following administration of SR MT formulations and 5-10 times following administration of IR MT, respectively.

REFERENCES

1. Dement, W.C., Miles, L.E., Carskadon, M.A. "White Paper" on sleep and aging, JAGS 30, 25-50 (1982).

2. Prinz, P.N., Vitiello, M.V., Raskind, M.A., Theropy, M.J. Geriatrics: Sleep disorders and aging, NEJM 323, 520-526 (1990).

3. Lerner, A.B., Case, J.D., Heinzelman, R.V. Structure of melatonin, J. Am. Chem. Soc. 81, 6084-6085 (1959).

4. Waldhauser, F., Dietzel, M. Daily and annual rhythms in human melatonin secretion: Role in puberty, Ann. New York Acad. Sci. 453, 205-214 (1985).

5. Dawson, D., Encel, N. Melatonin and sleep in humans, J. Pineal Res. 15, 1-12 (1993).

6. Dollins, A.B., Zhdanova, I.V., Wurtman, R.J., Lynch, H.J., Deng, M.H. Effect of inducing nocturnal serum melatonin concentrations in daytime on sleep, mood, body temperature, and performance, Proc. Natl. Acad. Sci. 91, 1824-1828 (1994).

7. Singer, C., Jackson, J., Moffit, M., Blood, M., McArthur, A., Sack, R., Parrott, K.A., Lewy, A. Physiologic melatonin administration and sleep-wake cycle in Alzheimer's disease: a pilot study, Sleep Research 23, 84 (1994).

8. Singer, C., McArthur, A., Hughes, R., Sack, R., Kaye, J., Lewy, A. High dose melatonin administration and sleep in the elderly, Sleep Research 24, 151 (1995).

9. Singer, C., McArthur, A., Hughes, R., Sack, R., Kaye, J., Lewy, A. Physiologic melatonin administration and sleep in the elderly, Sleep Research 24, 152 (1995).

10. Garfinkel, D., Laudon, M., Nof, D., Zisapel, N. Improvement of sleep quality in elderly people by controlled-release melatonin, Lancet 346, 541-544 (1995).

11. Haimov, I., Lavie, P., Laudon, M., Herer, P., Vigder, C., Zisapel, N. Melatonin replacement therapy of elderly insomniacs, Sleep 18, 598-603 (1995).

12. Dahlit, M., Alvarez, B., Vignau, J., English, J., Arendt, J., Parkes, J.D. Delayed sleep phase syndrome response to melatonin, Lancet 337, 1121-1124 (1991).

13. Petrie, K., Conaglen, J.V., Thompson, L., Chamberlain, K. Effects of melatonin on jet lag after long haul flight, Br. Med. J. 298, 705-707 (1989).

14. Waldhauser, F., Vierhapper, H., Oirich, K. Abnormal circadian melatonin secretion in night-shift workers, The New Eng. J. Med. 7, 441-446 (1986).

15. Rosenthal, N.E., Sack, D.A., Gillin, J.C., Lewy, A.J., Goodwin, F.W., Davenport, Y., Mueller, P.S. Seasonal effective disorder. A description of the syndrome and preliminary findings with light therapy, Arch. Gen. Psychiatry 41, 71-80 (1984).

16. Singer, C., Wild, K., Sack, R., Lewy, A. High dose melatonin is well tolerated by the elderly, Sleep Research 23, 86 (1994).

17. Macfarlane, J.G., Cleghorn, J.M., Brown, G.M., Streiner, D.L. The effects of melatonin on the total sleep time and daytime alertness of chronic insomniacs: A primary study. Biol. Psych. 30, 371-376 (1991).

18. James, S.P., Mendelson, W.B., Sack, D.A., Rosenthal, N.E., Wehr, T.A. The effect of melatonin on normal sleep. Neuropsychopharmacology, 1, 41-44, (1987).

19. James, S.P., Sack, D.A., Rosenthal, N.E., Mendelson, W.B. Melatonin administration in insomnia. Neuropsychopharmacology, 3,19-23, (1990).

20. Lewy, A.J., Newsome, D.A. Different types of melatonin circadian secretory rhythms in some blind subjects, J. Clin. Endocrinol. Metab. 56, 1103-1107 (1983).

21. Lee, B., Parrott, K. A., Ayres, J.W., Sack, R.L. Development and characterization of an oral controlled release delivery system for melatonin, Drug Dev. Ind. Pharm., 22(3), 269-274 (1996).

22. Lee, B., Parrott, K.A., Ayres, J.W., Sack, R.L. Design and evaluation of an oral controlled release delivery system for melatonin in human subjects, Int. J. Pharm. 124, 119-127 (1995).

23. Arendt, J. in: Melatonin and the mammalian pineal gland, 1995, Chapman & Hall, UK pp. 40, 42.

24.	Lane, E. A.; Moss, H. B. Pharmacokinetics of melatonin in man: first pass hepatic metabolism. J. Clin. Endocrinol. Metab. 61, 1214-1216 (1985).

25.	Kopin, I.J., Pare, C.M.B., Axelrod, J., Weissbach, H. The fate of melatonin in animals, J. Bio. Chem. 236, 3072-3075 (1961).

26.	Matthews, C.D., Kennaway, D.J., Fellenberg, A.J.G., Phillipou, G., Cox, L.W., Seamark, R.F. Melatonin in man, Adv. Biosci. 29, 371-81 (1981).

27.	Vakkuri, O., Leppaluoto, J., Kauppila A. Oral administration and distribution of melatonin in human serum, saliva and urine. Life Sci. 37, 489-495 (1985).

28.	Iguchi, H., Kato, K.I., Ibayashi., H. Melatonin serum levels and metabolic clearance rate in patients with liver cirrhosis., J. Clin. Endocrinol. Metab. 54, 1025-1027 (1982).

29.	Mallo, C., Zaidan, R., Galy, G., Brun, J., Chazot, G., Claustrat, B. Pharmacokinetics of melatonin after intravenous infusion and bolus injection. Eur. J. Clin. Pharmacol. 38, 297-301 (1990).

30.	Bojkowski, C.J. 6-sulphatoxymelatonin as an index of pineal function in human physiology. Thesis, University of Surrey, UK.

31.	Waldhauser, F., Waldhauser, M., Lieberman, H.R., Deng, M.H., Lynch, H.J., Wurtman, R.J. Bioavailability of oral melatonin in humans, Neuroendocrinology 39, 307-313 (1984).

32.	Gilad, E., Zisapel, N. High-affinity binding of melatonin to hemoglobin Biochemical & Molecular Medicine 56(2), 115-120 (1995).

33.	DiPiro JT, Talbert RL, Hayes PG, et al., eds. Pharmacotherapy, a pathophysiologic approach. 2th ed. Connecticut: Appleton & Lane Norwalk, 1993, p 37.

34.	Ouslander JG. Drug therapy in the elderly Ann. Intern. Med. 95, 711-722 (1981).

35.	Evans WE, Schentag JJ, Jusko WJ. Applied Pharmacokinetics, Applied Therapeutics, Inc. 1992.

36.	Swift CG, Homeida M., Halliwell M, et al. Antipyrine disposition and liver size in the elderly. Eur. J. Clin. Pharmacol. 12, 149-152 (1978).

37.   Vestal RE, Norris AH, Tobin JD, et al. Effect of age and cigarette smoking on propanolol disposition. Clin. Pharmmacol. Ther. 26, 8-15 (1979)

38.   Lewy, A.J., Markey, S.P. Analysis of melatonin in plasma by gas chromatography negative chemical ionization mass spectroscopy, Science 201, 741-743 (1978).

39.   Aldhous, M.E., Arendt, J. Radioimmunoassay for 6-sulphatoxymelatonin in urine using an iodinated trace, Ann. Clin. Biochem. 25, 298-303 (1988).

40.   Jusko, W.J. Guidelines for collection and analysis of pharmacokinetic data. In: Evans, Schentag, Jusko, eds. Applied Pharmacokinetics, 2nd ed. Spokane, Washington: Applied Therapeutics, 1986.

41.   Yeh, K.C., Kwan, K.C. A comparison of numerical integrating algorithms by trapezoidal, lagrange, and spline approximation. J. Pharm. Biopharm. 6(1), 79-98 (1978).

42.   RSTRIP II version 1.0 copyright 1992. Micromath Inc.

43.   P-PHARM, Population pharmacokinetic/pharmacodynamic data modeling program. Simed S.A., France.

44.   Gough, K., Hutchison, M., Keene, O., Byrom, B., Ellis, S., Lacey, L., McKellar, J. Assessment of dose proportionality: report from the statisticians in the pharmaceutical industry/pharmacokinetics UK joint working party. Drug Inform. J. 29, 1039-1048 (1995).

45.   Cochran WC, Cox GM. Experimental Designs, 2th ed. New York: John Wiley and Sons, 1957.

46.   STATGRAPHICS Plus version 2.1 (for Windows), Portion copyright 1996 Manugistics, Inc. Statistical Graphics Corporation.

47.   Sanford, B. in: Pharmaceutical statistics, practical and clinical appliaction, third edition, 1997, Marcel Dekker, Inc., New York pp. 203-210.

48.   Snedecor, G.W. and Cochran, W.G. Statistical methods, eight edition, 1991, Iowa State University Press, Ames, Iowa pp. 68-70.

CHAPTER 2

EVALUATION OF ORAL CONTROLLED RELEASE FORMULATIONS FOR
MELATONIN IN YOUNG HUMAN SUBJECTS USING TRACKING URINARY
6-SULPHATOXYMELATONIN DATA

ABSTRACT

Biostudy of three formulations of melatonin (MT) was carried out in 7 females

and 5 males aged between 21-25 years using tracking urinary 6-sulphatoxymelatonin

(6STMT), MT chief metabolite, data. A solution of MT (formulation A) and two MT

sustained release formulations (formulation B and C) were orally given to each subject

at 750 μg in three separate occasions with space of one week. Formulation A was

freshly prepared prior to the study. Formulation B and C were 10% Aquacoat® coated

beads, and 9% Eudragit® L 30D coated on 20% Aquacoat® coated beads, respectively.

Blood samples were additionally collected following administration of formulation A

to investigate effect of gender on MT pharmacokinetics using a noncompartmental

method. Effects of gender and weight on pharmacokinetic parameters were also

investigated using P-PHARM (a one compartment open model). There was no

statistically significant difference in MT pharmacokinetics between males and females.

There was much larger variation in Cmax and AUC of MT plasma profiles than those

of 6STMT urinary excretion rate-time profiles following administration of formulation

A. As a result, AUC of MT plasma profiles and AUC of 6STMT urinary excretion

rate-time profiles did not correlated well. MT was rapidly absorbed following

administration of formulation A with peak concentration within 1 hour. Delay in onset

of drug release for approximate 2 hours by enteric coating (9% Eudragit®L30D) occurred in 3 subjects. The use of Aquacoat® coating at 20% level provided better controlled delivery for MT than at 10% level.

INTRODUCTION

Melatonin (N-acetyl-5-methoxytryptamine, MT) is an indole neurohormone secreted primarily by the pineal gland in a circadian rhythm. It has a short plasma half-life, approximately 45 minutes (1). Endogenous MT concentration is low during the daytime, usually below 30 pg/ml (2). MT concentration increases in the evening about 9-10 p.m. and is maintained at about 25-120 pg/ml for approximately 6-8 hours (3). Exogenous MT acts as "chronobiotics" (4). Chronobiotics are substances which can therapeutically adjust the timing of circadian rhythm (5). The primarily therapeutic potential of MT is to improve conditions where rhythm abnormalities are associated with lack of well being and/or poor performance (3, 6). Other possible significance to human health of MT including antitumor effect (7), oncostatic effect (8), as well as effects on human reproductive function (9), cardiovascular function (10), and immune system were also reported (11). Though efficacy of MT given at physiological versus pharmacological concentration needs to be fully clarified (12), there are several studies suggesting the benefit of exogenous MT administered in physiological quantities to the circadian rhythm sleep disorders (13, 14) including jet lag (15), shift work syndrome (16), and seasonal affective diseases (17).

Due to MT short plasma half life, sustained release drug delivery system is needed to deliver exogenous MT to mimic the nighttime physiological secretion. Oral administration is the most convenient and economical method for systemic drug delivery (18). Development and pharmacokinetic evaluation of oral controlled-release formulations of MT in human subjects were previously described (19, 20). In this pilot study, MT controlled release formulation containing 20% immediate release (IR) MT and 80% sustained release (SR) MT produced a rapid onset of systemic MT and maintained MT plasma concentrations above physiological concentrations for more than 8 hours (20, 21). Additional pharmacokinetic studies of MT following oral administration would provide useful information to optimize oral drug delivery systems for MT.

Application of urinary 6STMT as an index for plasma MT was supported (22, 23, 24) and previously used (25, 26) by other investigators. Collection of urine samples over period of time is non-invasive and provides ability to perform long-term studies (26). Though, power in analysis of the parent drug pharmacokinetics could be limited, urinary metabolite profiles can roughly be used to compare and evaluate formulations given to the same subjects. In this study, *in vivo* performance of three formulations of MT, including a solution, and two MT SR formulations, orally given at physiological dose was investigated in young healthy volunteers using tracking urinary 6-sulphatoxymelatonin (6STMT), urinary chief metabolite of MT. Effect of gender on MT pharmacokinetics was also studied using MT plasma concentration data following administration of the solution.

MATERIALS AND METHODS

Materials

MT was purchased from Regis Chemical Co. (Morton Grove, IL). Core sugar spheres (USP/NF) were purchased from Paulaur Co. (Robbinsville, NJ, USA). Polyvinylpyrrolidone (PVP, average molecular weight 40, 000, Lot # 05907 CW) and hydroxypropylcellulose (HPC, average molecular weight 300,000, Lot # 80253BP) were from Aldrich Chemical Co. (Milwaukee, WI). Aquacoat® (aqueous polymeric ethylcellulose suspension, Type ECD-30, Lot # J7211) was purchased from FMC Corp. (Philadelphia, USA). Eudragit® L30D (aqueous methacrylic acid copolymer suspension, Type A, Lot # 12-936-1280) was purchased from Rhom Pharma GMBH, FRG. Sebatic acid dibutyl ester (DBS, dibutyl pthalate 99%, grade II, Lot # 40H0279) was from Sigma Chem. Co. (St. Louis, MO), and triethyl citrate (TEC, triethyl citrate 99%) was from Aldrich Chemical Co. (Milwaukee, WI, USA) as plasticizers, respectively. 95% ethanol (USP grade) was from Georgia-pacific Co. Chemicals used were reagent grade and were used without further purification.

Preparation of SR formulation for MT

SR formulation, developed previously (19), consisting of MT-loaded sugar beads coated with Aquacoat®. For completeness of the present work, dosage form preparation procedures of previous MT studies are described below.

Preparation of MT beads

      300 grams of nonpareil sugar beads (8-10 Mesh) were coated with 1.2 grams of

MT dissolved in 200 ml 95% ethanol USP. Polyvinylpyrrolidone (0.24 g) and

hydroxypropylcellulose (0.12 g) were added to the alcoholic solution as binders. Total

binders were 30% (w/w) based on MT content. The beads were prewarmed in a fluid-

bed coating chamber at 40 °C for 15 minutes. The MT ethanolic solution was then

applied to the beads with continuos fluidizing air supply. The solution was delivered

at 4 ml/min using a peristaltic pump. After application of ethanolic MT solution, drug

coated beads were allowed to dry for 30 min at 40 °C in order to remove residual

ethanol. Beads were removed from the bed coating chamber and assayed to evaluate

the total amount of drug loaded per total weight of beads. MT content was

approximately about 3.2 mg of MT per gram of beads. Summary of formulation for

application of MT to nonpareil sugar beads are shown below in Table 2.1.

Table 2.1:   Formulation for application of MT to nonpareil sugar beads.

MT	1.2 g
Nonpareil sugar beads (8-10 mesh)	300 g
Polyvinylpyrrolidone (PVP, MW 40,000) [a]	0.24 g
Hydroxypropylcellulose (HPC, MW 300,000) [a]	0.12 g
95% ethanol	200 ml

[a] Total binders, 30% (w/W) based on MT content.

Production of the SR beads

Polymer film coating technology was used to produce controlled release (sustained action) MT. The coating apparatus consisted of a spray coating chamber, with a 2×7 inch Wurster column (STREA-1, Aeromatic Inc., Columbia, MD) inside clear plexiglass column mounted on a fluid-bed dryer (lab-Line/P.R.L. Hi-Speed Fluid-Bed Dryer, Lab-Line Instruments, Inc., Melrose Park, IL). Drawing of cross section of STREA-1 SPRAY COATER fully assembled is shown in Figure 2.1. A peristaltic pump is used to deliver solutions to the spray nozzle. The entire equipment is located in a ventilating hood. Ethylcellulose (Aquacoat®) was used as coating materials. Two plasticizers; DBS, and TEC, were used at 30% (15% each) based on the solid content of Aquacoat®. Loading of polymers was calculated as weight percent of polymer solids per unit weight of MT beads. The coating solution was prepared as listed in Table 2.2. Amount of application was 62.7 g, and 125.4 g per 90 g of MT beads to produce a 10%, and 20% theoretical coating based on solids content of Aquacoat®. The coated beads were dried in the chambers for 30 minutes and then further air dried in a hood. All processes were undertaken at 40 °C. The coated beads contained about 2-3 mg of MT per gram of coated beads (approximate 2 mg/g of 20% coated beads, and 3 mg/g of 10% coated beads).
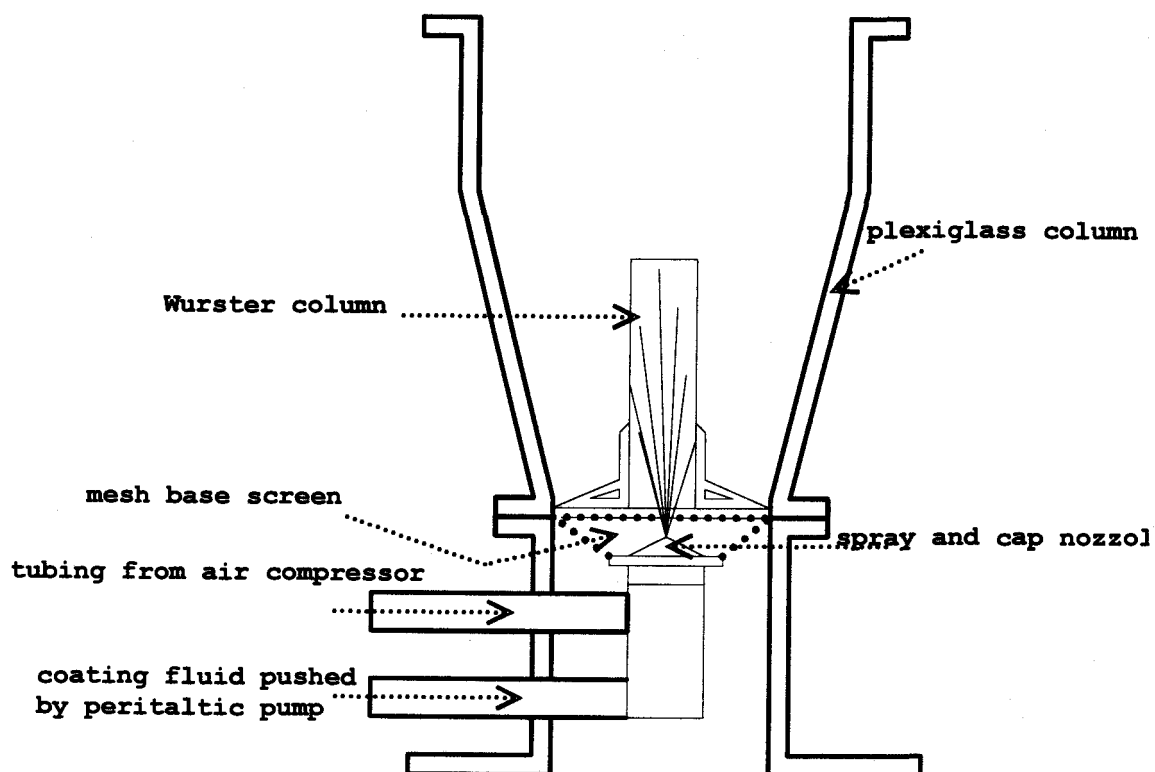
Figure 2.1: Cross section of STREA-1 SPRAY COATER fully assembled.

Table 2.2: Coating formulation for application of ethyl cellulose to MT beads.

Ethylcellulose suspension (Aquacoat®, 30% (w/w) of solids)	100 g
Dibutyl sebacate (DBS) [a]	4.5 g
Triethyl citrate (TEC) [a]	4.5 g
Water	100 g

[a] Total amount of plasticizers added was 30% based on solids content of Aquacoat® suspension.

Note   Coating formulation approximately contained 14.35% (w/w) polymer solids as described below.

Total weight of SR coating solution   209 g.

Total weight of polymer solids   30 g.

% Content of polymer solids per coating solution $= (30 \times 100) / 209 = 14.35\%$.

Production of enteric coating SR beads

20 % Aquacoat® coated MT beads was further coated with Eudragit® L30D to provide enteric coating action. Loading of enteric polymers was calculated as weight of polymer solids per unit weight of SR MT beads. DBS, 15% of total solids, and TEC, 15% of total solids, were used as plasticizers. The coating solution was prepared as listed below in Table 2.3.

Table 2.3: Formulation for application of Eudragit® L30D (enteric coat) to SR MT beads.

Eudragit®L30D, 30% (w/w) of solids (Methacrylic acid copolymer suspension)	100 g
Dibutyl sebacate (DBS) [a]	4.5 g
Triethyl citrate (TEC) [a]	4.5 g
Water	100 g

[a] Total amount of plasticizers added was 30% based on solids content of Eudragit®L30D suspension.

Note   Coating formulation approximately contained 14.35% (w/w) polymer solids as shown below.

Total weight of enteric coating solution   209 g.

Total weight of polymer solids   30 g.

% Content of polymer solids per coating solution = (30 × 100) / 209 = 14.35%.

Amount of application was weighted per 70 g of SR MT beads to produce a range of 3%, 6%, 9%, 12%, and 15% theoretical enteric coat based on solids content of Eudragit® L30D. The enteric coated beads were dried in the chambers for 30 minutes and then further air dried in a hood. All processes were undertaken at 40 °C. The coated beads contained about 2 mg of MT per gram of coated beads. Five different levels of enteric coating SR beads were prepared to investigate effect of different amount of enteric coating on dissolution profiles of 20% Aquacoat® MT loaded beads. 20% Aquacoat® coated beads in combination with immediate release MT were

previously evaluated in the pilot study in human subjects (20). Structure of SR

formulations used in the study are shown in Figure 2.2

In vitro dissolution

In vitro release rate of MT was determined using the USP dissolution apparatus

I (Basket method) at 37 ± 0.5 °C. The stirring rate was 50 rpm. SR MT beads and

enteric coating SR MT beads were weighed to contain about 500 µg of MT before they

were placed in 900 ml of simulated gastric fluid (enzyme free, pH 1.4) for the first 2

hours of dissolution. At 2 hours gastric fluid was decanted. For hours 2 to 24 hours

beads were exposed to simulated intestinal fluid (enzyme free, pH 7.4), equilibrated to

37 °C. 1 ml samples of dissolution media were collected, with replacement, over a

period of 24 hours and analyzed using an HPLC system with UV detection. The HPLC

was equipped with an M-45 pump, WISP® 710B injector, reversed-phase C18 (4µ)

radial compression column and Model 441 detector with a 229-nm light source (all

from Waters® Associates). Retention time and sensitivity for MT (mobile phase:

methanol/water, 50:50) were 4 minutes and 10 ng/ml, respectively, at a flow rate of 1.2

ml/minute. Methylparaben was used as the internal standard. Its retention time was

6.5 minute.
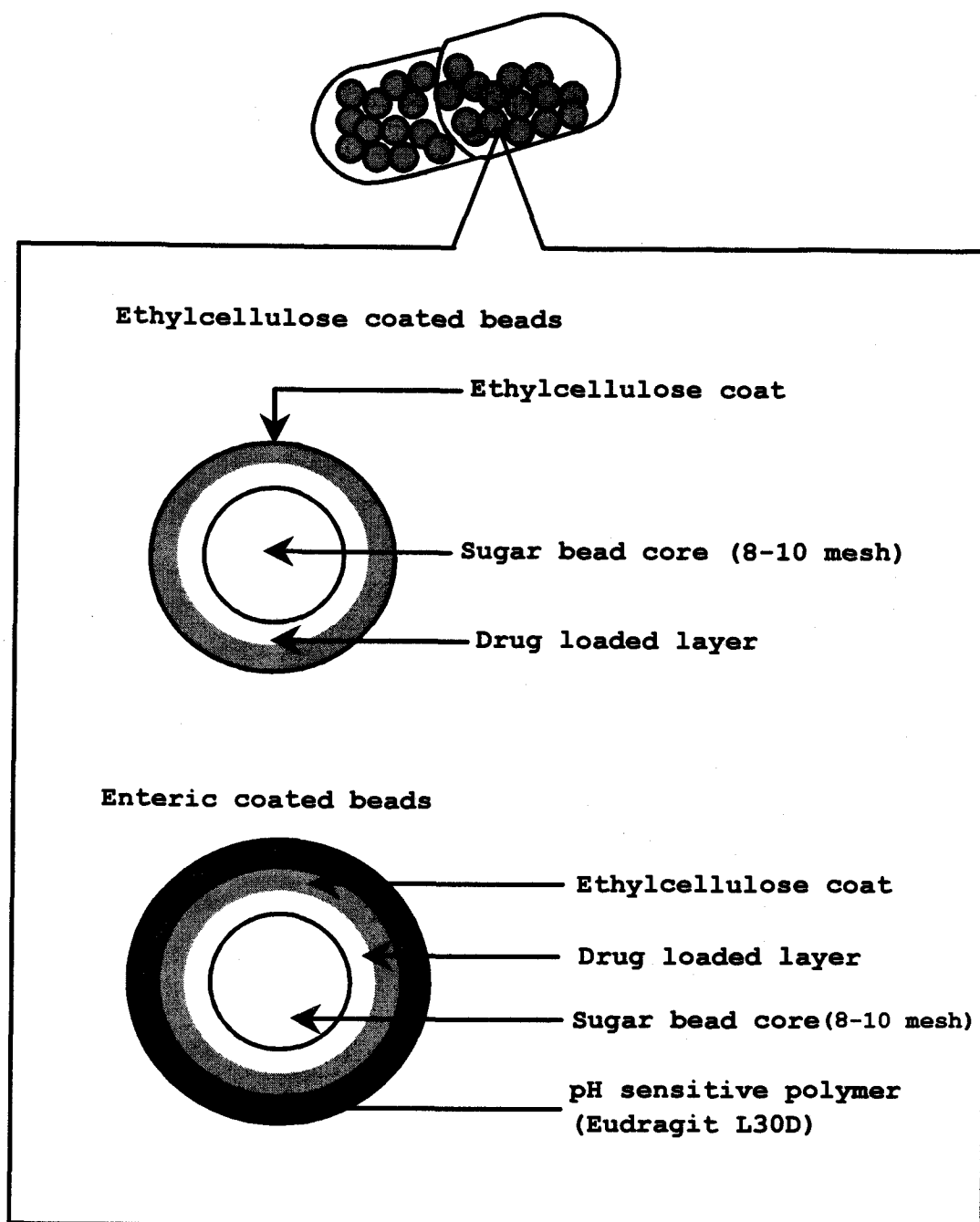
Figure 2.2: Structure of sustained release (SR) drug delivery systems (formulation B, and C) for MT used in the study.

Experimental section

Dosage Forms

Three different oral formulations of MT at 750 μg dose; formulation A, B, and C, were used in the study. Formulation A was a 750 ml solution of MT which was freshly prepared before the study by adding 1 ml of MT stock solution (MT dissolved in 95% ethanol, 0.75 mg/ml) to 749 ml of water. Formulation B, and C were 10% Aquacoat® coated beads, and 9% Eudragit® L30D coated on 20% Aquacoat® coated beads, respectively (Figure 2.2). The beads filled in gelatin capsules (No. 1) were administered with 750 ml of water.

Subjects

Twelve healthy nonsmoking volunteers, 7 females and 5 males under age 25 were recruited from Oregon State University in February, 1995. The mean age and was 22.3 ± 1.2 years. The mean weight of females and males was 56.0 ± 13.7 kg, and 65.8 ± 4.5 kg, respectively. Subjects taking medications on a regular basis, using tobacco or alcohol within two weeks of the study were excluded. Protocol and informed consents for the pharmacokinetic study were approved by the Investigational Review Board, Oregon State University (OSU), Corvallis, OR. An investigational new drug (IND) application was filed with FDA and was approved.

Study design

      In an open-label, three-period crossover, single dose design, they received all three MT formulations in the same sequence, at dose of 750 µg with treatments spaced one week apart. MT was administered at 8 am after a ten hour overnight fast. Subjects continued fasting for 2 hours after dosing. Water and juices were given orally ad lib during fasting. After administration of formulation A, both blood and urine samples were collected for measurement of MT and 6STMT, respectively. Only urine samples were collected for measurement of 6STMT following administration of formulation B, and C. In the study of formulation A, blood samples were taken by direct venipuncture at 10 min prior to dosing to provide baseline values and at 0.25, 0.5, 1, 1.5, 3, 5, 8, and 10 h post dosing. Urine samples were collected at approximately 15 min prior to dosing and every 1 hour for the first 6 h after dosing, and at subject convenient occasions for a 24 h study period. Total urine volume was measured and an aliquot was saved for subsequent measurement of 6STMT concentration. Twenty four hour baseline data for endogenous 6STMT in each subject was obtained from urine samples collected the day before the study of formulation A, was conducted (no MT administration). Plasma MT concentrations were determined by high-sensitivity GC/MS (27). Urinary 6STMT concentrations were determined by radioimmunoassay (28). Summary of study design and the formulations are shown in Table 2.4.

Table 2.4: Summary of study design and oral formulations of melatonin used in the study.

Formulations	Dose (µg)	Drug release rate	First polymer coat	Second polymer coat	Biological collected samples
A	750	IR	-	-	Blood Urine
B	750	SR	10% Aquacoat®	-	Urine
C	750	SR	20% Aquacoat®	9% Eudragit®	Urine

Pharmacokinetic and statistical analysis

Following administration of formulation A, individual endogenous MT plasma concentrations received at 10 minutes prior to dosing was used as baseline MT plasma concentration. Both of the plasma concentrations with and without baseline adjustment were analyzed using the noncompartmental (SHAM) method (29). Thus, peak plasma concentration (Cmax) and time to Cmax (Tmax) were taken directly from the observed data. The area under the plasma concentration versus time curve (AUC_T) truncated at the last measurable plasma concentration at time T (C_T) was calculated using linear trapezoidal rule for incremental trapezoids and log-trapezoidal rule for decremental trapezoids (30). The terminal-phase elimination rate constant (λz) was estimated by a log-linear regression of the last three to five observed plasma concentrations, and the terminal-phase disposition half life ($t_{1/2}$) was calculated as $t_{1/2} =$

ln2/λz. Total AUC was then estimated by AUC = $AUC_T + C_T/\lambda z$. The oral dose mean residence time (MRT_{oral}) was estimated using the statistical moment approach. MRT_{oral} is estimated by MRT_{oral} = AUMC/AUC, where AUMC is the area under the first moment curve. AUMC is calculated as AUMC = $\int t \cdot Cdt$ = $AUMC_T + (T \cdot C_T/\lambda z)$ + $(C_T/\lambda z^2)$.

Either a mono- or bi-exponential pharmacokinetic equation with a first-order input (see below) was applied to best fit individual MT plasma data using RSTRIP® (31). Data is fitted to models, mono-, and biexponential based on model selection criteria (Akaike Information Criteria) and graphical fitting.

$$C = A_2 e^{-\lambda 1t} - A_2 e^{-kat}$$

$$C = A_1 e^{-\lambda 1t} + A_2 e^{-\lambda 2t} - (A_1+A_2) e^{-kat}$$

Relationship between pharmacokinetic parameters and covariates (gender and weight) was investigated using graphical and statistical analysis options provided in P-PHARM (32). The plasma data was fitted to one compartment open model. A lag time was also included in the model to satisfactorily fit data. Average population pharmacokinetic parameters together with intersubject variance are estimated. P-PHARM fits the data of all the subjects simultaneously and estimates the parameters and their variances.

Following administration of formulation A, comparison between young males and young females with respect to the mean pharmacokinetic parameters were made by using analysis of variance; ANOVA (33). Pairwise comparisons among gender groups were made using Tukey's multiple range test at a significant level of $\alpha = 0.05$.

Following administration of formulation A, B, and C, cumulative amount of 6STMT in urine, with baseline correction, were statistically compared using ANOVA and Tukey's multiple range test.

In vivo performance of the three formulations based on 6STMT urinary excretion rate-time profiles was evaluated only within the same subject to minimize other confound effects since complete mechanistic modeling of MT and its metabolites, which could be extremely varied from one subject to another, has not yet been determined.

STATGRAPHIC (version 7) was used for statistical analysis (34).

RESULTS AND DISCUSSION

In Vitro dissolution

Dissolution profiles of MT from formulation B, and C over period of 24 hours are shown in Figure 2.3. MT was completely released from formulation B within 9 hours based on dissolution test. For formulation C, in addition to 20% ethylcellulose (Aquacoat®) coating, enteric coat (Eudragit®L30D) at theoretical 9% was applied to delay the onset of drug release from the SR formulation by insolubility of enteric polymers in low pH media (i.e. gastric fluid). MT was not detected during 2 hours testing in pH 1.4 acid media. When the beads were placed in medium pH media (simulated intestinal fluid, pH 7.4), enteric coat dissolved and drug was slowly released from formulation C during 2-24 hour period. After 24 hours in simulated intestinal fluid, about 87% of MT was released. The release of MT from formulation
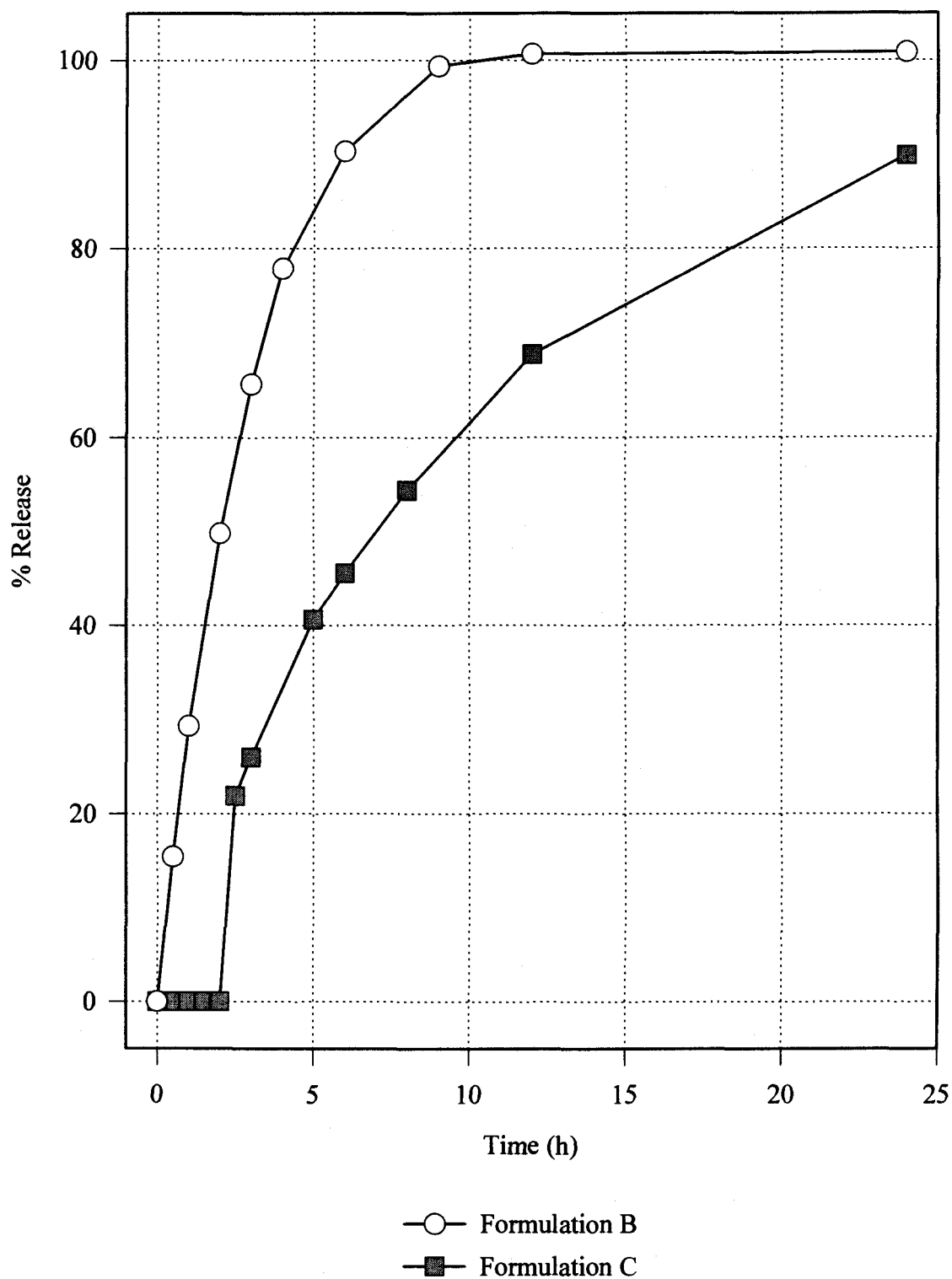
Figure 2.3: Mean dissolution profiles of MT from sustained release
formulation B, and C (n=3).

B was much faster than that of formulation C i.e. $T_{50\%}$ of formulation B was 2 hours and $T_{50\%}$ of formulation C was 7 hours.

In Figure 2.4, dissolution profiles of MT from enteric coating SR formulations with different amount of enteric polymers were compared. It required at least 9% (w/w) of Eudragit®L30D to perform enteric coating action for 20% Aquacoat® coated beads (8-10 mesh). Different amount of enteric coating ranging from 9% to 15% showed no significant effect (p-value > 0.05 at 95% confidence level) on release of MT after the beads were placed in medium pH media. Comparison of dissolution profiles of 3%, 6%, 9%, 12% and 15% of Eudragit® L30D coating, also showed that percent drug release of MT in simulated intestinal fluid among these beads was not significantly different.

Comparison of dissolution profiles of MT from formulation C and 20% Aquacoat® coated beads was also shown in Figure 2.5. Time-adjusted dissolution profiles of 20% Aquacoat® coated beads was generated by adding 2 hours to every time point of original dissolution profiles of 20% Aquacoat® coated beads in order to roughly compare effect of enteric coat at 9% level on the release profile of 20% Aquacoat® coated beads. Addition of the enteric coat on 20% Aquacoat® coated beads slightly accelerated drug release rate in the first ten hours based on rough comparison described in Figure 2.5. The change may be due to slightly thinning in Aquacoat® film and small migration of MT to the outer layer during the introduction of enteric polymer coating. Formation of enteric layer film on the 20% Aquacoat® layer required contact
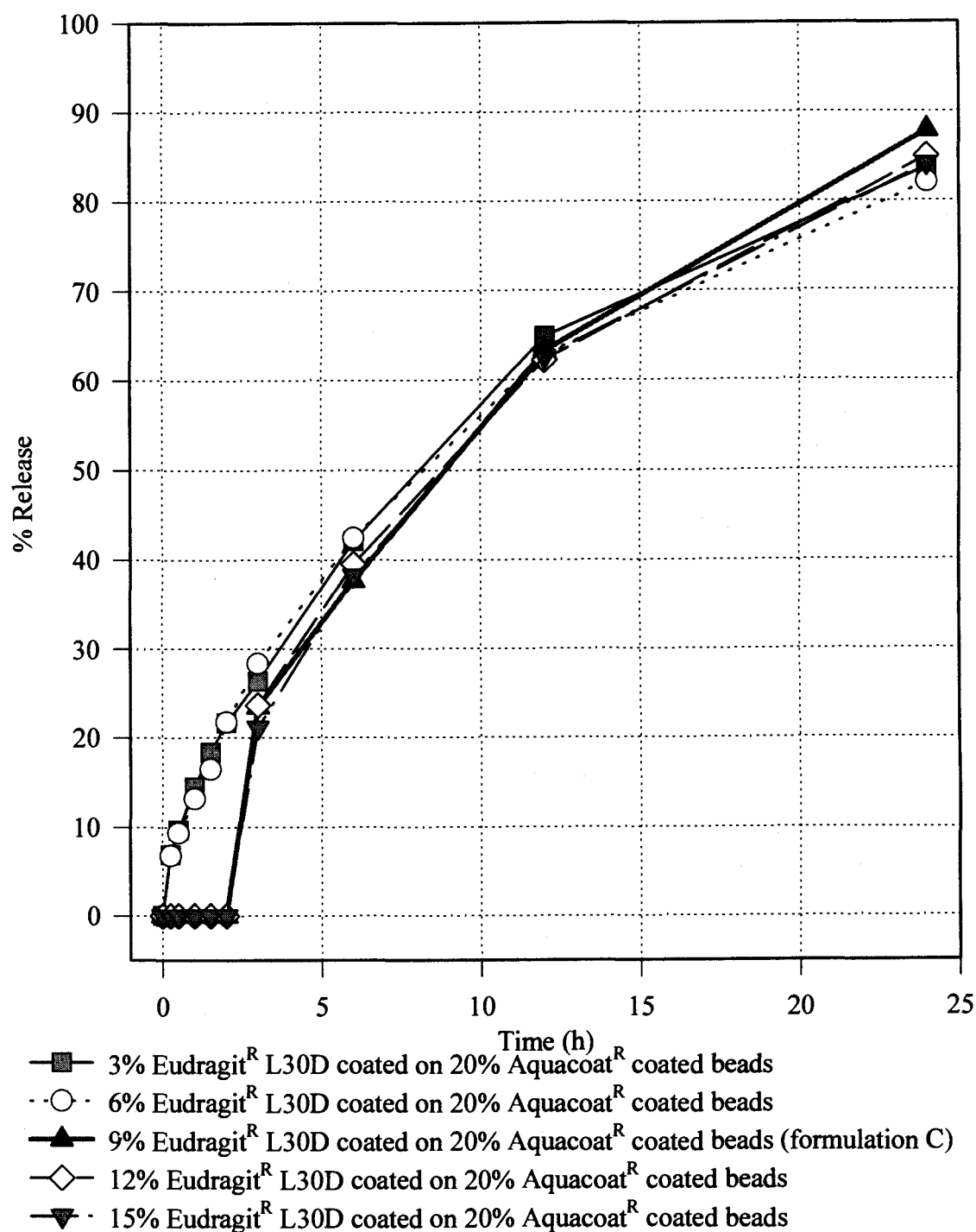
Figure 2.4: Comparison of dissolution profiles of MT from sustained release beads (20% Aquacoat[R]) with enteric coat (Eudragit[R]L30D) in different amount. Standard error of each data piont is too small to shown.
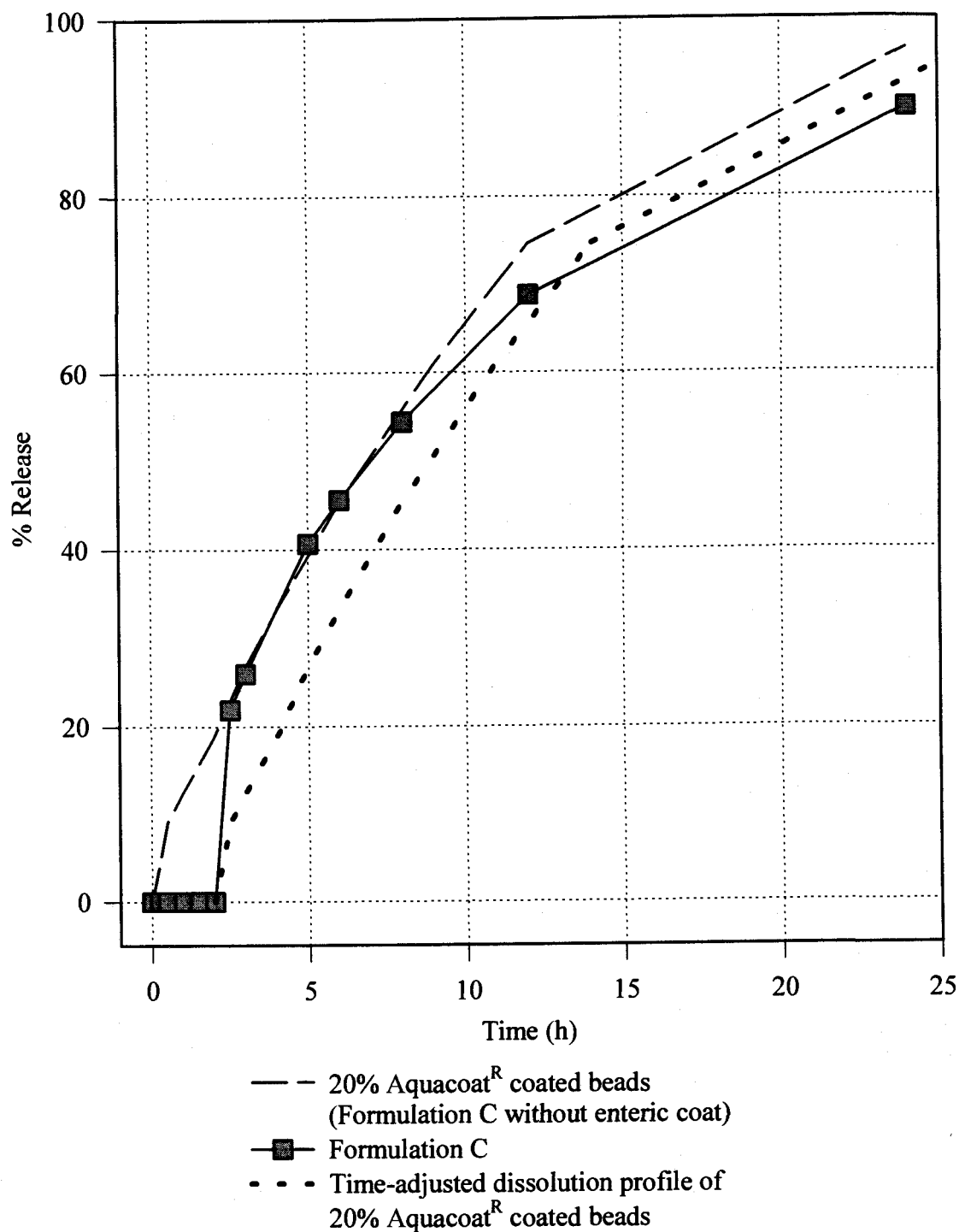
Figure 2.5: Comparison of dissolution profiles of MT from sustained release formulation C (9% Eudragit[R] L30D coated on 20% Aquacoat[R] coated beads) and 20% Aquacoat[R] coated beads.

between coating droplets and the Aquacoat® layer. With the presence of water serving as a carrier for dispersed particles in the enteric coating suspension, as well as plasticizers softening and enhancing flexibility of coating polymers, small amount of MT dissolved in the Aquacoat® layer may diffuse into the outer layer when coating particles coalesced to form a continuous film. The original thickness of the Aquacoat® coat may also slightly decrease during the formation of the enteric coating film.

Pharmacokinetic study

Demographic data of twelve subjects included in the study is presented in Table 2.5. Summary of pharmacokinetic parameters of MT, following administration of formulation A, estimated using noncompartmental method, RSTRIP®, and P-PHARM, are reported in Table 2.6 and 2.7, respectively. Simulation of MT plasma concentrations based on pharmacokinetic parameters fitted by P-PHARM is shown in Figure 2.6. MT plasma concentration-time curves together with 6STMT urinary excretion rate-time profiles following administration of formulation A are presented as mean values (Figure 2.7) and individual profiles (Figure 2.8 to 2.13). For subject MS (Figure 2.13), collection of blood samples was not possible due to difficulty in blood drawing. A plot of AUC of MT plasma concentration-time profile vs. total urinary 6STMT recovery and a plot of AUC of MT plasma concentration-time profile vs. AUC of 6STMT urinary excretion rate-time profile following administration of formulation A, are presented in Figure 2.14 and 2.15, respectively.

Table 2.5: Demographic data of twelve healthy volunteers involved in the study.

Subjects	Gender	Weight (kg)	Height	Age	Race
JD	female	55	168	23	WHITE
AC	female	86	160	22	WHITE
MS	female	48.6	162	22	WHITE
RJ	female	54.5	160	21	WHITE
NP	female	45	150	24	ORIENTAL
YC	female	50	165	24	ORIENTAL
NY	female	53	155	24	ORIENTAL
SC	male	65	180	21	WHITE
CW	male	62	169	22	WHITE
JS	male	73	190	23	WHITE
GW	male	62	174	21	ORIENTAL
SP	male	67	184	21	WHITE
Mean ± SE		60.1 ± 11.6	168.1 ± 12.0	22.3 ± 1.2	

Table 2.6: Pharmacokinetic parameters of MT following oral administration of MT solution in 11 subjects. Parameters are estimated using noncompartmental method.

Subjects	Cmax (pg/ml)	Tmax (h)	AUC_T (pg h/ml)	AUC (pg h/ml)	AUMC (pg h^2/ml)	λz (h^{-1})	$t_{1/2}$ (h)	MRT (h)	CL/F (L/h)	Vd/F (L)
JD	922.5	0.25	1281	1285	1649	0.61	1.1	1.3	583.6	962.1
AC	2276.2	0.67	2914	2916	3540	0.61	1.1	1.2	257.2	424.3
RJ	1595.0	0.52	2915	2917	3559	0.34	2.0	1.2	257.1	752.3
NP	1532.0	1.00	2881	2893	4917	0.63	1.1	1.7	259.2	409.8
YC	6980.0	0.42	5199	5207	5524	0.62	1.1	1.1	144.0	231.7
NY	1173.0	0.50	1426	1440	1937	0.27	2.6	1.3	520.9	1919.3
SC	1743.0	0.52	1082	1084	1306	0.69	1.0	1.2	692.1	1003.1
CW	1706.0	0.50	1962	1963	2042	0.73	1.0	1.0	382.1	524.2
JS	50.8	0.23	2460	2467	3507	0.56	1.2	1.4	304.0	544.0
GW	856.4	0.32	79	80	141	0.89	0.8	1.8	9338.1	10476.9
SP	765.8	1.02	1269	1274	1762	0.59	1.2	1.4	588.9	999.6
Mean	1781.9	0.54	2133	2139	2717	0.59	1.3	1.3	1211.6	1658.8
(SE)	(1826.6)	(0.27)	(1364)	(1366)	(1627)	(0.17)	(0.5)	(0.2)	(2700.9)	(2960.6)
%CV	102.5	49.12	64	64	60	28.52	40.4	17.2	222.9	178.5
Geometric mean	1138.4	0.49	1548	1554	2039	0.57	1.2	1.3	482.7	850.1

Young males

	Cmax	Tmax	AUC_T	AUC	AUMC	λz	$t_{1/2}$	MRT	CL/F	Vd/F
Mean	1024.4	0.52	1370	1374	1752	0.69	1.0	1.4	2261.0	2709.6
(SE)	(711.3)	(0.31)	(908)	(910)	(1220)	(0.13)	(0.2)	0.3	3959.3	4348.4

Young females

	Cmax	Tmax	AUC_T	AUC	AUMC	λz	$t_{1/2}$	MRT	CL/F	Vd/F
Mean	2413.1	0.56	2769	2776	3521	0.51	1.5	1.3	337.0	783.3
(SE)	(2283.9)	(0.26)	(1413)	(1412)	(1548)	(0.16)	(0.6)	0.2	173.6	615.8

p-value from ANOVA of log transformed data: source of variation = gender

	Cmax	Tmax	AUC_T	AUC	AUMC	λz	$t_{1/2}$	MRT	CL/F	Vd/F
	0.140	0.706	0.122	0.121	0.101	0.102	0.131	0.752	0.121	0.274

Table 2.7: Pharmacokinetic parameters of MT following oral administration of MT solution in 11 subjects. Parameters are estimated using either a monoexponential equation (RSTRIP®) or one compartment open model (P-PHARM).

Subjects	Calculation using RSTRIP®					Calculation using P-PHARM				
	ka (h^{-1})	λ_1 (h^{-1})	CL/F (L/h)	V/F (L)	AUC (pg h/ml)	ka (h^{-1})	k (h^{-1})	CL/F (L/h)	V/F (L)	AUC (pg h/ml)
JD	6.39	1.01	555.1	549.6	1351	3.47	1.10	504.7	460.3	1486
AC	4.13	1.83	267.0	145.9	2809	3.74	1.10	236.2	213.9	3175
RJ	100	1.89	360.9	191.0	2078	3.82	1.11	441.6	398.0	1698
NP	1.36	1.36	244.1	179.5	3072	2.25	1.08	265.7	246.1	2823
YC	100	1.88	107.8	57.4	6956	4.26	1.11	115.2	103.6	6512
NY	5.41	1.32	535.3	405.6	1401	3.6	1.10	456.7	417.0	1642
SC	1.77	1.77	315.8	178.4	2375	3.47	1.10	588.0	534.9	1276
CW	1.62	1.62	301.0	185.8	2492	3.25	1.10	323.7	294.0	2317
JS	7.43	0.92	9740.3	10587.2	77	2.82	1.09	300.6	276.5	2495
GW	4.26	1.3	675.7	519.8	1110	3.23	1.09	9051.4	8274.6	83
SP	1.61	1.6	559.3	349.6	1341	2.97	1.09	553.9	508.4	1354
Mean	21.27	1.50	1242.0	1213.6	2278	3.35	1.10	1167.1	1066.1	2260
(SE)	(38.98)	(0.34)	(2823.7)	(3113.0)	(1778)	(0.52)	(0.01)	(2497.1)	(2283.1)	(1570)
%CV	183.25	22.82	227.3	256.5	78	15.47	0.84	214.0	214.2	69
Geometric mean	5.87	1.46	472.8	323.6	1586	3.31	1.1	463.3	422.3	1619
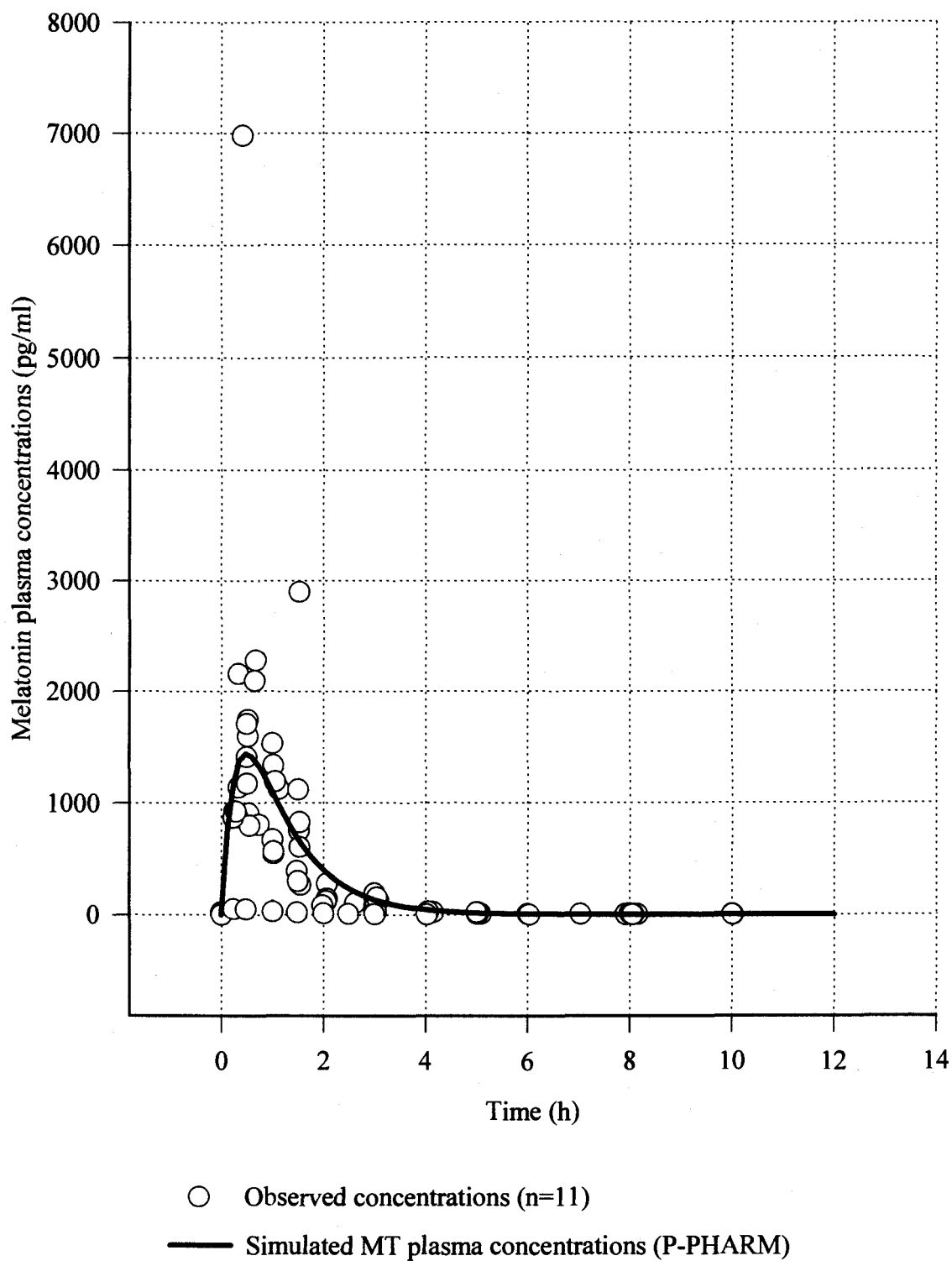
Figure 2.6: Simulation of MT plasma profiles based on population pharmacokinetic parameters estimated using P-PHARM.
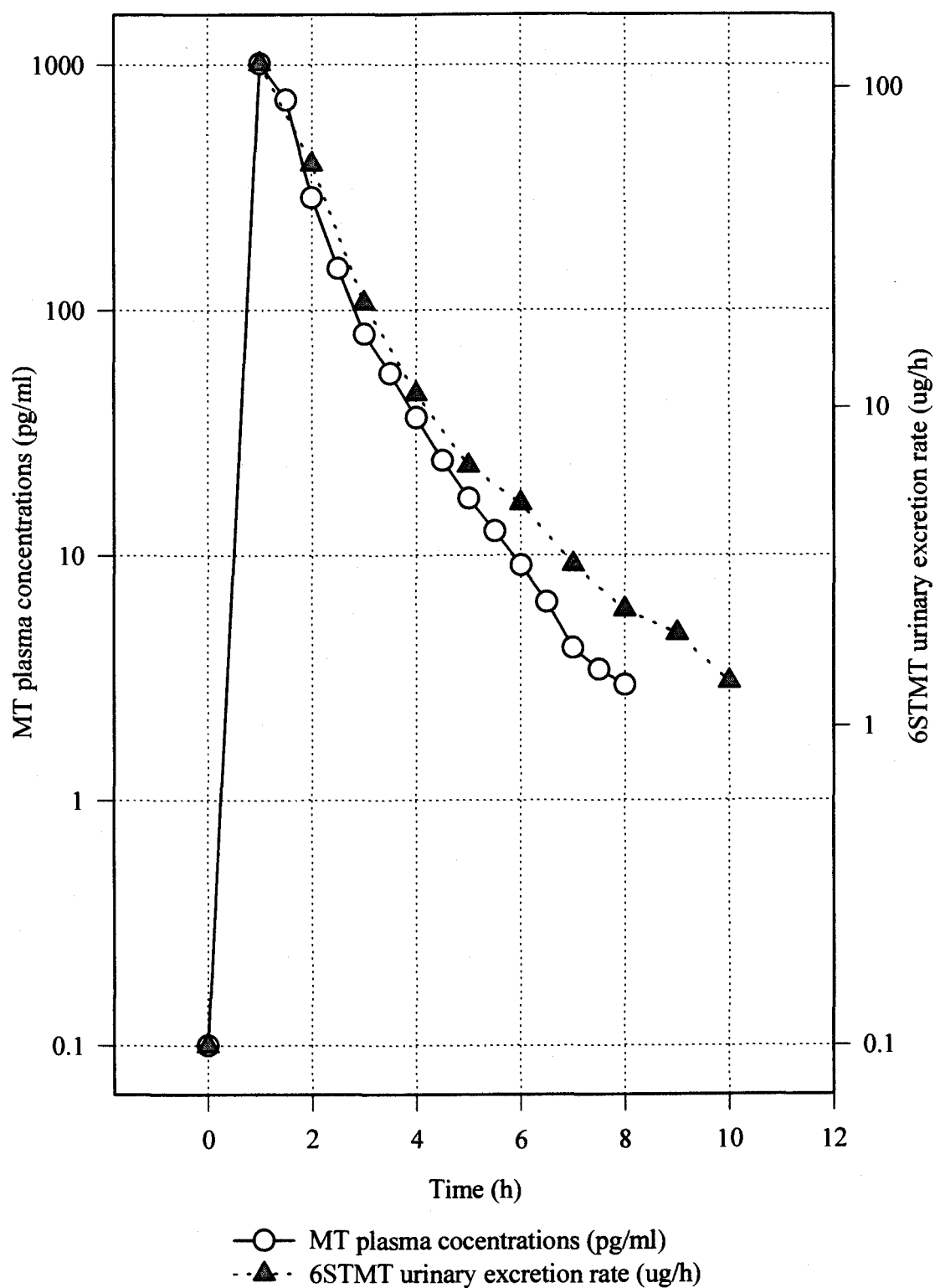
Figure 2.7: Mean MT plasma concentration and 6STMT urinary excretion rate following oral administration of formulation A (n=11).
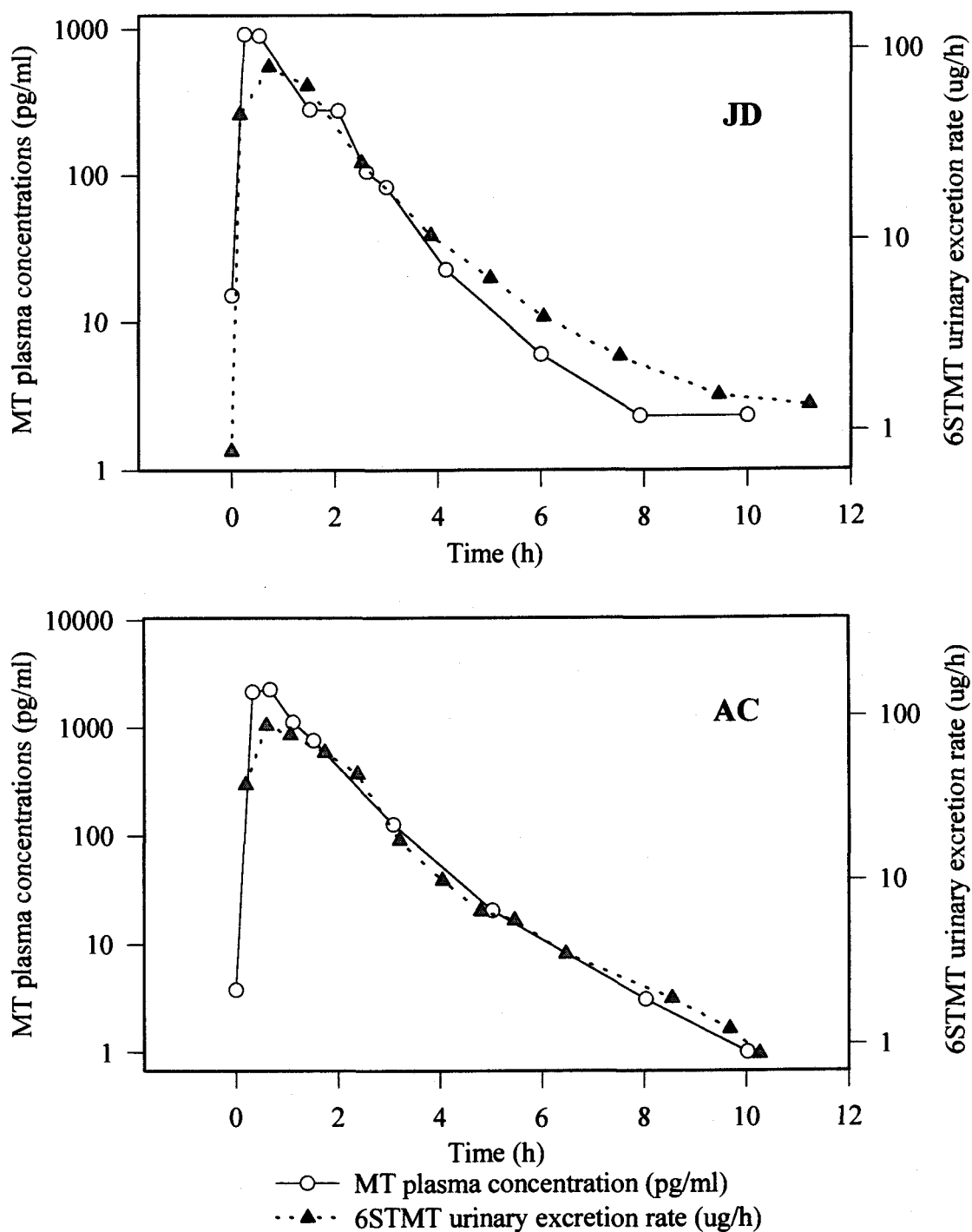
Figure 2.8: Profiles of MT plasma concentrations and 6STMT urinary excretion rate following oral administration of solution of MT in subject JD and AC.
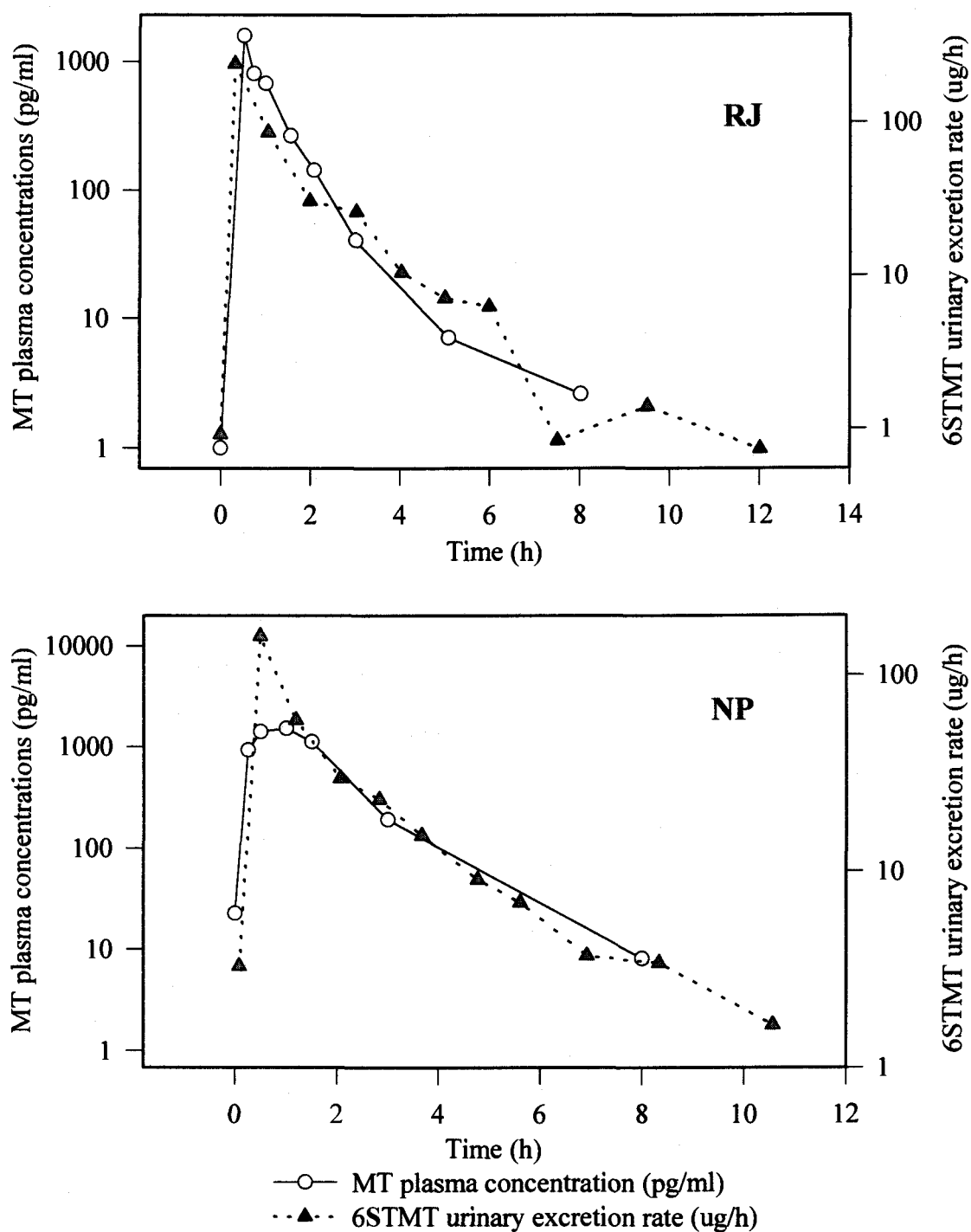
Figure 2.9: Profiles of MT plasma concentrations and 6STMT urinary excretion rate following oral administration of solution of MT in subject RJ and NP.
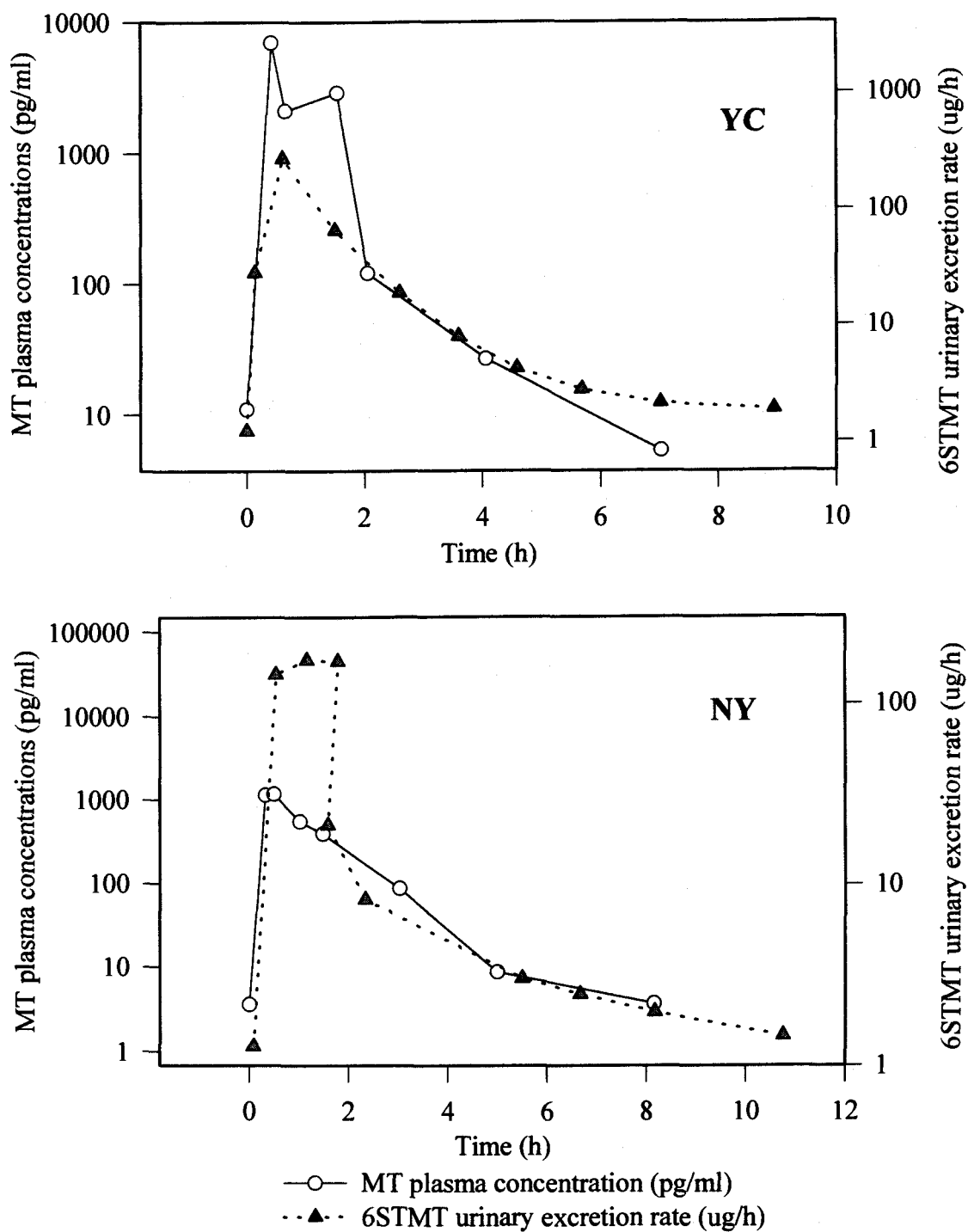
Figure 2.10: Profiles of MT plasma concentrations and 6STMT urinary excretion rate following oral administration of solution of MT in subject YC and NY.
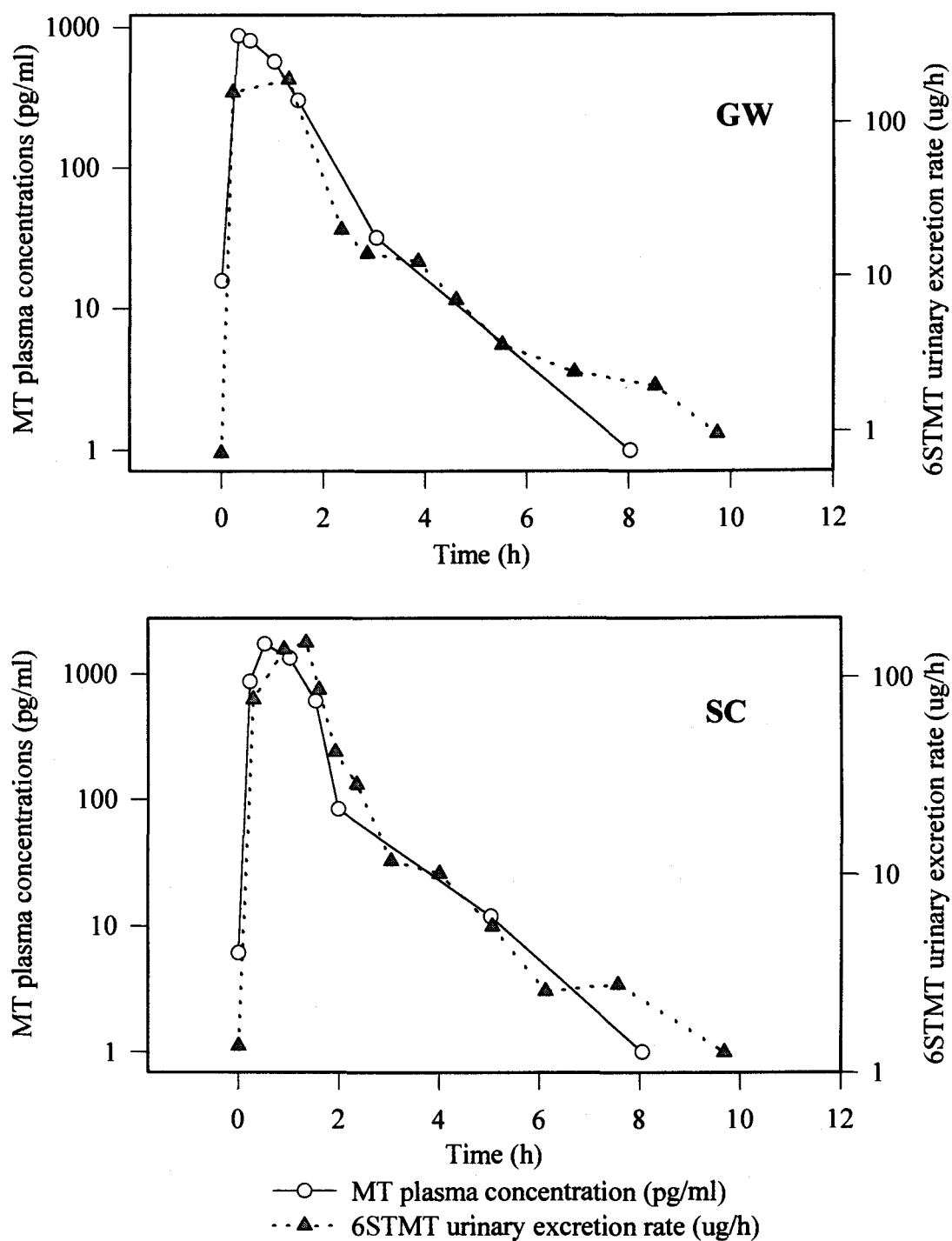
Figure 2.11: Profiles of MT plasma concentrations and 6STMT urinary excretion rate following oral administration of solution of MT in subject GW and SC.
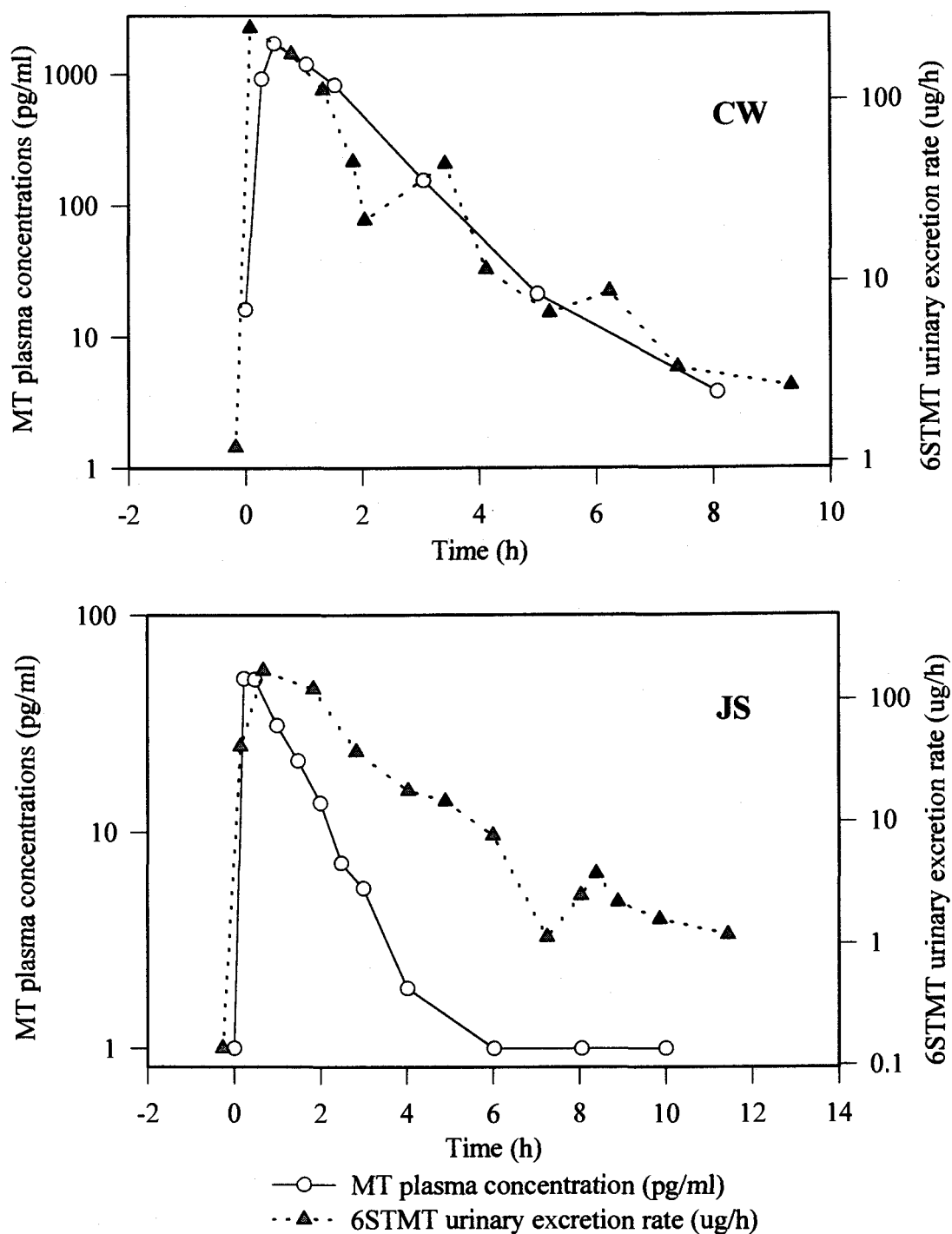
Figure 2.12: Profiles of MT plasma concentrations and 6STMT urinary excretion rate following oral administration of solution of MT in subject CW and JS.
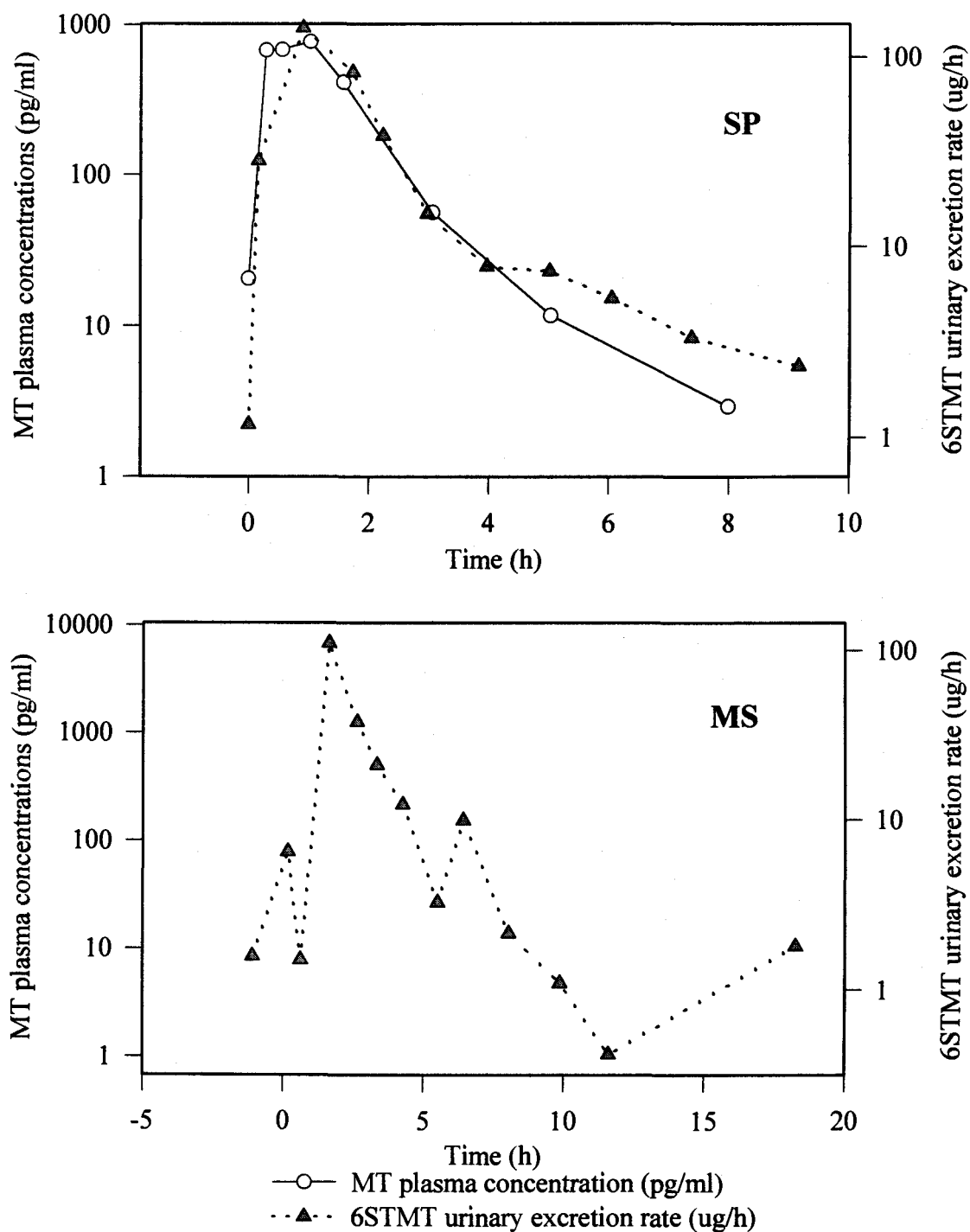
Figure 2.13: Profiles of MT plasma concentrations and 6STMT urinary excretion rate following oral administration of solution of MT in subject SP and MS (only 6STMT urinary excretion rate).
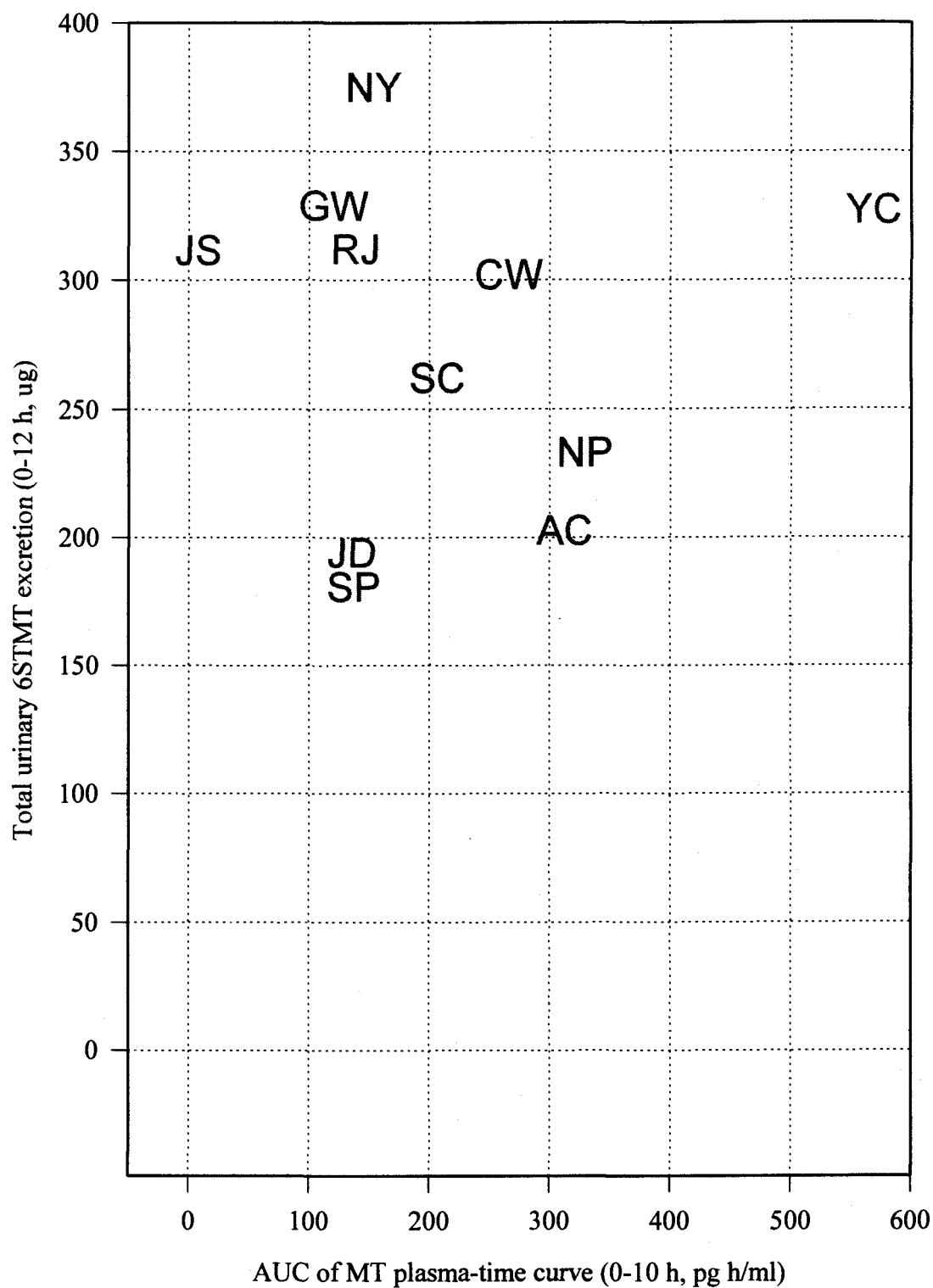
Figure 2.14 : Area under the curve (AUC) of MT plasma-time profile (0-10 h) versus total urinary 6STMT excretion (0-12 h) in 11 subjects received a solution of MT.
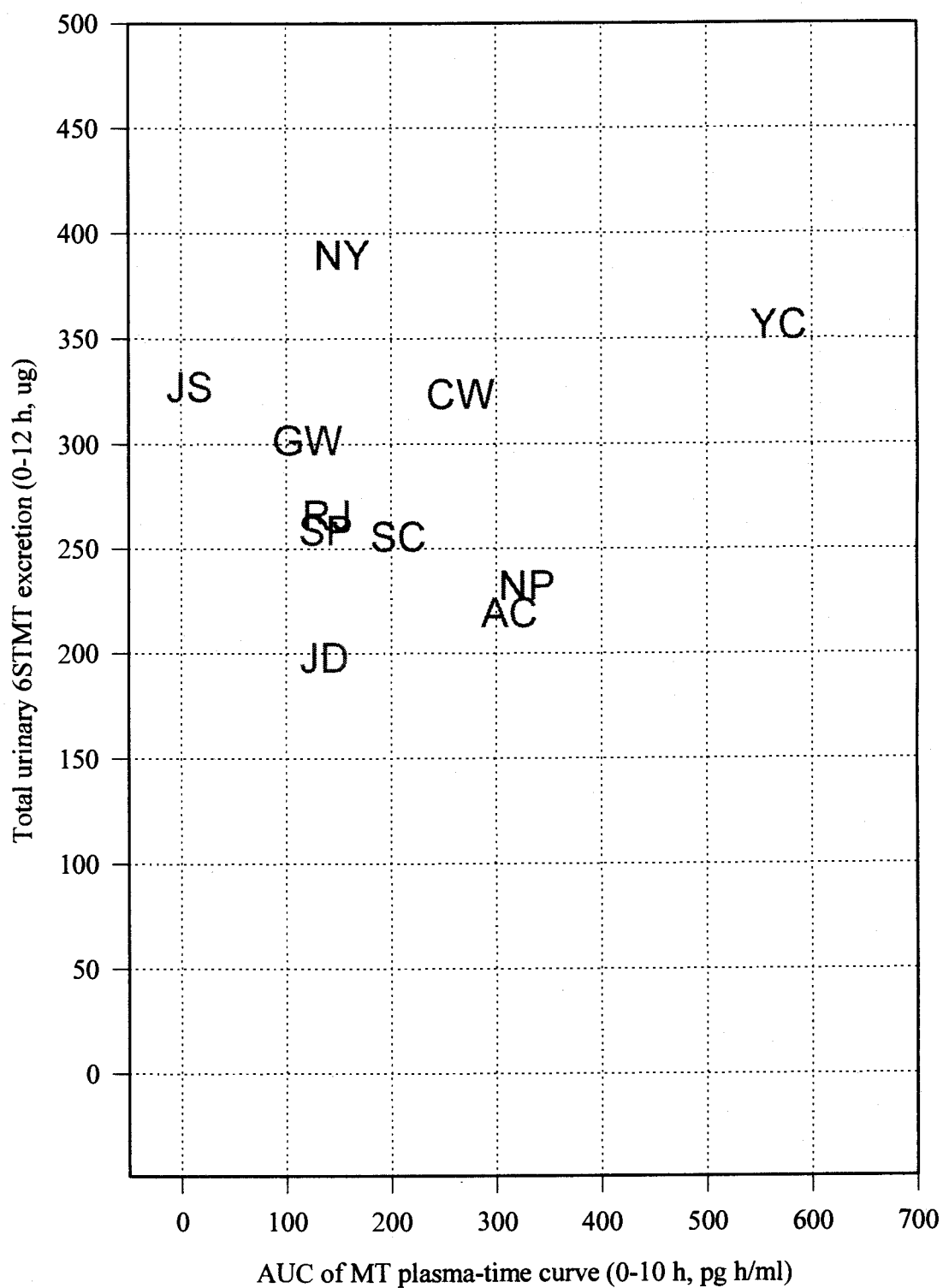
Figure 2.15 : Area under the curve (AUC) of MT plasma-time profile (0-10 h) versus AUC of 6STMT urinary excretion rate-time profile (0-10 h) in 11 subjects received a solution of MT.

Following administration of formulation A, absorption of MT following the solution was fast. Tmax values were within 1 hour. There was an extremely large variation in Cmax (103%), and AUC of MT plasma profile (64%) following administration of formulation A (n=11). High variation in Cmax and MT plasma AUC were possibly due to large variation in first pass metabolism which has been reported previously (35). MT is extensively metabolized by a first pass effect (3, 35, 36). The variation in Cmax and AUC dropped to 36% after exclusion of data from two subjects whose MT plasma concentrations was extremely low (JS-young male) and high (YC-young female).

There was no statistically significant difference between gender. Estimation of the values of ka obtained from the study may not be accurate in some subjects due to limit in sample collection during the first hour postdosing which could effect pharmacokinetic curve stripping and least squares parameter optimization in RSTRIP®. The values of ka in some subjects are extremely high (Table 2.7). Average value of λ_1 derived from RSTRIP® was higher than the values previously reported; herein $\lambda_1 = 1.5$ h^{-1} (n=11) compared to 0.87 h^{-1} (1), and 0.95 h^{-1} (37). Data best fitted with 2 exponential terms based on both statistical and graphical analysis.

Data resulted from RSTRIP® was applied as initial values for parameters in P-PHARM. The iterative two-stage method with simplex method was employed in P-PHARM to estimate individual and population pharmacokinetic parameters. In simplex method estimation of parameters is based on minimization of unweighed residuals and is applicable for sparse data set. Therefore, estimation of

pharmacokinetic parameters may be more reliable than that of RSTRIP® in this data set. k values estimated from P-PHARM were similar to those of previous studies (1, 37). ka values were larger than the values reported previously in study of oral administration of crystalline MT at 80 mg (1). The extremely large values of estimated CL/F and V/F were likely due to small bioavailability (F). MT was reported to be potentially well absorbed based on *in vitro* study of COCA-2 cells (38). If 100% of MT in the solution (formulation A) was absorbed in this young subjects, F could range from about 40% to 0.4%. Investigation of covariates showed neither gender nor weight had significant effect on the pharmacokinetic parameters.

In Figure 2.8 to 2.13, after log transformation shapes of 6STMT urinary excretion rate-time profiles from 7 out of 11 subjects (JD, AC, RJ, NP, GW, SC, and CW) were similar to those of MT plasma concentration-time profiles. The result was similar to the finding of the pilot study (20, 21) in which shapes of profiles of 6STMT urinary excretion rate and MT plasma profiles were comparable in all subjects (n=6).

Less than 1 percent of MT present in blood escapes into the urine in the unchanged form (39, 40), and 6-STMT is extensively excreted in the urine (37, 39, 40, 41). Since most drugs and metabolites are eliminated by a first-order rate process, the rate of drug or metabolite excretion is dependent on the first-order elimination rate constant and its systemic concentration (42). Thus, shape of 6STMT urinary excretion rate-time profile should be similar to that of 6STMT plasma concentration-time curve. When metabolite elimination is much faster than formation and no flip-flop occurs with the concentration profiles of the parent drug (the elimination rate is much faster

than the absorption rate), both parent drug and metabolite should have the same log terminal slope representing the elimination rate constant of the parent drug (43, 44). This could be one explanation of pattern seen in the profiles of the 7 subjects following oral administration of MT solution. In subject JS, it was possible that the elimination rate of 6STMT was much slower than the rate of its formation; therefore, MT plasma profile and 6STMT urinary excretion rate-time profile had different log terminal slope. In the latter case, log terminal slope of MT and 6STMT plasma concentration time profile should represent elimination rate constants of parent drug and metabolite, respectively, if there is no flip-flop in parent drug concentration-time profile (42, 43).

Based on the results of the present work and previous studies of SR formulations including oral, transmucosal, and transdermal drug delivery systems illustrating comparable shapes between MT plasma profiles and 6STMT plasma profiles (45) or MT plasma profiles and 6STMT urinary excretion rate time profiles (20, 24), it is possible to assume that a shape of 6STMT urinary excretion rate-time profile could represent shape of MT plasma profiles following oral administration of SR formulations used in the study. Especially when the drug is administered in a SR formulation, the absorption of MT into the body is controlled by drug release rate from the formulation. Thus, comparison between Tmax and duration of SR obtained from 6STMT urinary excretion rate-time profiles following oral administration of formulation B and C should be useful. However, direct interpretation of magnitude of 6STMT urinary excretion rate for concentration of plasma MT across the subjects may not be appropriate herein due to obscure correlation between the two values. As seen

in Figure 2.14 and 2.15, there was no significant correlation between total urinary 6STMT excretion or AUC of 6STMT urinary excretion rate-time and AUC of MT plasma profiles.

STMT urinary excretion rate time profiles following oral administration of the three formulations; formulation A, B, and C, are shown in Figure 2.16 to 2.22. Individual values of AUC of MT plasma concentration-time profile, AUC of 6STMT urinary excretion rate-time profile, and Tmax following oral administration of the three formulations in each subject are presented in Table 2.8. Comparison among individual values of AUC of MT plasma concentration-time profile and AUC of 6STMT urinary excretion rate-time profile is shown in Figure 2.23. Despite large variation in AUC of MT plasma concentration-time profile following oral administration of formulation A (78 %CV), there was much lower variation in AUC of 6STMT urinary excretion rate-time profile (23 %CV) as seen in Table 2.8.

Following oral administration of formulation B, 6STMT urinary excretion rate quickly rose above the baseline values after dosing and reached peak within 3 hours and dropped to the baseline values within 5 to 10 hours postdosing. Evaluation of *in vivo* performance of formulation C based on 6STMT urinary excretion rate-time profile showed delay in onset time of drug release for about 2 hours in 3 subjects (JD, NY, and CW). Peak of 6STMT urinary excretion rate following formulation C were generally lower than that of formulation B. Duration of the rate above the base line following administration of formulation C was slightly longer maintained than that of formulation B. Comparison of 6STMT urinary excretion rate-time profiles following
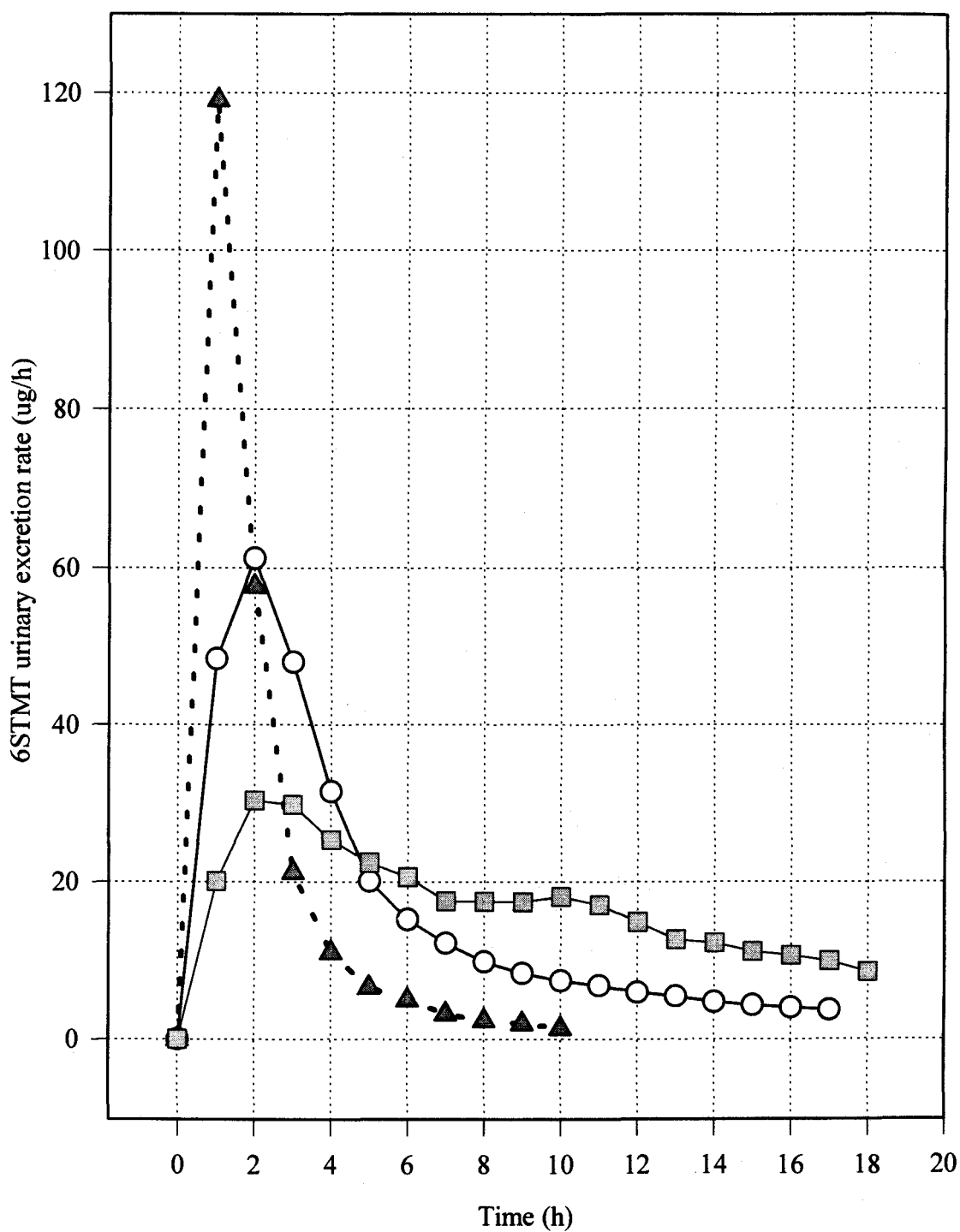
Figure 2.16: Mean 6STMT urinary excretion rate-time profiles following oral administration of formulation A (- ▲ -), formulation B (—O—), and formulation C (—■—).
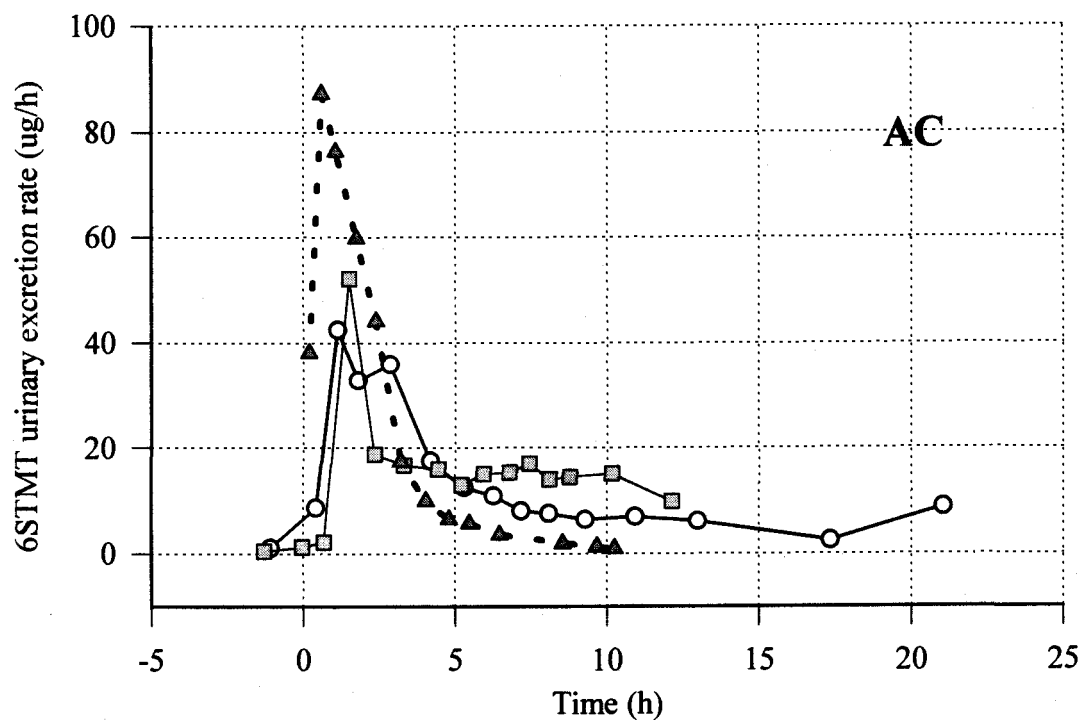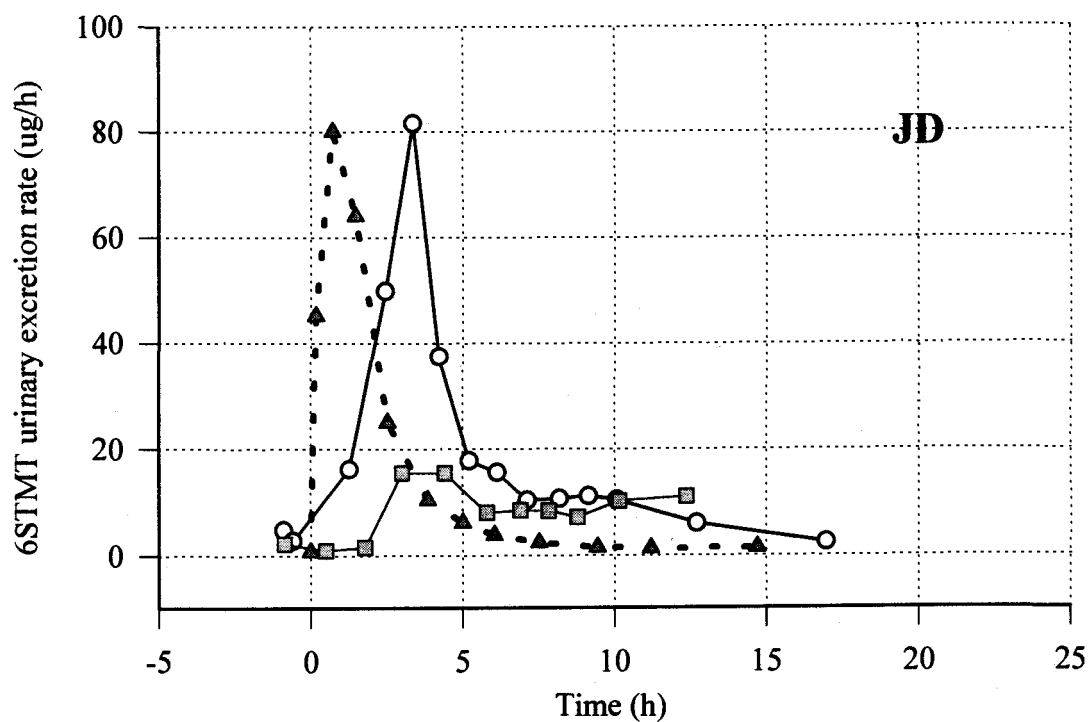
Figure 2.17: 6STMT urinary excretion rate-time profiles following oral administration of formulation A (•••▲•••), formulation B (—O—), and formulation C (—□—) in subject JD and AC.
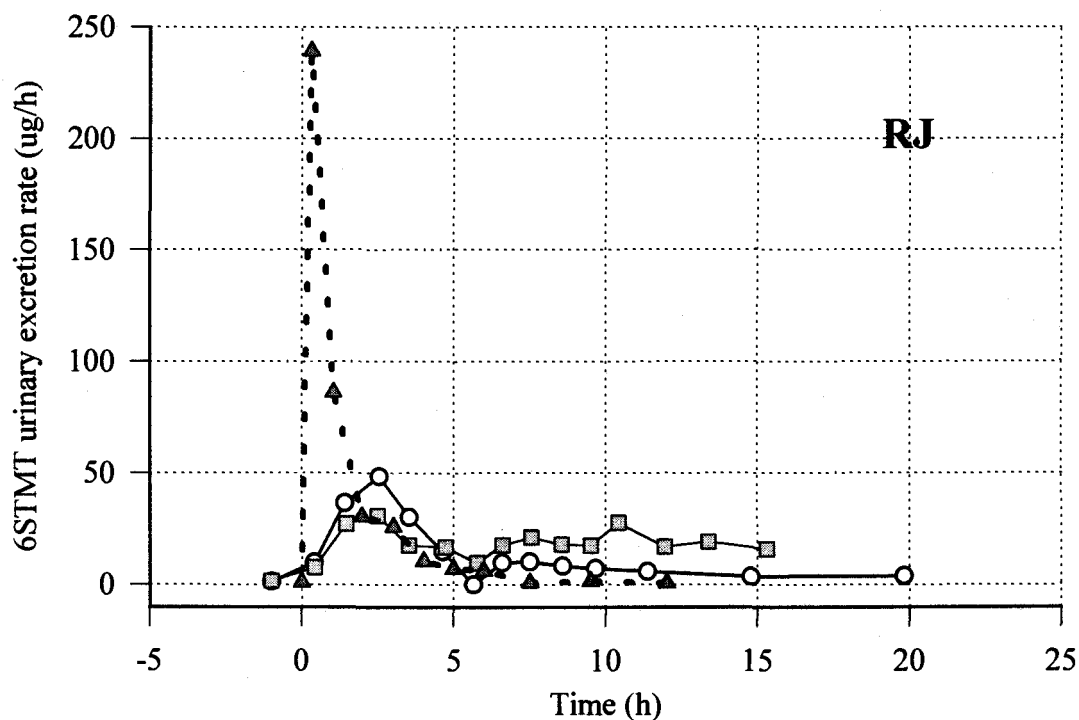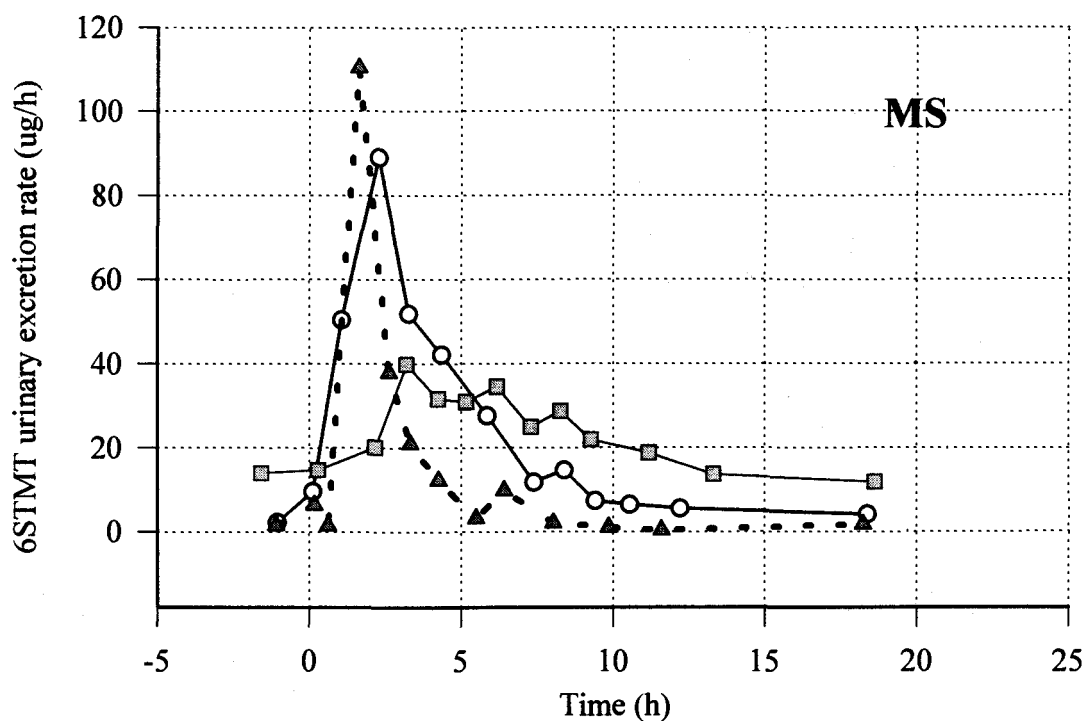
Figure 2.18: 6STMT urinary excretion rate-time profiles following oral administration of formulation A (- ▲ -), formulation B (—O—), and formulation C (—▣—) in subject MS and RJ.
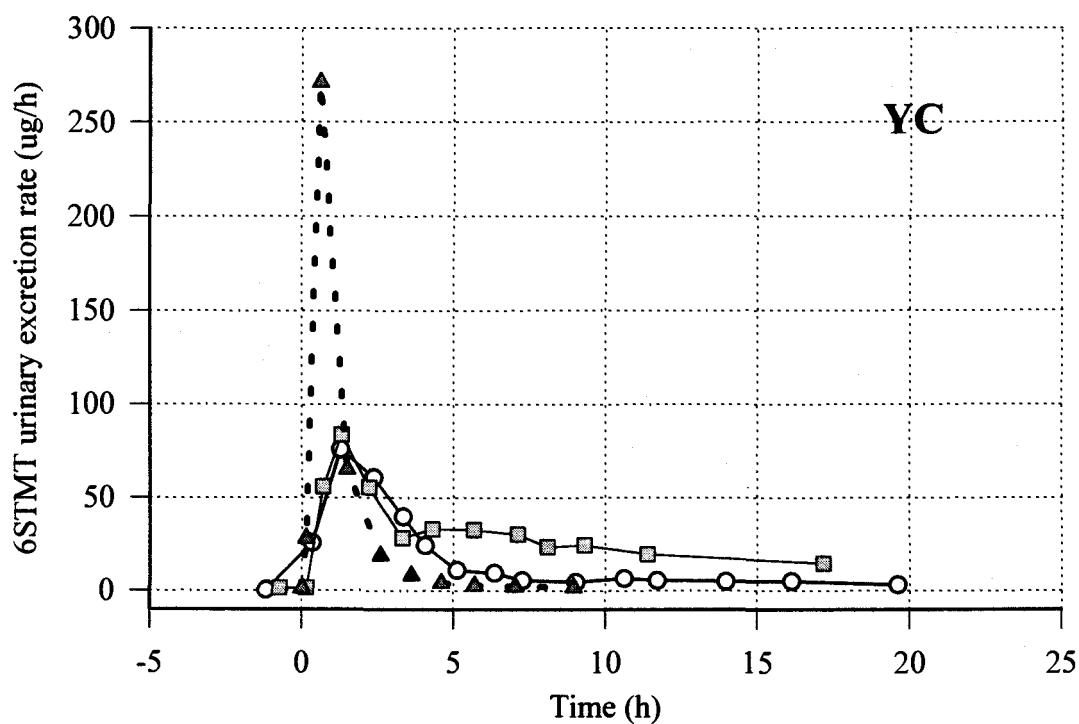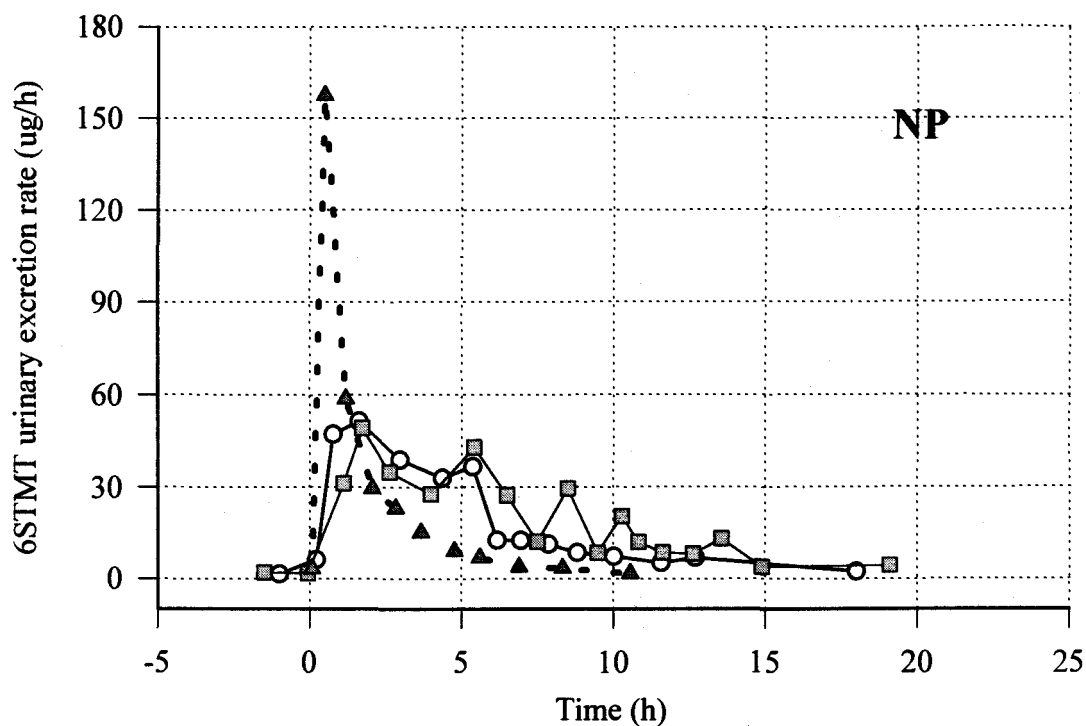
Figure 2.19: 6STMT urinary excretion rate-time profiles following oral administration of formulation A (▪ ▲ ▪), formulation B (—O—), and formulation C (—▪—) in subject NP and YC.
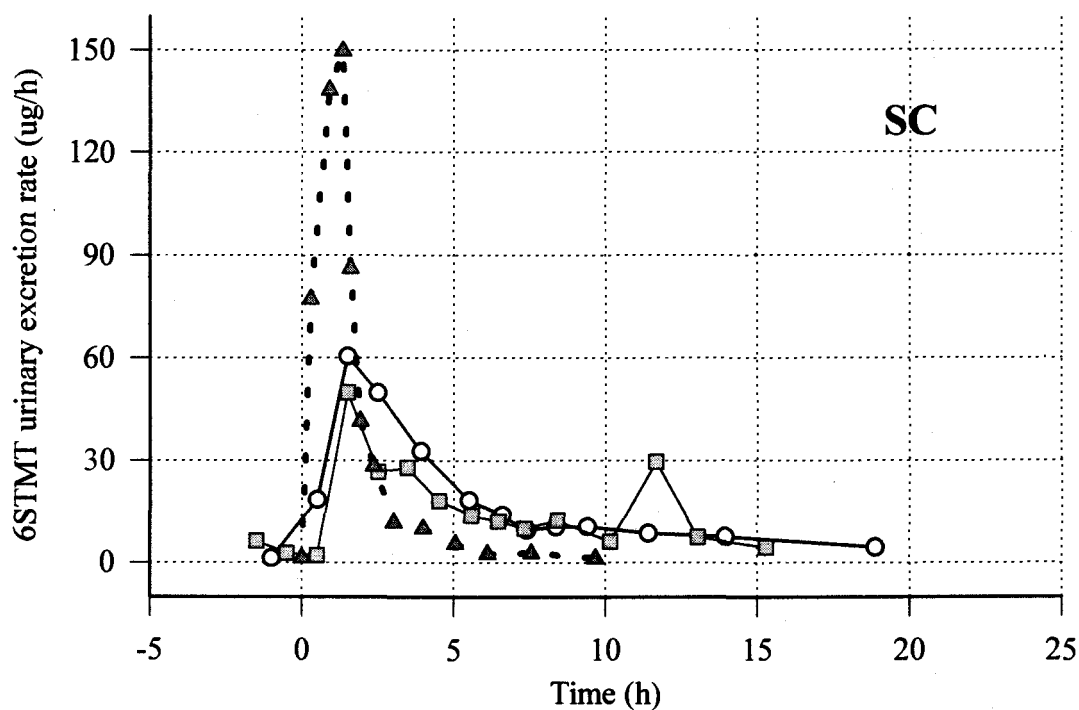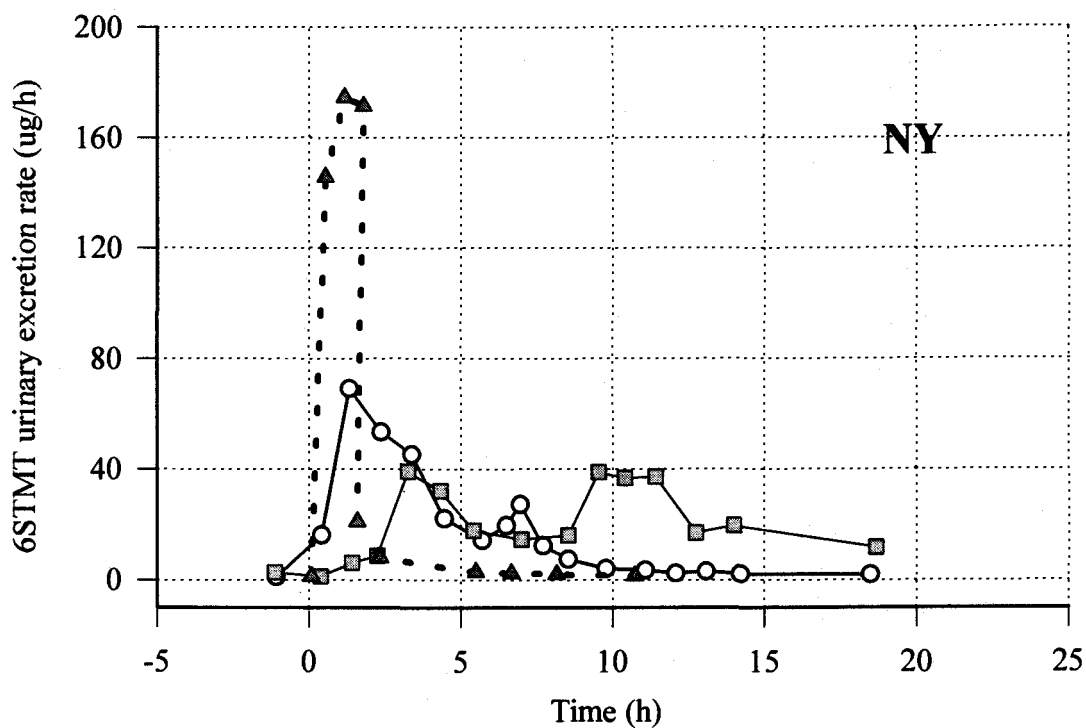
Figure 2.20: 6STMT urinary excretion rate-time profiles following oral administration of formulation A (● ▲ ●), formulation B (—O—), and formulation C (—□—) in subject NY and SC.
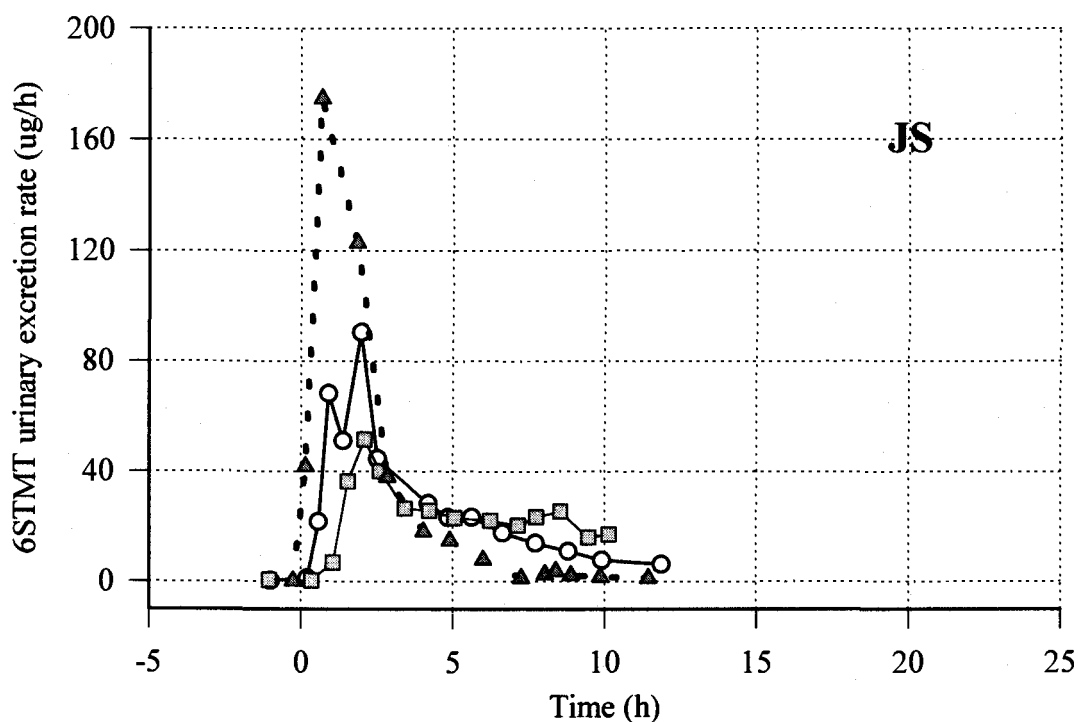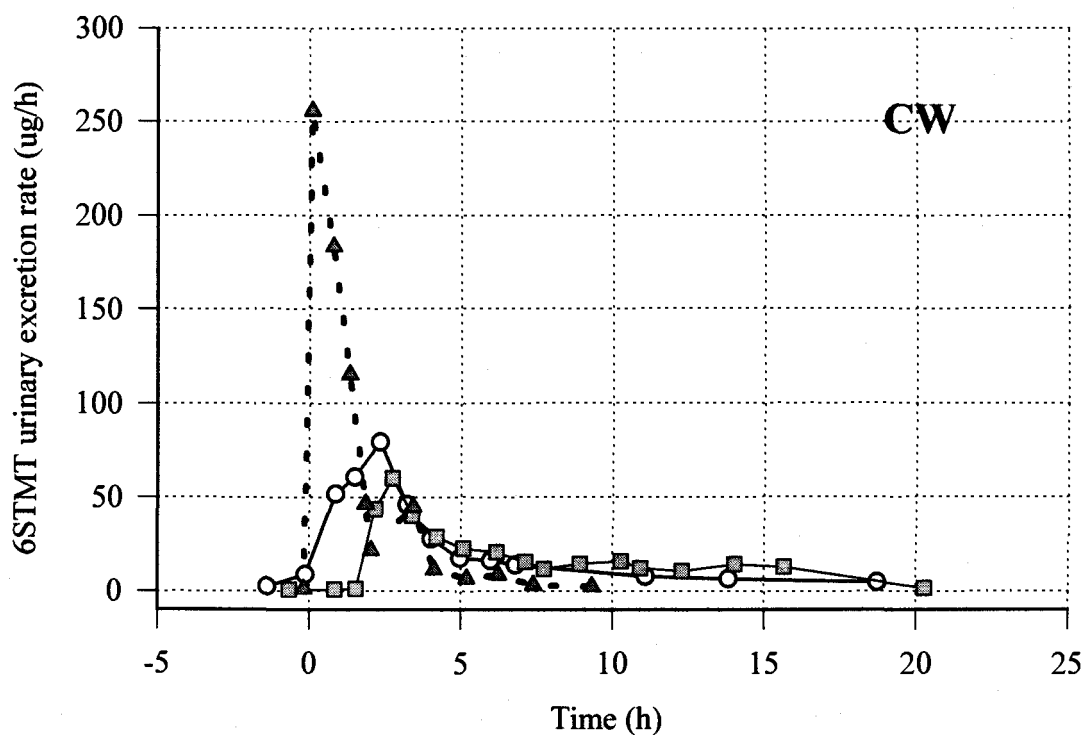
Figure 2.21: 6STMT urinary excretion rate-time profiles following oral administration of formulation A (- ▲ -), formulation B (—O—), and formulation C (—▣—) in subject CW and JS.
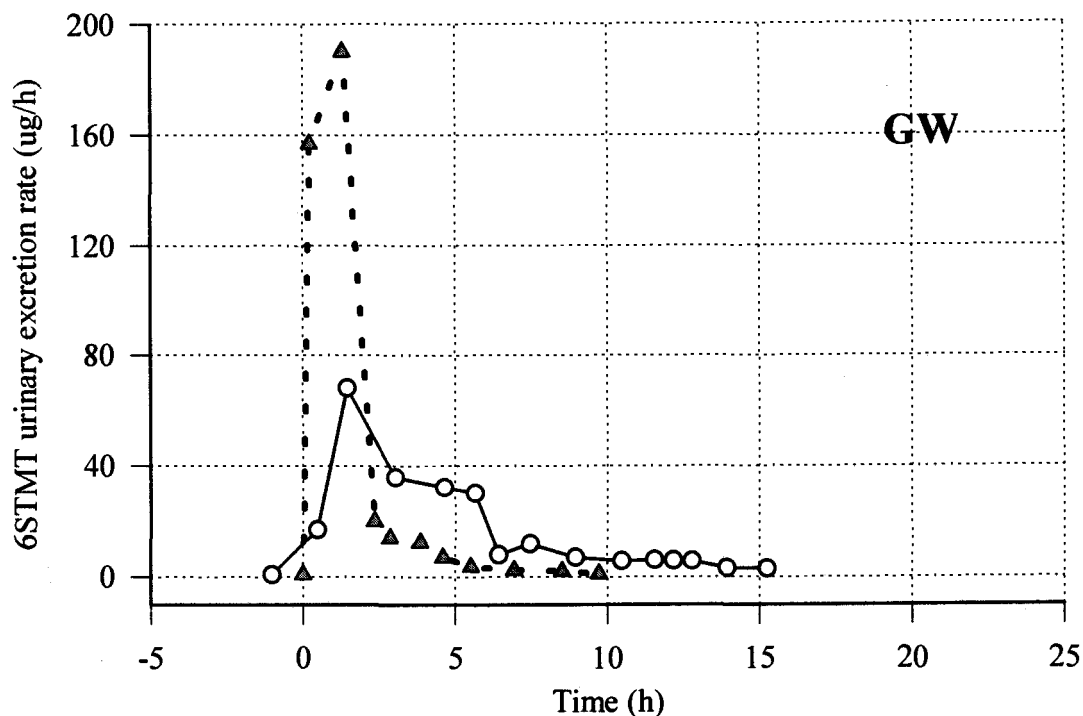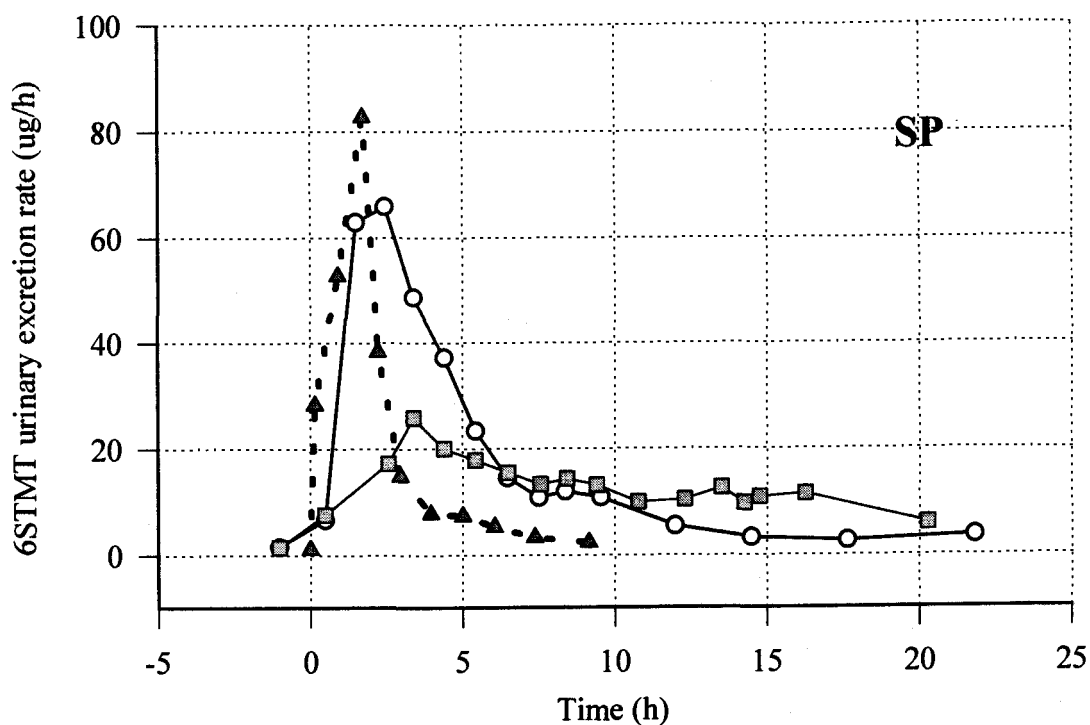
Figure 2.22: 6STMT urinary excretion rate-time profiles following oral administration of formulation A (- ▲ -), formulation B (—O—), and formulation C (—□—) in subject SP, and formulation A and B in subject GW.
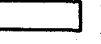
Table 2.8: Area under the curve of melatonin (MT) plasma concentration-time profiles and 6-sulphatoxymelatonin (6STMT) urinary excretion rate-time profiles, and Tmax (time to maximum MT plasma concentration or maximum 6STMT urinary excretion rate) following oral administration of formulation A, B, and C given at 750 µg dose.

| Subjects | MT plasma profile | | 6STMT urinary excretion rate-time profile | | | | | |
| | Formulation A | | Formulation A | | Formulation B | | Formulation C | |
	AUC (0-10h) (pg h/ml)	Tmax [a] (h)	AUC (µg)	Tmax* [a] (h)	AUC (µg)	Tmax* [b] (h)	AUC (µg)	Tmax* [b] (h)
JD	1285	0.25	198	0.73	257	3.37	100	4.41
AC	2916	0.67	219	0.60	186	1.13	195	1.51
MS	-	-	189	1.63	355	2.28	300	3.21
RJ	2917	0.52	266	0.32	191	2.54	230	2.49
NP	2893	1.00	232	0.49	237	1.63	295	1.73
YC	5207	0.42	356	0.61	259	1.28	394	1.31
NY	1440	0.50	390	1.17	275	1.33	261	3.25
SC	1084	0.52	255	1.35	267	1.50	211	1.50
CW	1963	0.50	323	0.09	309	2.33	232	2.73
JS	2467	0.23	327	0.68	294	1.98	256	2.08
SP	80	0.32	258	1.73	300	1.45	158	3.39
GW	1274	1.02	302	1.31	274	2.45	-	-
Mean	2177	0.54	276	0.89	267	1.94	239	2.51
(SE)	(1696)	(0.27)	(64)	(0.53)	(47)	(0.67)	(78)	(0.99)
%CV	78	49	23	59	18	34	32	39
Geometric mean	1553	0.49	270	0.70	263	1.84	227	2.34

* Tmax is the midpoint time.

[a] and [b] are homogenous groups based on Tukey's multiple comparison.
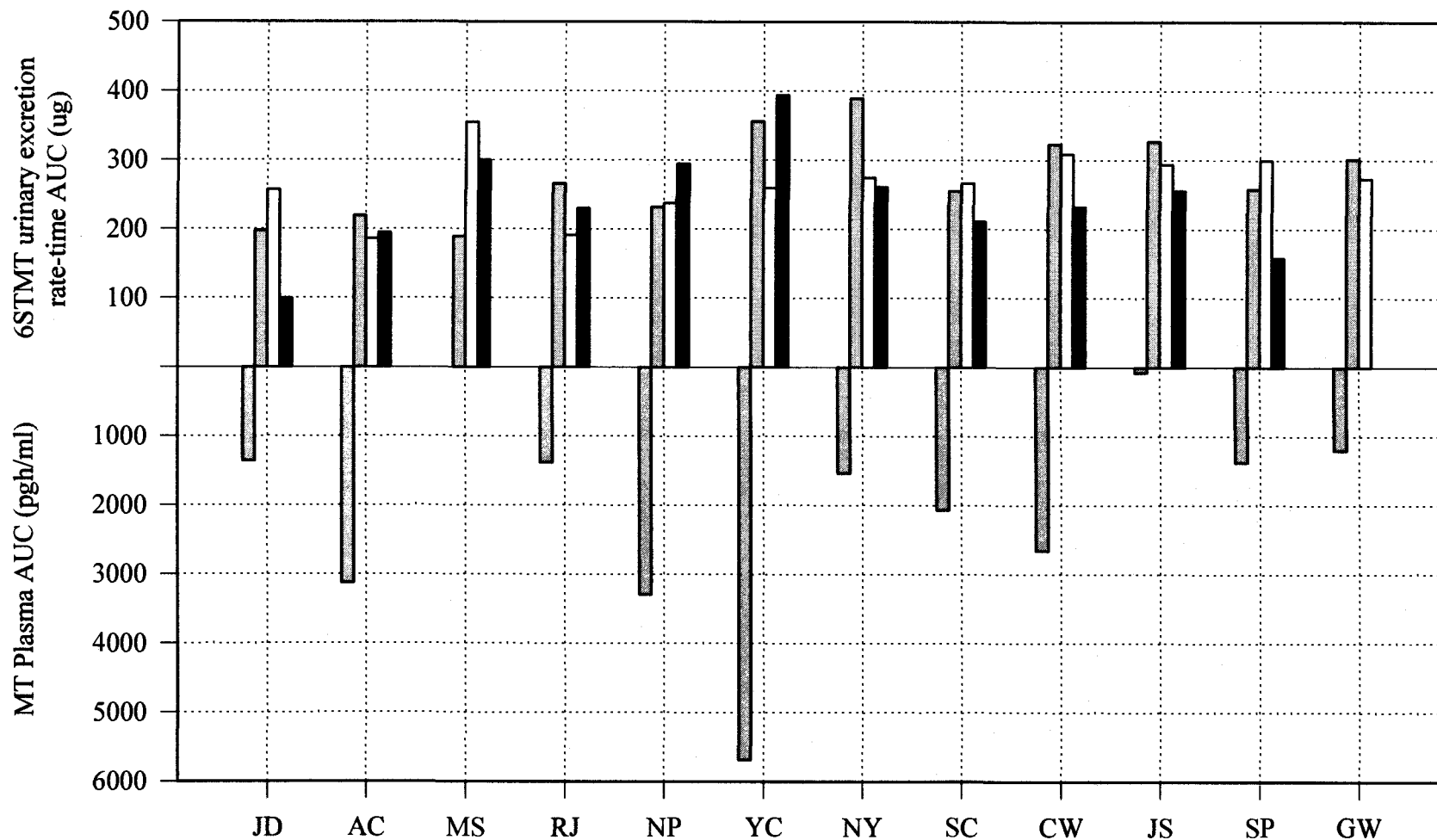
Figure 2.23: Comparison of area under curves (AUC) of MT plasma concentration-time profiles (▨) following oral administration of formulation A, and AUC of 6STMT urinary excretion rate-time profiles following oral administration of formulation A (▨), formulation B (▢), and formulation C (■).

each formulation within the same subject should be useful, if MT and 6STMT

pharmacokinetics are linear within dose and drug release rate involved in the study.

Formulation A produced a spike in MT plasma and 6STMT urinary excretion rate-time

profiles with the fastest Tmax and maximum in peak of 6STMT urinary excretion rate.

Statistical comparison of Tmax values (Table 2.8) obtained from profiles of plasma

MT and 6STMT urinary excretion rate following administration of formulation A

showed no significant difference. Therefore, estimation of Tmax based on 6STMT

urinary excretion rate-time profile may be used as an approximate index for Tmax of

MT plasma concentration-time profiles in this study where urine sample collection is

adequately collected. Tmax obtained from 6STMT urinary excretion rate-time profiles

following administration of formulation B and C was significantly longer than that of

formulation A. There was no significant difference among AUC of 6STMT urinary

excretion rate-time profiles following formulation A, B, and C. The finding suggested

that MT released from formulation A, B, and C might be absorbed into the body in the

similar quantity if metabolism of MT is linear at this dose/drug release rate.

Comparison of *in vivo* performance of the three dosage forms using 6STMT

urinary excretion rate-time profiles supported the use of 20% Aquacoat® coat as

controlled release layer rather than 10% Aquacoat® coat. Attempt on delaying onset

time of drug released from the Aquacoat® beads with the use of additional enteric coat

was not fully achieved. In this study, only 6STMT urinary excretion rate-time profiles

of 3 subjects out of 11 subjects showed delayed in onset of drug absorption for about 2

hours in fasted condition. The delay in onset time is highly dependent on the gastric

emptying which can be largely variable ranging from a few minute to 3 hours at fasted state (46).

CONCLUSION

There was high variation in Cmax and AUC of MT plasma concentration-time profiles following oral administration of formulation A (MT solution). No significant correlation was found between AUC of MT plasma profiles (0-10 hours) and total 6STMT excretion (0-12 hours) or AUC of 6STMT urinary excretion rate-time profiles across subjects. The large variation in MT plasma concentrations among subjects and lack of the correlation may be due to difference in first pass metabolism. Shapes of profiles of MT plasma concentrations and 6STMT urinary excretion rate were comparable in 7 out of 11 subjects supporting possibility of using 6STMT urinary excretion data as index for MT plasma profile. There was no significant difference in pharmacokinetic parameters between gender.

The release of MT from formulation B was faster than that of formulation C both *in vitro* and *in vivo*. Delay in onset of MT absorption by enteric coating on 20% Aquacoat® beads (formulation C) occurred in 3 subjects under fasted condition for about 2 hours. Comparison between 6STMT urinary excretion rate-time profiles following administration of formulation B and C supported the use of 20% Aquacoat® coating as the controlled release layer rather than 10% coating.

REFERENCES

1. Waldhauser, F.; Waldhauser, M.; Lieberman, H. R.; Deng, M. H.; Lynch, H. J.; Wurtman, R. J. Bioavailability of oral melatonin in humans. Neuroendocrinol. 39, 307-313 (1984).

2. Waldhauser, F. Dietzel, M. Daily and annual rhythms in human melatonin secretion: Role in puberty. Ann., New York Acad., 453, 205-214 (1985).

3. Arendt, J. In Melatonin and the mammalian pineal gland; Chapman & Hall, London, UK, 1995, pp. 40, 42, 207, 248.

4. Dawson, D., Armstrong, S.M. Chronobiotics-Drugs that shift rhythms. Pharmacol. Ther. 69, 15-36 (1996).

5. Simpson, H.W. Chronobiotics: Selected agents of potential value in jet lag and other desynchronisms. In: Chronobiology: principles and applications to shifts in schedules. L.E. Scheving and F. Halberg (Eds.), Sijthoff and Noordhoff, the Netherlands, 1980, pp. 443-446.

6. Robert, S.L., Lewy, A.J., Hughes, R.J., McArthur, A.J., Blood, M.L. Melatonin as a Chronobiotic Drug. DN&P, 9(6), 325-332 (1996).

7. Bartsch, H., Bartsch, C. Effect of melatonin on experimental tumors under different photoperiods and times of administration. J. Neural Trans., 52, 269-279 (1981).

8. Blask, D.E., Hill, S.M., Pelletier, D.B. Oncostatic signaling by the pineal gland and melatonin in the control of breast cancer In The pineal gland and cancer Gupta, D.; Attanasio, A.; Rieter, R.J., Ed; Muller & Bass, Tubingen, Germany, 1988, pp 195-206.

9. Cagnacci, A., Elliott, J.A., Yen, S. Amplification of pulsatile LH secretion by exogenous melatonin in women. J. Clin. Endocrinol. Metab. 73, 210-212 (1991).

10. Wynn, V.T., Arendt, J. The effect of melatonin on the human electrocardiogram and simple reaction time responses. J. Pineal Res., 5, 427-436 (1988).

11. Maestroni, G.J.M., Conti, A., Pierpaoli, W. Melatonin stress and the immune system. Pineal. Res. Rev., 7, 268 (1989).

12. Sack, R.L. Melatonin: advising patients about the use of melatonin ASDA News, 3(3), 15, 27 (1996).

13. McArthur, A.J., Lewy, A.J., Sack, R.L. Non-24-hour sleep-wake syndrome in a sighted man: circadian rhythm studies and efficacy of melatonin treatment. Sleep, 19(7), 544-553 (1996).

14. Dahlit, M., Alvarez, B, Vignau, J., English, J., Arendt, J., Parkes, J.D. Delayed sleep phase syndrome response to melatonin, Lancet 337, 1121-1124 (1991).

15. Petrie, K., Conaglen, J. V., Thompson, L., Chamberlain, K. Effects of melatonin on jet lag after long haul flight, Br. Med. J. 298, 705-707 (1989).

16. Waldhauser, F., Vierhapper, H., Oirich, K. Abnormal circadian melatonin secretion in night-shift workers, The New Eng. J. Med. 7, 441-446 (1986).

17. Rosenthal, N.E., Sack, D.A., Gillin, J.C., Lewy, A.J., Goodwin, F.W., Davenport Y., Mueller, P.S. Seasonal effective disorder. A description of the syndrome and preliminary findings with light therapy, Arch. Gen. Psychiatry 4, 171-180 (1984).

18. DiPiro JT, Talbert RL, Hayes PG, et al., eds. Pharmacotherapy, a pathophysiologic approach. 2th ed. Connecticut: Appleton & Lane Norwalk, 1993, pp. 37.

19. Lee, B., Parrott, K.A., Ayres, J.W., Sack, R.L. Development and characterization of an oral controlled release delivery system for melatonin Drug Dev. Ind. Pharm., 22(3), 269-274 (1996).

20. Lee, B., Parrott, K.A., Ayres, J.W., Sack, R.L. Design and evaluation of an oral controlled release delivery system for melatonin in human subjects Int. J. Pharm. 124, 119-127 (1995).

21. Lee, B. Development of an oral controlled release and a transdermal delivery system for melatonin. Ph.D. Thesis Oregon State University 1992.

22. Nowak, R., McMillen, I.C., Redman, J., Short, R.V. The correlation between serumand salivary melatonin concentration and urinary 6-hydroxymelatonin sulphate excretion rate: Two non-invasive techniques for monitoring human circadian rhythmicity, Clin. Endocrinol. 27, 445-452 (1987).

23. Arendt, J., Bojkowski, C., Franey, C., Wright, J., Marks, V. Immunoassay of 6-hydroxymelatonin sulfate in human plasma and urine: abolition of the urinary 24-hour rhythm with atenolo, J. Clin. Endocrinol. Metab. 60, 1166-73 (1985).

24. Lee, B., Parrott, K.A., Ayres, J.W., Sack, R.L. Preliminary evaluation of transdermal delivery of melatonin in human subjects, Res. Commun. Mol. Pathol. Pharmacol. 85, 337-346 (1994).

25. Garfinkel, D., Laudon, M., Nof, D., Zisapel, N. Improvement of sleep quality in elderly people by controlled-release melatonin, Lancet 346, 541-544 (1995).

26. Bojkowski, C.J., Arendt, J. Factors influencing urinary 6-sulphatoxymelatonin, a major melatonin metabolite, in normal human subjects. Clin. Endocrinol., 33, 435-444 (1990).

27. Lewy, A.J., Markey, S.P. Analysis of melatonin in plasma by gas chromatography negative chemical ionization mass spectroscopy, Science 201, 741-743 (1978).

28. Aldhous, M.E., Arendt, J. Radioimmunoassay for 6-sulphatoxymelatonin in urine using an iodinated trace, Ann. Clin. Biochem. 25, 298-303 (1988).

29. Jusko, W.J. Guidelines for collection and analysis of pharmacokinetic data. In: Evans, Schentag, Jusko, eds. Applied Pharmacokinetics, 2nd ed. Spokane, Washington: Applied Therapeutics, 1986.

30. Yeh, K.C., Kwan, K.C. A comparison of numerical integrating algorithms by trapezoidal, lagrange, and spline approximation. J. Pharm. Biopharm. 6(1), 79-98 (1978).

31. RSTRIP II version 1.0 copyright 1992. Micromath Scientific Software Salt Lake City, UT.

32. P-PHARM, Population pharmacokinetic/pharmacodynamic data modeling program. Simed S.A., France.

33. Cochran WC, Cox GM. Experimental Designs, 2th ed. New York: John Wiley and Sons, 1957.

34.   STATGRAPHIC version 7.0, Portion copyright 1993 Manugistics, Inc.
        Statistical Graphics Corporation.

35.   Lane, E. A.; Moss, H. B. Pharmacokinetics of melatonin in man: first pass
        hepatic metabolism. J. Clin. Endocrinol. Metab. 61, 1214-1216 (1985).

36.   Vakkuri, O., Leppaluoto, J., Kauppila A. Oral administration and distribution
        of melatonin in human serum, saliva and urine. Life Sci. 37, 489-495 (1985).

37.   Iguchi, H., Kato, K.I., Ibayashi., H. Melatonin serum levels and metabolic
        clearance rate in patients with liver cirrhosis., J. Clin. Endocrinol. Metab. 54,
        1025-1027 (1982).

38.   Yeleswaram, K., Mclaughlin, L.G., Knipe, J.O., Schabdach, D. Oral
        bioailability of melatonin in the rat, dog, and monkey J. Pineal. Res. in press
        (1997).

39.   Matthews, C.D., Kennaway, D.J., Fellenberg, A.J.G., Phillipou, G., Cox,
        L.W., Seamark, R.F. Melatonin in man, Adv. Biosci. 29, 371-81 (1981).

40.   Jones, R.L., Mc Geer, P.L., Greiner, A.C. Clin. Chim. Acta. 26, 281 (1969).

41.   Fellenberg, A.J., Phillipou, G., Seamark, R.F. Urinary 6-sulphatoxymelatonin
        excretion and melatonin production rate: studies in sheep and man. In Pineal
        function (C.D. Matthews and R.F. Seamark, Ed.), 1981, Elsevier/North
        Holland Biomedical Press, Amsterdam, pp. 143-50.

42.   Shargel, L., Yu, A.B.C. In Applied biopharmaceutics and pharmacokinetics;
        Appleton&Lange, Connecticut,1993, pp. 200-201.

43.   Balant, L.P., McAinsh, J. Use of metabolite data in the evaluation of
        pharmacokinetics and drug action. In: Jenner, P., Testa, B., eds. Concepts in
        drug metabolism. Part A Marcel Dekker, Inc. New York, 1980, pp. 311-371

44.   Lee, P.I.D., Amidon, G.L. Influence of dosage on pharmacokinetics-Dose
        proportionality In Pharmacokinetic analysis Technomic Publishing
        Company, Inc., Pennsylvania, 1996, pp. 143-165.

45.   Benes, L.; Brun, J.; Claustrat, B.; Degrande, G.; Ducloux, N.; Geoffriau, M.;
        Horriere, F.; Karsenty, H.; Lagain, D. In Melatonin and the pineal gland -
        From basic science to clinical application; Touitou, Y.; Arendt, J.; Pevet, P.,
        Ed.; Elsevier science publishers, Amsterdam, the Netherlands, 1993; pp. 347.

46.   Wilson, C.G., Washington, N. The stomach: its role in oral drug delivery. In Physiological Pharmaceutics, biological barriers to drug absorption. John Wiley & Sons. New York, 1989, pp. 47-70.

CHAPTER 3

MODELING OF MELATONIN PLASMA PROFILES FOLLOWING ORAL SUSTAINED RELEASE DOSAGE FORM ADMINISTRATION

ABSTRACT

Simulation of melatonin (MT) plasma concentration-time curves from administration of MT controlled-release oral dosage forms is described using a mathematical relationship between *in vitro* release rate and *in vivo* absorption. Two simulation approaches are described. Data from an initial formulation studied in six human subjects are evaluated *in vitro* and *in vivo* and the resultant models assuming linear pharmacokinetics applied to two new formulations given to twelve and four subjects, respectively. The following steps are used to relate *in vitro* dissolution profiles with expected plasma concentration profiles: 1) Deconvolution of plasma MT concentrations following dosage form administration to estimate *in vivo* absorption rate. 2) Correlation of *in vivo* absorption rate with *in vitro* dissolution rate. 3) Estimation of *in vivo* absorption rate for dosage forms with different *in vitro* dissolution profiles based on the correlation derived in step 2. 4) Computer simulation of expected plasma concentrations based on the estimated *in vivo* absorption rate. Satisfactory prediction resulting from the two models was obtained with the formulations containing IR MT, as well as the formulation containing only SR MT given at higher dose. Results suggest possible dependence of MT bioavailability

on release rate from the formulation since models assuming linear pharmacokinetics overestimates plasma drug concentrations produced by a low dose SR formulation.

INTRODUCTION

Melatonin (MT) is an indole neurohormone produced by the pineal gland. Its chronobiological secretion helps set the "biological clock" of many animals, including humans. Giving MT to people may help treat various disorders occurring from inappropriate physiological MT release patterns associated with certain sleep disorders, jet-lag, shift work syndrome, and seasonal affective disease (1). MT is an experimental drug; however, it has recently become available in conventional tablets as a supplementary nutrient. Drug delivery systems for controlled release of melatonin, such as transdermal (2), oral (3), and transmucosal (4, 5), have been developed in order to deliver melatonin to mimic a physiological pattern.

Controlled release formulations of old drugs are usually developed and tested firstly *in vitro* followed by *in vivo*. Optimization of the formulations for oral administration is likely to be facilitated by appropriate management of *in vitro* testing and preliminary *in vivo* evaluation (6). The more relevant the *in vitro* test to *in vivo* performance, the more likely the success in predicting obtainable plasma concentrations (7). Complete pharmacokinetic studies such as iv bolus, iv infusion, or oral solution administration are usually not carried out in the same subjects as involved in studying for new prolonged release formulations for old drugs. In this case, literature values of pharmacokinetic parameters may be employed for prediction of

plasma drug concentrations which will be produced by the new formulation. Although results obtained from application of data from different studies must be used with caution, it may still be useful as an additional tool for screening different product formulations prior to performing *in vivo* evaluation.

In this work, the use of computer simulation in order to predict MT plasma concentration-time curves from dissolution data is presented. Two modeling techniques are developed in order to obtain *in vitro-in vivo* correlations using data from a pilot study of MT SR oral formulation (3) as an initial source of approximate correlations. The process involves application of pharmacokinetic literature data from different studies in different subjects. Accuracy of modeling results is discussed based on simulation results.

METHODS

Assumptions

Simulations made by the mathematical model are based on several assumptions including (8, 9): *i)* rate of absorption of MT from the gastrointestinal tract is limited by the dosage form. *ii)* there is no " absorption window " for MT. *iii)* changes in rate of absorption from the gastrointestinal tract are associated with a concomitant change in drug concentrations in plasma. *iv)* distribution pharmacokinetics of MT in sustained-release (SR) products do not differ from those with other products (i.e. immediate release (IR) product) *v)* pharmacokinetics of the drug are linear.

Model Development

Data from a pilot study of an oral delivery system for MT in human subjects (3) are used for model development. Details of the formulation (A) have been published (3). Briefly, formulation A consisted of 20% IR and 80% SR MT, and was given as a single dose of 500 μg (100 μg IR + 400 μg SR) to four subjects, or 1000 μg (200 μg IR + 800 μg SR) to two subjects. MT plasma concentrations were collected over an 8 hour period. In addition, new results are now presented with different dosage of SR, but no IR MT.

Two techniques of simulation are developed. Technique 1 ignores the separate contributions of IR and SR mechanisms of *in vitro* release from the formulation. Thus, only total amounts of MT released *in vitro* are employed to generate an estimated *in vivo* input of drug into the body. In technique 2, release of the drug *in vitro* is first identified as a fast release (IR), or a slow release (SR) portion, then the two parts are treated separately as *in vivo* input for the IR plus *in vivo* input for the SR, respectively.

Modeling Technique 1

Modeling technique 1 was previously described and employed as a stochastic simulation model to estimate bioavailability of KCL from sustained release dosage forms (9). It involved application of point to point estimated bioavailability to simulate KCL urinary excretion rate profiles. A similar approach can be applied for simulation of the MT plasma concentration-time profile to be expected from MT sustained release formulations.

In Vivo Absorption Rate Estimation

Initially, known MT plasma concentration vs. time data are used to obtain the cumulative amount of MT absorbed at any time (t) following oral administration with the dosage form of interest. Cumulative amount absorbed *in vivo* (t) is obtained from deconvolution results in subjects given formulation A at 500 µg or 1000 µg using PCDCON (version 1.0 courtesy of Dr. William Gillespie, University of Texas at Austin). Because data for iv. bolus or oral solution were not available in the pilot study, plasma MT concentrations following an IV bolus of 10 µg MT by Iguchi et. al. (10) were employed as a source for impulse response specification of MT to estimate cumulative amount absorbed *in vivo (t)*. The cumulative amount absorbed at any time (t) can then be related to the amount dissolved at any time (t) using equation 1.

Equation 1.

$$\text{Fvr (t)} = \frac{\text{Cumulative amount absorbed, } \textit{in vivo} \text{ (t)}}{\text{Cumulative amount released, } \textit{in vitro} \text{ (t)}}$$

Thus, Fvr (t) is a normalization factor obtained from the relationship expressed in equation 1 and is comparable to relative (to the literature iv bolus study (10)) bioavailability at time t. Cumulative amount released *in vitro* (t) of formulation A is estimated from the Weibull equation (11) fitted to dissolution data of formulation A. The Weibull equation is one of appropriate mathematical models for simulation of dissolution time profile. Fvr (t) employed in equation 1 is the arithmetic average of all Fvr (t) (n = 6). Once obtained, Fvr (t) can now be combined with dissolution data for various formulations of MT to predict or "simulate" expected MT plasma concentration vs. time profiles based on drug release from the rate controlling dosage

form. Simulation of plasma concentrations from formulation A is, of course, both

trivial and necessary. It is trivial since Fvr (t) was generated from dissolution and

absorption data for formulation A, and necessary to confirm that all computer

programs work as expected. Simulation of predicted drug plasma concentrations vs.

time occurs as follows.

Simulation of *in vivo* input rate can be generated from amount of drug
predicted

to be absorbed over time as described below.

$$\text{\textit{In vivo} absorption rate at mid point between } t_{i+1} \text{ and } t_i = \frac{\text{Simulated amount absorbed \textit{in vivo} } (t_{i+1} - t_i)}{(t_{i+1} - t_i)}$$

Simulated cumulative amounts absorbed *in vivo* at time t are obtained from equation

2 (now simulated if dissolution data are used for formulations tested *in vitro* but not

previously tested *in vivo*). Note that dissolution need not only represent real data, but

may also include theoretical dissolution release profiles.

Equation 2.

$$\left(\begin{array}{l} \text{Simulated cumulative} \\ \text{amount drug} \\ \text{absorbed \textit{in vivo} (t)} \end{array} \right) = \text{Fvr (t)} \times \left(\begin{array}{l} \text{Simulated or real} \\ \text{cumulative amount drug} \\ \text{release \textit{in vitro} (t)} \end{array} \right)$$

where simulated amount of MT released *in vitro* at time t can be estimated from

dissolution curve fitting of an investigated formulation by the Weibull equation (11).

A general form of Weibull equation is shown in equation 3.

Equation 3.

$$A_t = A_\infty \{ 1 - \exp[-(t/\beta)^\alpha] \}$$

Where A_t is the cumulative release in %, A_∞ is the cumulative % release at time

infinity, t is time, β is a time scaling parameter, and α is a parameter associated with

shape of the dissolution profile ($\beta > 0$ and $\alpha > 0$).

Generation of MT Plasma Concentration Curves

MT administered intravenously is best described by assuming a two

compartment model (10). However, like most two compartment drugs, when MT is

administered orally the absorption is slower than distribution and the resultant data are

best described by assuming a one-compartment model behavior (12). MT plasma

concentration curve is generated from estimated *in vivo* absorption rate which is

approximated as a large series of zero order input functions. For time during which an

input i occurs, change in plasma concentration is given by assuming a one-

compartment open model with multiple changing zero-order inputs at many different

as shown in equation 4.

Equation 4.

$$C(t) = \frac{(k_i)}{VK} \{ 1 - \exp[-K(t - t_{begin, i})] \}$$

Where k_i is the input rate, $t_{begin, i}$, is the time that the ith input begins, $K = 1.24$ h^{-1} is

the elimination rate constant, and $V = 32.47$ L is the volume of distribution (10). k_i

changes every 2.4 minutes (determined by stepsize) to provide a good fit to the

observed MT plasma concentration vs. time curve. After the ith infusion has ended, change in MT plasma concentration is expressed as in equation 5.

Equation 5.

$$C(t) = \frac{k_i}{VK} \{ 1 - \exp[-K (t - (t_{end,i} - t_{begin, i}))] \} \exp[-K (t - t_{begin, i})]$$

Where $t_{end, i}$ is the time that the ith infusion ends. The contribution of all infusions are summed. Thus the simulated plasma concentration at time (t) is:

Equation 6.

$$\text{Simulated plasma conc.} = \Sigma C_i (t)$$

The convolution program is written in EXCEL 5.0 (Microsoft Corporation, Seattle, WA). The simulation allowed input to occur for up to 8 hours (could be more or less if desired) according to results of deconvolution of the pilot study (3).

Modeling Technique 2

Unlike in modeling technique 1, which prediction is less flexible due to the rather fixed values of Fvr (t), simulation of MT plasma profiles using modeling technique 2 are generated from two separated parts based on drug release rate. In this method, determination of the fraction of IR and SR in a MT formulation is required. Convolution of blood drug concentration data is generated by determining the plasma concentration to be expected from each of the two apparent drug input functions (first-order absorption from the IR part, and a series of zero-order inputs (as ki) determined by the SR part), and summing them (8), i.e.,

Equation 7.

$$C(t) = C_{sus}(t) + C_{im}(t)$$

Where $C_{sus}(t)$ is plasma concentration at time t following the SR drug input , and $C_{im}(t)$ is plasma concentration at time t resulting from first order absorption from the IR portion in a dosage form. As a result, if there is difference in bioavailability between IR and SR MT formulation, simulation can be separately evaluated. A polyexponential function is fitted to dissolution curves by a method of residuals (8) in order to determine the fraction of IR and SR portion in a SR dosage form, as well as to simulate dissolution-time profiles. The general equation is (8):

Equation 8.

$$A_t = A_{im} + \Sigma A_{sus\,i} \{1\text{-exp}\,[-K_{sus\,i}\,t\,]\}$$

Where A_t is the cumulative release in % at time t , A_{im} is the percentage of immediate release in a dosage form, $A_{sus\,i}$ is the percentage of the i sustained exponential portion, $K_{sus\,i}$ is the dissolution rate constant for the i sustained exponential part, and t is time.

Estimation of *In Vivo* Absorption Rate

In vivo absorption rate resulting from the *in vitro* SR portion of a formulation is estimated from the relationship in equation 9.

Equation 9.

$$\left(\begin{array}{l} \text{Simulated absorption rate} \\ in\ vivo\text{(t) resulting from a} \\ \text{sustained release portion} \end{array} \right) = R_{sus} \times \left(\begin{array}{l} \text{Simulated slow release} \\ \text{rate } in\ vitro\text{(t) of a} \\ \text{sustained release portion} \end{array} \right)$$

Where R_{sus} (described below) is 0.152 ± 0.045 (n=6) for formulation A, obtained from the slope of linear regression of plots between cumulative amount of MT released *in vitro* vs. cumulative amount of MT absorbed *in vivo* from 5 to 8 hours after administration of formulation A (given at 500 µg and 1000 µg) in six subjects as seen in Figure 3.1. It was assumed that after 5 hours of administration, absorption of the IR MT was complete, and all additional absorption was due only to the SR MT from the dosage form. Note that R_{sus} is an estimate of F, the function of dose absorbed from the SR portion of the formulation only.

Derivation of R_{sus}

From Figure 3.1, R_{sus} is obtained from the slope of linear regression of a plot between cumulative amount of MT released *in vitro* vs. cumulative amount of MT absorbed *in vivo* from 5 to 8 hours after administration of formulation A (given at 500 µg and 1000 µg). It was assumed that after 5 hours of administration, absorption of the IR MT was complete, and all additional absorption was due only to the SR MT from the dosage form.

t_i is time (h) after 5h. Then

$$\text{Slope} = \frac{\text{Cumulative MT absorbed } \textit{in vivo}\ (t_{i+1} - t_i)(\mu g)}{(t_{i+1} - t_i)\ (h)} \times \frac{(t_{i+1} - t_i)\ (h)}{\text{Cumulative MT absorbed } \textit{in vivo}\ (t_{i+1} - t_i)(\mu g)}.$$

$$R_{sus} = \frac{\text{Absorption rate } \textit{in vivo}\ (t_{i+1} - t_i)\ (\mu g/h)}{\text{Release rate } \textit{in vitro}\ (t_{i+1} - t_i)\ (\mu g/h)}$$

$$= \frac{\text{Cumulative MT absorbed, } \textit{in vivo}\ (t_{i+1} - t_i)\ (\mu g)}{\text{Cumulative MT released, } \textit{in vitro}\ (t_{i+1} - t_i)\ (\mu g)}$$
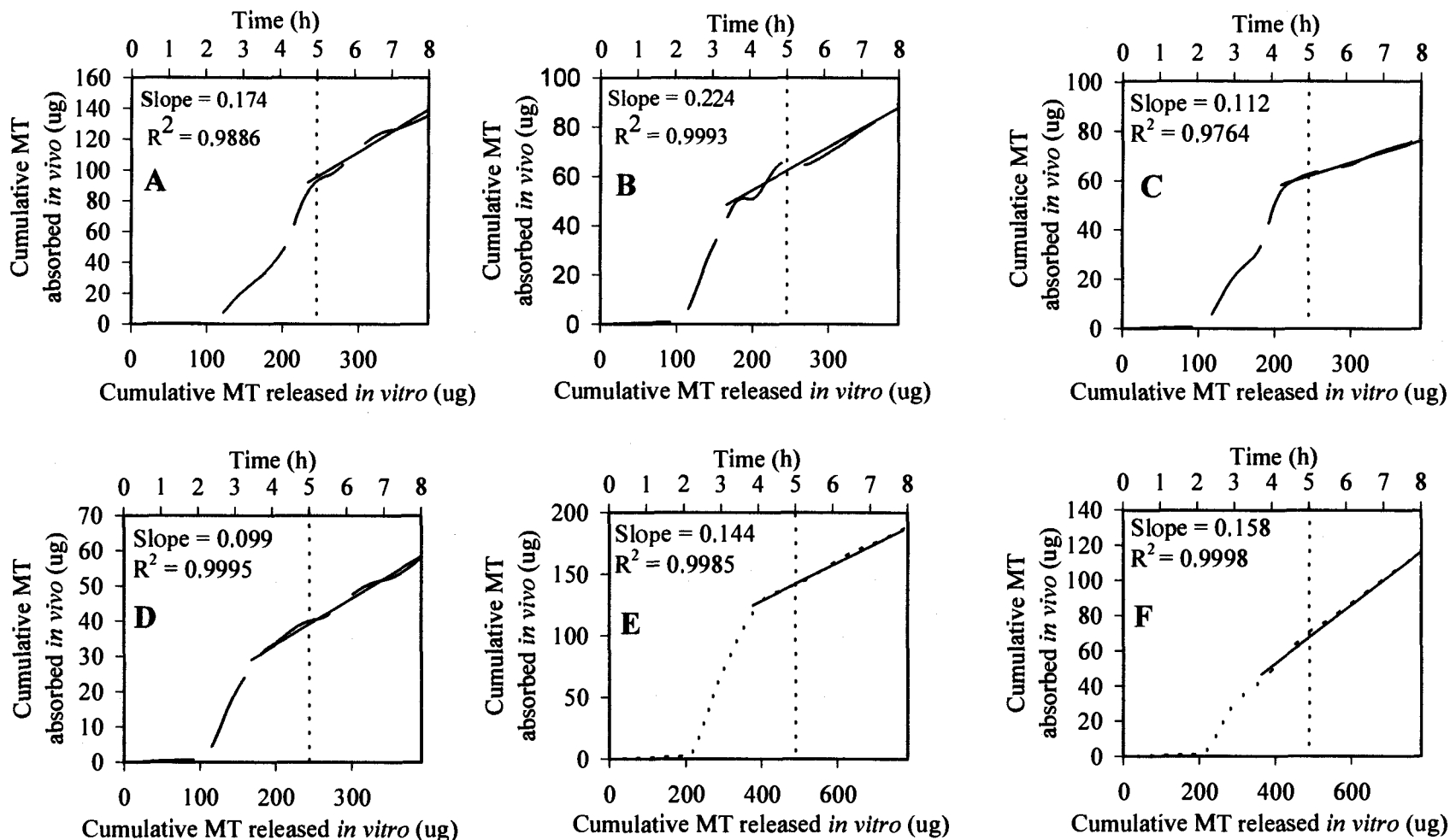
Figure 3.1: Cumulative amount of MT absorbed *in vivo* (µg) versus cumulative amount of MT released *in vitro* (µg) following administration of formulation A given at 500 µg (A, B, C, and D) and 1000 µg (E and F).

Since it was assumed that after 5 h absorption of MT was due only to the SR MT from the dosage form. Bioavailability of SR MT can be estimated from Rsus as shown above.

Generation of MT Plasma Concentration Curves

Convolution of MT plasma concentration data requires simulation of $C_{sus}(t)$ and $C_{im}(t)$ for modeling technique 2 as mentioned earlier. $C_{sus}(t)$ can be generated from the simulated absorption rate *in vivo* obtained from equation 9 by applying equations 4, 5, and 6 in technique 1. $C_{im}(t)$ is change in plasma concentration at time t resulting from first order absorption of the IR portion in a dosage form, and can be described as in equation 10 (one compartment open model with first-order absorption).

Equation 10.

$$C(t) = \frac{K_a \, F_{im} \, D_{im}}{(K_a - K) \, V} \, [\exp(-K \, t) - \exp(-K_a \, t)]$$

Where $K_a = 1.74 \ h^{-1}$ is the absorption rate constant (12), $K = 1.24 \ h^{-1}$ is the elimination rate constant, and $V = 32.47 \ L$ is volume of distribution (10). F_{im} is the fraction of IR dose (D_{im}) which is absorbed. D_{im} is the total IR dose in the dosage form. For example, formulation A consisted of 22.86 % A_{im}; thus, total IR dose in a formulation given to subjects in the pilot study is 114.3 µg and 228.6 µg of the total dose of 500 µg and 1000 µg, respectively. F_{im} was estimated from deconvolution of the pilot study data i.e.,

Equation 11.

$$
F_{im} = \left(\begin{array}{c} \text{Total amount} \\ \text{absorbed } in \ vivo \\ \text{after 8 h} \end{array} - \begin{array}{c} \text{Total amount absorbed } in \\ vivo \text{ from the slow release} \\ \text{part after 8 h} \end{array} \right) \div D_{im}
$$

Total amount absorbed *in vivo* after 8 hours was obtained from deconvolution. Total

amount absorbed *in vivo* from the SR portion after 8 hour was received from

integration of equation 9. When product A was given at a dose of 500 μg or 1000 μg,

the corresponding F_{im} were 0.30 and 0.31, respectively. Thus, average of F_{im} (= 0.305)

was then used for prediction of MT plasma concentration data.

Experimental Section

General Procedures

Simulation results for expected plasma concentrations are now compared to

observed plasma concentrations using both modeling techniques and MT plasma

concentration data obtained from oral administration of a new formulation (B) in 13

subjects. This formulation contained exactly the same SR MT formulation as that of

formulation A (3) except formulation B consisted of less IR MT (10% IR and 90% SR

MT). Seven healthy subjects (4 females and 3 males) over age seventy and five

healthy subjects (4 females and 2 males) under age thirty, were all given formulation B

at three different doses of 200 μg (20 μg IR plus 180 μg SR MT), 400 μg (40 μg IR

plus 360 μg SR MT), and 800 μg (80 μg IR plus 720 μg SR MT).

Another SR formulation C, which was similar to formulation A except formulation C did not contain any IR MT was administered to a panel of four healthy volunteers (males aged between 35 to 50). Oral single doses of either 380 μg or 760 μg of MT SR were administered at 9.00 a.m. with 8 oz of water. Subjects were fasted overnight and four hours after dosing. Area under MT plasma concentration-time curves (AUC) was computed using the trapezoidal rule. Time to reach peak (Tmax) and peak plasma concentration (Cmax) were obtained by visual inspection of concentration-time curves. Dissolution tests were performed in triplicate using the USP dissolution apparatus I (basket method). Resultant dissolution data were fitted to mathematical functions: the Weibull equation and a polyexponential function using nonlinear least squares regression (EXCEL 5.0).

Analytical Methods

Plasma MT concentrations were determined by a highly sensitive and specific GC/MS assay (13). MT concentration in non-biological fluids was determined using an HPLC system with UV detection (2).

RESULTS AND DISCUSSION

Comparison of observed and predicted plasma concentrations based on the deconvolution/convolution methods after oral administration of formulation A (500 mg, and 1000 mg) are shown in Figure 3.2. Results are quite good, as expected, since the model was built using data from formulation A.
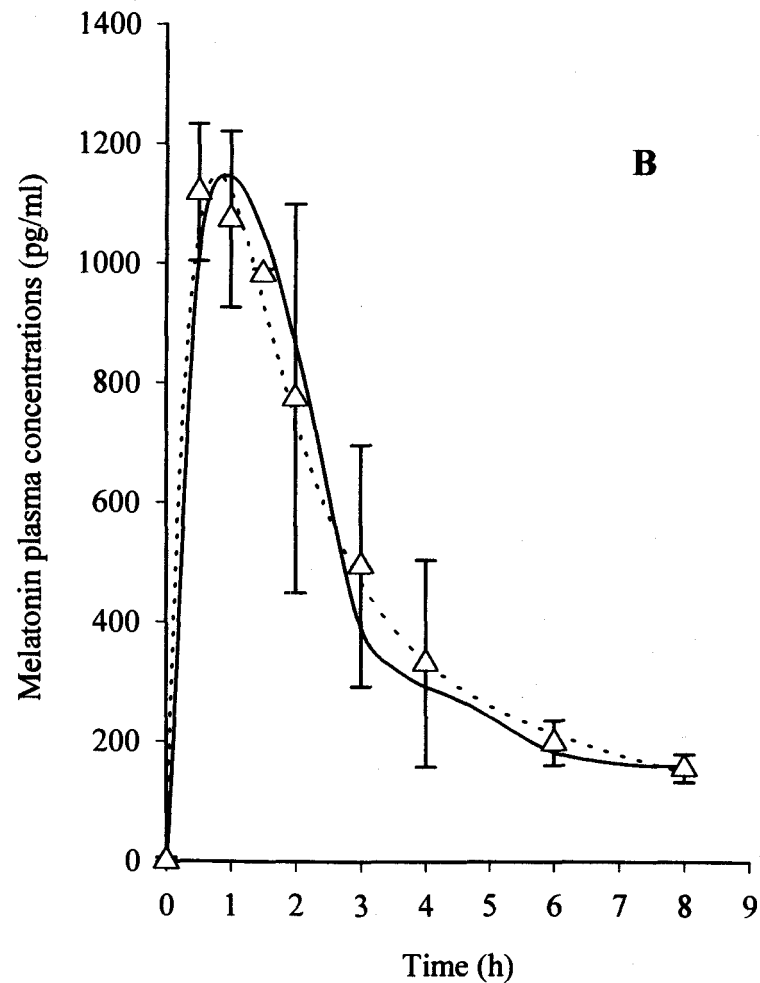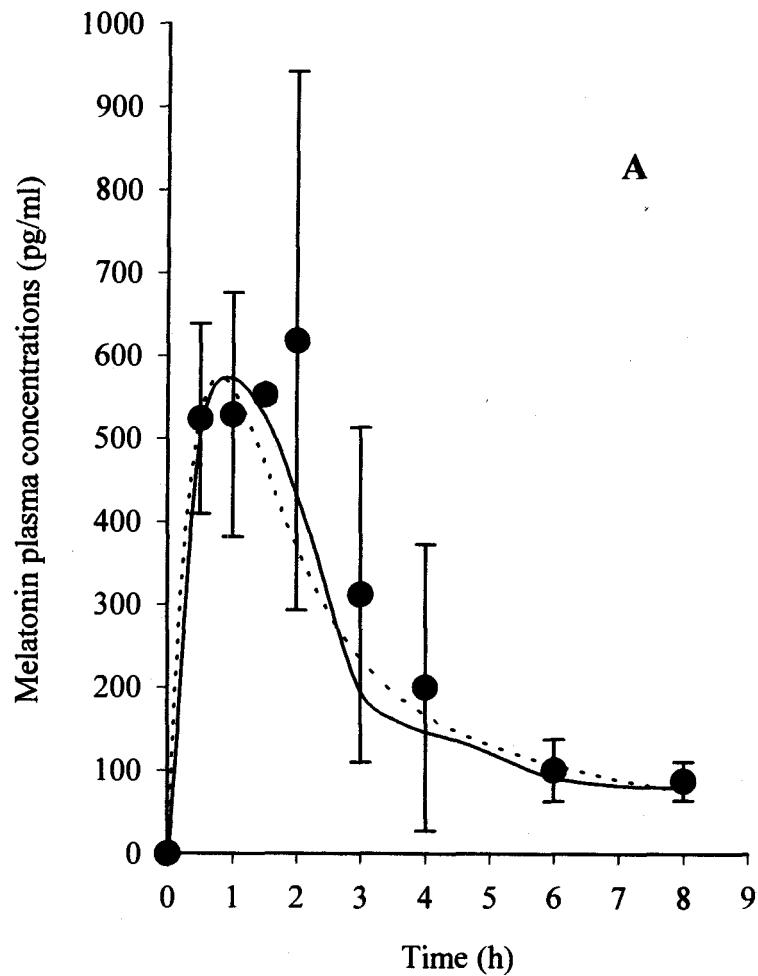
Figure 3.2: Comparison between observed and predicted MT plasma concentration time curves following oral administration of formulation A at doses of (●) 500 µg (n=4), and (△) 1000 µg (n=2), with simulation (——) technique 1, and (------) technique 2.

Good prediction from both modeling techniques is also obtained when they are applied to MT plasma concentration time profiles following oral administration of a different MT sustained release formulation B (containing 10% IR and 90% SR) at total doses of 200 mg, 400 mg, and 800 mg in both old and young subjects (n=13). Results of the simulation are shown in Figure 3.3.

Although the use of pharmacokinetic data from other studies in different subjects has limitations, the application of literature reported parameter values used in the modeling (10, 12) were supported by the relatively good fits in Figures 3.2 and 3.3.

Comparison of mean observed dissolution data fitted with both the Weibull and polyexponential equations for formulations A and C are presented in Figure 3.4. Although formulation C does not contain IR MT, about 6.6% is rapidly dissolved (Figure 3.4). 25 mg and 50 mg are used as Dim in Equation 8 when applying technique 2 to formulation C given at doses of 380 mg and 760 mg, respectively. Formulation C releases MT at a slower rate than formulation A but is still predicted to produce significant plasma MT concentrations when administered at doses of either 380 mg or 760 mg as shown in Figure 3.5. Observed plasma concentrations following the 380 mg dose are far below what is predicted based on the models as derived from evaluation of formulation A and certainly does not fit as well as is observed with formulation B (compare fits in Figures 3.2, 3.3 and 3.5(i)). The observed curves for formulation C are close to the expected plasma concentration profiles obtained through simulation techniques 1 and 2 only for the dose of 760 mg (Figure 3.5(ii)). However, the good fit of MT plasma profile following 380μg dose can be obtained when
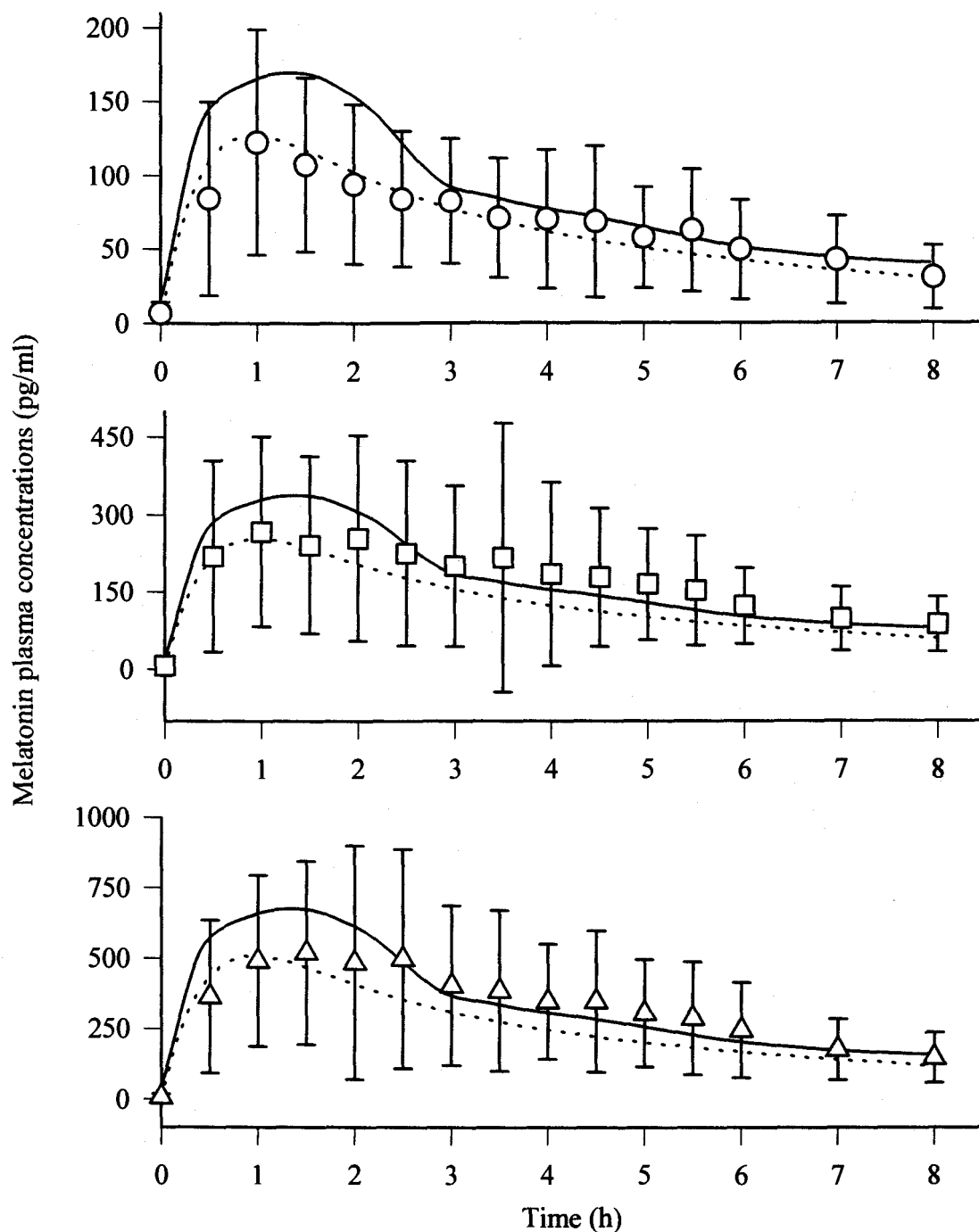
Figure 3.3: Observed and expected MT plasma concentrations following
formulation B given to old and young subjects (n=13) at
(◯) 200 µg, (☐) 400 µg, and (△) 800 µg,
with simulation (———) technique 1, and (· · · · ·) technique 2
with Fim = 0.305 and Rsus = 0.152 derived from evaluation of
formulation A.
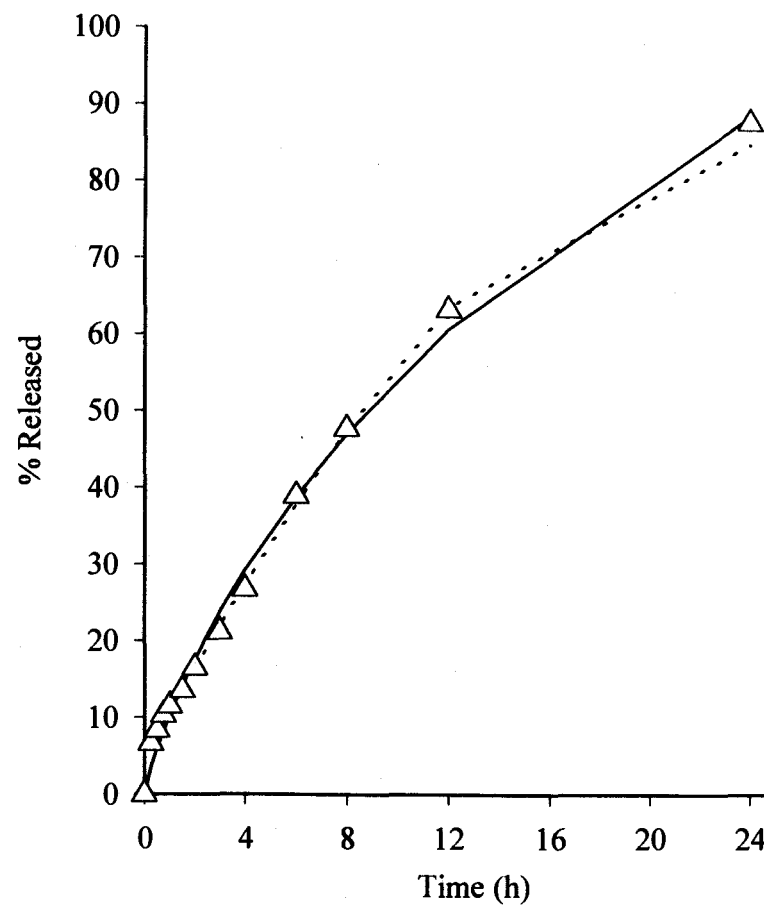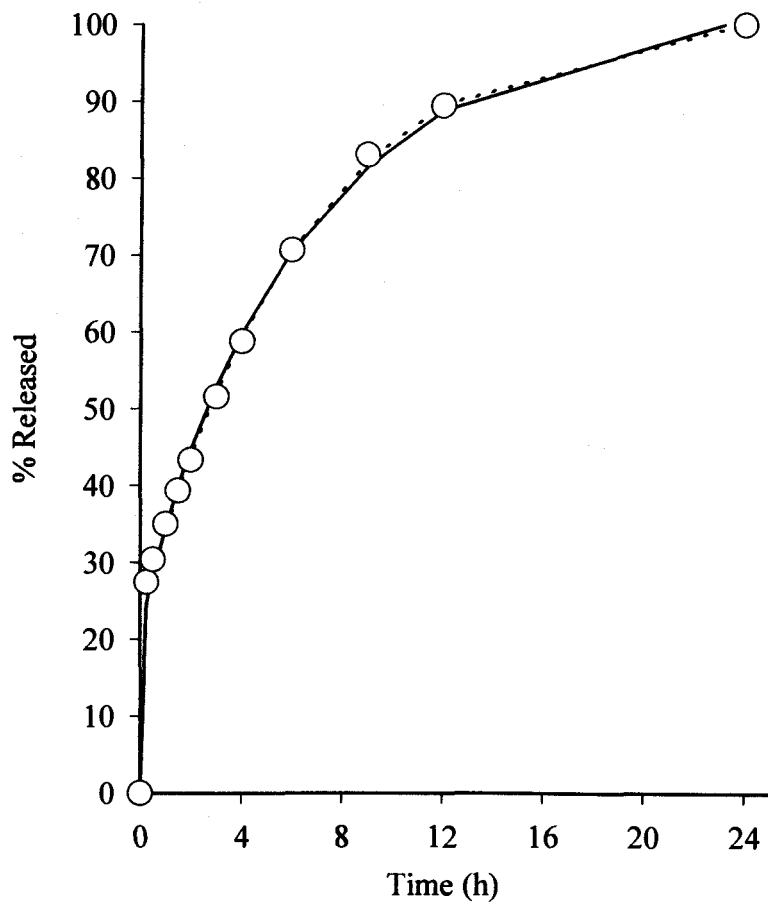
Figure 3.4: Release profiles of MT from SR formulations, (◯) formulation A, and (△) formulation C with (———) Weibull equation and (· · · · ·) polyexponential equation simulation. Sample standard error (n=3) are too small to show. Formulation C releases MT at slower rate than formulation A ($t_{50\%}$ = 8.6 hours and 2.8 hours for formulation C and A, respectively).
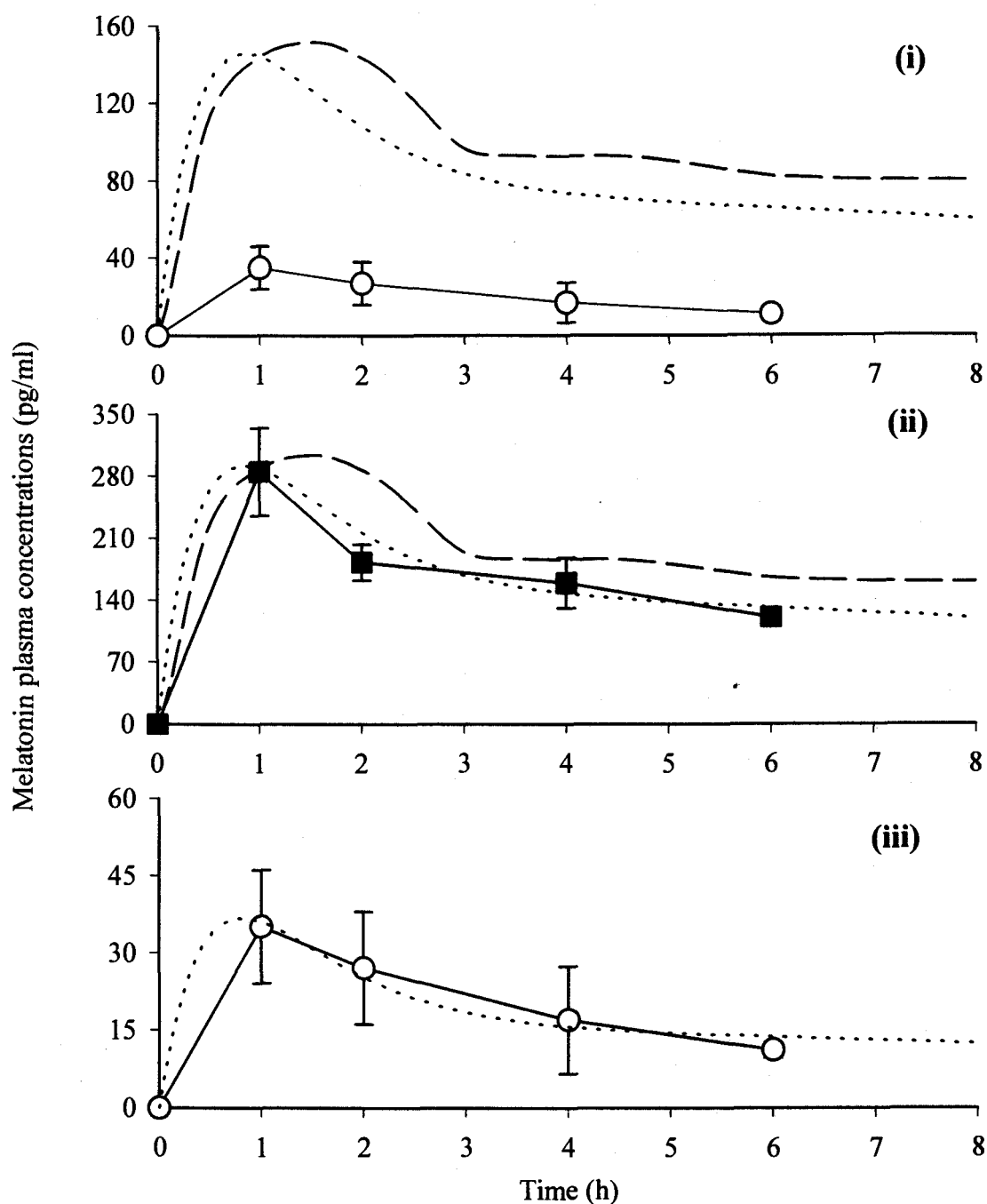
Figure 3.5: Comparison between observed and expected MT plasma concentrations following formulation C given at (—O—) 380 μg (n=2), and (—■—) 760 μg (n=2), with simulation (— —) technique 1, and (·····) technique 2. For (i) and (ii) the simulations based on *in vitro-in vivo* correlation derived from evaluation of formulation A, (iii) the simulation generated by technique 2 with adjusted Fim and Rsus (Fim = 0.08 and Rsus = 0.03) using non-linear regression best fit to the observed data of 380 μg.

technique 2 was applied with "adjusted" Fim and Rsus using non-linear regression (Figure 3.5(iii)). The optimized fit in Figure 3.5(iii) revealed reduce in bioavailability of both IR (Fim) and SR MT (Rsus) at 380 μg SR dose. Bioavailability of IR MT and of SR MT reduced from 30% and 15% (after administration of formulation A at 500 μg and 1000 μg) to 8% and 3% (after administration of formulation C at 380 mg), respectively.

Noncompartmental pharmacokinetic parameters of formulations A, B and C are displayed in Table 3.1. Disproportional increase in Cmax and AUC were found after administration of formulation C at 380 mg and 760 mg. In an additional trial with the 380 mg dose of formulation C in three subjects in France (unpublished data), negligible plasma concentrations of MT were produced. Using technique 2 to fit the observed plasma concentration-time profiles, bioavailability of SR MT given at 760 mg and 380 mg can be estimated to be about 13% and 3%, respectively.

Reduced bioavailability due to gastrointestinal and hepatic first-pass metabolism of orally administered drug is a well-known pharmacokinetic phenomenon (14, 15, 16). MT is extensively metabolized by a first pass effect (17, 18, 19). Slow input rates can become very important if MT first pass metabolism is saturable. As input rate is decreased, bioavailability is decreased. Study of oral bioavailability of MT carried out in dogs also indicated dose-dependent bioavailability (20). Significant reduce in input rate may pronounce change in systemic bioavailability. The very low plasma concentrations of MT in 5 subjects from the 380 μg SR dose is not predicted by non-saturable first pass metabolism and linear pharmacokinetics. The finding of dose-

Table 3.1: Pharmacokinetic parameters (mean ± S.E.) of SR formulations A, B and C.

Dose (μg)	Cmax (pg/ml)	Tmax (h)	AUC (pg h/ml)
Formulation A			
500 (n=4)	651 ± 144.1	1.07 ± 0.54	2364 ± 947 (from 0 to 8 h)
1000 (n=2)	1178 ± 690.4	0.59 ± 0.19	4281 ± 652 (from 0 to 8 h)
Formulation B			
200 (n=11)	123 ± 69.0	1.15 ± 0.36	565 ± 348.0 (from 0 to 12 h)
400 (n=11)	313 ± 229.9	1.38 ± 0.81	1572 ± 1092.8 (from 0 to 12 h)
800 (n=11)	573 ± 40.1	1.8 ± 1.70	3990 ± 1891.0 (from 0 to 12 h)
Formulation C			
380 (n=2)	35 ± 11.0	0.96 ± 0.056	125 ± 48.7 (from 0 to 6 h)
760 (n=2)	285 ± 49.5	0.97 ± 0.001	1019 ± 34.8 (from 0 to 6 h)

dependent bioavailability of MT after administration of low dose (380 µg) SR

formulations was not found previously in the study of higher dose (500 µg, and 1000

µg) SR formulation A (3).

Lane and Moss reviewed MT bioavailability by applying a calculation using

hepatic extraction ratio and suggested prominent first pass hepatic metabolism and

reduced bioavailability for orally administered MT (18). Bioavailability for 2.5 mg of

IR MT was estimated to be 3-6% (18). If a dose of 2.5 mg IR is input over one hour or

less, then the input rate is about 2.5 mg/h. A 1 mg or 0.4 mg dose in SR might be

input over 6 hours (0.167 mg/h or 0.067 mg/h). This fifteen to thirty-eight fold

decrease in input rate is expected to decrease bioavailability. Wagner et. al suggested

that the sensitivity of the change in bioavailability with change in input rate will

depend on the magnitude of the Km* (15). An accurate relative decrease in MT

bioavailability as input is decreased cannot be calculated without Km*. However, the

bioavailability of a SR MT releasing 0.167 mg/h or 0.067 mg/h is expected to be less

than 1% if 2.5 mg IR MT only has a bioavailability of about 3%. Thus, the poor fit for

predicted plasma concentrations compared to the very low MT concentrations

produced by a 380 mg dose of slow input from formulation C in five subjects is

consistent with the literature. Disproportionally low bioavailability from a low dose

coupled with a slow input rate results in violation of the model requirement for linear

pharmacokinetics; which means the predicted lines should not fit the observed data if

estimated bioavailability used in the prediction is dose dependent. It is surprising that

the 760 mg dose of formulation C and all doses of formulation B are well described by

the modeling which suggests a much higher bioavailability than expected from the literature on IR MT coupled with what is known regarding drug input rates and first pass metabolism, i.e. dose calculation and bioavailability from model simulation and observed data are inconsistent with estimation based on literature. Average production of MT by the pineal gland is 28.8 mg/day (18). Oral SR doses necessary to provide 28.8 mg/day are predicted to be more than 3 mg if bioavailability is a maximum of 1% for slow input rates. However, both data and modeling presented herein demonstrate that normal MT plasma concentrations may be mimicked or supplemented to normal concentrations with SR formulations of much smaller doses than previously recognized.

Summary of the two modeling techniques based on deconvolution/convolution of MT plasma concentration-time profiles following oral SR dosage form administration is presented in Table 3.2.

Table 3.2: Summary of modeling techniques based on deconvolution/convolution of MT plasma concentration-time profiles following oral sustained release dosage form administration.

Issue	Modeling technique 1	Modeling technique 2
Equation used for fitting a dissolution- time profile	The Weibull equation is used to estimate cumulative amount of MT released *in vitro* at each time (t).	A multiexponential equation is used to separate a portion of MT in a formulation that is a fast or slow release as well as to estimate cumulative amount of MT released *in vitro* from the SR portion.
Connection between *in vitro/in vivo* drug behavior	Fvr(t) = ratio of cumulative amount of MT absorbed *in vivo* at time t over cumulative amount of MT released *in vitro* (dissolution) at time t Fvr(t) is a function of time	Rsus = slope of linear regression fitting on cumulative amount of MT absorbed *in vivo* versus cumulative amount of MT released *in vitro* from 5 to 8 h. It is assumed that first-order absorption from IR portion is complete after 5 h. Rsus is a fraction of the release rate *in vitro* that becomes the absorption rate *in vivo*.
Convolution process	Application of a series of zero-order inputs to a one compartment open model	Application of one compartment open model with parallel first order and a series of zero order inputs.
Pharmacokinetic parameters used in the convolution process	K, V from Iguchi et. al. (10) Fvr(t)	K, V from Iguchi et. al (10) Ka from Waldhauser et. al. (12) Fim (fraction of dose absorbed) for first-order absorption, estimated in the modeling process. Rsus
Comment	Less flexible than technique 2.	Also useful as a tool for estimation of both IR and SR MT bioavailability.
Model improvement	Need more *in vitro/in vivo* data for different input (release) rates.	Better estimation of Fim and Rsus as IR dose/input rate changes
Limitation of the model	Applicable only in the range of linear MT pharmacokinetics/dose-independent MT bioavailability, and doses examined herein.	Optimum prediction is based on good estimation of MT bioavailability.

CONCLUSION

Two simulation approach to predict MT plasma profiles following oral controlled release formulations based on *in vitro* dissolution were proposed. The simulation is useful for product development of MT. In modeling technique 1, an *in vitro-in vivo* correlation is valid only in the range of linear pharmacokinetics/dose independent bioavailability. However, it appears that oral MT bioavailability may be dependent upon input rate from the formulation. In the presence of dose-dependent bioavailability, the correlation between *in vitro* dissolution and *in vivo* absorption changes. In this case, application of modeling technique 2 is still valid for prediction when characteristics of MT dose-dependent bioavailability are fully described. Further study is needed to define the relative change in bioavailability with change in input rate. The general model approach may also be applied to other drugs to obtain a high correlation between *in vitro* dissolution and *in vivo* drug behavior.

REFERENCES

1. Petterborg, L.J.; Thalen, B.E.; Kjellman, B.F.; Wetterberg, L. Effects of melatonin replacement on serum hormone rhythm in a patient lacking endogenous melatonin. Brain. Res. Bull. 27(2), 181-185 (1991).

2. Konsil, J.; Parrott, K. A.; Ayres, J. W. Development of a transdermal delivery device for melatonin *in vitro* study. Drug Dev. Ind. Pharm. 21(12), 1377-1387 (1995).

3. Lee, B., Parrott, K.A., Ayres, J.W., Sack, R.L. Design and evaluation of an oral controlled release delivery system for melatonin in human subjects Int. J. Pharm. 124, 119-127 (1995).

4. Benes, L.; Brun, J.; Claustrat, B.; Degrande, G.; Ducloux, N.; Geoffriau, M.; Horriere, F.; Karsenty, H.; Lagain, D. In Melatonin and the pineal gland from basic science to clinical application; Touitou, Y.; Arendt, J.; Pe'vet, P.; Eds.; Elsevier Science Publishers B.V., Amsterdam, the Netherlands, 1993; pp 347.

5. Benes, L.; Degrande, G.; Ducloux, N.; Horriere, F.; Karsenty, H.; Proceed Intern.Symp. Control. Rel. Bioact. Mater., Controlled Release Society, Inc., 21, 551-552 (1994).

6. Brockmeier, D. Acta Pharm. Technol. 32(4) 164-167 (1986).

7. Rossi, S.; Ferri, F.; Bonferoni, M. C.; Caramella, C.; La Manna, A.; De Bernardi Di Valserra, M.; Feletti, F. A computer-aided simulation approach in the development of prolong release formulation. Boll. Chim. Farmaceutico. 130(11), 443-448 (1991).

8. Leeson, L. J.; Adair, D.; Clevenger, J.; Chiang, N. The *in vitro* development of extended-release solid oral dosage forms J. Pharm. and Biopharm. 13(5), 493-514 (1985).

9. Kalns, J. E. Pharmacokinetic and pharmacodynamics of 1) Oral sustained release acetaminophen suspension in children; 2) Potassium chloride in adults. Ph.D. Thesis, Oregon State University, 1993, pp. 64 -104.

10. Iguchi, H., Kato, K.I., Ibayashi., H. Melatonin serum levels and metabolic clearance rate in patients with liver cirrhosis., J. Clin. Endocrinol. Metab. 54, 1025-1027 (1982).

11. Lagenbucher, F. Linearization of dissolution rate curves by the Weibull distribution. J. Pharm. Pharmacol. 24, 979-981 (1972).

12. Waldhauser, F.; Waldhauser, M.; Lieberman, H. R.; Deng, M. H.; Lynch, H. J.; Wurtman, R. J. Bioavailability of oral melatonin in humans. Neuroendocrinol. 39, 307-313 (1984).

13. Lewy, A.J., Markey, S.P. Analysis of melatonin in plasma by gas chromatography negative chemical ionization mass spectroscopy, Science 201, 741-743 (1978).

14. Keller, F.; Kunzendorf, U.; Walz, G.; Haller, H.; Offermann, G. Saturable first-pass kinetics of propanolol J. Clin Pharmacol, 29, 240-245 (1989).

15. Wagner, J.G., Antal, E.J., Elvin, A.T., Gillespie, W.R., Pratt, E.A., Albert, K.S. Theoretical decrease in systemic availability with decrease in input rate at steady-state for first-pass drugs Biopharm. Drug Disposit. 6, 341-343 (1985).

16. Robinson, J. R., Vincent, H. L., Ed, Controlled Drug Delivery Fundamentals and applications, Marcel Dekker, Inc.: New York, 1987; pp 24-25

17. Vakkuri, O.; Leppaluoto, J.; Kauppila, A. Oral administration and distribution of melatonin in human serum, saliva and urine. Life Sci. 37, 489-495 (1985).

18. Lane, E. A.; Moss, H. B. Pharmacokinetics of melatonin in man: first pass hepatic metabolism. J. Clin. Endocrinol. Metab. 61, 1214-1216 (1985).

19. Arendt, J. In Melatonin and the mammalian pineal gland; Chapman & Hall, London, UK, 1995, pp. 40.

20. Yeleswaram, K., Mclaughlin, L.G., Knipe, J.O., Schabdach, D. Oral bioavailability of melatonin in the rat, dog, and monkey J. Pineal. Res. in press (1997).

CHAPTER 4

THEORETICAL APPROACH TO SATURABLE FIRST PASS METABOLISM OF MELATONIN

ABSTRACT

Melatonin (MT) plasma concentrations following oral administration are highly variable among subjects. This variation is probably caused by differences in individual first pass metabolism which may be dose-dependent. In this work an attempt to describe change in bioavailability (F) with change in drug release rate from formulation was made using the theoretical model previously published by Wagner et al. Data was employed from previous study of MT SR formulation orally given to 13 young and old healthy subjects at three different doses (200 μg, 400 μg, and 800 μg). F at any time was estimated from *in vitro* dissolution and *in vivo* absorption. Steady state bioavailability (Fss) was determined as F at which its first derivative with respect to time was zero. The slopes and intercept of plots between Ln(Fss) and steady state drug release rate (Rss) were used to estimate the individual parameters of saturable first pass effect; 1/QK*m and V*m (Q = liver blood flow, Km = the Michaelis Menten constant, and V*m = the maximum velocity of metabolism). Prediction of F with different drug release rate was then possible using these obtained parameters. Accuracy of modeling results was based on simulation result of individual MT plasma profiles using predicted F and modeling technique 2 (Chapter 3). The plots between Ln(Fss) and Rss fitted well with the theoretical equations in 7 subjects. Application of

predicted F improved predictability of modeling technique 2. Simulation results of MT plasma concentrations were generally acceptable. The predicted concentrations were within 30% of the observed values. Combination of the approach to MT saturable first pass effect and modeling technique 2 may be useful for optimization of drug release rate from SR formulation of MT.

INTRODUCTION

Power in prediction of melatonin (MT) plasma concentration-time curve following oral administration using the two modeling techniques described earlier in Chapter 3 will be limited when there is large variation among individual MT plasma profiles. Exogenous MT orally administered undergoes extensive first pass effect (1, 2). Very large individual variation are seen in its peak plasma concentrations (at least 25 fold) and attributed to differences in absorption (1, 3). Oral bioavailability of MT could vary from less than 1% to higher than 70% depending on dose and nutritional status (1, 2).

Possibility of dose-dependent bioavailability of MT was experimentally supported in animal study (4). Study of oral bioavailability of MT in dogs indicated dose-dependent bioavailability i.e. the oral bioavailability decreased with reduction in dose (4). The studies in our laboratory revealed that MT bioavailability following oral SR formulations is probably drug release rate-dependent (bioavailability reduced with decrease in dose/drug release rate). Administration of sustained release (SR) formulation C (Chapter 3) at 380 µg and 760 µg to four human subjects showed

disproportional increase in area under plasma concentration-time curve (AUC) and maximum plasma concentration (Cmax). In this case, bioavailability needed to be adjusted to obtain good prediction result using modeling technique 2 (Chapter 3). Thus, assumption of MT linear pharmacokinetics or non-saturable first-pass effect may not be sufficiently described the *in vitro/in vivo* correlation. However, due to small number of subjects included in the study as well as history of high variation in individual MT plasma profiles, it is difficult to conclude that saturable first-pass metabolism of MT involves in the poor prediction result. Development of a model to predict change in bioavailability with change in drug release rate may provide not only a better estimation of individual MT plasma profile but also a rough investigation of possibility of saturable first pass metabolism of MT orally given to human subjects.

The purposes of this work were to investigate possibility of saturable first-pass effect based on theoretical model previously proposed by Wagner et al. (5) as well as to improve accuracy in prediction of individual MT plasma concentrations following oral administration. Mathematical technique to estimate change in bioavailability with change in drug release rate was developed using data from previous study of MT SR formulation given to 13 young and old subjects at three different doses (Chapter 1). Accuracy of modeling results is discussed based on simulation results using predicted bioavailability obtained from the new modeling approach and modeling technique 2 (Chapter 3).

MATERIALS AND METHODS

Background information

The sinusoidal perfusion model of hepatic elimination.

Mathematical equations of theoretical decrease in bioavailability with decrease in input rate at steady-state for first-pass drugs previously described by Wagner et al. (5) were based on the sinusoidal perfusion model, a model describing pharmacokinetics of hepatic elimination. Equations for the sinusoidal perfusion ('parallel tube') model were developed by Bass et al.(6, 7, 8, 9, 10). The original model was an undistributed model (6) which later led to a distributed model (7). The word 'distribution' was referred to the distribution of enzyme in the sinusoids of the liver which metabolize drug. In this model, the liver is viewed as a set of parallel tubes (representing the sinusoids) (6, 11, 12, 13, 14, 15). Blood flow rate is said to be the same in all tubes. Uptake by the hepatocytes is a function of concentration. Concentration decreases exponentially along the tubes in the direction of flow (16). Studies of drugs including bromsulphthalein, propanolol, and thyroxine demonstrated such gradients (17, 18, 19, 20). The net result of the model is that the logarithmic average of the inflow and outflow drug concentrations in the liver must be used in calculating parameters of the model (21). Calculation of nonlinear pharmacokinetic parameters of first pass metabolism was previously demonstrated using the single dose oral and intravenous and steady-state oral plasma concentration time data (21). Herein,

a new mathematical technique was developed using the single oral plasma concentration time profile of MT SR formulation given at 3 different doses.

Theoretical decrease in oral bioavailability with reduction in drug input rate

Theoretical decrease in systemic availability with decrease in input rate at steady-state for first-pass drugs was previously proposed by Wagner et. al (5). The theoretical model suggests possibility of applying bioavailability received from oral administration of drug at two or more doses/drug release rate to predict bioavailability of new doses/formulations with different drug release rate. For a comprehensive explanation of the application of this theoretical model to prediction of individual MT plasma concentration-time curve, the concept of the model is described below.

Wagner et. al (5) described a mathematical function relating all important variables for the sinusoidal perfusion model at steady-state as

<u>Equation 1</u>

$$v = Q K^*m \, Ln \frac{Co}{Ci} + V^*m$$

Where

v = the velocity of metabolism of the drug in the liver (mass/time)

Q = the liver blood flow (volume/time)

K^*m = the Michaelis Menten constant (mass/volume) of the sinusoidal perfusion model

Co = the outlet (venous concentration) of unchanged drug being metabolized (mass/volume)

C_i = the inlet (arterial) concentration of drug (mass/volume)

V^*_m = the maximal velocity of metabolism (mass/volume) of the sinusoidal

perfusion model

The velocity of metabolism of the drug in the liver (v) was said to be equal to constant rate of input of the drug (R, mass/time) at steady-state. In addition, the ratio of drug concentration after and before metabolism (C_o/C_i) at the steady-state would be the same as bioavailability of the drug (F).

Therefore,

Equation 2

$$Ln\ F = -\frac{(V^*_m - R)}{Q\ K^*_m} = \frac{-V^*_m}{Q\ K^*_m} + \left(\frac{1}{Q\ K^*_m}\right) R$$

Equation 3

$$F = exp^{\frac{-(V^*_m - R)}{Q\ K^*_m}}$$

F = C_o/C_i is the bioavailability of the drug.

R = drug input rate (mass/time)

Wagner at. al (5) also pointed out that a plot between Ln F and R should yield a straight line with positive slope (if F increases with R) and negative intercept. The slope is equal to $1/QK^*_m$ and the intercept is equal to $-V^*_m/QK^*_m$.

The relationship between relative bioavailability (F_n/F_i) from two oral treatments (n and I) with difference in drug release rate (R_n and R_i) was derived as shown in Equation 4 and 5.

Equation 4

$$\frac{Fn}{Fi} = \exp^{\frac{-(Ri - Rn)}{Q K^*m}}$$

Equation 5

$$-\operatorname{Ln}\frac{Fn}{Fi} = \frac{(Ri - Rn)}{Q K^*m}$$

where

Fn   = bioavailability at given drug input rate of Rn

Fi   = bioavailability at given drug input rate of Ri

Rn and Ri   = drug input rate (mass/time)

Wagner et al. (5) suggested that if bioavailability decreased with reduction in dose/drug release rate or Ri > Rn and Fi > Fn, the plot between - Ln (Fn / Fi) versus (Ri - Rn) would yield a straight line, passing through the origin, with positive slope equal to 1/Q K*m. The sensitivity of the change in relative bioavailability with change in drug release rate after oral administration would depend on the magnitude of the K*m value if Q is constant. The relative bioavailability is independent of V*m value. They also pointed out advantage of using the relationship to optimize rate for a SR products to obtain satisfactory bioavailability during development.

Saturable first pass metabolism and modeling of MT plasma profile

In this study, approach for estimation of saturable first-pass kinetic parameters using bioavailability at steady-state, deconvolution technique, and *in vitro/in vivo* correlation is proposed. Data from previous study of oral SR formulation of MT

administered at 3 different doses in 13 old and young subjects was used in simulation (Chapter 1). For completion of this work, data collection procedures of previous MT study is briefly described below.

Data collection (Chapter 1)

Seven healthy subjects (4 females and 3 males) over age seventy and six healthy subjects (4 females and 2 males) under age thirty were included in the study. They received oral administration of SR formulation containing 10% immediate release (IR) and 90% SR of MT at total dose of 0.2 mg (0.02 mg IR MT plus 0.18 mg SR MT), 0.4 mg (0.04 mg IR MT plus 0.36 mg SR MT), and 0.8 mg (0.08 mg IR MT plus 0.72 mg SR MT) in a crossover fashion. IR MT and SR MT, filled separately in gelatin capsules (no. 4), were simultaneously administered to the subjects at the dosing time. Subjects fasted over night and for twelve hours after dosing. Caloric and fluid replacement with fruit juice and corn starch supplements were given orally ad lib. Blood samples were collected at 0.5 h prior to the dosing to provide baseline values and at 0, 0.5, 1, 1.5, 2, 2.5, 3, 3.5, 4, 4.5, 5, 5.5, 6, 7, 8, 9, 10, 11, and 12 h post dosing. Plasma MT concentrations were determined by a highly sensitive and specific GC/MS assay (22).

Modeling approach

Scheme of modeling approach on MT saturable first pass metabolism is illustrated in Figure 4.1. Assumptions of the model are
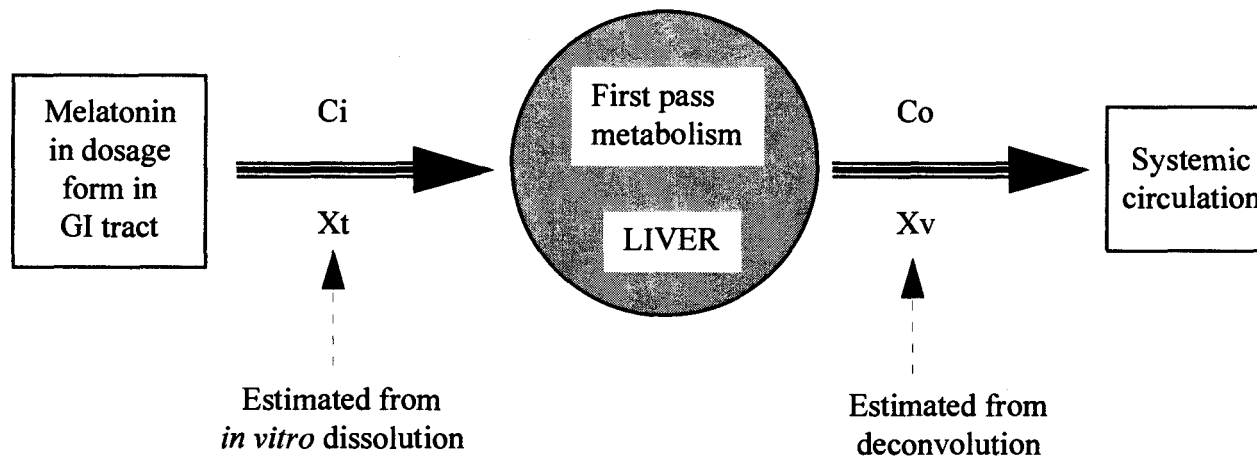
Ci = the inlet concentration of melatonin (μg/ml) (Equation 1)

Co = the outlet of unchanged melatonin being metabolized (μg/ml) (Equation 1)

Xt = total amount of melatonin released from dosage form (μg)

Xv = total amount of melatonin absorbed into the systemic circulation (μg)

Assumption : Co / Ci ≈ Xv / Xt ≈ F

: Hepatic first pass effect is the dominant process.

Figure 4.1: Scheme of theoretical approach on saturable first pass effect of melatonin.

1. The ratio of drug concentration after and before first pass effect is approximately equal to ratio of amount of drug absorbed in the body and amount drug released from formulation. The ratio is also equal to bioavailability.

2. Hepatic elimination mainly contributes to MT first pass metabolism.

Steps involved in simulation

1. Determination of steady-state bioavailability (Fss) and steady-state drug release rate (Rss) for each individual subject following oral administration of MT SR formulation given at 3 different doses.

2. Determination of 1/QK*m and V*m using linear regression fit between Fss and Rss to steady-state first pass effect equations previously described by Wagner et al. (5) (Equation 5 and 2, respectively).

3. Prediction of bioavailability based on the fitted V*m, 1/QK*m, and *in vitro* dissolution rate (Equation 3).

4. Simulation of MT plasma concentration-time profiles using modeling technique 2 (Chapter 3) and predicted bioavailability from step 3.

Step 1: *Determination of individual Fss and Rss.*

Bioavailability of MT at anytime after administration, F(t), can be estimated from

Equation 6

$$F(t) = \frac{\text{total drug absorbed } in\ vivo\ (t)}{\text{total drug release } in\ vitro\ (t)}$$

Total drug absorbed *in vivo* (t) can be estimated by deconvolution (PCDCON (23)) of MT plasma concentration-time profiles using i.v. bolus data (24) as the impulse response (24). Total drug release *in vitro* (t) can be estimated from dissolution profile fitted with either Weibull, polyexponential, or cubic spline equation. However, polyexponential equation is preferred herein since the fit to the equation assists in identifying fast release fraction of SR formulation. This fast release portion is significant in simulation of MT plasma profiles using modeling technique 2 (see Chapter 3).

F in Equation 6 can be compared to F described in Equation 1 (i.e. Co $\approx$ drug absorbed *in vivo* and Ci $\approx$ drug release *in vitro*) if it is assumed that gastrointestinal first pass effect can be ignored and drug release *in vitro* (dissolution test) represents drug release *in vivo* (in gastrointestinal tract). However, all F(t) in Equation 6 may not represent F at steady-state because these F(t) change with time. Steady-state bioavailability (Fss) is determined as the bioavailability at which the first derivative of F(t) with respect to time (t) is zero (dF(t)/dt $\approx$ 0).

Drug release rate at steady-state (Rss) can be obtained from Equation 7.

<u>Equation 7</u>

$$Rss = \frac{\text{total drug released } \textit{in vitro} \text{ (tss)}}{\text{tss}}$$

Practically, dF(t)/dt of experimental data set can be done by taking a slope between points of a plot between F(t) and time. The point at which its slope with respect to time is closest to zero were used to identify an approximate value of Fss.

From data of 13 subjects, the smallest slope (or $d(F(t)/dt \approx 0$) range from -1×10^{-7} to $+1 \times 10^{-7}$ (very small, and closest to zero compared to those of the other points). Fss is the average of the two values of F(t) calculated for the smallest slope, time to steady-state (tss) is the mid-time point corresponding to those two F(t), and Rss can be calculated from Equation 7. Dissolution profile of SR formulation used in the study is shown in Figure 4.2. Individual plots of F(t) versus time are presented in Figure 4.3 and 4.15.

Step 2: *Determination of individual value of 1/QK*m and V*m*

1/QK*m and V*m can be determined from a plot between Ln F versus R as shown in Equation 2. Application of Equation 2 for the estimation of 1/QK*m and V*m needs at least two sets of data to draw a line (i.e. administration of 2 different doses or formulations with different drug release in the same subject).

1/QK*m can also obtain from the slope of the plot between -Ln (Fn/Fi) versus Ri - Rn (Equation 5). Unlike Equation 2, the minimum set of data needed for the plot in Equation 5 is three sets of data (i.e. administration of 3 different doses or formulations with different drug release in the same subject). Wagner et al. (5) suggested that the plot of Equation 5 should be a straight line with positive slope passing through the origin if bioavailability increased with input rate (or drug release rate). Equation 5 may be the most important equation to roughly explore correlation between relative bioavailability following different drug release rate. The sensitivity of
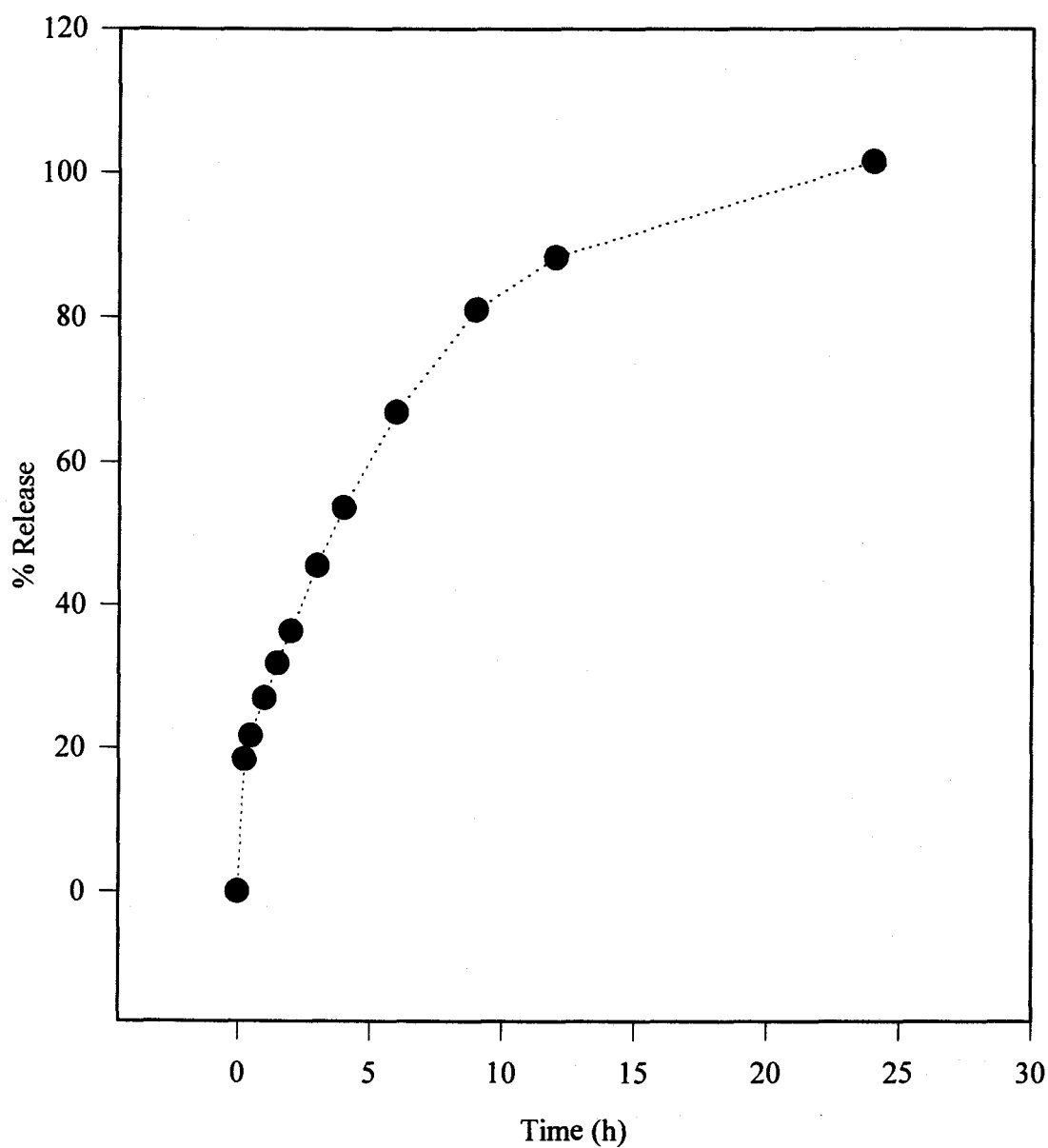
Figure 4.2: Release profile of the sustained release formulation (10% IR + 90% SR MT). Sample standard error (n=3) are too small to show.
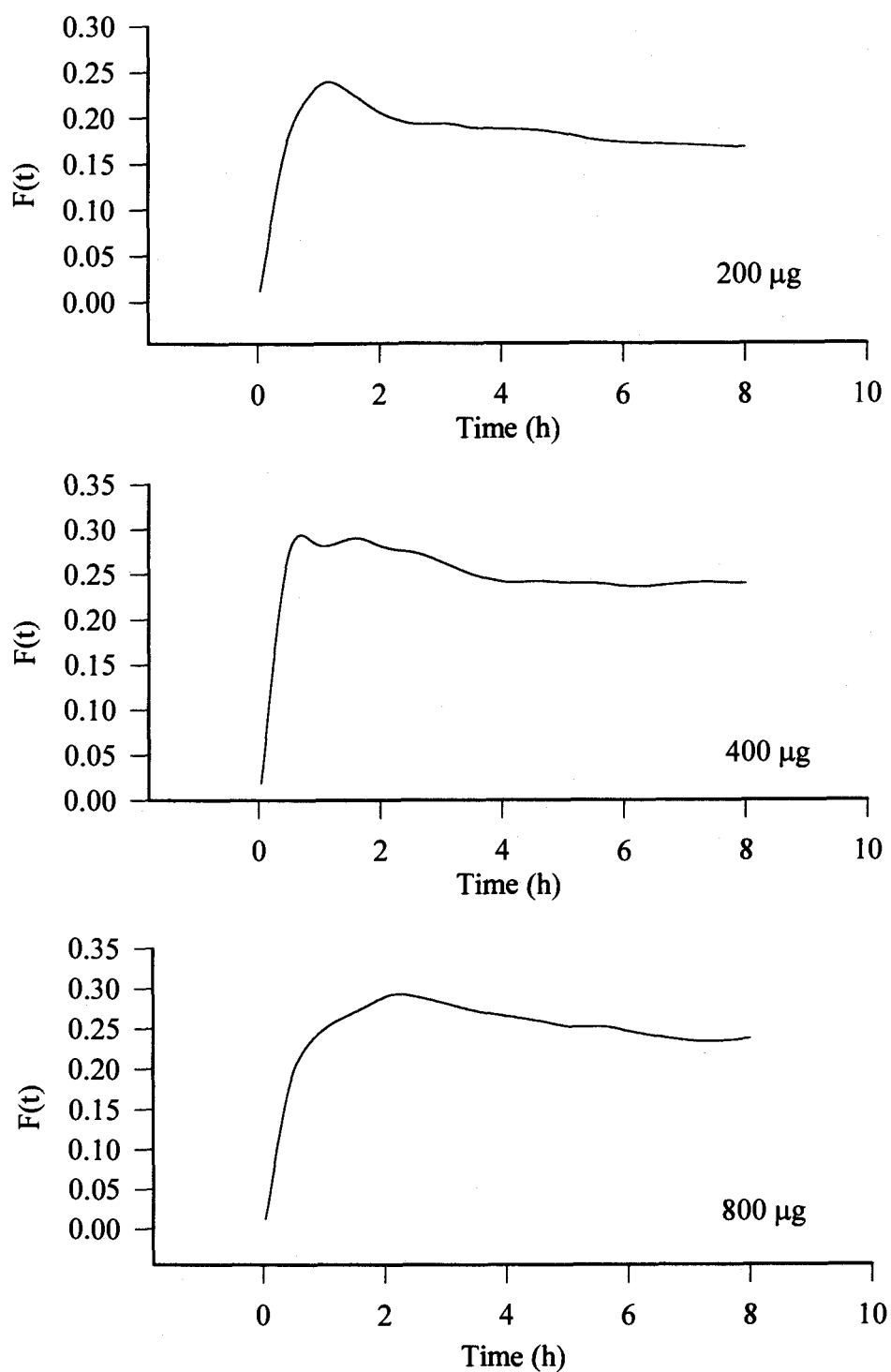
Subject code: AK

Figure 4.3: Plots of bioavailability F(t) estimated from Equation 6 as a function of time (t) following administration of 200 μg, 400 μg, and 800 μg of MT SR formulation in subject AK.
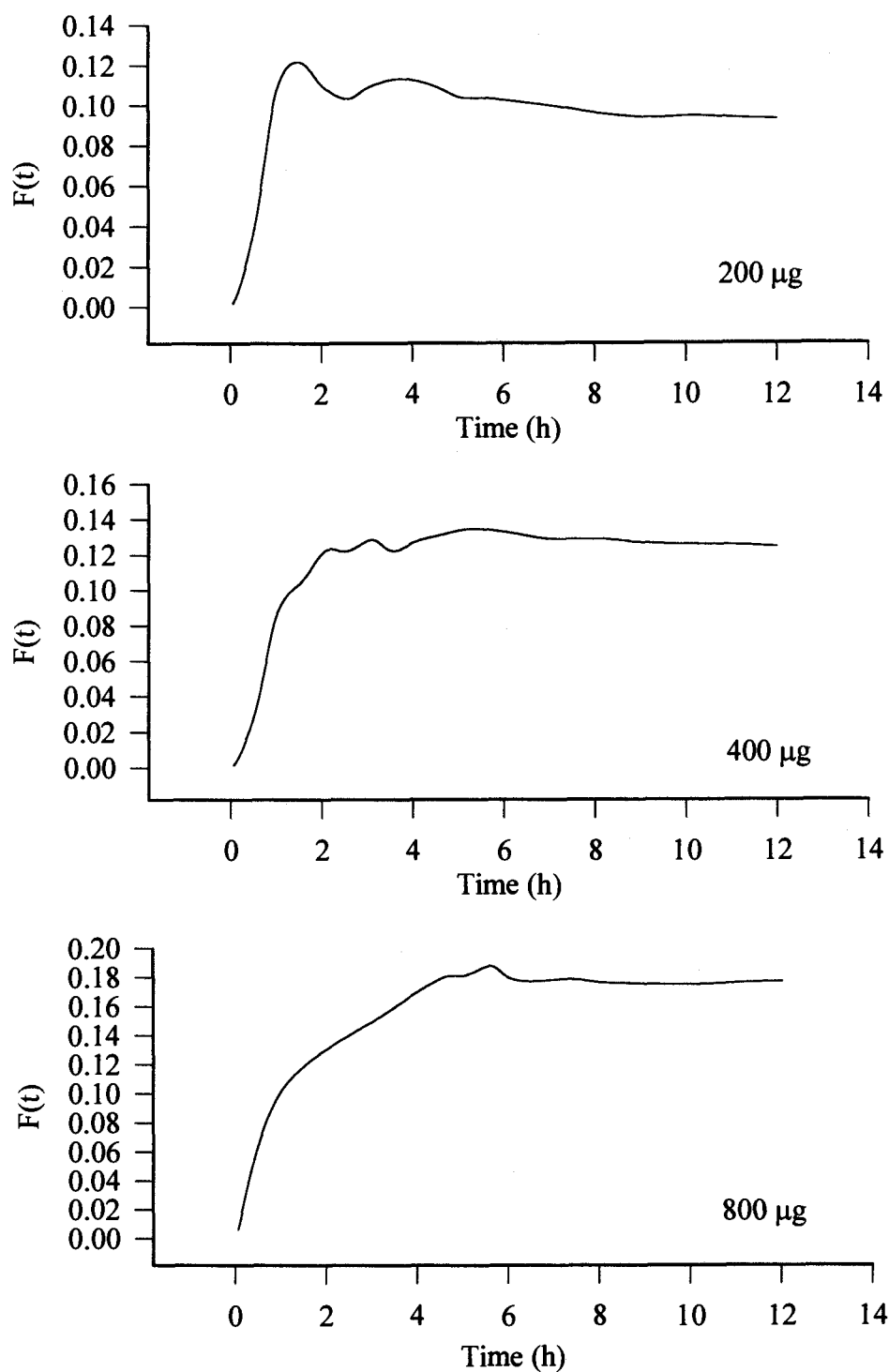
Subject code: HF

Figure 4.4: Plots of bioavailability F(t) estimated from Equation 6 as a function of time (t) following administration of 200 μg, 400 μg, and 800 μg of MT SR formulation in subject HF.
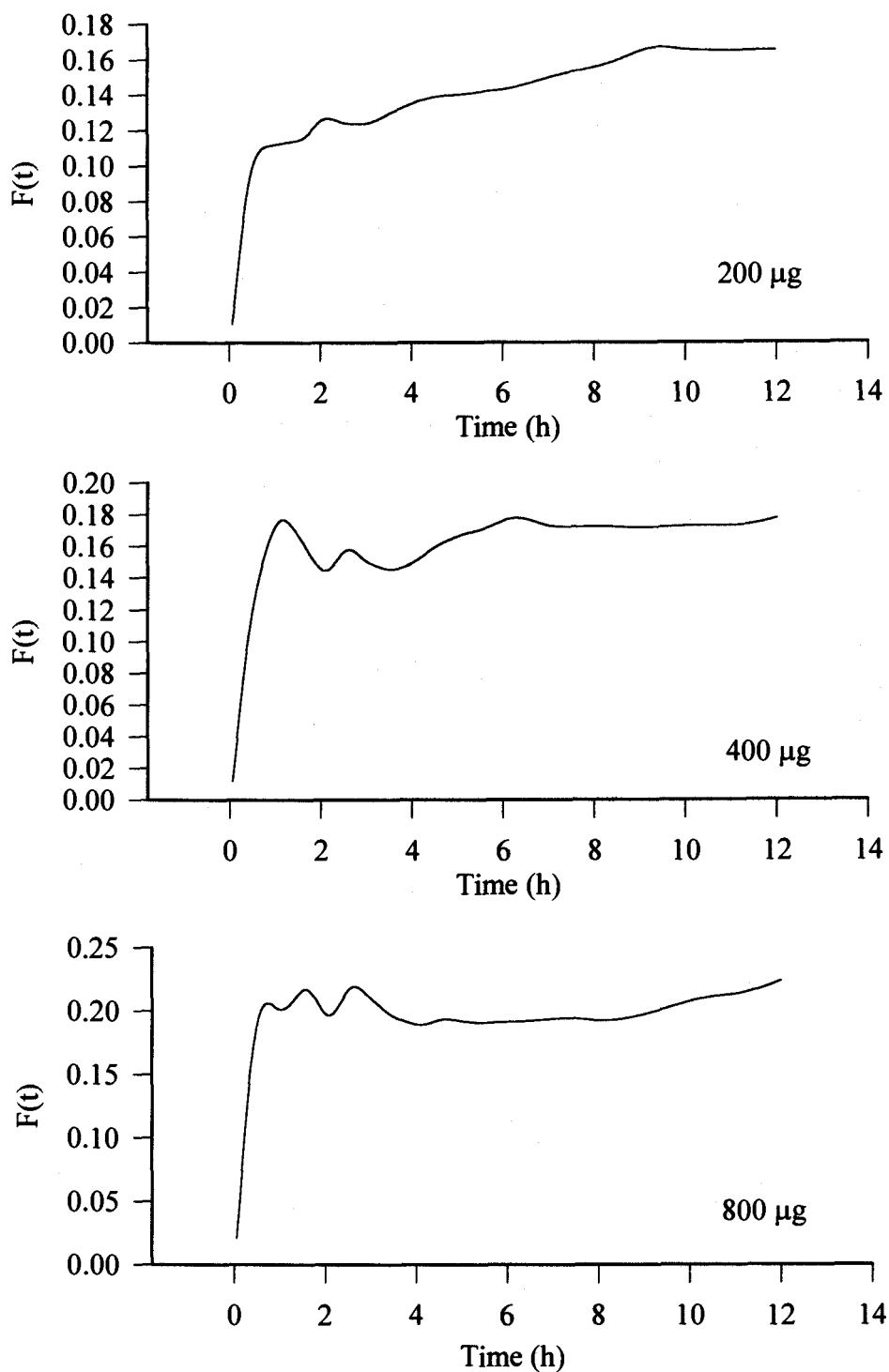
Figure 4.5: Plots of bioavailability F(t) estimated from Equation 6 as a function of time (t) following administration of 200 µg, 400 µg, and 800 µg of MT SR formulation in subject KT.
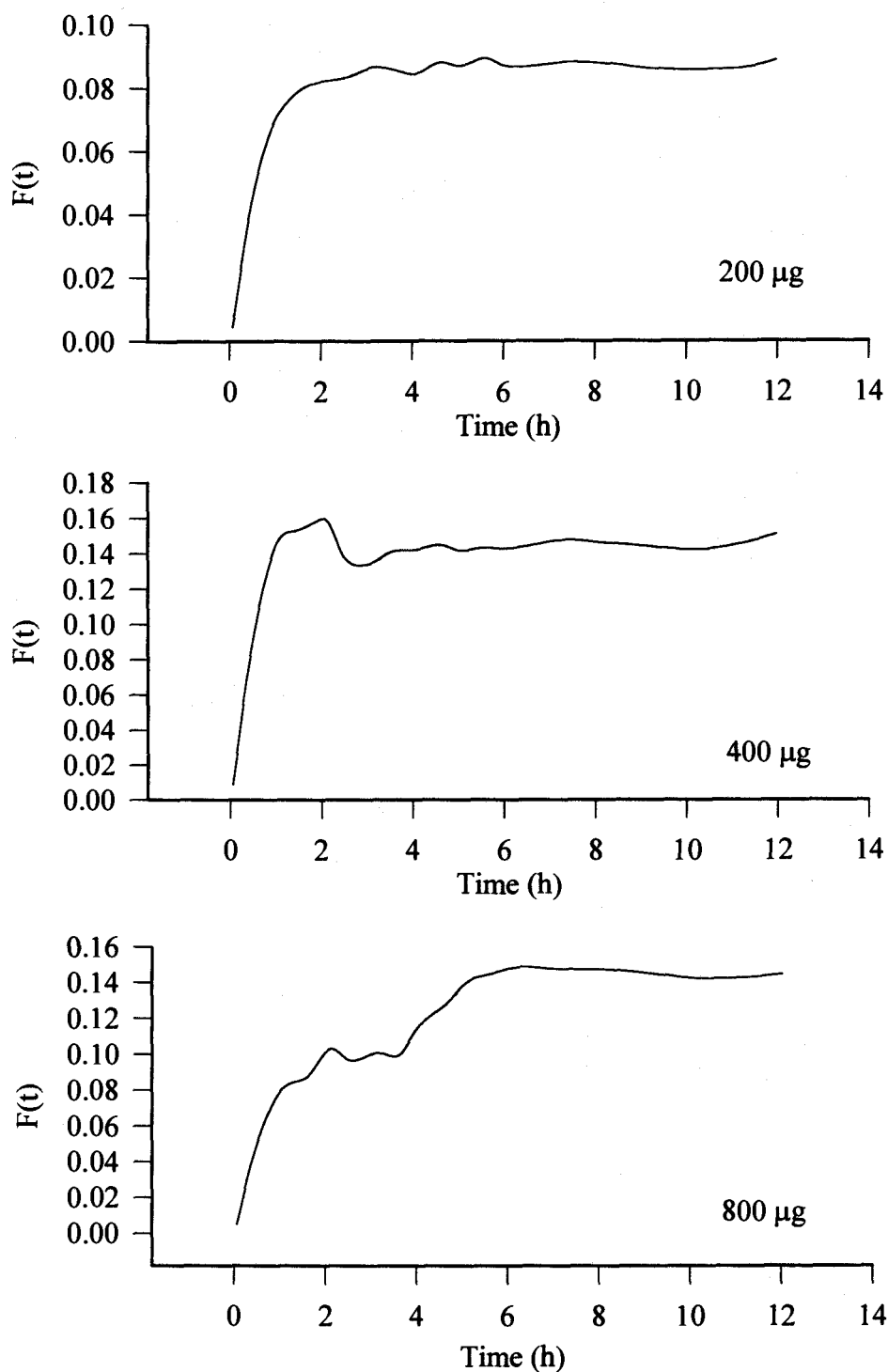
Subject code: RC

Figure 4.6: Plots of bioavailability F(t) estimated from Equation 6 as a function of time (t) following administration of 200 µg, 400 µg, and 800 µg of MT SR formulation in subject RC.
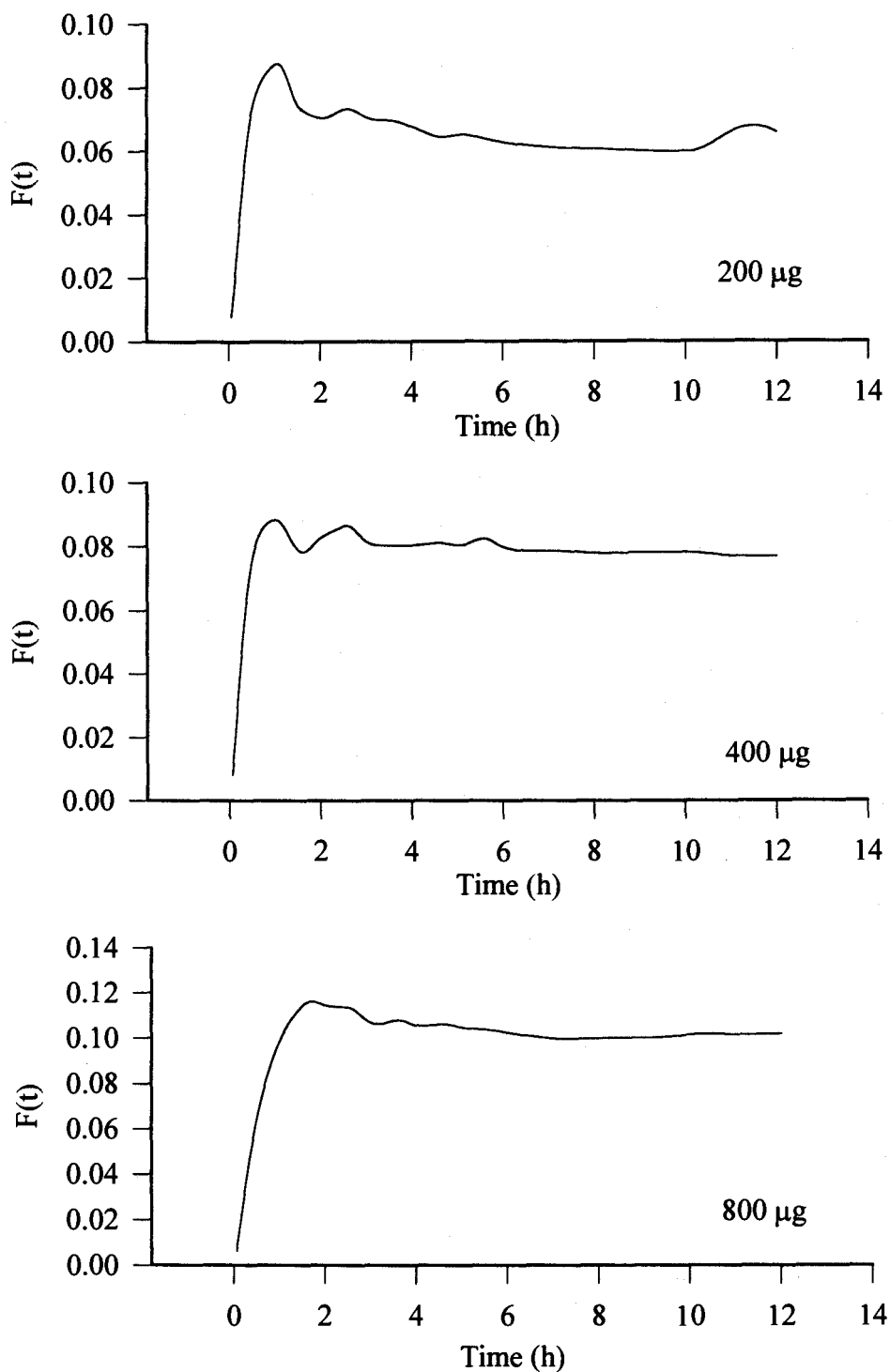
Subject code: SK

Figure 4.7: Plots of bioavailability F(t) estimated from Equation 6 as a function of time (t) following administration of 200 μg, 400 μg, and 800 μg of MT SR formulation in subject SK.
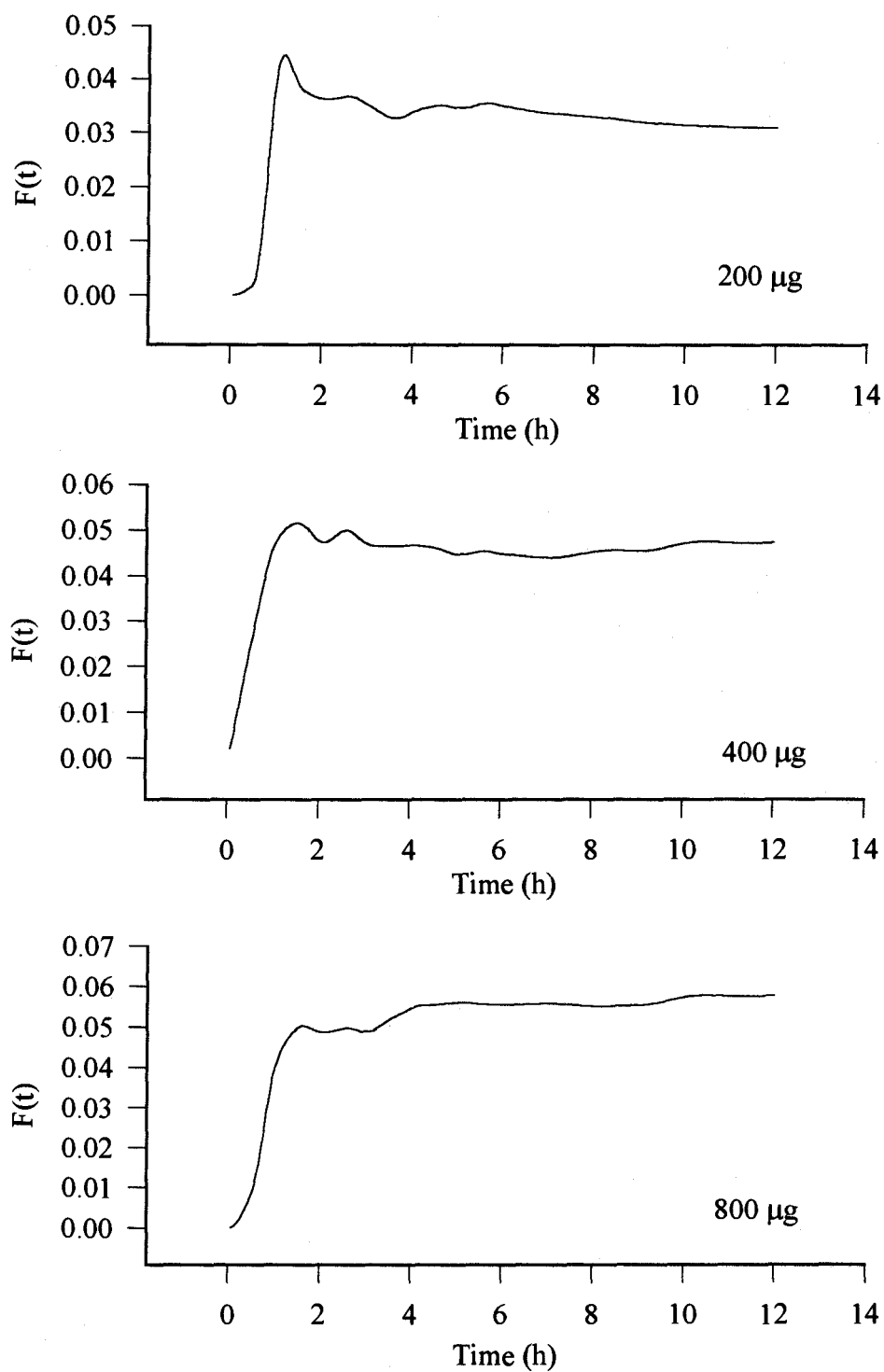
Subject code: SL

Figure 4.8: Plots of bioavailability F(t) estimated from Equation 6 as a function of time (t) following administration of 200 µg, 400 µg, and 800 µg of MT SR formulation in subject SL.
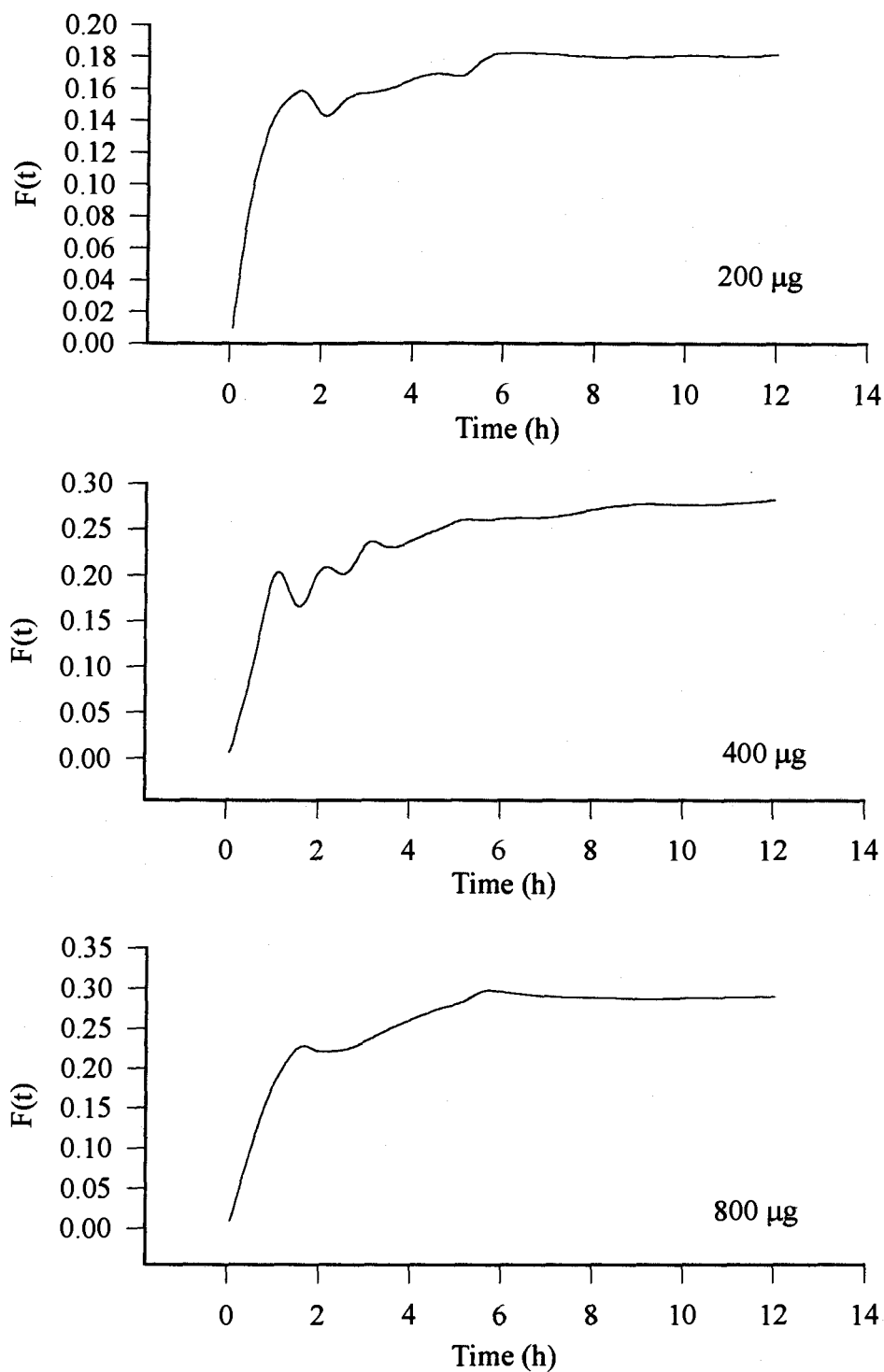
Subject code: AT

Figure 4.9: Plots of bioavailability F(t) estimated from Equation 6 as a function of time (t) following administration of 200 μg, 400 μg, and 800 μg of MT SR formulation in subject AT.
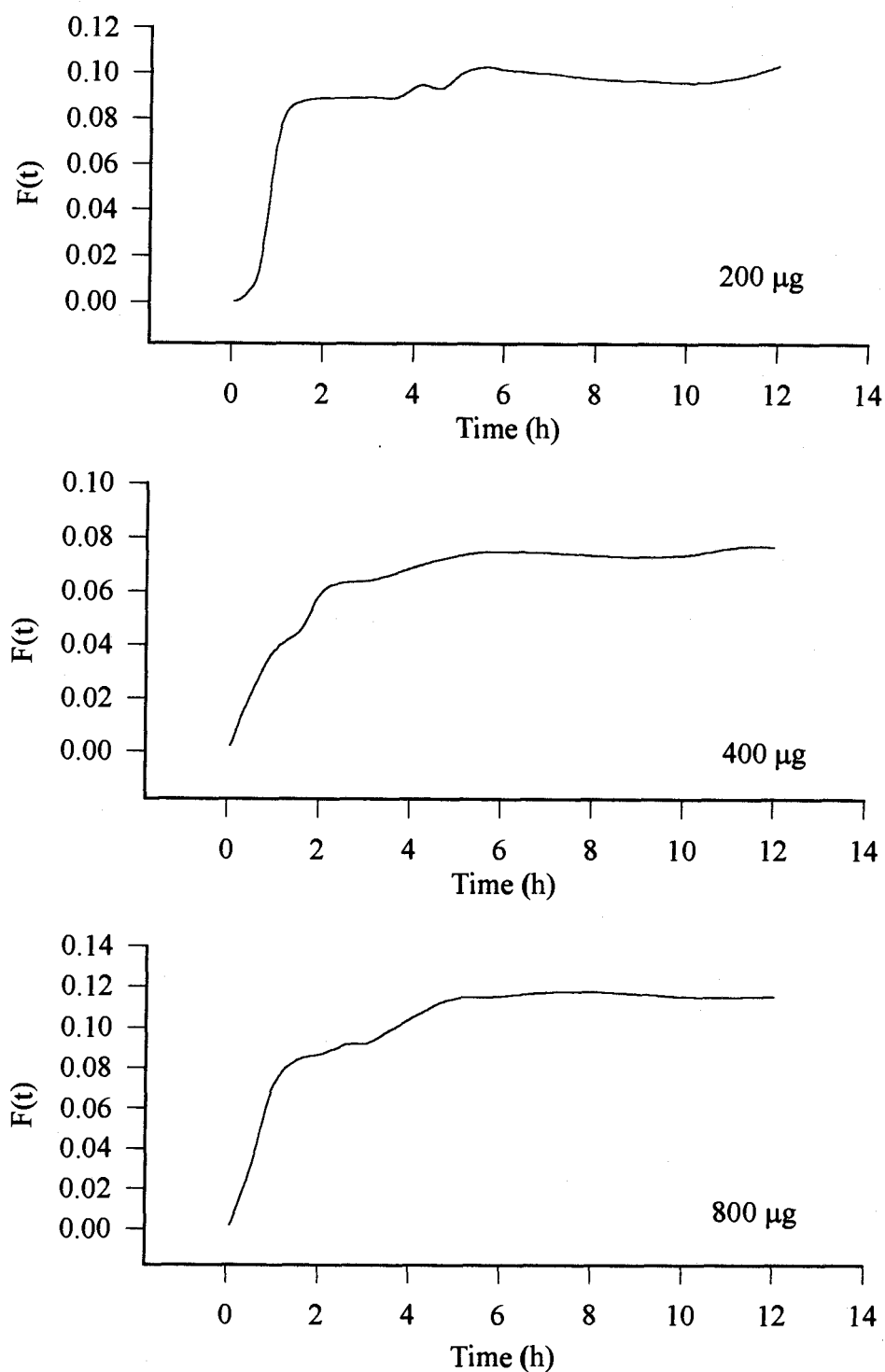
Subject code: CB

Figure 4.10: Plots of bioavailability F(t) estimated from Equation 6 as a function of time (t) following administration of 200 µg, 400 µg, and 800 µg of MT SR formulation in subject CB.
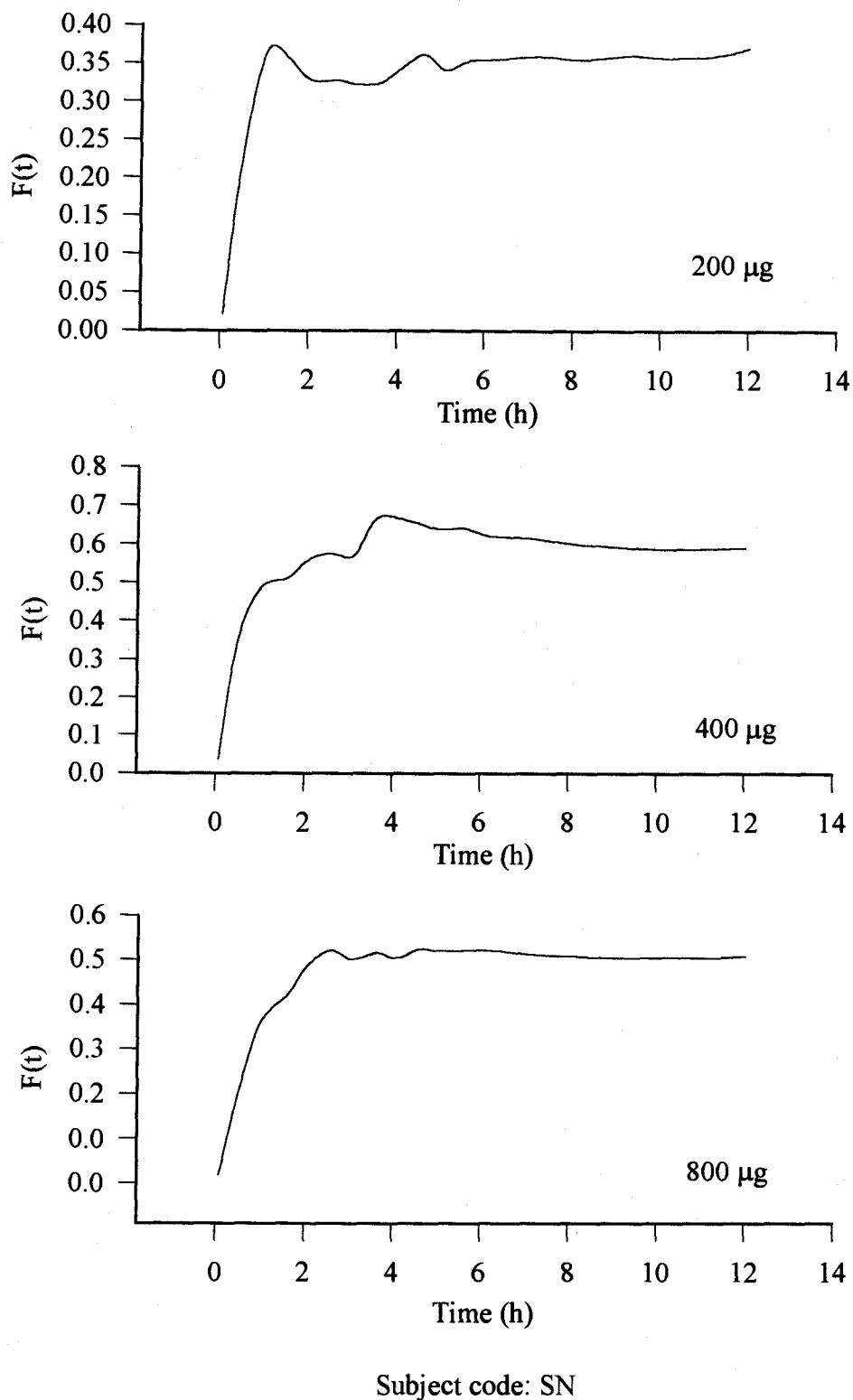
Subject code: SN

Figure 4.11: Plots of bioavailability F(t) estimated from Equation 6 as a function of time (t) following administration of 200 μg, 400 μg, and 800 μg of MT SR formulation in subject SN.
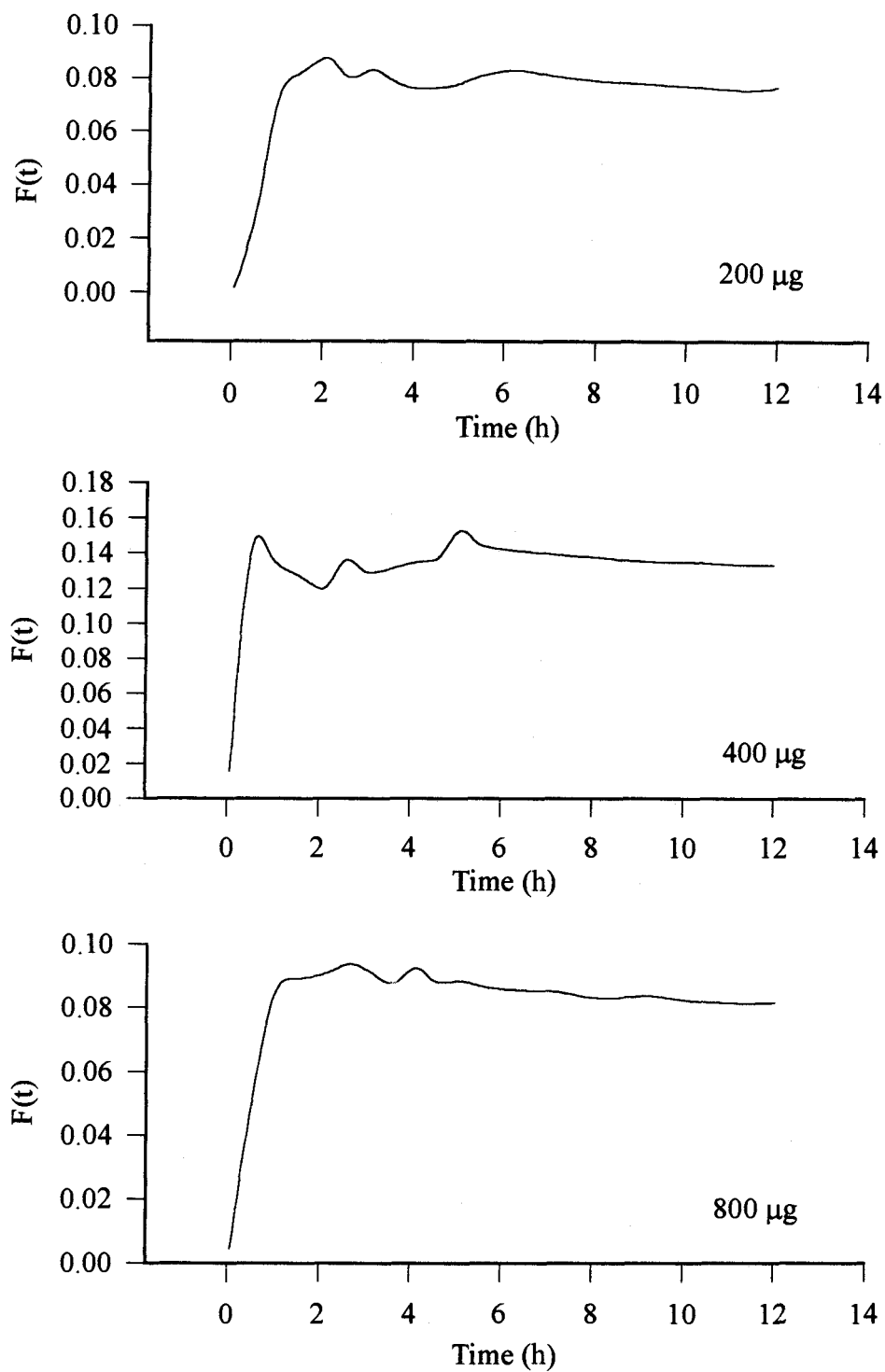
Subject code: VB

Figure 4.12: Plots of bioavailability F(t) estimated from Equation 6 as a function of time (t) following administration of 200 μg, 400 μg, and 800 μg of MT SR formulation in subject VB.
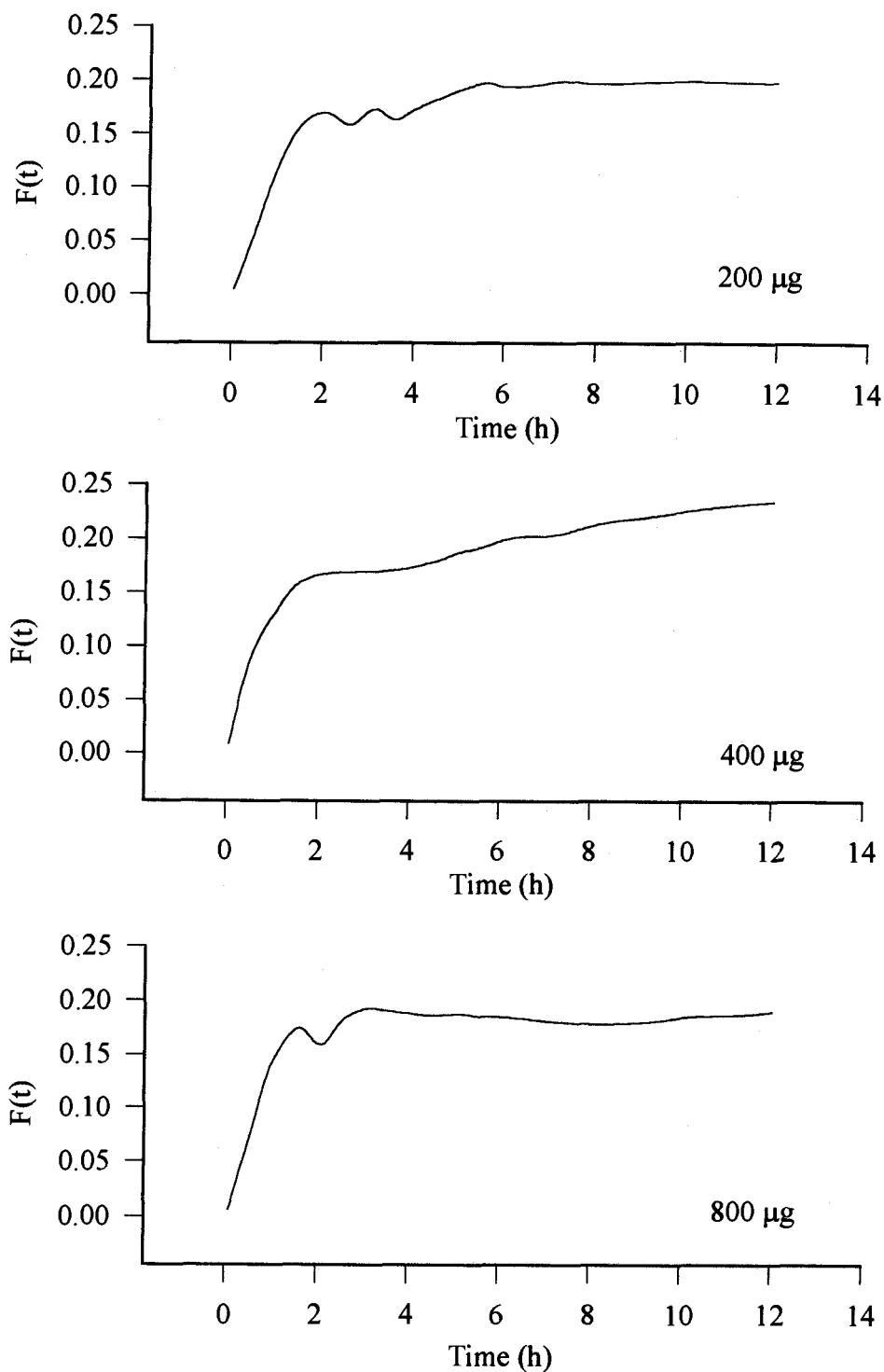
Subject code: AO

Figure 4.13: Plots of bioavailability F(t) estimated from Equation 6 as a function of time (t) following administration of 200 μg, 400 μg, and 800 μg of MT SR formulation in subject AO.
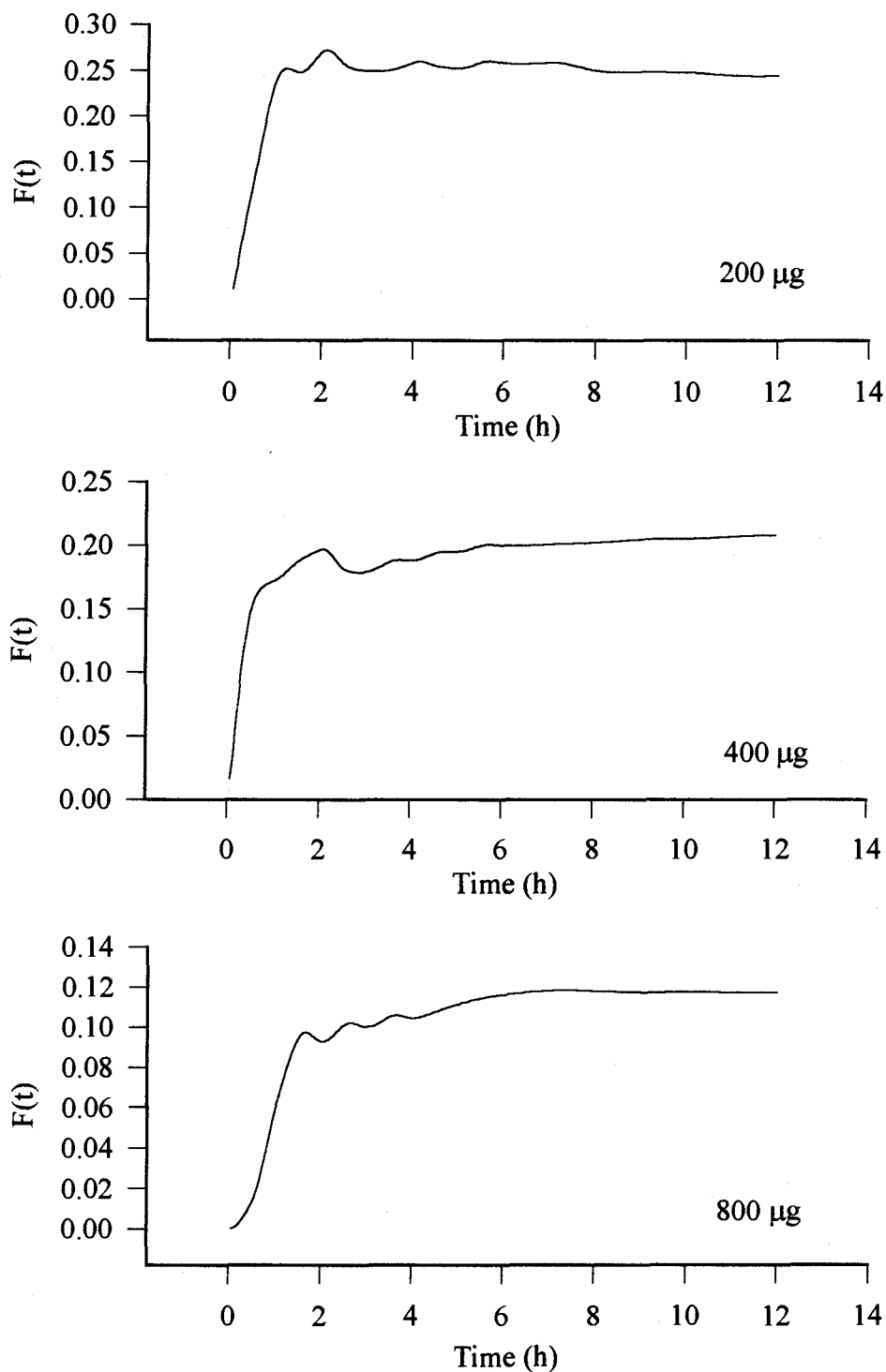
Figure 4.14: Plots of bioavailability F(t) estimated from Equation 6 as a function of time (t) following administration of 200 μg, 400 μg, and 800 μg of MT SR formulation in subject GL.
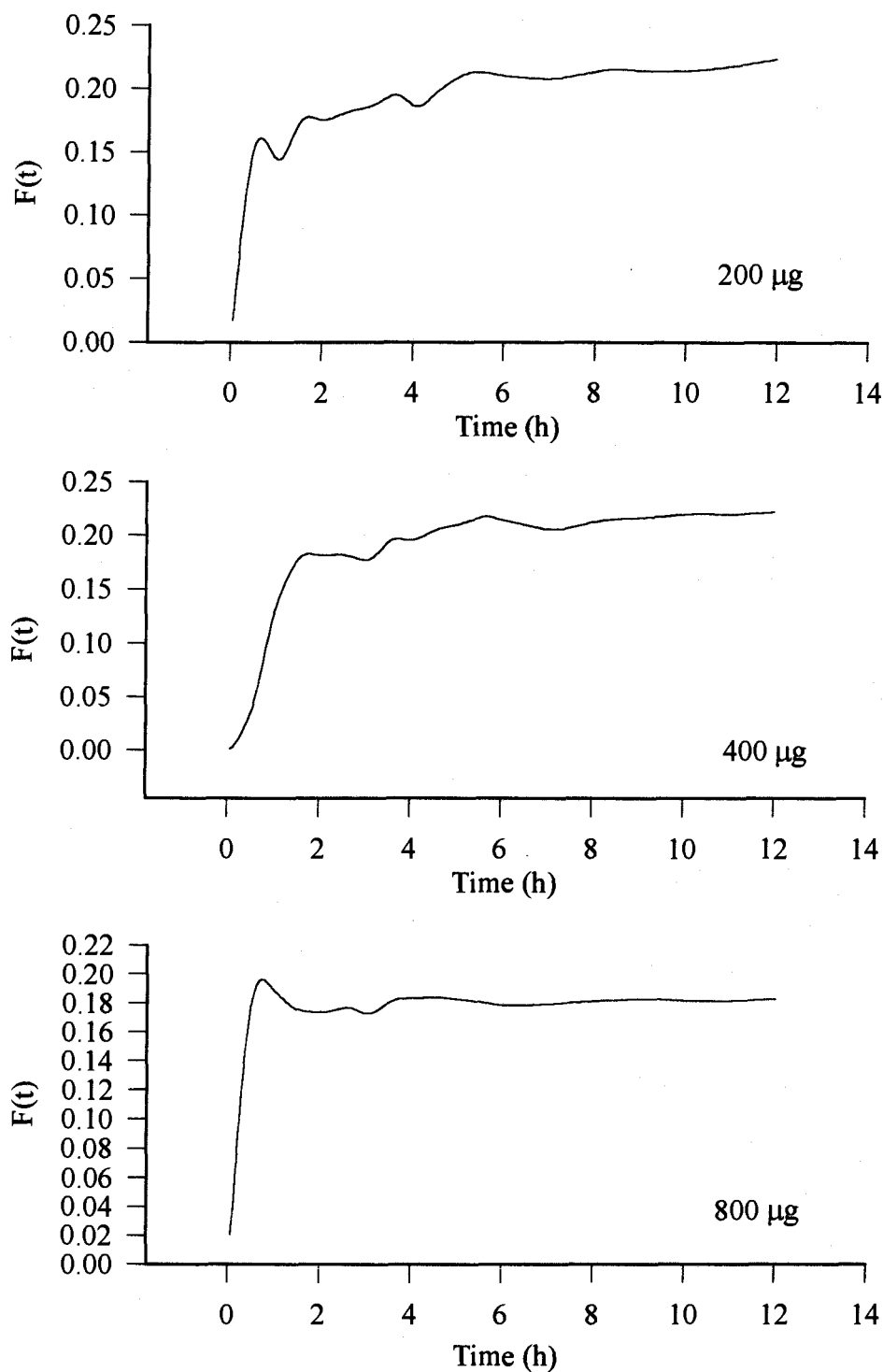
Subject code: LA

Figure 4.15: Plots of bioavailability F(t) estimated from Equation 6 as a function of time (t) following administration of 200 µg, 400 µg, and 800 µg of MT SR formulation in subject LA.

the change in relative bioavailability with change in constant input rate/drug release rate will depend upon the magnitude of the K*m value if Q is constant (5).

Step 3: *Prediction of bioavailability using the fitted values of V*m, 1/QK*m, and in vitro dissolution rate*

If the values of V*m and 1/QK*m can be defined from step 1 and 2, we can apply both parameters to predict theoretical bioavailability of MT with known drug release rate by using Equation 3. Drug release rate of IR MT portion (R_{IR}) in the dosage form is estimate by assuming that total IR dose is completely absorbed within one hour i.e. IR MT is delivered at approximate drug release rate of R_{IR} = total IR dose / 1 hour. On the other hand, drug release rate of SR MT portion (R_{SR}) is estimated from *in vitro* dissolution data over desired period of prediction time i.e. R_{SR} = total amount released *in vitro* over 12 hours / 12 hours if one would like to predict drug plasma concentrations up to 12 hour period. R_{IR} and R_{SR} were then used to estimated bioavailability of IR MT and SR MT in the formulation.

Step 4: *Simulation of MT plasma concentration-time profiles*

MT plasma concentration-time profiles can be simulated using modeling technique 2 described earlier in Chapter 3 by substitute Fim with predicted bioavailability of IR MT and Rsus with predicted bioavailability of SR MT obtained from step 3. Total IR dose (Dim) based on the fitted polyexponential equation was 25.6

µg for 200 µg dose, 51.2 µg for 400 µg dose, and 102.4 µg for 800 µg dose, respectively (Chapter 3).

RESULTS AND DISCUSSION

Graphical results are presented according to each subject for convenience in comparing goodness of fits to Equation 5 and 2 with simulation results using modeling technique 2. The results may be divided into three cases based on the fits to Equation 5 and 2. Experimental data obtained from 7 subjects were fitted well with the theoretical equations (case I). For the other 6 subjects, the experimental data did not fit very well to the theoretical model with the data from 5 subjects demonstrating poor fits with small magnitude of slope (1/QKm) (case II) and the data from 1 subject clearly showing decrease in bioavailability with increase in drug release rate (case III).

In the first case, data from seven subjects (AK, HF, KT, RC, SK, SL, and AT) are fitted fairly well with the theoretical model (Equation 5 and 2). The fits to Equation 5 and 2 have positive slopes which means that bioavailability increases with increase in drug release rate from the formulation. The individual fits to Equation 5 and 2 together with simulation results of MT plasma profiles are presented in Figure 4.16 to 4.29. Simulation results are generally good. However, prediction of maximum concentration (Cmax) in some subjects are not very accurate. This error is likely attributable to inaccurate estimation of R_{IR}, and/or deviation of individual pharmacokinetic parameters from the literature values used in the prediction such as the drug absorption rate constant, the drug elimination rate constant, and the volume of distribution.
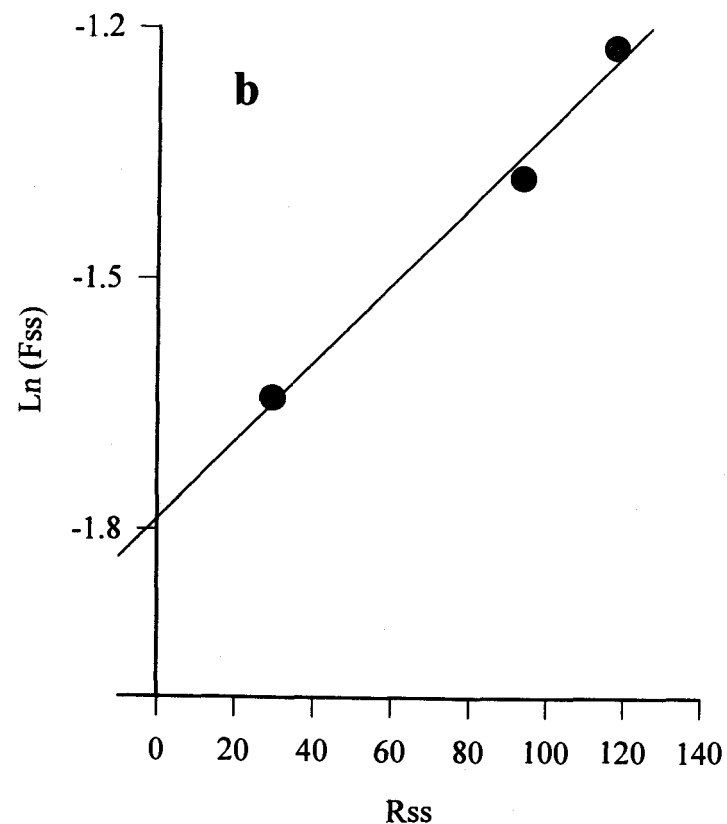
Figure 4.16: The fits to Equation 5 (a) and 2 (b) using experimental data following administration of MT SR formulation given at 200 μg, 400 μg, and 800 μg in subject AK

In the figure:

a axis labels: y-axis $-Ln\ (Fn/Fi)$, x-axis $Ri - Rn$

Equation 5: $-Ln\dfrac{Fn}{Fi} = \dfrac{(Ri - Rn)}{Q\,K^*m}$

b axis labels: y-axis $Ln\ (Fss)$, x-axis Rss

Equation 2: $Ln\ (Fss) = \dfrac{-V^*m}{Q\,K^*m} + \dfrac{Rss}{Q\,K^*m}$

● Experimental data
—— Regression line
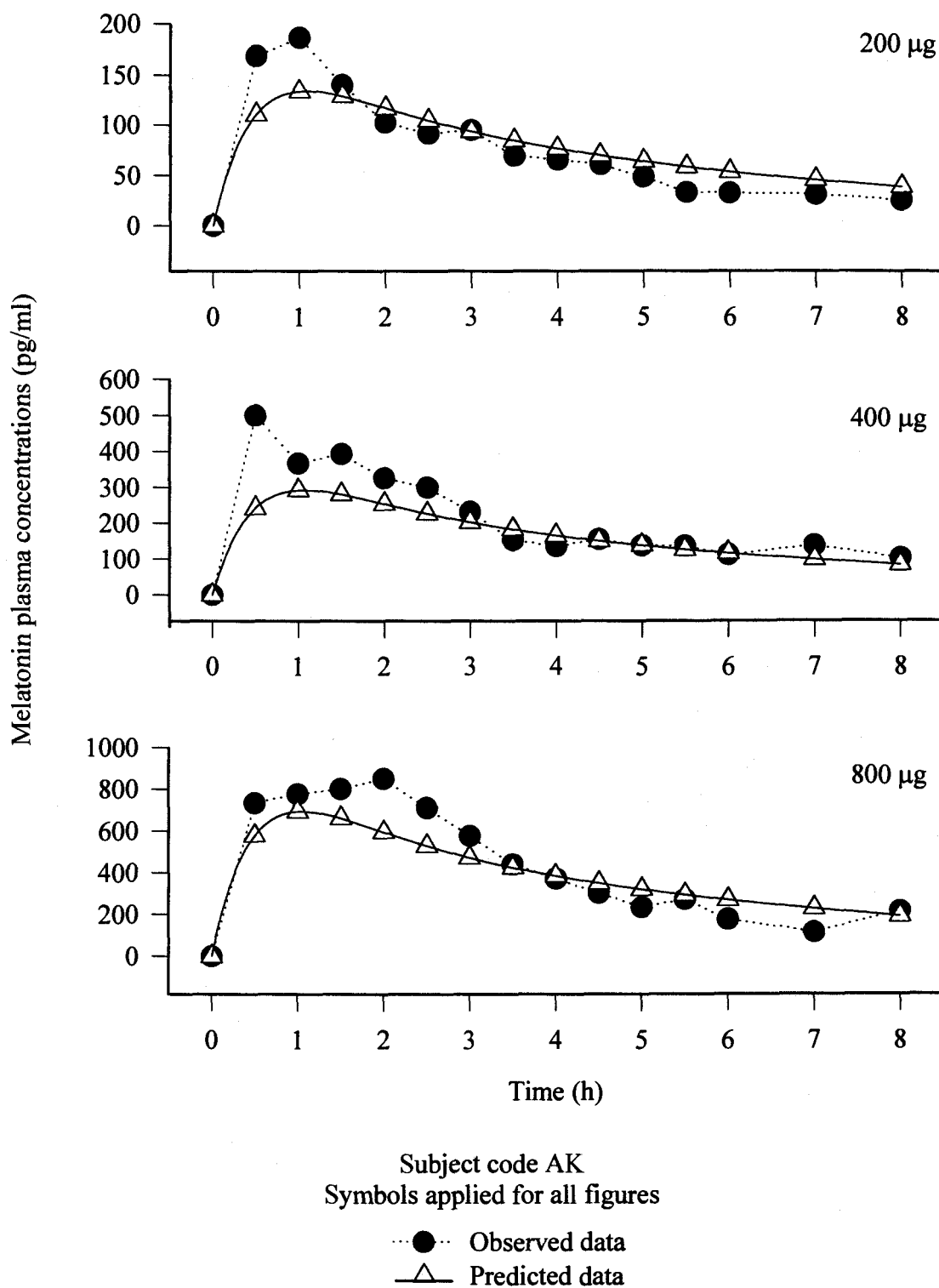
Figure 4.17: Observed versus predicted MT plasma concentration-time profiles following administration of MT SR formulation given at 200 μg, 400 μg, and 800 μg to AK.
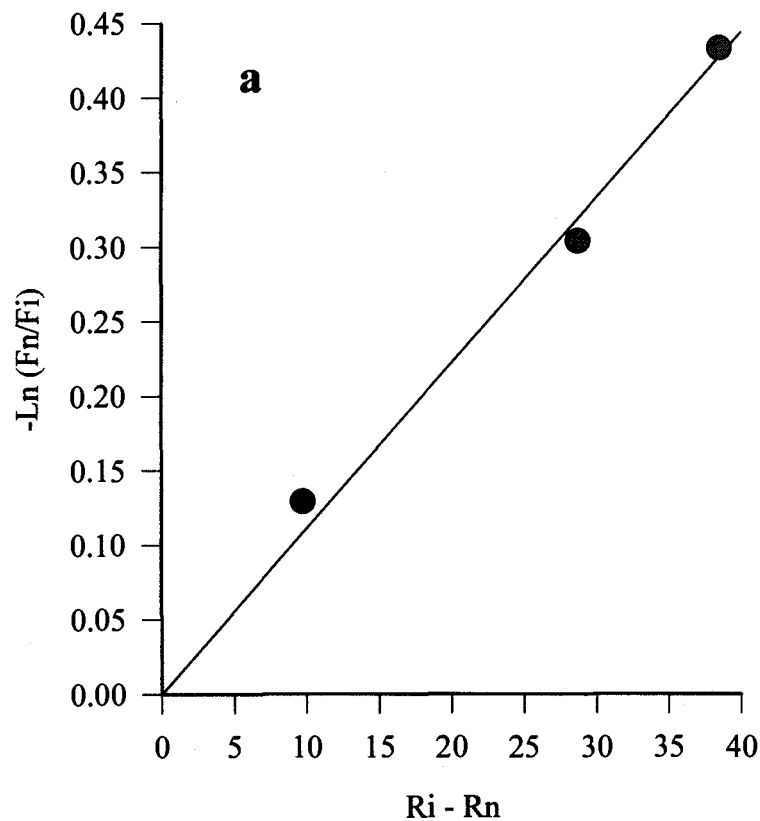
Equation 5: $-\ln \dfrac{F_n}{F_i} = \dfrac{(R_i - R_n)}{Q\, K^{*} m}$

Equation 2: $\ln(F_{ss}) = \dfrac{-V^{*} m}{Q\, K^{*} m} + \dfrac{R_{ss}}{Q\, K^{*} m}$

● Experimental data
—— Regression line

Figure 4.18: The fits to Equation 5 (a) and 2 (b) using experimental data following administration of MT SR formulation given at 200 μg, 400 μg, and 800 μg in subject HF.
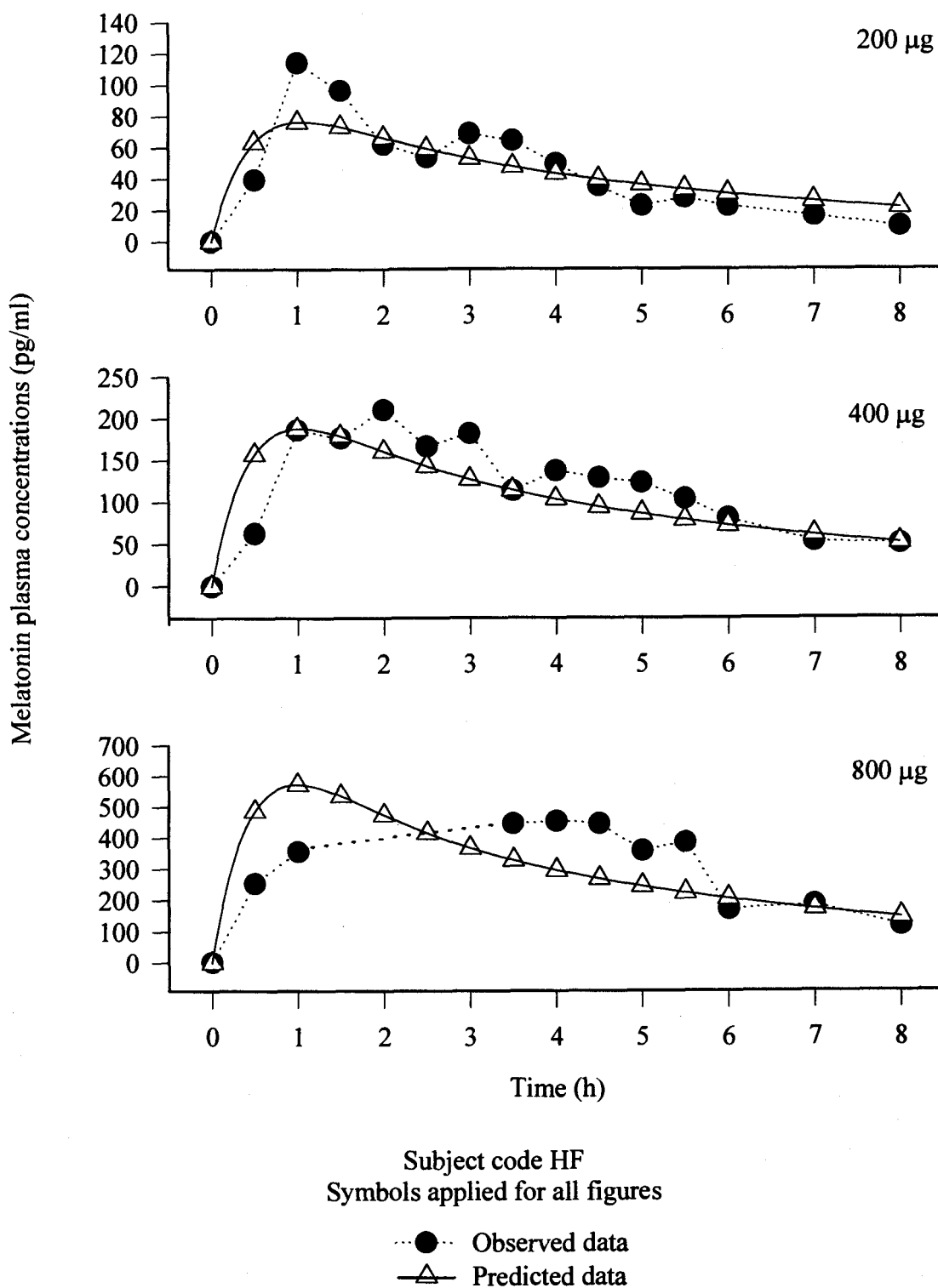
Figure 4.19: Observed versus predicted MT plasma concentration-time profiles following administration of MT SR formulation given at 200 µg, 400 µg, and 800 µg to HF.
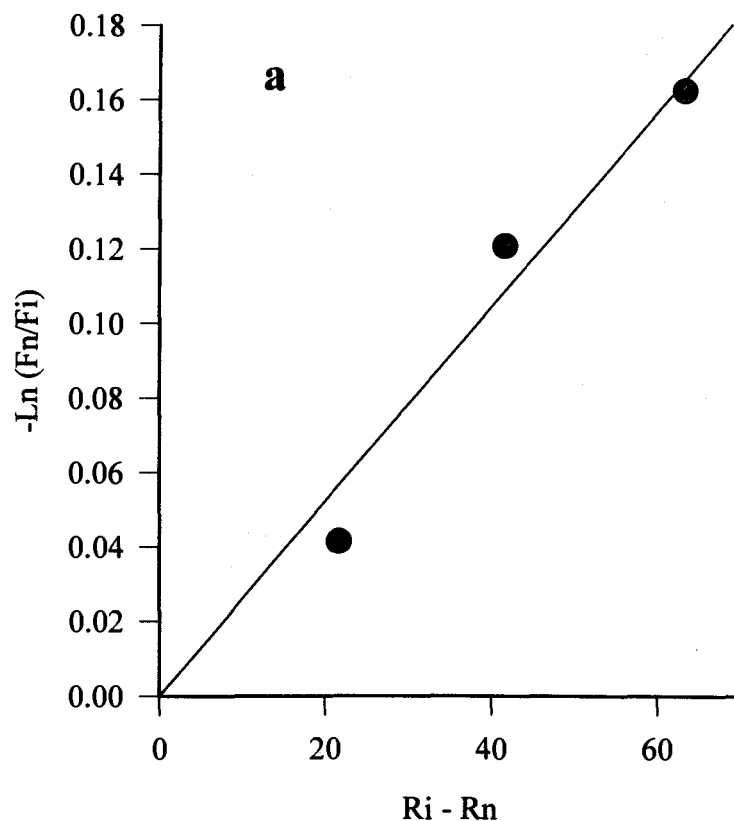
Equation 5: $-\mathrm{Ln}\,\dfrac{Fn}{Fi} = \dfrac{(Ri - Rn)}{Q\,K^*m}$

Equation 2: $\mathrm{Ln}\,(Fss) = \dfrac{-V^*m}{Q\,K^*m} + \dfrac{Rss}{Q\,K^*m}$
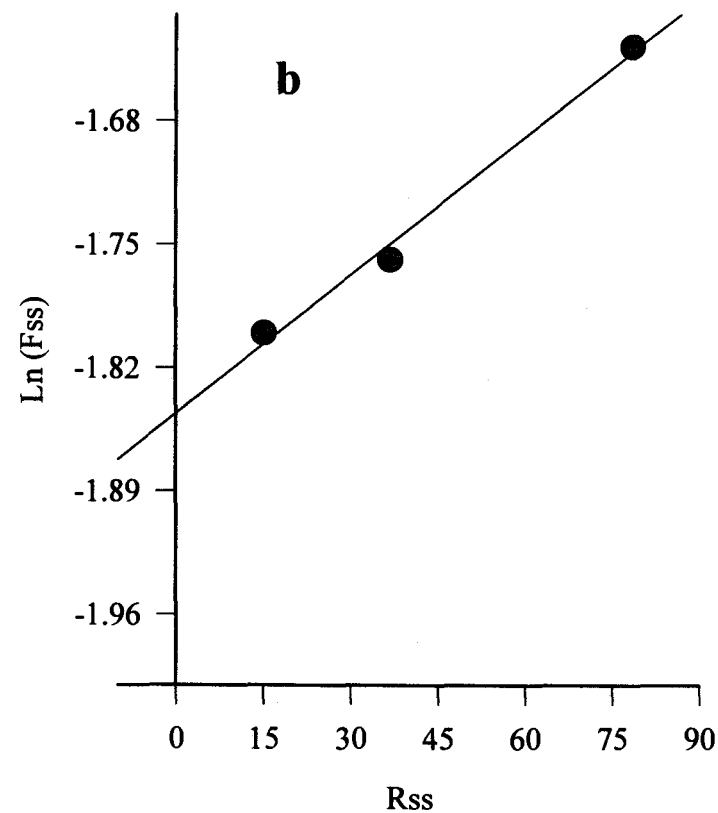
● Experimental data
── Regression line

Figure 4.20: The fits to Equation 5 (a) and 2 (b) using experimental data following administration of MT SR formulation given at 200 μg, 400 μg, and 800 μg in subject KT.
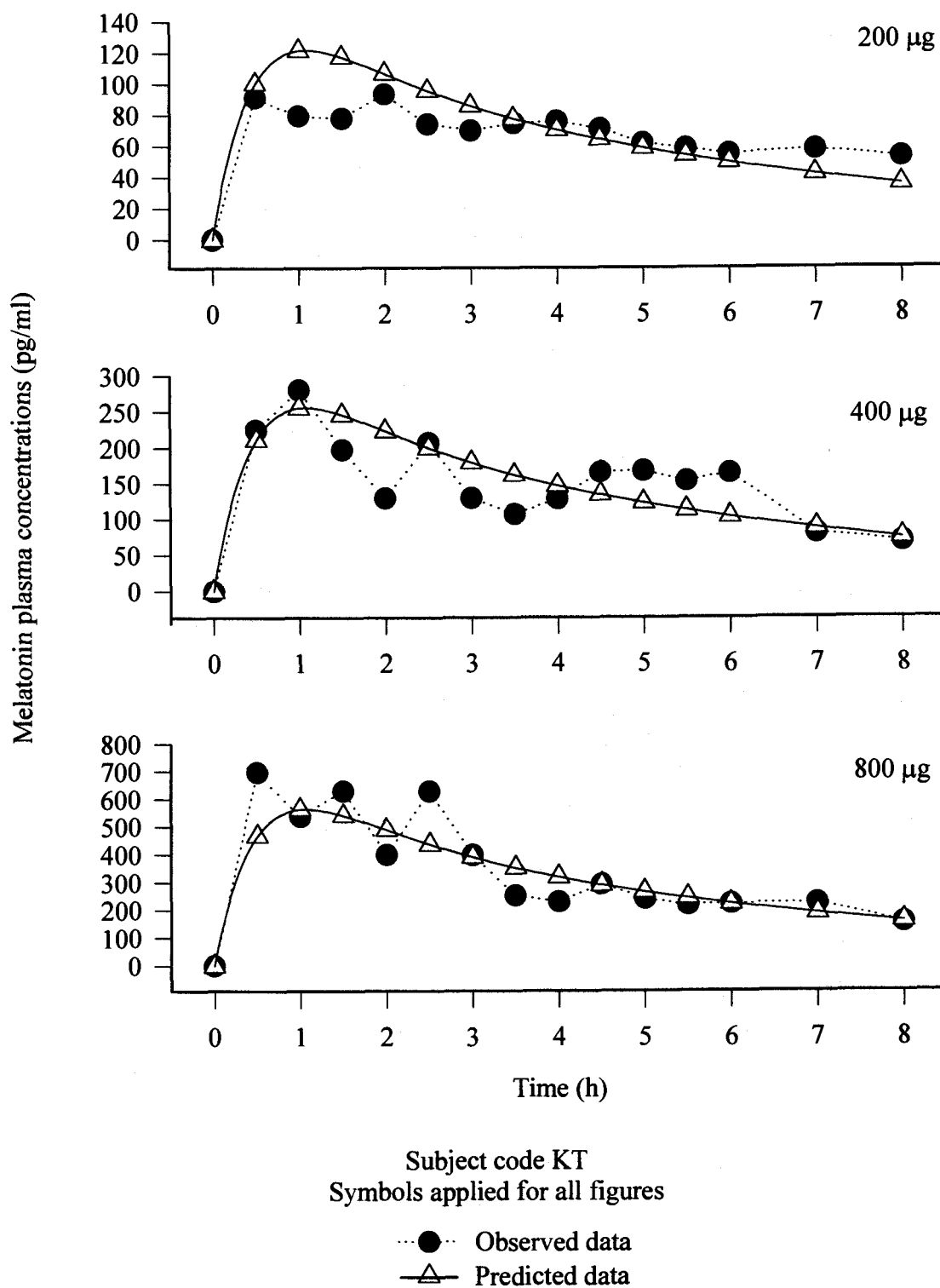
Figure 4.21: Observed versus predicted MT plasma concentration-time profiles following administration of MT SR formulation given at 200 µg, 400 µg, and 800 µg to KT.
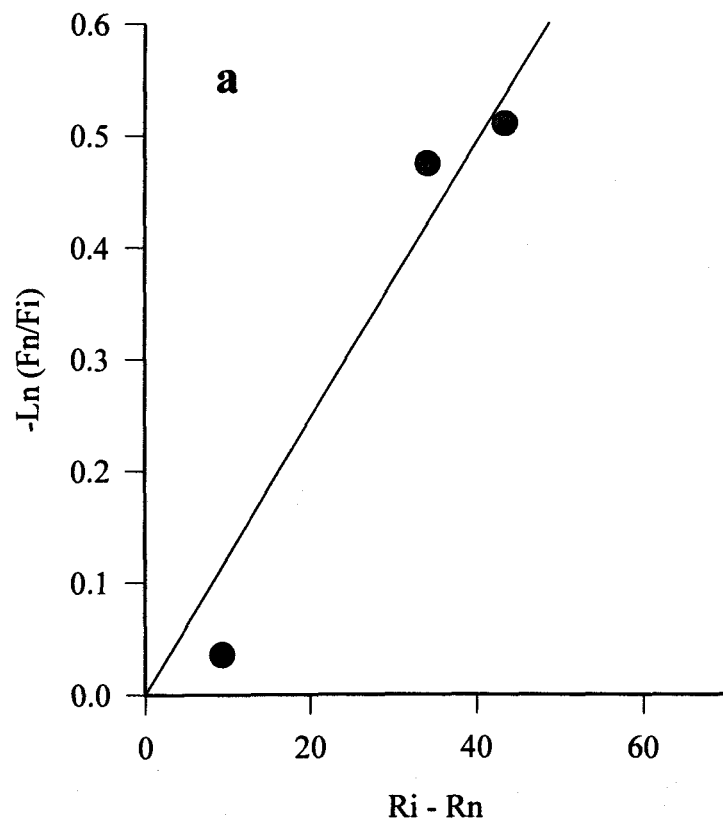
Equation 5: $-\mathrm{Ln}\ \dfrac{Fn}{Fi} = \dfrac{(Ri - Rn)}{Q\ K^*m}$
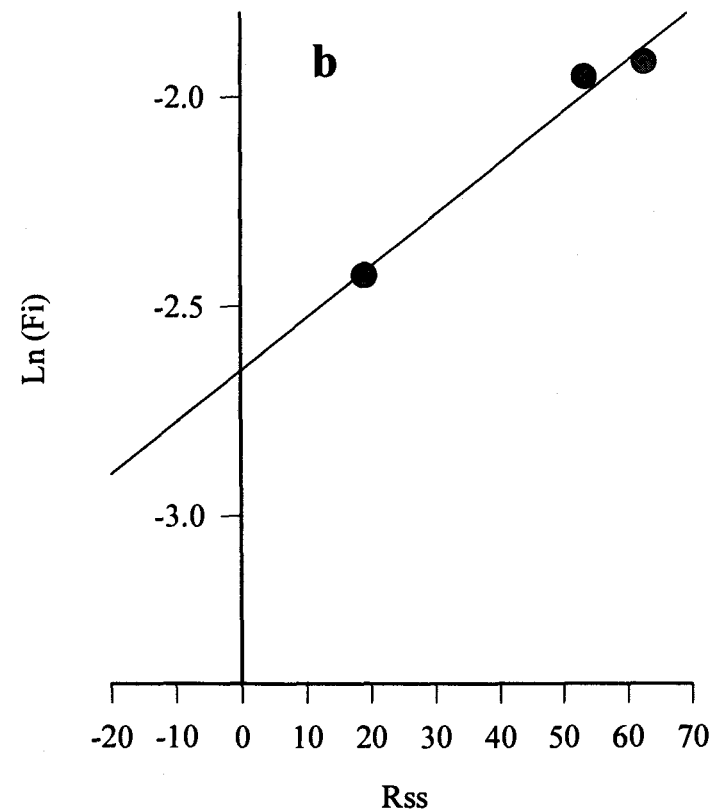
Equation 2: $\mathrm{Ln}\ (Fss) = \dfrac{-V^*m}{Q\ K^*m} + \dfrac{Rss}{Q\ K^*m}$

● Experimental data
—— Regression line

Figure 4.22: The fits to Equation 5 (a) and 2 (b) using experimental data following administration of MT SR formulation given at 200 μg, 400 μg, and 800 μg in subject RC.
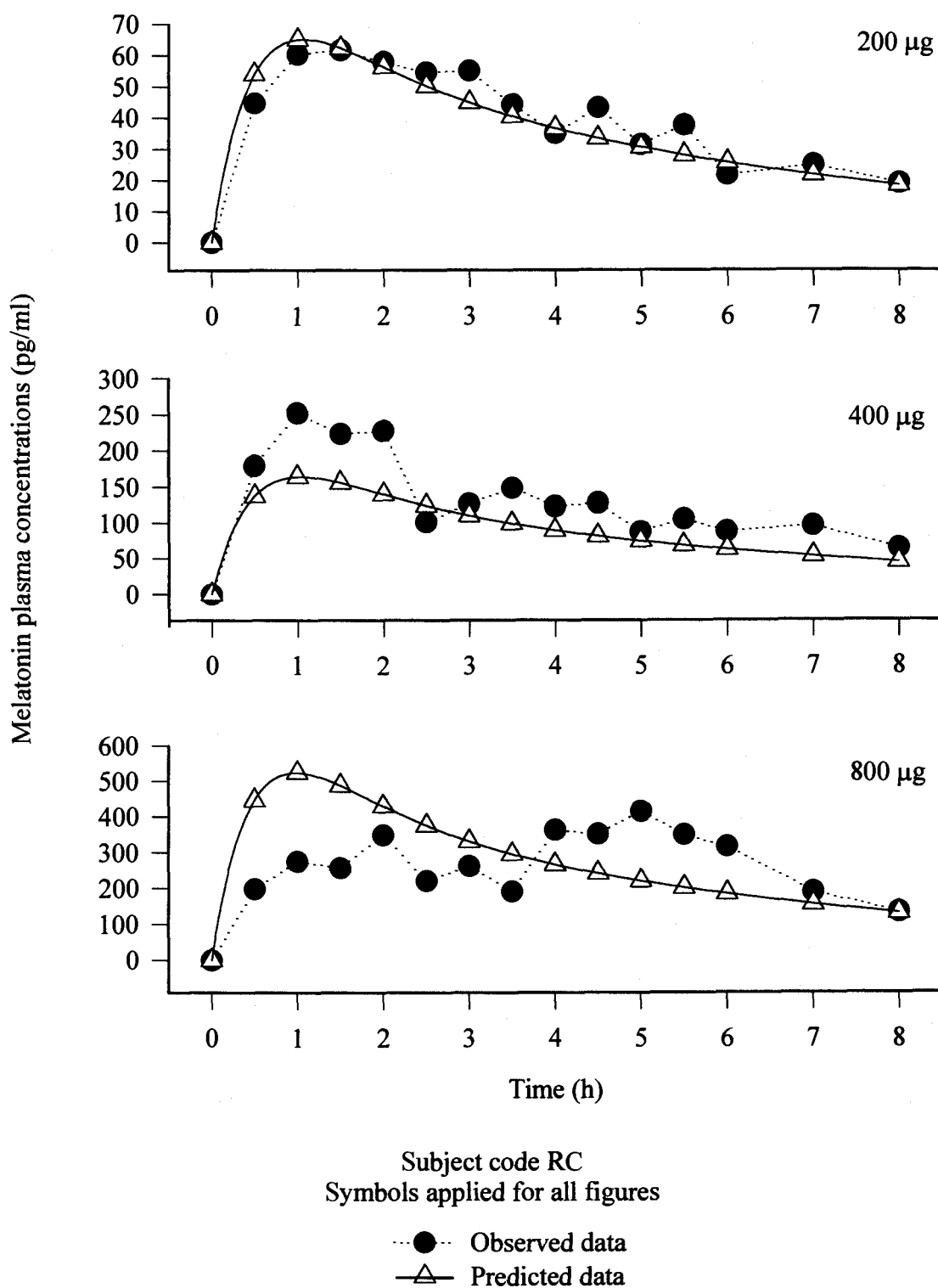
Figure 4.23: Observed versus predicted MT plasma concentration-time profiles following administration of MT SR formulation given at 200 μg, 400 μg, and 800 μg to RC.
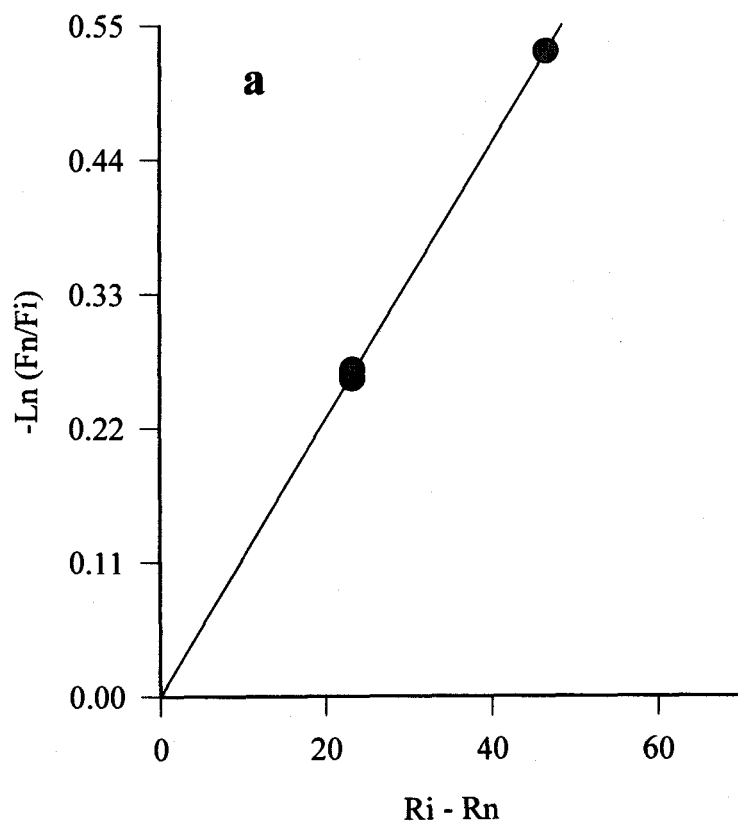
Equation 5: $- \ln \dfrac{F_n}{F_i} = \dfrac{(R_i - R_n)}{Q\,K^*m}$

Equation 2: $\ln(F_{ss}) = \dfrac{-V^*m}{Q\,K^*m} + \dfrac{R_{ss}}{Q\,K^*m}$
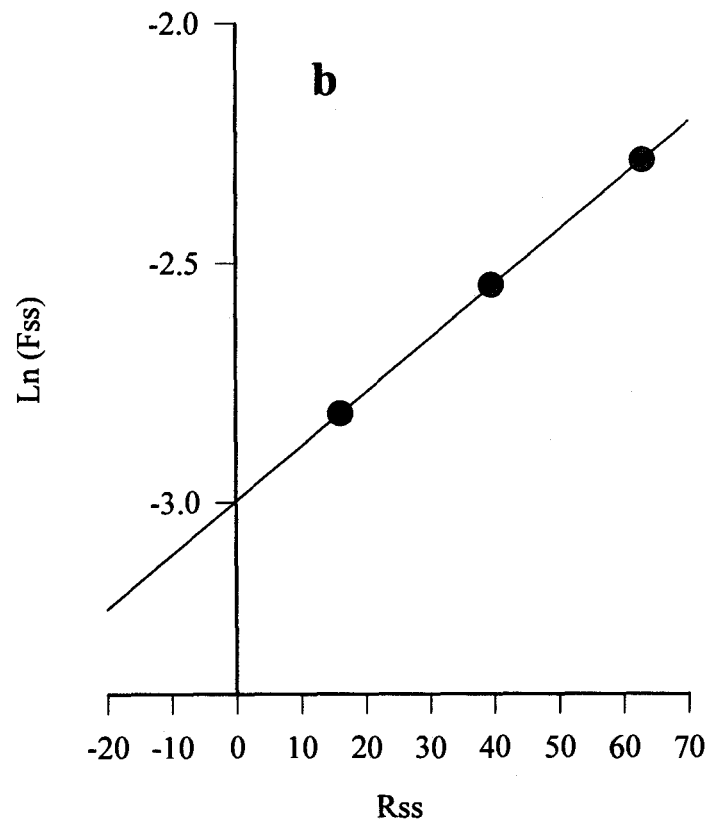
● Experimental data
—— Regression line

Figure 4.24: The fits to Equation 5 (a) and 2 (b) using experimental data following administration of MT SR formulation given at 200 µg, 400 µg, and 800 µg in subject SK.
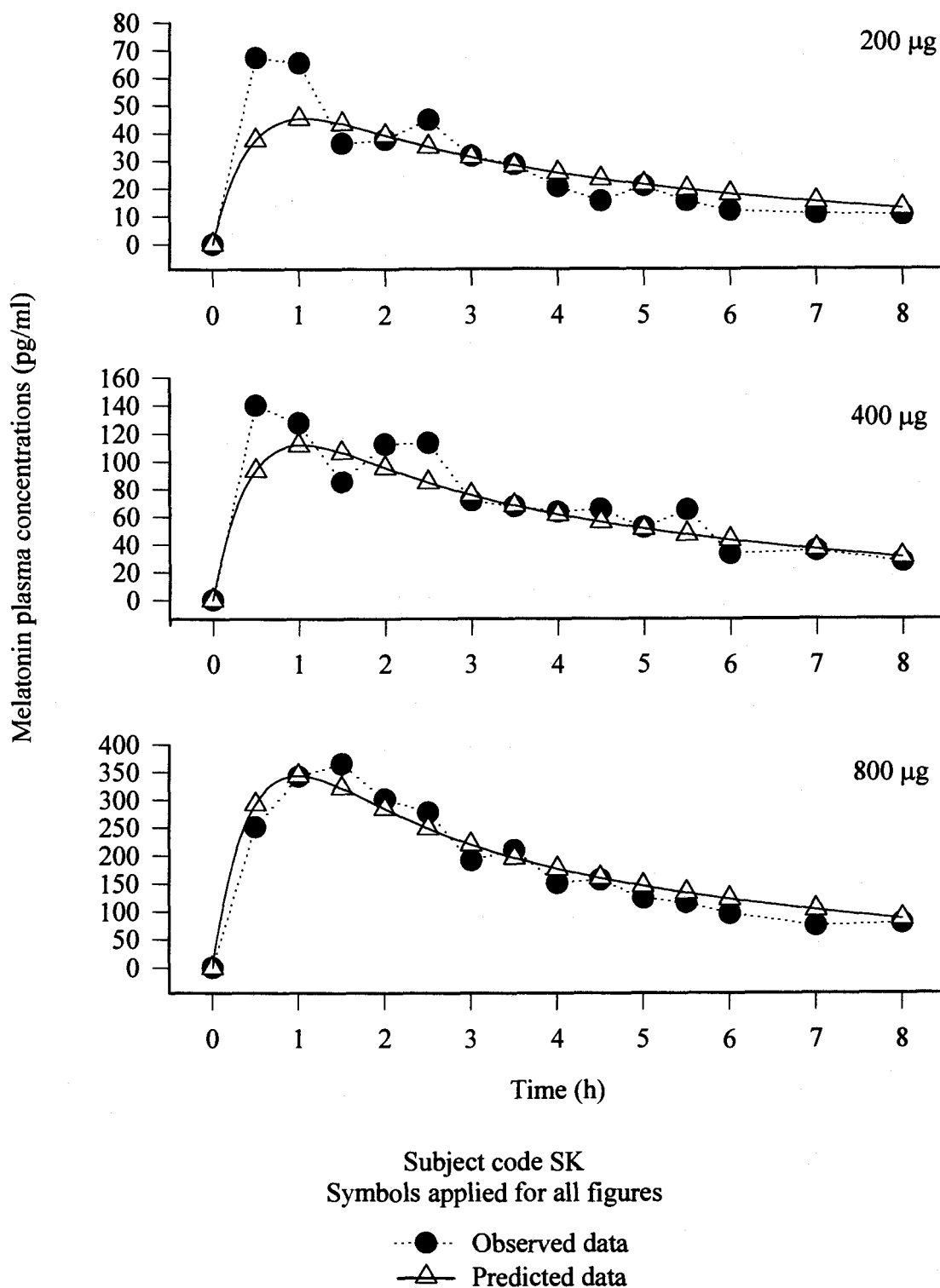
Figure 4.25: Observed versus predicted MT plasma concentration-time profiles following administration of MT SR formulation given at 200 μg, 400 μg, and 800 μg to SK.
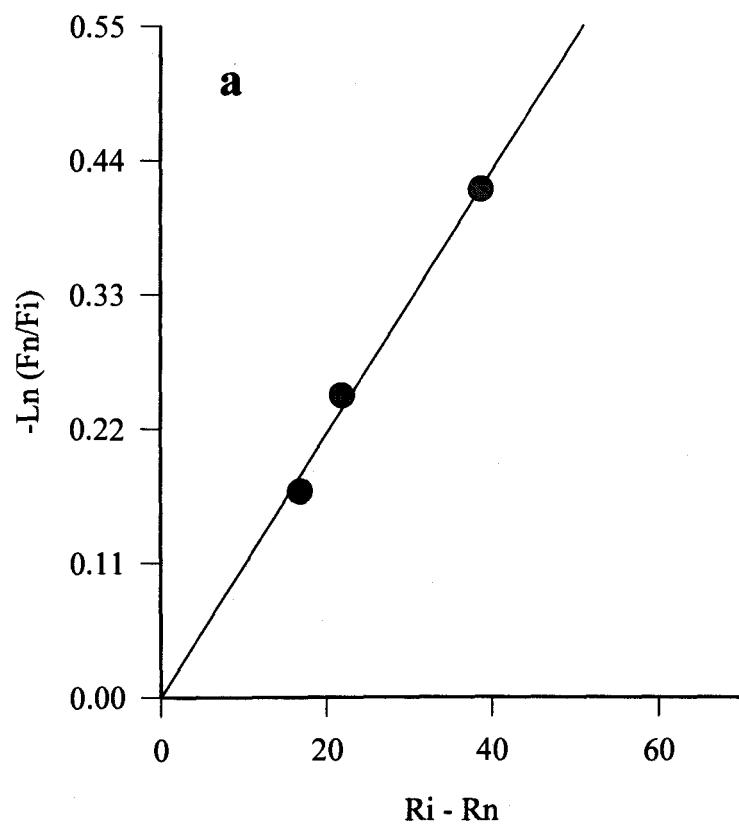
Equation 5: $-\text{Ln}\,\dfrac{Fn}{Fi} = \dfrac{(Ri - Rn)}{Q\,K^{*}m}$
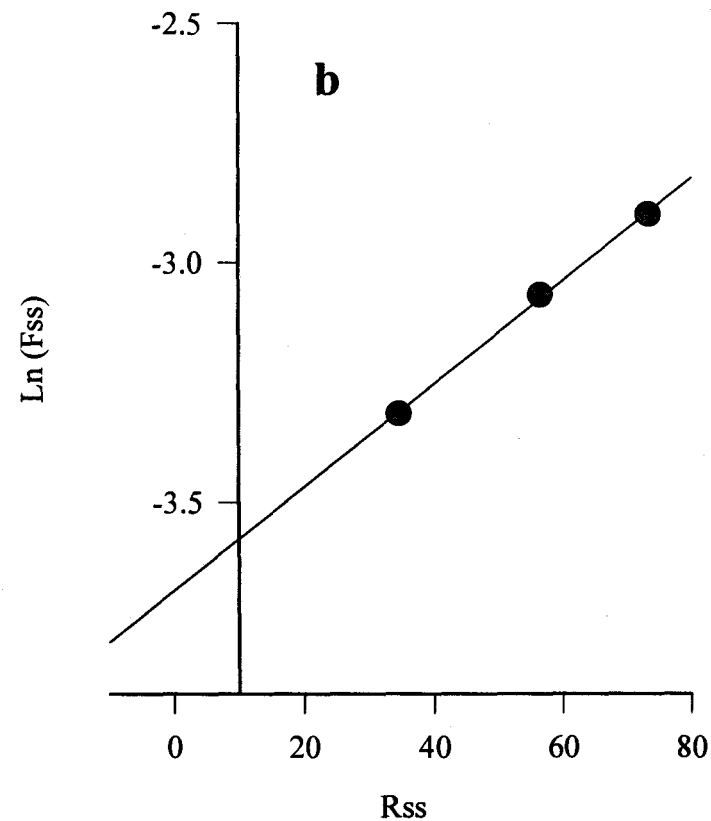
Equation 2: $\text{Ln}\,(Fss) = \dfrac{-V^{*}m}{Q\,K^{*}m} + \dfrac{Rss}{Q\,K^{*}m}$

● Experimental data
—— Regression line

Figure 4.26: The fits to Equation 5 (a) and 2 (b) using experimental data following administration of MT SR formulation given at 200 µg, 400 µg, and 800 µg in subject SL.
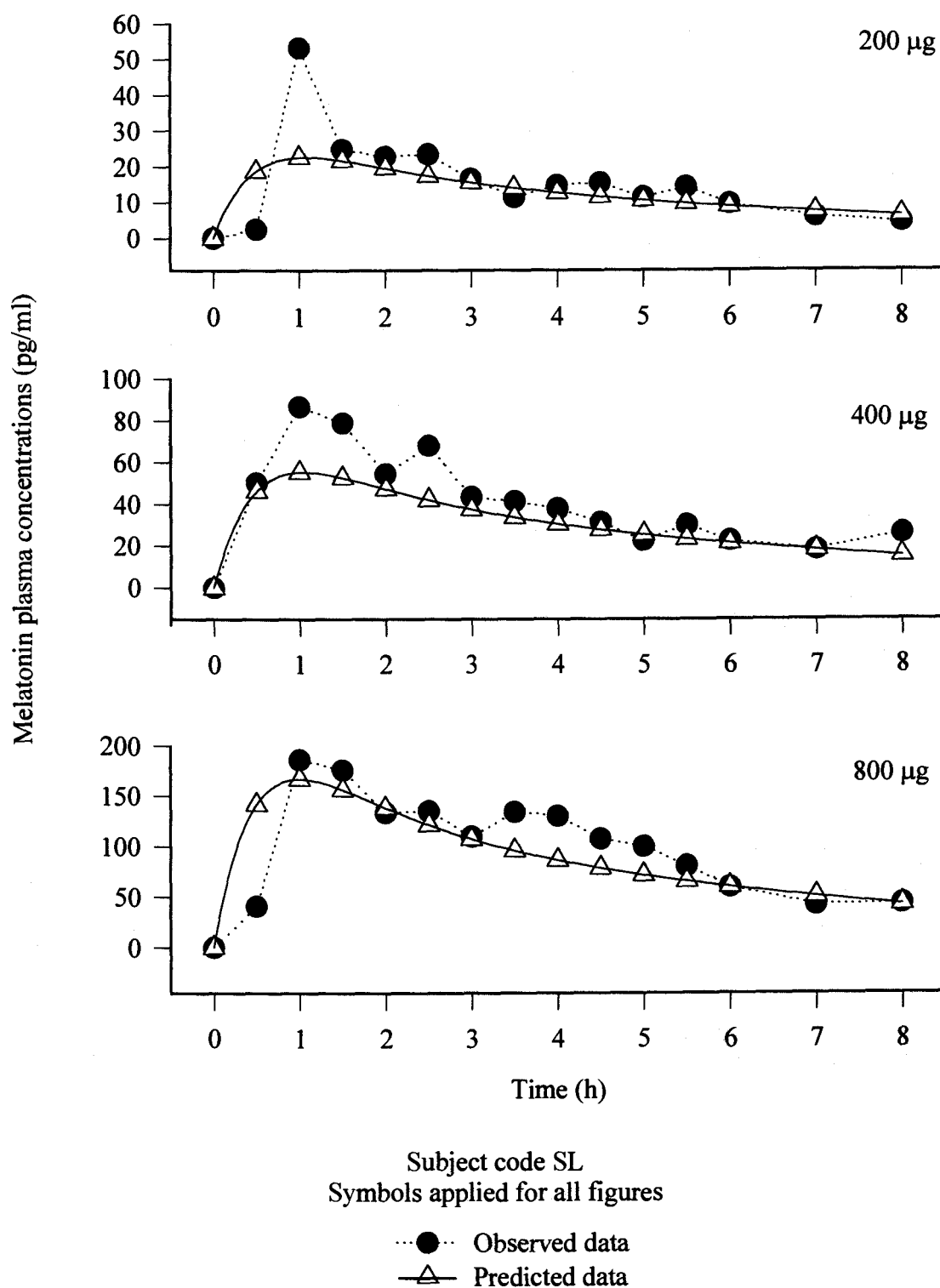
Figure 4.27: Observed versus predicted MT plasma concentration-time profiles following administration of MT SR formulation given at 200 μg, 400 μg, and 800 μg to SL.
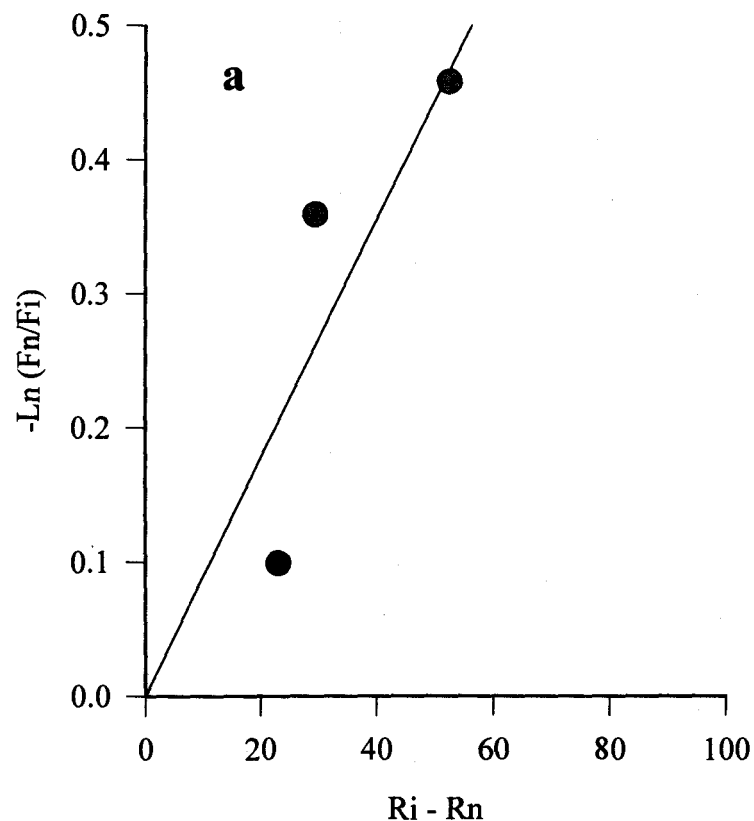
Equation 5: $-\mathrm{Ln}\,\dfrac{Fn}{Fi} = \dfrac{(Ri - Rn)}{Q\,K^*m}$

Equation 2: $\mathrm{Ln}\,(Fss) = \dfrac{-V^*m}{Q\,K^*m} + \dfrac{Rss}{Q\,K^*m}$

● Experimental data

—— Regression line
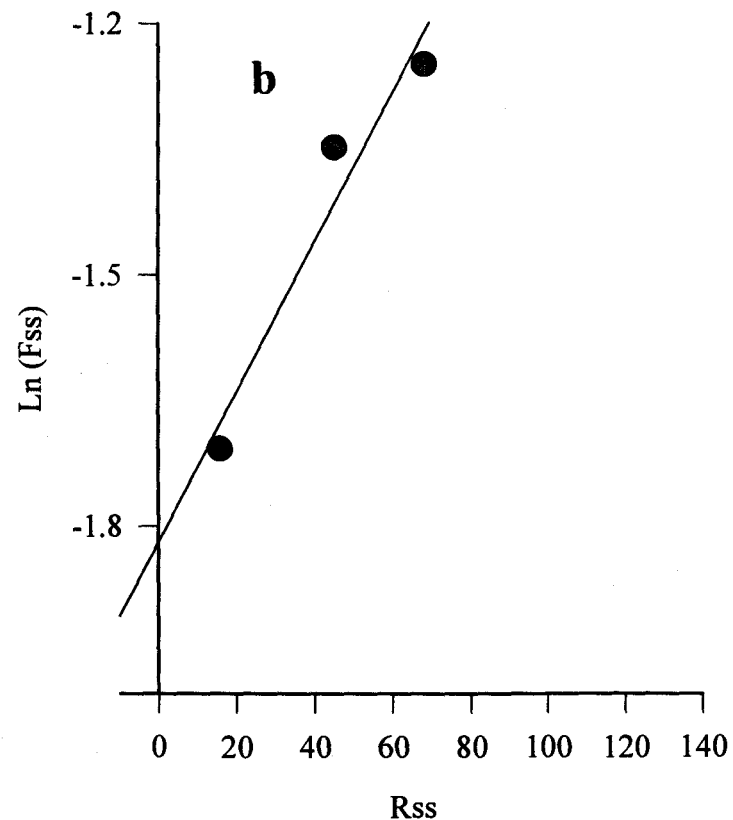
Figure 4.28: The fits to Equation 5 (a) and 2 (b) using experimental data following administration of MT SR formulation given at 200 µg, 400 µg, and 800 µg in subject AT
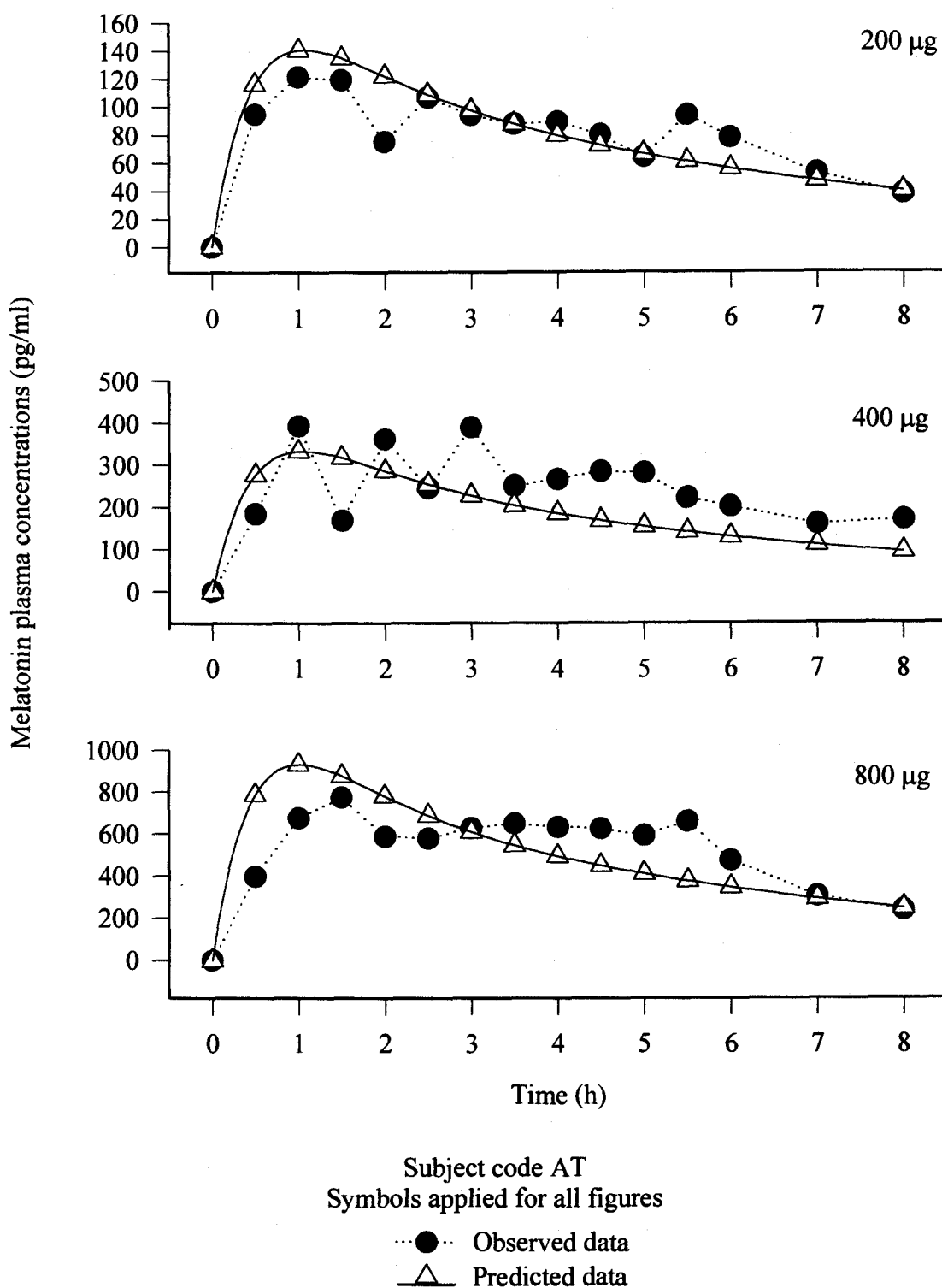
Figure 4.29: Observed versus predicted MT plasma concentration-time profiles following administration of MT SR formulation given at 200 µg, 400 µg, and 800 µg to AT.

The second case is the poor fit of experimental data to Equation 5 and 2 with small magnitude of slope which indicates less sensitiveness in change in bioavailability with change in drug release rate. Simulation results of MT plasma profiles are generally acceptable based on graphical and statistical goodness of fit. The fits to Equation 5 and 2 together with simulation results are shown in Figure 4.30 to 4.39 (subjects: CB, VB, SN, AO, and LA) .

The last case is where the fits to Equation 5 and 2 clearly go in opposite direction to what described by the theoretical model. The slopes of plots between - Ln (Fn/Fi) versus Ri - Rn and between Ln (Fss) versus Rss are negative or bioavailability decreases as drug release rate increases. As a result, the estimated values of $1/QK^*m$ and V^*m are negative and have no physiological meaning. However, prediction of bioavailability is mathematically possible. Thus, MT plasma concentration-time profiles can be generated using the predicted bioavailability. The fits to Equation 5 and 2 together with simulation results of this subject (GL) are shown in Figure 4.40 and 4.41, respectively. It is interested that subject GL is the elderly.

The proportionality between the dose (input) and AUC (output) of drug is an important criterion used to determine whether the drug exhibits linear or non-linear kinetics in the body (25). Table 4.1 showed dose-normalized AUC and Cmax to those of 200 μg following administration of MT SR formulation used in the study (presented earlier in chapter 1, but herein data were grouped together according to the results in this chapter). Correlation between individual bioavailability and drug release rate of MT generally followed relationship between the dose-normalized AUC and dose. In
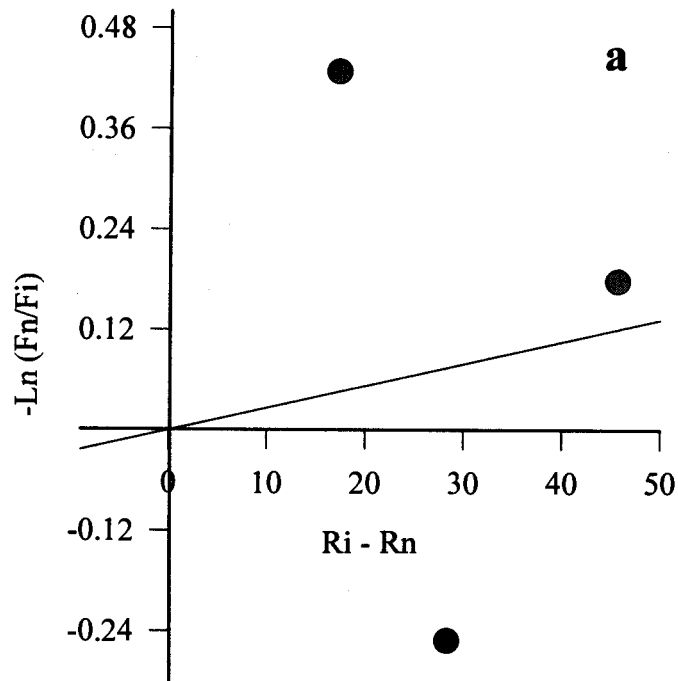
Equation 5: $-\operatorname{Ln}\dfrac{Fn}{Fi} = \dfrac{(Ri - Rn)}{Q\,K^{*}m}$
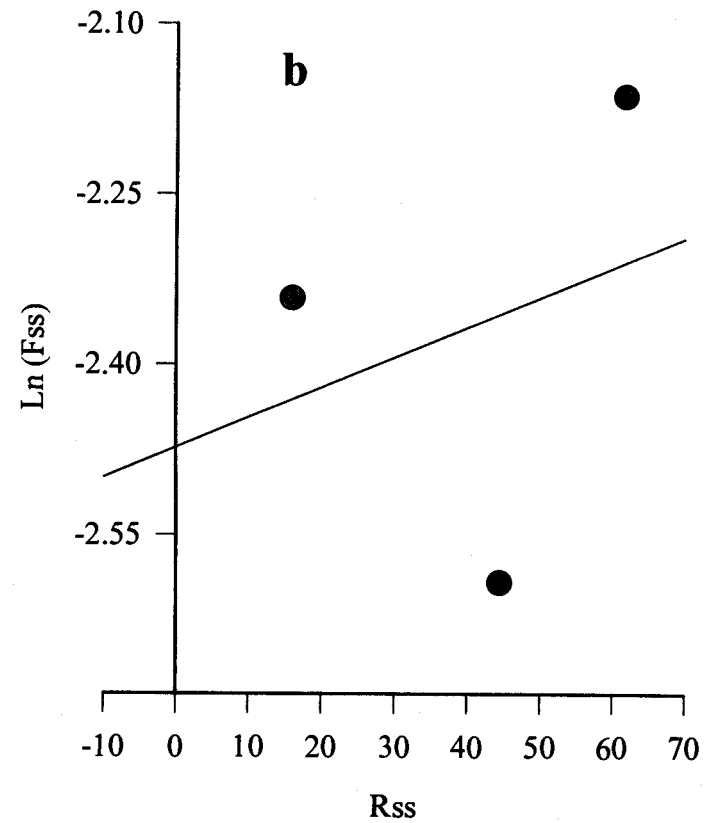
Equation 2: $\operatorname{Ln}(Fss) = \dfrac{-V^{*}m}{Q\,K^{*}m} + \dfrac{Rss}{Q\,K^{*}m}$

● Experimental data
—— Regression line

Figure 4.30: The fits to Equation 5 (a) and 2 (b) using experimental data following administration of MT SR formulation given at 200 μg, 400 μg, and 800 μg in subject CB
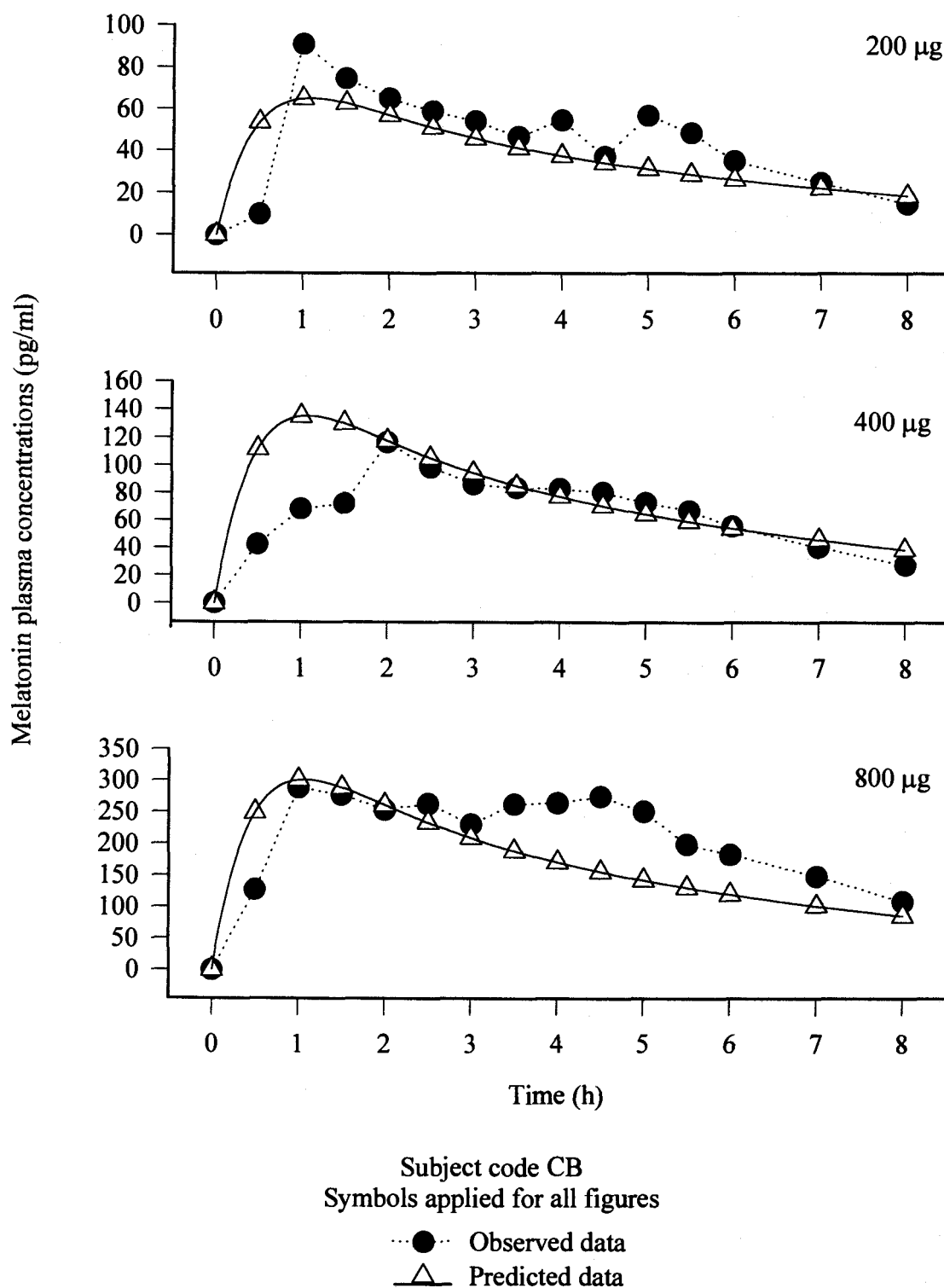
Figure 4.31: Observed versus predicted MT plasma concentration-time profiles following administration of MT SR formulation given at 200 μg, 400 μg, and 800 μg to CB.
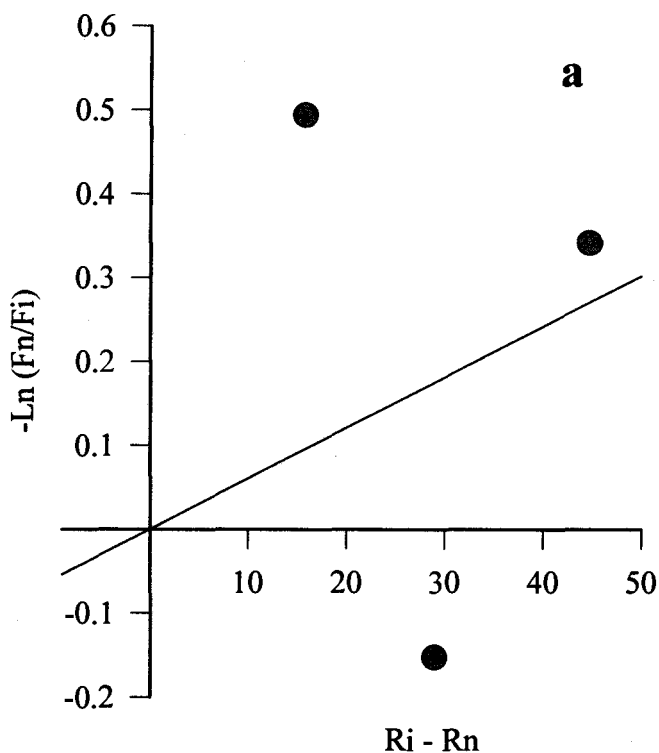
Equation 5: $-\ln \dfrac{Fn}{Fi} = \dfrac{(Ri - Rn)}{Q\,K^*m}$
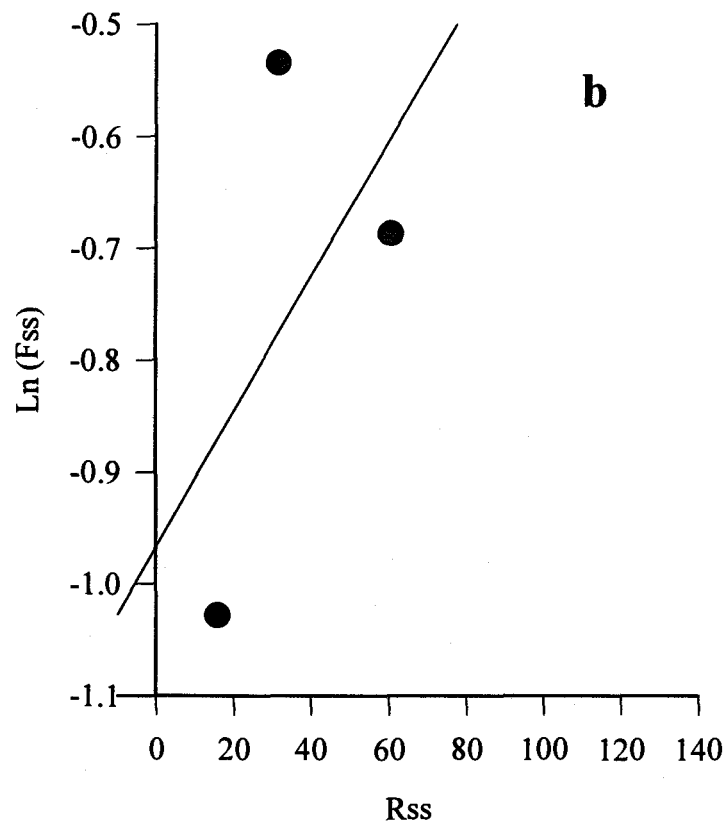
Equation 2: $\ln (Fss) = \dfrac{-V^*m}{Q\,K^*m} + \dfrac{Rss}{Q\,K^*m}$

● Experimental data
— Regression line

Figure 4.32: The fits to Equation 5 (a) and 2 (b) using experimental data following administration of MT SR formulation given at 200 µg, 400 µg, and 800 µg in subject SN
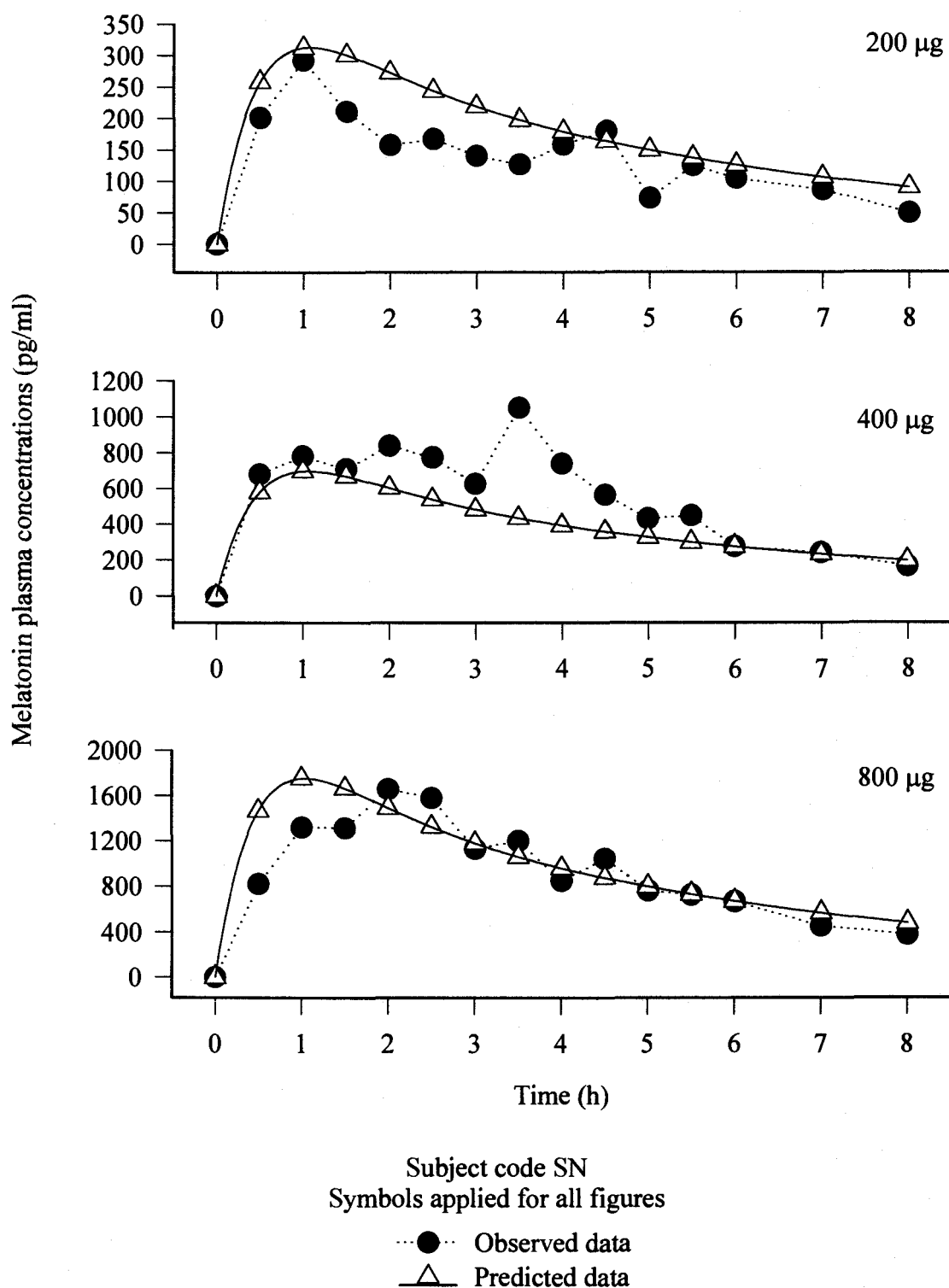
Figure 4.33: Observed versus predicted MT plasma concentration-time profiles following administration of MT SR formulation given at 200 µg, 400 µg, and 800 µg to SN.
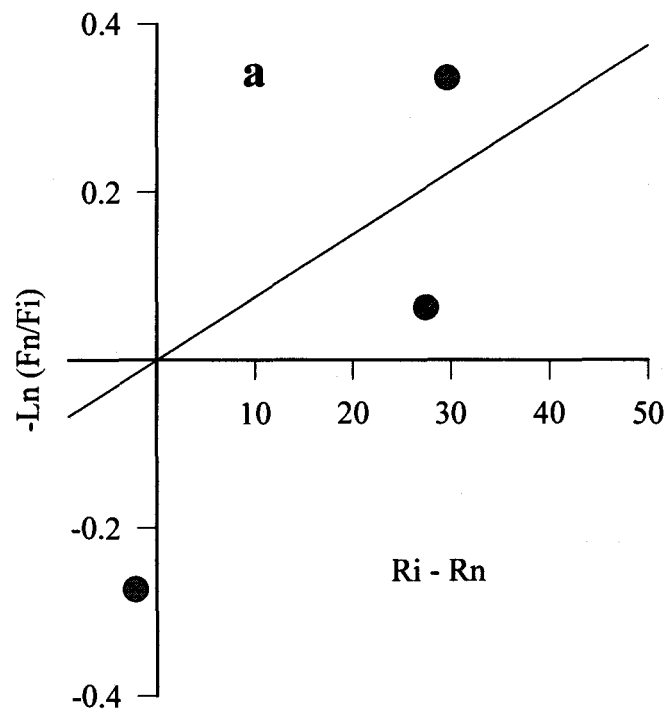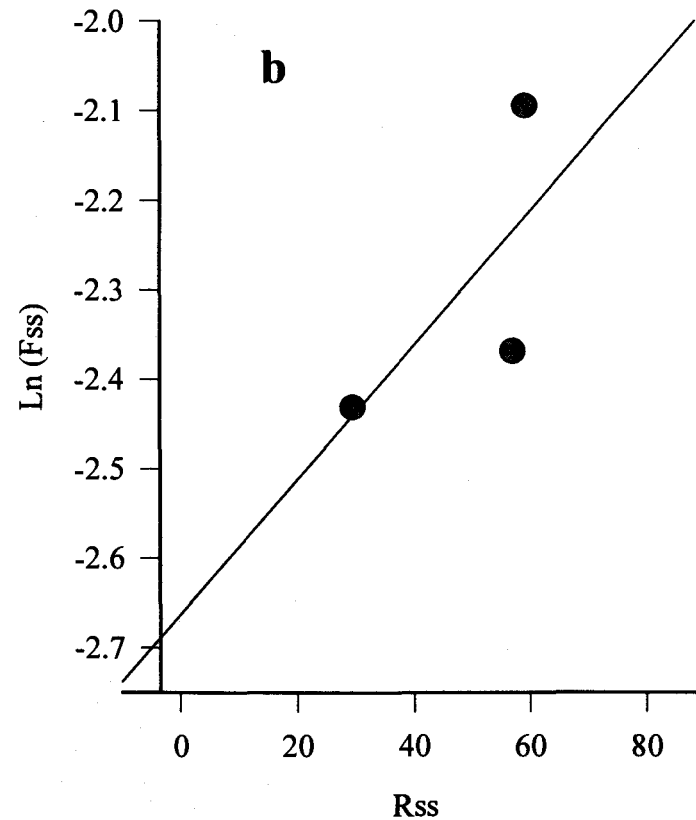
Figure 4.34: The fits to Equation 5 (a) and 2 (b) using experimental data following administration of MT SR formulation given at 200 μg, 400 μg, and 800 μg in subject VB

Equation 5: $-Ln \dfrac{Fn}{Fi} = \dfrac{(Ri - Rn)}{Q\,K{*}m}$

Equation 2: $Ln\,(Fss) = \dfrac{-V{*}m}{Q\,K{*}m} + \dfrac{Rss}{Q\,K{*}m}$

● Experimental data
— Regression line
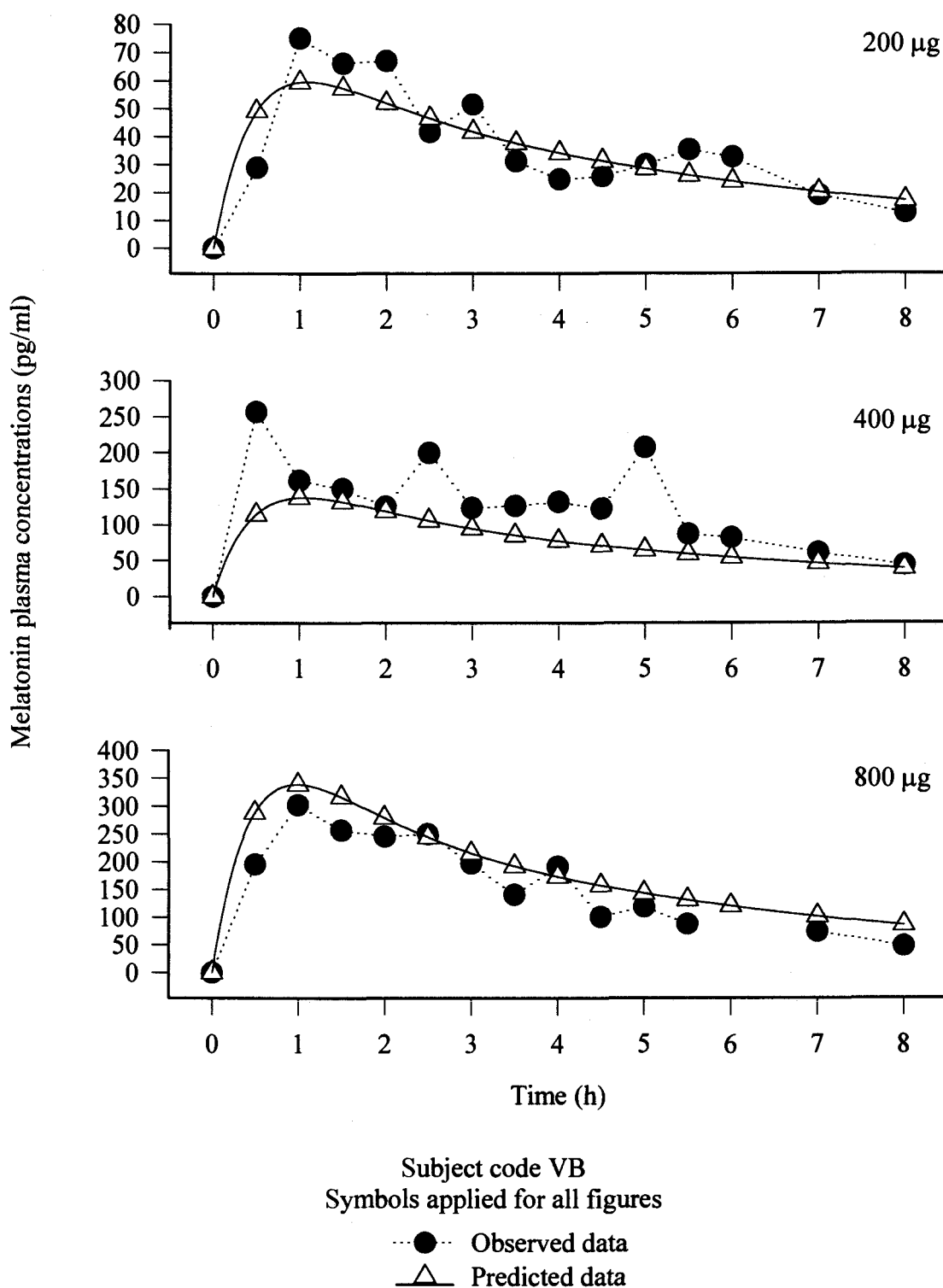
Figure 4.35: Observed versus predicted MT plasma concentration-time profiles following administration of MT SR formulation given at 200 µg, 400 µg, and 800 µg to VB.
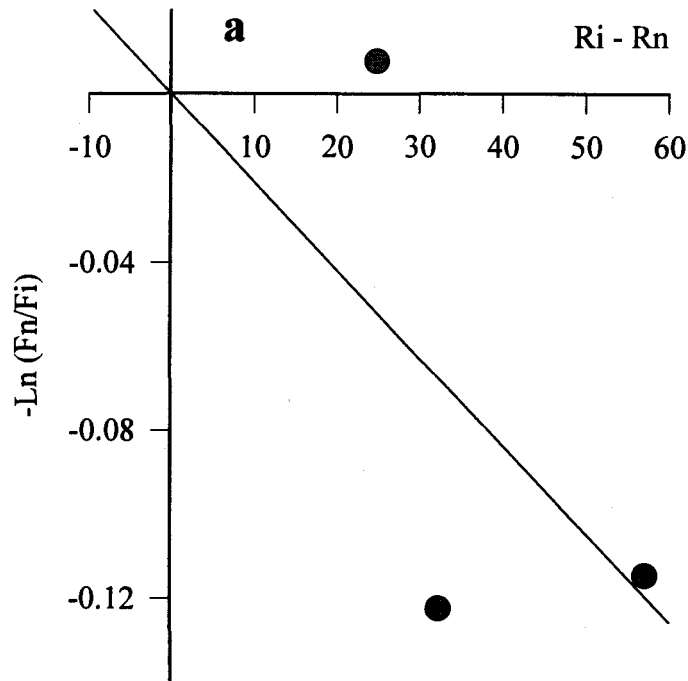
Equation 5: $-\ln \dfrac{Fn}{Fi} = \dfrac{(Ri - Rn)}{Q\,K^{*}m}$
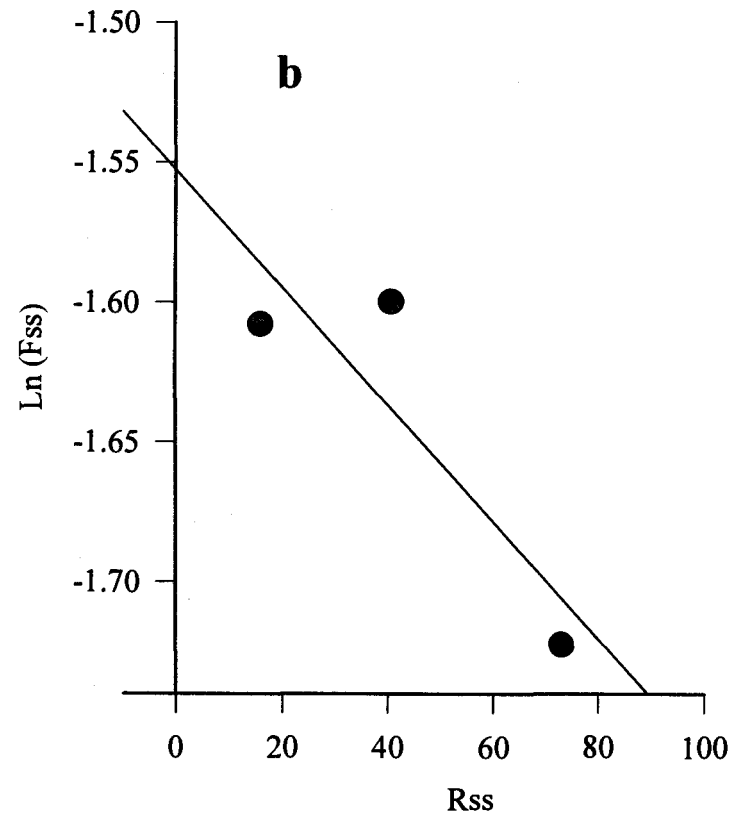
Equation 2: $\ln (Fss) = \dfrac{-V^{*}m}{Q\,K^{*}m} + \dfrac{Rss}{Q\,K^{*}m}$

● Experimental data
—— Regression line

Figure 4.36: The fits to Equation 5 (a) and 2 (b) using experimental data following administration of MT SR formulation given at 200 µg, 400 µg, and 800 µg in subject AO
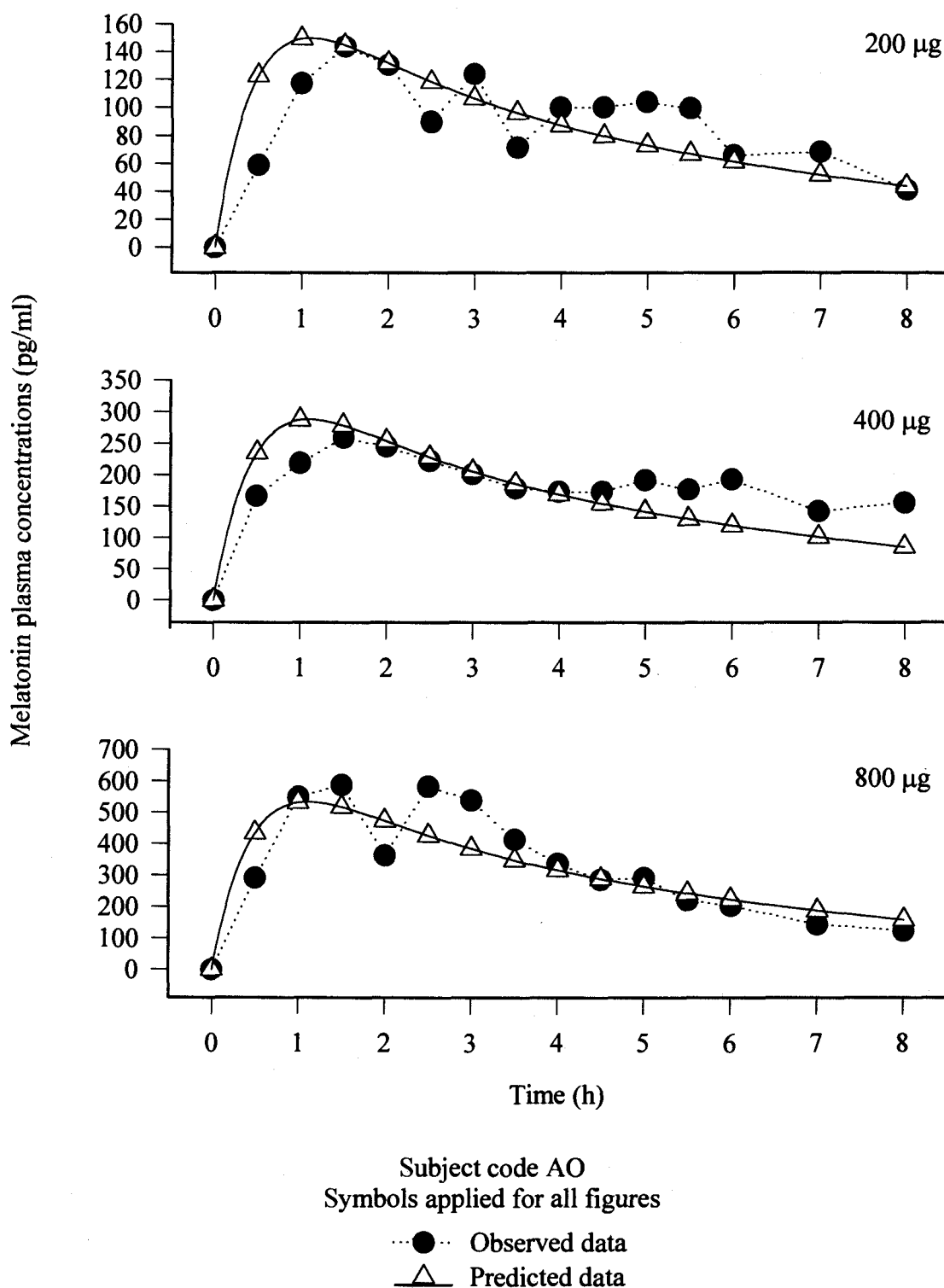
Figure 4.37: Observed versus predicted MT plasma concentration-time profiles following administration of MT SR formulation given at 200 µg, 400 µg, and 800 µg to AO.
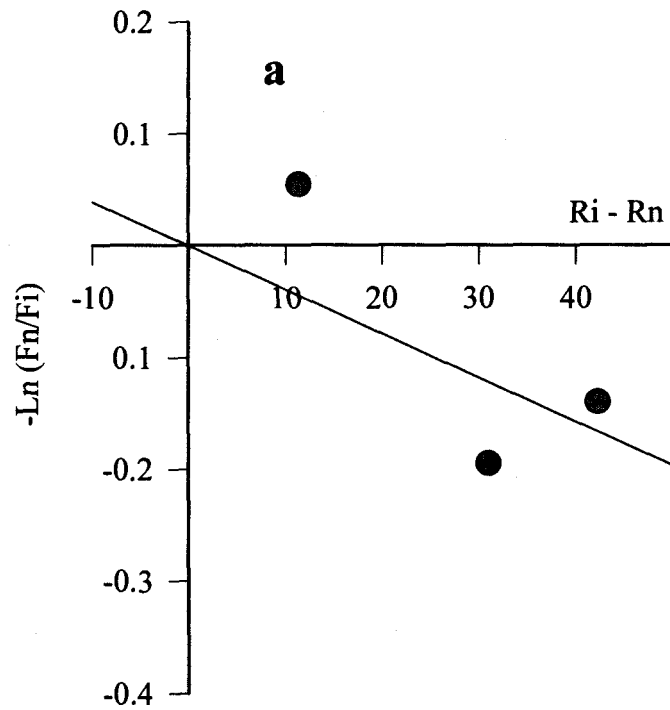
Equation 5: $-\ln \dfrac{Fn}{Fi} = \dfrac{(Ri - Rn)}{Q\,K^*m}$
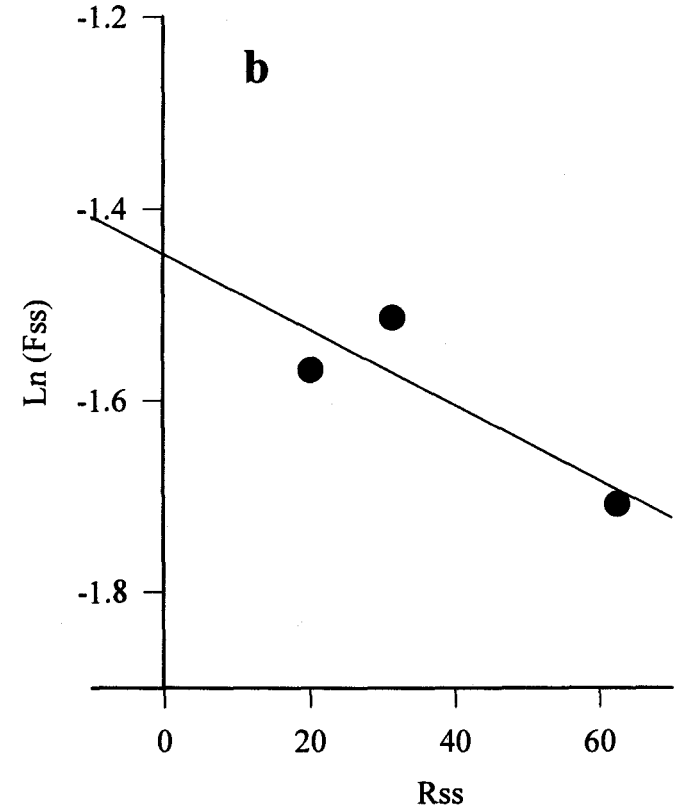
Equation 2: $\ln (Fss) = \dfrac{-V^*m}{Q\,K^*m} + \dfrac{Rss}{Q\,K^*m}$

● Experimental data
—— Regression fit

Figure 4.38: The fits to Equation 5 (a) and 2 (b) using experimental data following administration of MT SR formulation given at 200 μg, 400 μg, and 800 μg in subject LA
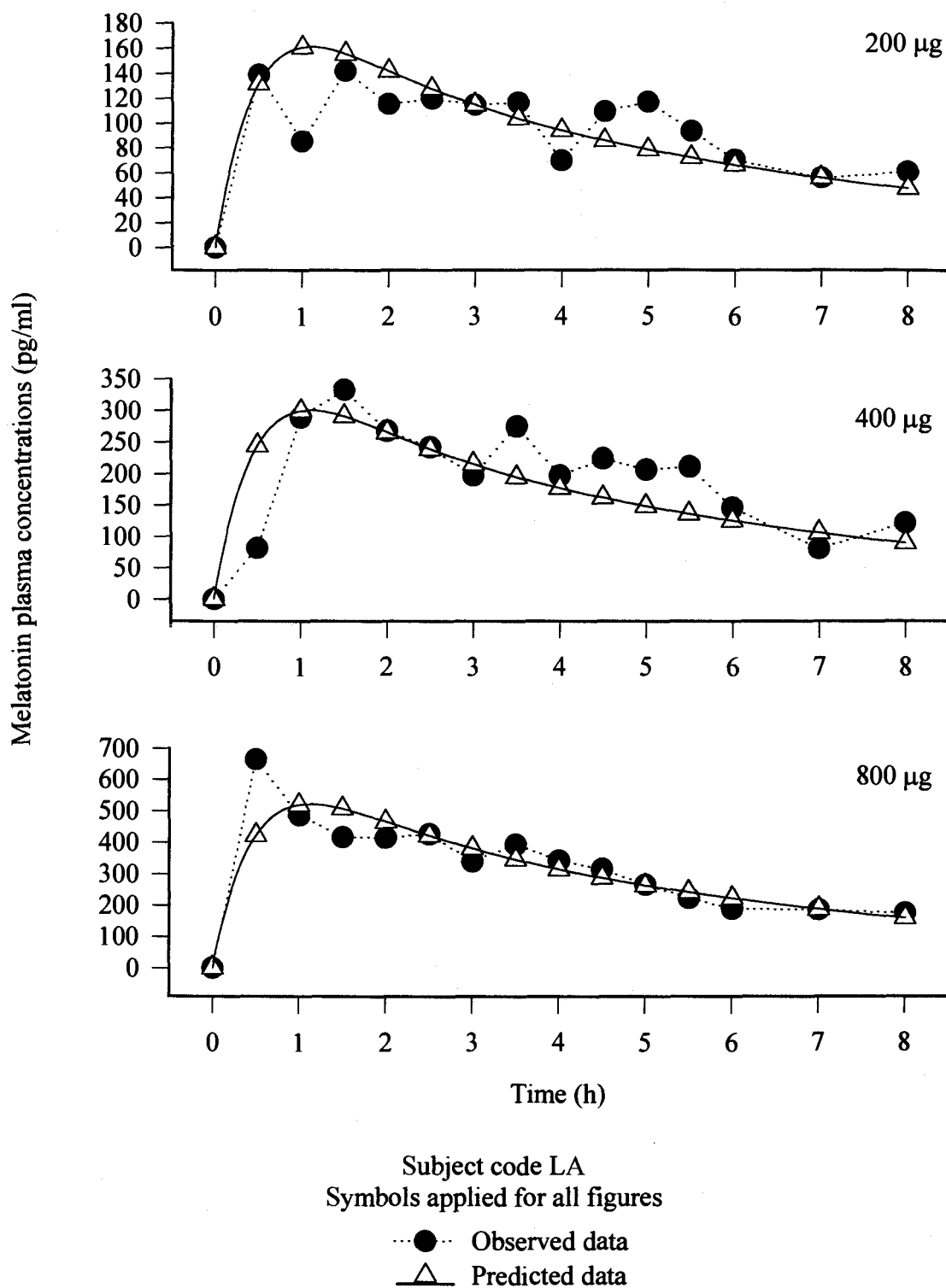
Figure 4.39: Observed versus predicted MT plasma concentration-time profiles following administration of MT SR formulation given at 200 µg, 400 µg, and 800 µg to LA.
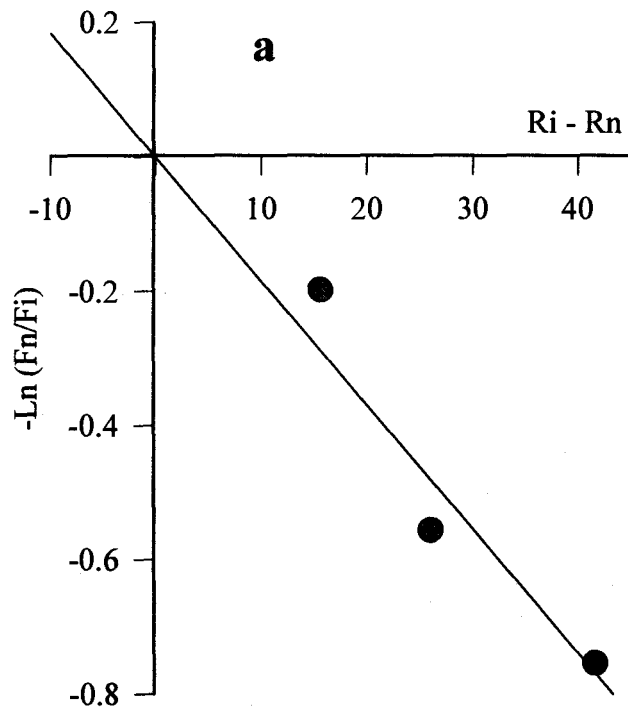
Equation 5: $-\text{Ln}\dfrac{Fn}{Fi} = \dfrac{(Ri - Rn)}{Q\,K^{*}m}$

● Experimental data
—— Regression fit
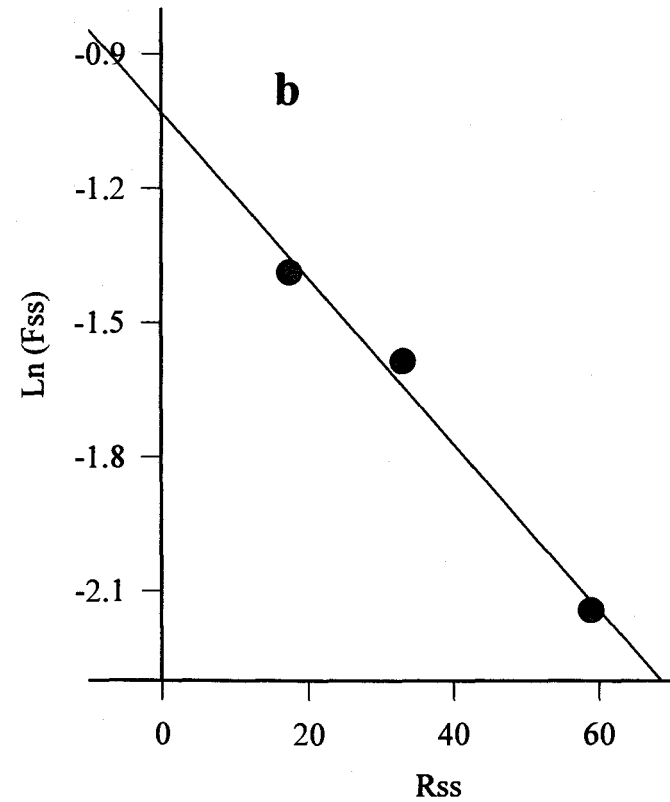
Equation 2: $\text{Ln}\,(Fss) = \dfrac{-V^{*}m}{Q\,K^{*}m} + \dfrac{Rss}{Q\,K^{*}m}$

Figure 4.40: The fits to Equation 5 (a) and 2 (b) using experimental data following administration of MT SR formulation given at 200 µg, 400 µg, and 800 µg in subject GL
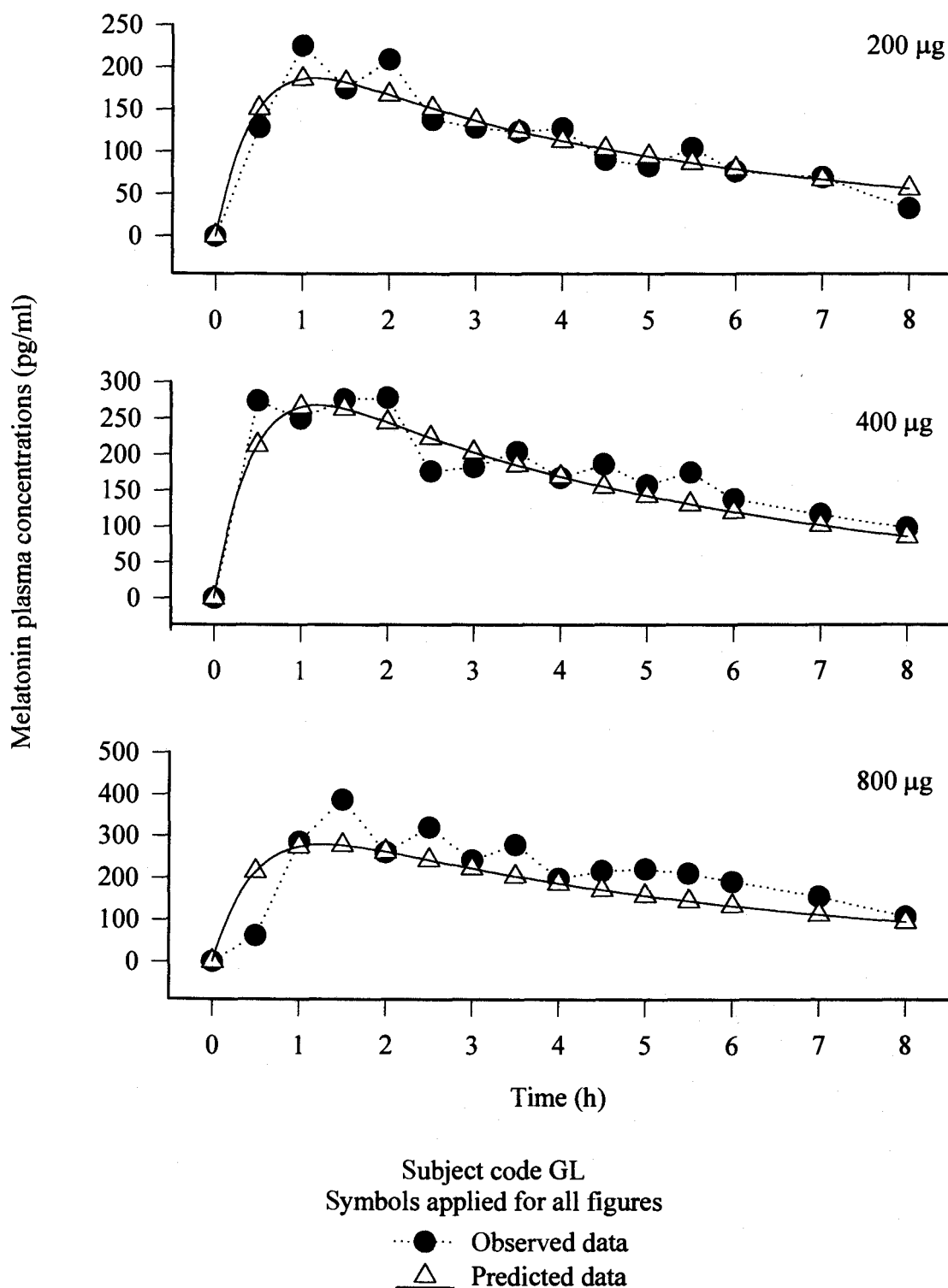
Figure 4.41: Observed versus predicted MT plasma concentration-time profiles following administration of MT SR formulation given at 200 μg, 400 μg, and 800 μg to GL.

Table 4.1: Dose normalized AUC and Cmax (to those of 200 µg dose) in 13 old and young subjects (EF = elderly female, EM = elderly male, YF = young female, and YM = young male).

AUC	CASE I							CASE II					CASE III
Expected ratio	AK (EF)	HF (EF)	KT (YF)	RC (YF)	SK (EM)	SL (YM)	AT (EF)	CB (YF)	SN (YF)	VB (YM)	AO (EF)	LA (EM)	GL (EM)
1	1	1	1	1	1	1	1	1	1	1	1	1	1
2	3	2.7	2.1	3.4	2.4	3	3.1	1.5	3.2	3.4	2.3	2	1.7
4	6.2	7.4	5.2	6.6	6.3	7.1	6.4	4.6	5.5	4.2	3.8	3.3	1.9
Cmax	CASE I							CASE II					CASE III
Expected ratio	AK (EF)	HF (EF)	KT (YF)	RC (YF)	SK (EM)	SL (YM)	AT (EF)	CB (YF)	SN (YF)	VB (YM)	AO (EF)	LA (EM)	GL (EM)
1	1	1	1	1	1	1	1	1	1	1	1	1	1
2	2.7	1.8	3.1	4.1	2.6	1.3	3.2	1.3	3.3	3.4	1.8	2.3	1.2
4	4.6	4	7.4	6.7	6.8	2.8	6.3	3.2	5.3	4	4.1	4.7	1.7

CASE I: good fits to Equation 5 and 2 (positive slope).
CASE II: poor fits to Equation 5 and 2.
CASE III: The fits to Equation 5 and 2 have negative slopes.

the first case, the AUC disproportionally increased with dose. Degree of deviation from linearity ranged from small to large. In the second case, correlation between the AUC and dose seemed to be inconsistent. Finally, in the last case the AUC generally decreased with increase in dose. Although MT pharmacokinetics appeared to be generally linear within the dose range of 200 - 800 μg, based on statistical comparison of the dose normalized ratio of AUC, Cmax, and urinary STMT, it was interesting that analysis of individual data showed deviation of the normalized parameters from the expected values.

Disproportional increase in AUC with dose can be caused by nonlinearity in absorption, distribution, and elimination. Based on previous studies of MT in both human (studies in our laboratory) and animals (4), nonlinearity of MT pharmacokinetics was found following oral administration. It is likely that the nonlinearity occurs due to saturable first pass metabolism of MT. The normalized ratio of AUC were generally greater than the expected ratio (1.0 : 2.0 : 4.0), whereas the ratio of urinary STMT appeared to be fairly linear. This observation is often found in drug demonstrating saturable first pass metabolism i.e. there is a nonlinearity in pharmacokinetics of the parent drug, whereas there is linearity in pharmacokinetics of metabolites (26). Additionally, the results in this work also support possibility of the saturable first pass effect.

There are at least three possible reasons that can cause less than proportional increase in AUC/bioavailability with dose including dissolution rate, transit time of drugs remaining in the regions of the gastrointestinal (GI) tract, and the ability or

inability of drugs to cross intestinal barriers (25). Possibility of MT incomplete absorption was previously reported (2). It was less likely that in *vivo* dissolution of the formulation decreased at higher doses since more than half of the subjects' dose-normalized AUC increased with dose. Differences in subject GI physiology may account for differences in MT absorption. It was noted that subjects whose dose-normalized AUC/bioavailability reduced with increase in dose/drug release rate were in old age (greater than 70 years). Age may affect drug absorption because the gastric acid secretion, GI blood flow, number of absorbing cells in GI tract, and GI motility are reduced in the elderly (27).

Theoretical values of V^*m and QK^*m obtained from ten subjects whose data followed the saturable first pass equations (Equation 5 and 2) are presented in Table 4.2. The data used in the modeling was obtained from the study which was not designed for development of the saturable first pass metabolism. The estimated values of the parameters are only observational data predicted by the mathematical model. Besides, the values of V^*m and K^*m are dependent on a model describing pharmacokinetic of hepatic elimination used in the calculation (21). Therefore, there is no verification of the estimated parameters.

Table 4.2: Fitted values of V*m, 1/QK*m, and QK*m of each individual subject.

Subject code	V*m (µg/h)	1/QK*m (h/µg)	QK*m (µg/h)
AK	388.6	0.0046	217.4
HF	222.6	0.0111	90.1
KT	710.0	0.0026	384.6
RC	215.7	0.0123	81.3
SK	265.2	0.0113	88.5
SL	341.1	0.0108	92.6
AT	204.4	0.0089	112.4
CB	951.3	0.0026	384.6
SN	161.2	0.006	166.7
VB	355.1	0.0075	133.3
AO	-739.4	-0.0021	-476.2
GL	-55.8	-0.0185	-54.1
LA	-371.2	-0.0039	-256.4

CONCLUSION

The fits between change in estimated bioavailability and change in drug release rate were linearly correlated, as theoretically described by Wagner et al. (5), in 7 out of 13 subjects. The plots between -Ln (Fn/Fi) versus Ri - Rn were straight lines with positive slopes passing through the origin indicating that MT bioavailability increased with increase in drug release rate. Simulation of individual MT plasma profiles were generally good. Application of predicted bioavailability together with modeling technique 2 reduced error in prediction of individual MT plasma concentrations, which varied up to 8 folds in Cmax and 15 folds in AUC. The finding of this study suggest that MT oral bioavailability could be dose-dependent and may be predictable using theoretical saturable first pass equations of the sinusoidal perfusion model (5). However, future experiments are needed to confirm the hypothesis of saturable first pass metabolism of MT in humans.

REFERENCES:

1.   Arendt, J. In Melatonin and the mammalian pineal gland; Chapman & Hall, London, UK, 1995, pp. 40, 42, 207, 248.

2.   Lane, E. A.; Moss, H. B. Pharmacokinetics of melatonin in man: first pass hepatic metabolism. J. Clin. Endocrinol. Metab. 61, 1214-1216 (1985).

3.   Waldhauser, F.; Waldhauser, M.; Lieberman, H. R.; Deng, M. H.; Lynch, H. J.; Wurtman, R. J. Bioavailability of oral melatonin in humans. Neuroendocrinol. 39, 307-313 (1984).

4.   Yeleswaram, K., Mclaughlin, L.G., Knipe, J.O., Schabdach, D. Oral bioavailability of melatonin in the rat, dog, and monkey J. Pineal. Res. in press (1997).

5.   Wagner, J.G., Antal, E.J., Elvin, A.T., Gillespie, W.R., Pratt, E.A., Albert, K.S. Theoretical decrease in systemic availability with decrease in input rate at steady-state for first-pass drugs Biopharm. Drug Disposit. 6, 341-343 (1985).

6.   Bass, L., Keiding, S., Winkler, K., Tygstrup, N. Enzyme elimination of substrates flowing through the intact liver. J. Theor. Biol. 61, 393-409 (1976).

7.   Bass, L., Robinson, P.J., Bracken, A.J. Hepatic elimination of flowing substrates: the distributed model. J. Theor. Biol. 72, 161-184 (1978).

8.   Bass, L., Winkler, K. A method of determining intrinsic hepatic clearance from the first-pass effect. Clin. Exp. Pharmacol. Physiol. 7, 339-343 (1980).

9.   Bass, L., Robert, M.S., Robinson, P.J. On the relation between extended forms of the sinusoidal perfusion and the convection-dispersion models of hepatic elimination. J. Theor. Biol. 126, 457-482 (1987).

10.   Bass, L., Keiding, S. Physiologically based models and strategic experiments in hepatic pharmacology. Biochem. Pharmacol. 37, 1425-1431 (1988).

11.   Keiding S. Hepatic elimination kinetics: the influence of hepatic blood flow on clearance determinations. Scandinavian Journal of Clinical and Laboratory Medicine 36, 113-118 (1976).

12.   Keiding S., Andreasen, P.B. Hepatic clearance measurements and pharmacokinetics. Pharmacology 19, 105-110 (1979).

13. Winkler, K., Bass, L., Keiding S., Tygstrup, N. The effect of hepatic perfusion on the assessment of kinetic constants. In Lundqvist & Tygstrup (Eds) Regulation of hepatic metabolism, 1974, pp. 797-807, Munksgaard, Copenhagen.

14. Winkler, K., Bass, L., Keiding S., Tygstrup, N. The physiological basis for clearance measurements in hepatology. Scandinavian Journal of Gastroenterology 14, 439-448 (1979).

15. Winkler, K., Bass, L., Keiding S., Tygstrup, N. Clearance as a quantitative measurement of liver function. In Paumgartner & Preisig (Eds) The liver. Quantitative aspects of structure and function, 1973, pp. 144-155, Karger, Basel.

16. Morgan, D.J., Smallwood, R.A. Clinical significance of pharmacokinetic models of hepatic elimination Clin. Pharmacokinetic. 18(1), 61-76 (1990).

17. Anderson, J.H., Anderson, R.J., Iben, S. Hepatic uptake of propanolol. J. Pharmacol. Exp. Ther. 206, 172-180 (1978).

18. Groothius G.M.M., Hardonk, M.J., Keulemans, K.P.T., Niewenhuis, P., Meijer, D.K.F. Autoradiographic and kinetic demonstration of heterogeneity of taurocholate transport. American J. Physiol. 243, G455-G462 (1982).

19. Jones, A.L., Hradek, G.T., Renston R.H., Wong, K.Y., Karlaganis, G. et al. Autoradiographic evidence for hepatic lobular concentration gradient of bile acid derivative. American J. Physiol. 238, G233-G237 (1980).

20. Weisiger, R.A., Mendel, C.M., Cavalieri, R.R. The hepatic sinusoid is not well-stirred: estimation of the degree of axial mixing by analysis of lobular concentration gradients formed during uptake of thyroxine by the perfused rat liver. J. Pharm Sci. 75, 233-237 (1986).

21. Wagner, J.G. Comparison of nonlinear pharmacokinetic parameters estimated from the sinusoidal perfusion and venous equilibrium models. Biopharm. Drug Disposit. 6, 23-31 (1985).

22. Lewy, A.J., Markey, S.P. Analysis of melatonin in plasma by gas chromatography negative chemical ionization mass spectroscopy, Science 201, 741-743 (1978).

23.   Gillespie, W.R. PCDCON: Deconvolution for pharmacokinetic applications. AAPS Short Course of Convolution, deconvolution and linear systems. Miami Beach, FL, November 5, 1995.

24.   Iguchi, H., Kato, K.I., Ibayashi., H. Melatonin serum levels and metabolic clearance rate in patients with liver cirrhosis., J. Clin. Endocrinol. Metab. 54, 1025-1027 (1982).

25.   Lin, J.H. Dose-dependent pharmacokinetics: experimental observations and theoretical considerations. Biopharm. Drug Disposit. 15, 1-31 (1994).

26.   Lee, P.I.D., Amidon, G.L. Pharmacokinetics of metabolites. In Pharmacokinetic analysis Technomic Publishing Company, Inc., Pennsylvania, 1996, pp. 237-272.

27.   Benet, L.Z., Massoud, N., Gambertoglio, J.G. Pharmacokinetic basis for drug treatment, Raven Press, New York, 1984.

CHAPTER 5

MODELING OF MELATONIN PLASMA PROFILES FROM URINARY 6-SULPHATOXYMELATONIN.

ABSTRACT

Two new methods for simulation of melatonin (MT) plasma concentration-time profiles using urinary 6-sulphatoxymelatonin (6STMT, chief metabolite of MT) data are proposed. Data from previous studies of oral solution, oral sustained release formulation, and transdermal application in humans were used in development of the models. In technique 1, the relationship between MT plasma AUC (0 - t) and total urinary 6STMT (0 - t) were described by polynomial equations. Simulated MT plasma AUC (0-t) were then used to generate MT plasma concentration-time profiles. Results showed availability of total urinary 6STMT data allowed good prediction of MT plasma concentration-time profiles following the three formulations. In technique 2, deconvolution technique was applied to estimate weighting function describing 6STMT formation and excretion in urine. The weighting function was then employed to generate MT plasma profile. Deconvolution was performed using PCDCON. Satisfactory prediction was obtained for data set of oral solution, and oral sustained release formulation. Deconvolution failed to give reasonable estimation of weighting function when it was applied to data following MT transdermal application. Reason for this failure was unclear but it could be due to sensitiveness to nature of input data of deconvolution technique in PCDCON. Application of the two modeling techniques

for future prediction is valid only in range of MT linear pharmacokinetics. The polynomial relationships for prediction of MT plasma concentrations based on urinary 6STMT (technique 1) and the weighting function (technique 2) is restricted to each individual subject and type of dosage form due to large intersubject variability in excretion of 6STMT. The approaches are anticipated to be of value in formulation modification and to be useful for long term evaluation of different MT dosage forms given to the same subject where blood sampling is difficult.

INTRODUCTION

Melatonin (MT), an indole neurohormone secreted by the pineal gland in the brain, have caught attention of many people and investigators lately due to its therapeutic potentials and safety. Because of its short plasma half life of approximate 45 min (1), exogenous MT needs to be delivered in sustained release manner in order to mimic a physiological pattern. Basically, concentrations of drug in systemic circulation (blood/plasma) are used for pharmacokinetic evaluation of developed formulations. Collection of blood samples is an invasive method that needs special attention in both method of collection and total amount of blood drawing in the study. This requires admission of subjects at clinical research center throughout the period of study. Furthermore, it is difficult to perform such study in special population such as small children. Collection of other biological fluid such as urine, or saliva would be valuable alternative methods if significant amount of drug is excreted in the collected biological fluid.

Although only about 1 percent of MT present in blood escapes into the urine in the unchanged form (2). Previous studies have supported the use of urinary 6-sulphatoxymelatonin (6STMT), MT chief metabolite, as a non-invasive index of MT plasma concentrations resulting from both physiological production and exogenous administration (3, 4, 5, 6, 7,8). MT is mainly metabolized in the liver followed by the kidney. In phase 1, MT undergoes 6-hydroxylation, followed by sulfate or glucoronide conjugation in phase 2 (1), similarly to the metabolism of steroids and the deactivation and detoxification of many drugs, etc. (9).

More than 85% of MT is excreted in urine as 6STMT (1, 10, 11). Measurement of urinary 6STMT was recently used for relative evaluation of a controlled-release MT tablet in 12 elderly subjects (10). However, simulation of MT plasma concentration-time profiles based on tracking urinary 6STMT have not yet been proposed.

The purpose of this work is to develop simple and reliable methods to simulate MT plasma profiles using urinary 6STMT data. The process involves application of data from previous studies in different subjects. Accuracy of modeling results is discussed based on simulation results. The application of the approach may be useful for long term clinical evaluation of MT products, and MT dose regimens where blood sampling is difficult.

METHODS

The present work reports on modeling of data from a study of MT solution administered orally (Chapter 2), as well as other MT studies conducted previously, including oral sustained release (SR) formulations (7) and transdermal delivery (8).

Data collection

For completeness of the present work, data collection procedures of previous MT studies are briefly described below.

Solution (Chapter 2)

Eleven healthy volunteers, 6 females and 5 males under age 25 were recruited from Oregon State University. They were given an oral solution of MT (dose of 750 µg) at 9 am. Subjects fasted overnight and four hours after dosing. Water and juices were given orally ad lib during fasting. Blood and urine samples were collected for measurement of MT and 6STMT, respectively. Blood samples were collected 10 min prior to dosing to provide baseline values and at 0.25, 0.5, 1, 1.5, 2, 2.5, 3, 4, 6, 8, and 10 h post dosing. Urine samples were collected at approximately 15 min prior to dosing and every 1 hour for the first 6 h after dosing, and at subject convenient occasions for a 24 h study period. Twenty four hour baseline data for endogenous 6STMT in each subject was obtained from urine samples collected the day before the solution study was conducted but without any MT administration. MT plasma

concentrations were determined by high-sensitivity GC/MS (12). Urinary 6STMT

concentrations were determined by radioimmunoassay (13).

Oral sustained release formulation (7)

Six healthy volunteers (1 female and 5 males) participated in the study.

Subjects fasted at least 2 h before study and were given an oral SR MT formulation.

The products containing a combination of 20% immediate release (IR) and 80% SR

MT (14) were administered at 500 μg (100 IR + 400 SR) and 1000 μg (200 IR + 800

SR) in 4 and 2 subjects, respectively. Blood and urine samples were collected for 8 h

period of time. 24 h control urine study was carried out after 1 week washout period.

Transdermal delivery (15)

A Hill Top Chamber with Webril pad was used as the transdermal delivery

device (TDD). 200 μl solution of MT (10 mg/ml of 40% propylene glycol in

phosphate buffer pH 6.5) was placed in the device. Four TDD's were applied to a

hairless area of each subject's forearm. Total TDD surface area and MT content were

3.8 cm^2 and 8 mg, respectively. The study was conducted in 4 male volunteers. Blood

and urine samples were collected for 8 and 12 h period of time, respectively. Control

urine study (from 1 pm. to 7 pm.) was carried out after 2 week washout period.

Modeling approach

Two modeling techniques are proposed. In the first technique, simulation of MT plasma profile is generated using correlation between area under the curve (AUC) of MT plasma concentration-time profile and total urinary 6STMT excretion data. In the second technique, deconvolution technique is employed for the simulation.

Modeling technique 1

Modeling of MT plasma concentrations using urinary 6STMT data is based upon a relationship between MT plasma AUC and total urinary 6STMT. MT plasma AUC and total urinary 6STMT have been previously reported to be linearly correlated (3, 6). MT plasma concentrations and 6STMT plasma concentrations are fairly parallel to each other after oral administration of 2 mg IR MT in 6 subjects (1). However, biological half-life of MT was reported to be slightly shorter than that of 6STMT, 44 min and 58 min, respectively (1). Therefore, it may be appropriate to describe the relationship between MT plasma AUC and total urinary 6STMT using polynomial equations.

Steps involved in simulation of MT plasma concentrations based on tracking urinary 6STMT are

1. Derivation of a polynomial equation describing the relationship between total urinary 6STMT and MT plasma AUC, for each individual receiving the drug.

2. Simulation of MT plasma concentrations based on predicted MT plasma AUC using the polynomial equation and experimental total urinary 6STMT.

Derivation of the polynomial equation

To derive a polynomial equation describing MT plasma AUC using total urinary 6STMT data, experimental data of both variables need to be fitted at equal time points. This can be done using an interpolation technique such as polynomial, splines, etc. Here in, interpolating cubic splines was used to fit observed total urinary 6STMT and observed MT plasma concentrations at each stepsize time (i.e. 0.05 h). AUC was calculated from the interpolated MT plasma concentration-time profile. Relationship between the calculated AUC and urinary 6STMT was then defined by polynomial equation. General form of the polynomial equation is shown in equation 1. Cubic spline interpolation and polynomial fitting program were written in Sigma Plot (version 2.0).

<u>Equation 1</u>

$$\text{MT plasma AUC (0-t)} = \sum_{n}^{i=o} a_i \, [\text{urinary 6STMT (0-t)}]^i$$

Simulation of MT plasma concentrations

Experimental urinary 6STMT (0-t) data were applied as independent variables in equation 1 to obtain predicted MT plasma AUC (0-t). The simulated MT plasma AUC (0-t) was then used to generate MT plasma concentration-time profile. The calculation of MT plasma concentration at any mid point time (t_{midi}) is shown in equation 2.

Equation 2

Predicted Concentration (t_{midi}) = $\dfrac{[AUC\ (0\ to\ ti+1) - AUC\ (0\ to\ ti)]}{(ti+1 - ti)}$

" t_{midi} " is the mid point time between $ti+1$ and ti as displayed in equation 3.

Equation 3

$$t_{midi} = \frac{(ti+1 + ti)}{2}$$

The predicted MT plasma concentration at t_{midi} was plotted versus

" t_{midi} " to generate MT plasma profiles.

Modeling technique 2

Convolution and deconvolution algorithms, based on linear system theory, are

shown to be a general, flexible, and handy tool for correlating data in pharmaceutical

sciences (16, 17). System in convolution and deconvolution are composed of response

function, input function, and weighting function. Convolution is originated from

Laplace transform theory (17). Langenbucher has described the simplified

convolution/deconvolution concept used in pharmaceutical science which is shown

below (18).

Let

R(t) = response function

I(t) = input function

W(t) = weighting function

Algebraically it can be written as (16).

Equation 4

$$R(t) = \int_0^t I(\theta)\ W(t-\theta)\ d\theta$$

In a formal notation, convolution is symbolized as (17)

Equation 5

$$R(t) = I(t) * W(t)$$

The inverse operation of deconvolution calculates either input or weighting function by

Equation 6

$$I(t) = R(t)\ //\ W(t) \qquad \text{or}$$

Equation 7

$$W(t) = R(t)\ //\ I(t)$$

If two preparations A and B are given to the same body system, the basic assumption is that the weighting function is identical for both. Hence, the two inputs and responses are related by a "rule of three" proportion (16):

Equation 8

$$R_A(t)\ //\ I_A(t)\ =\ R_B(t)\ //\ I_B(t)\ =\ W(t)$$

Thus, either input or response of B can be calculated from the time functions of A, without exact description of the weighting function:

Equation 9

$$I_B(t)\ =\ R_B(t)\ //\ [\ R_A(t)\ //\ I_A(t)\ ]$$

Equation 10

$$R_B(t) = I_B(t) * [R_A(t) // I_A(t)]$$

The concept of deconvolution was employed to generate MT plasma concentration using 6STMT urinary excretion rate-time profile. In this case, response function [R(t)] is 6STMT urinary excretion rate-time profile; input function is MT plasma concentration time profile [I(t)]; and finally weighting function [W(t)] is a function describing metabolite (6STMT) formation and excretion in urine. If the function describing 6STMT formation in urine is assumed to be identical between dosage forms (Equation 8) i.e. in the same subject, the same route of administration, and following linear pharmacokinetics within applied dose range, MT plasma profile following administration of different dosage form can be generated using deconvolution technique (Equation 9).

Steps involved in simulation of MT plasma concentration time profile based on deconvolution technique are

1. Determination of the function describing 6STMT formation in urine by deconvolution i.e. applying 6STMT urinary excretion rate-time profile as response function and MT plasma profile as input function.

2. Simulation of MT plasma concentration time profile by deconvolution of 6STMT urinary excretion rate-time profile using the weighting function derived from step 1.

Deconvolution was performed using PCDCON (18). Scheme of deconvolution approach to simulate MT plasma profile from 6STMT urinary excretion rate-time profile are shown in Figure 5.1. Brief instruction for PCDCON is described below.

Estimation of weighting function [W(t)] using PCDCON:

1. Employ 6STMT urinary excretion rate-time profile as input response specification.

2. Employ MT plasma concentration-time profile as impulse response specification (use impulse dose of 1).

3. Perform deconvolution to estimate weighting function [W(t)] describing 6STMT formation and excretion in urine by selecting "plot cumulative input".

Simulation of MT plasma profile:

1. Employ 6STMT urinary excretion rate time profile as input response specification.

2. Employ the derived weighting function [W(t)] time profile as impulse response specification. Use impulse dose of 1 since dose was the same for both input response and impulse response. If dose is different, impulse dose is needed to be adjusted in appropriate proportion.

3. Perform deconvolution to simulate MT plasma profile by selecting "plot cumulative input".

other metabolites
formation

urine

MT in
dosage form

released   absorbed

GI tract

Systemic
circulation
MT plasma
profile
I(t)

less than 1%
of MT appears
in urine

Primary metabolism

metabolized

6STMT in
systemic
circulation

excreted

W(t)

Urine

6STMT urinary
excretion rate-time
profile
R(t)

$I(t)*W(t) = R(t)$
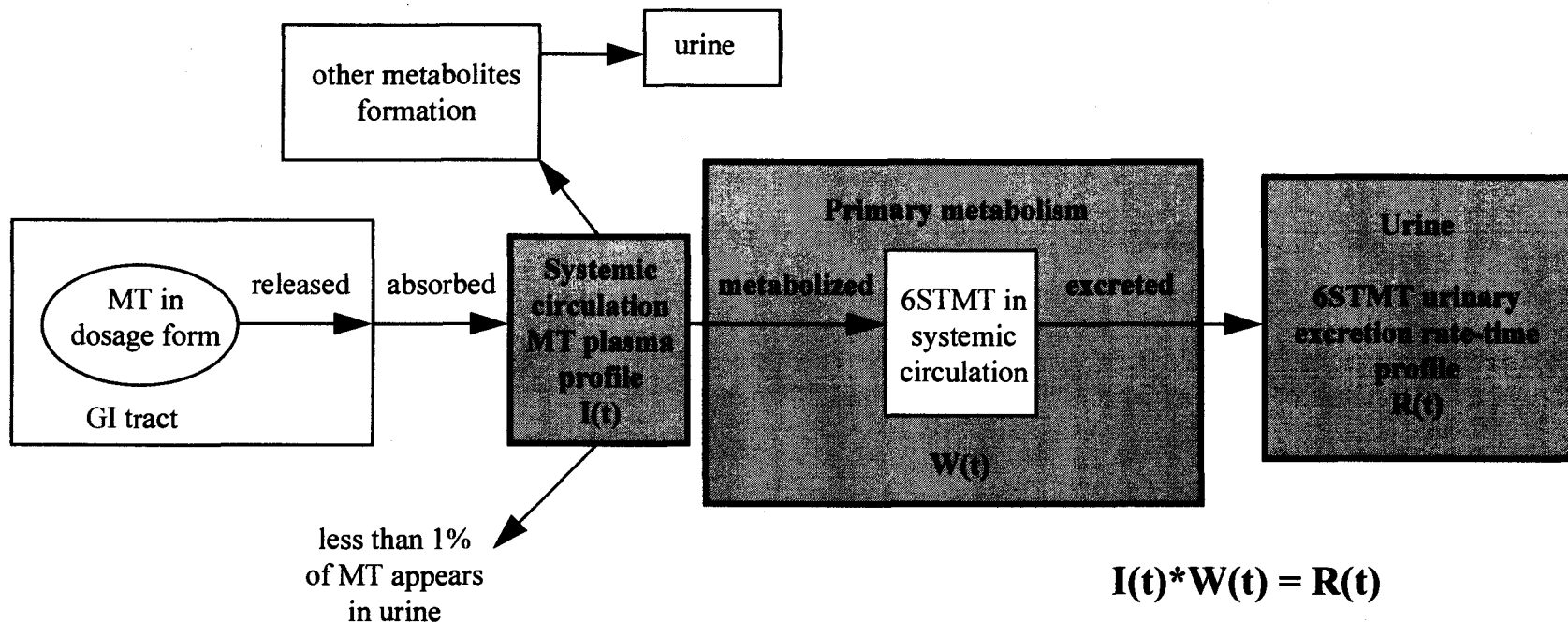
Figure 5.1: Scheme of deconvolution approach to simulate MT plasma profile from 6STMT urinary excretion rate-time profile.

RESULTS AND DISCUSSION

Modeling technique 1

Relationship between MT plasma AUC (0-t h, pg h/ml) and total urinary

6STMT (0-t h, µg) following administration of oral solution, oral SR formulation, and

transdermal application, are shown in Figure 5.2 to 5.5, respectively. Observed and

predicted MT plasma profiles following administration of the three formulations are

displayed in Figure 5.8 to 5.9. The data are displayed as experimental data, and

simulated data based on polynomial curve fitting derived from Equation 1.

The relationship between MT plasma AUC (0-t) and total urinary 6STMT (0-t)

was well described by polynomial equation. Almost half of the data show linear

relationship closed to a straight line between the two variables. Good prediction

results were obtained for data following the three dosage forms.

Application of the polynomial equation derived in Equation 1 for the future

prediction of MT plasma concentrations resulting from different studies is appropriate

only in the range of MT linear pharmacokinetics (i.e. MT plasma AUC (0-t) and

urinary 6STMT (0-t) proportional increase with increase in dose/release rate of MT

products). In addition, MT pharmacokinetics may differ among subjects and routes of

administration. Relationship between MT plasma AUC and 6STMT may not be the

same when MT is administered differently; for example, transdermally,

transmucosally, or orally due to differences in metabolism (i.e. first pass effect).

Therefore, application of the polynomial equation is restricted to each individual

subject and type of dosage form.
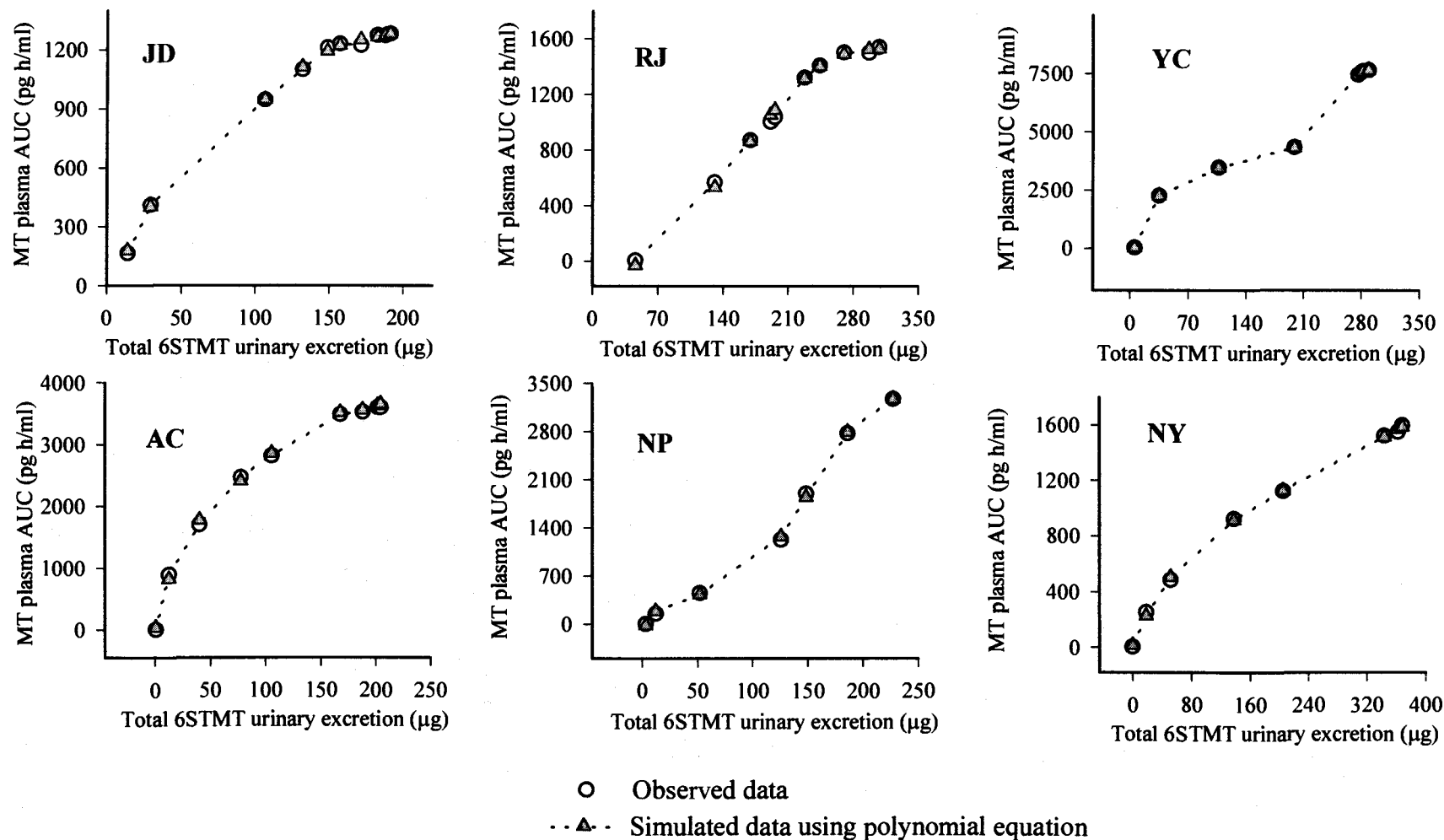
Figure 5.2 : Relationship between MT plasma AUC (0-t h, pg h/ml) and total 6STMT urinary excretion (0-t h, μg) following oral administration of a solution of MT (750 μg) in subject JD, AC, RJ, NP, YC, and NY.

○   Observed data

· · △ · ·   Simulated data using polynomial equation
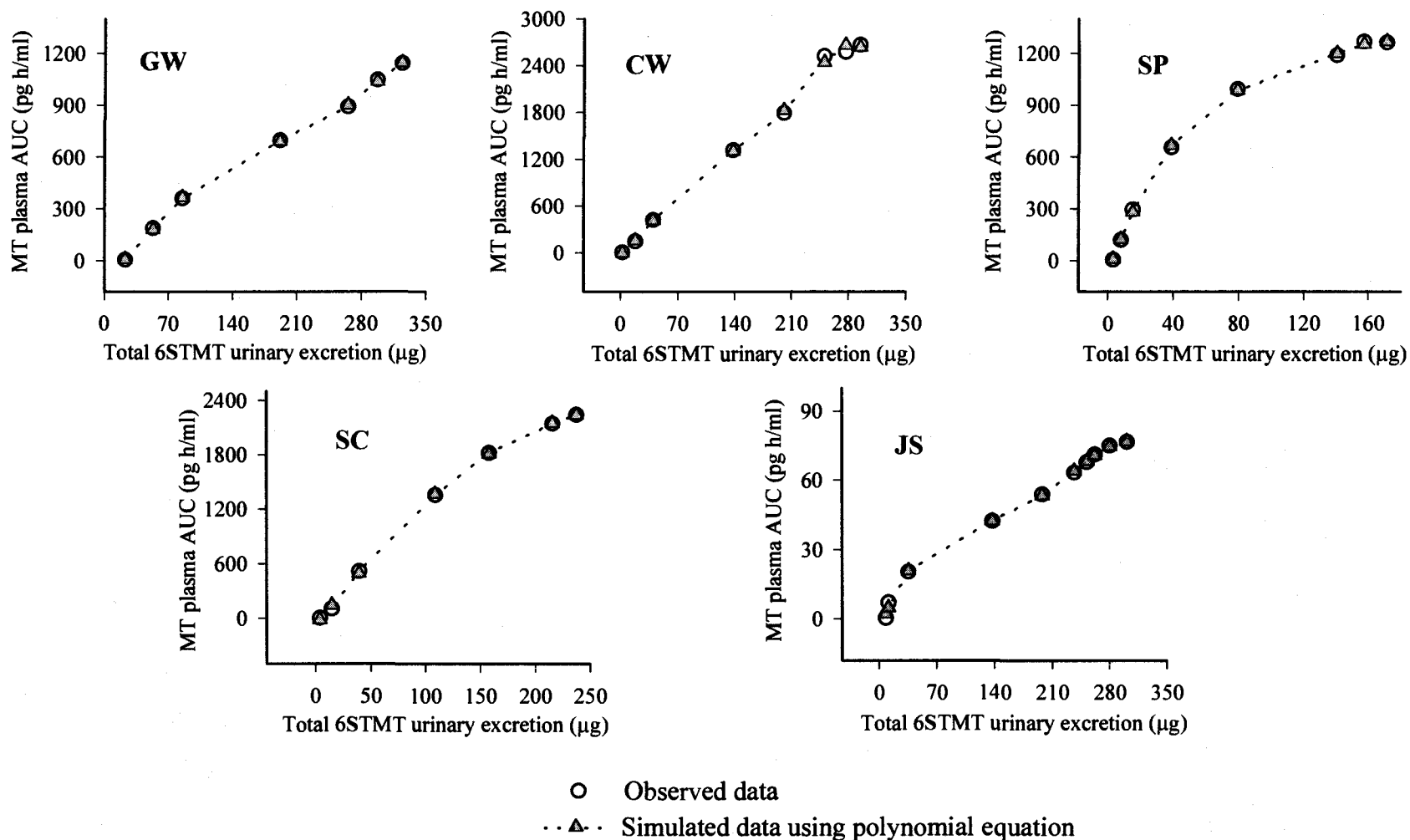
Figure 5.3 : Relationship between MT plasma AUC (0-t h, pg h/ml) and total 6STMT urinary excretion (0-t h, µg) following oral administration of a solution of MT (750 µg) in subject GW, SC, CW, JS, and SP.
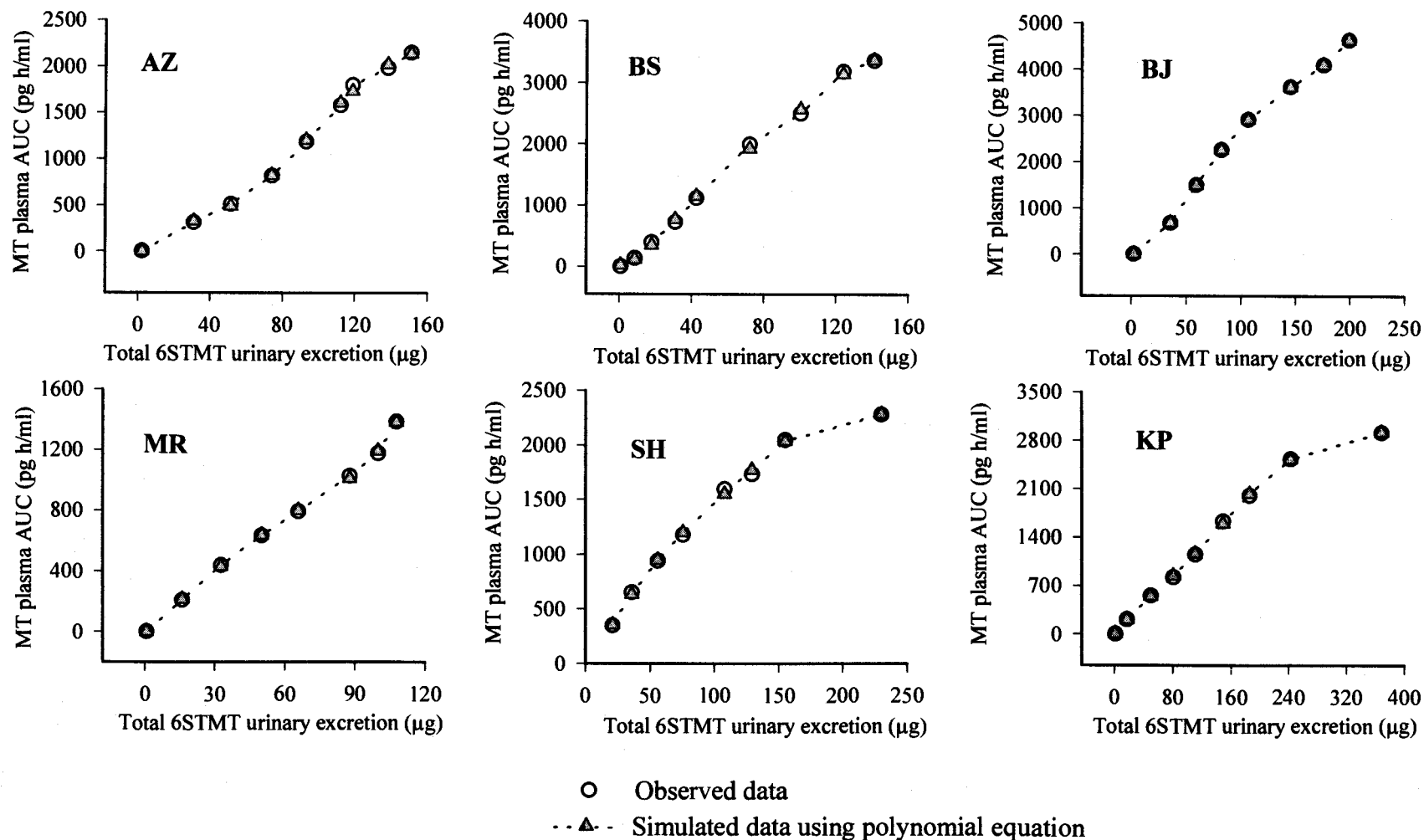
Figure 5.4 : Relationship between MT plasma AUC (0-t h, pg h/ml) and total 6STMT urinary excretion (0-t h, μg) following oral administration of MT SR formulation at 500 μg (AZ, MR, BS and SH) and at 1000 μg (BJ and KP).
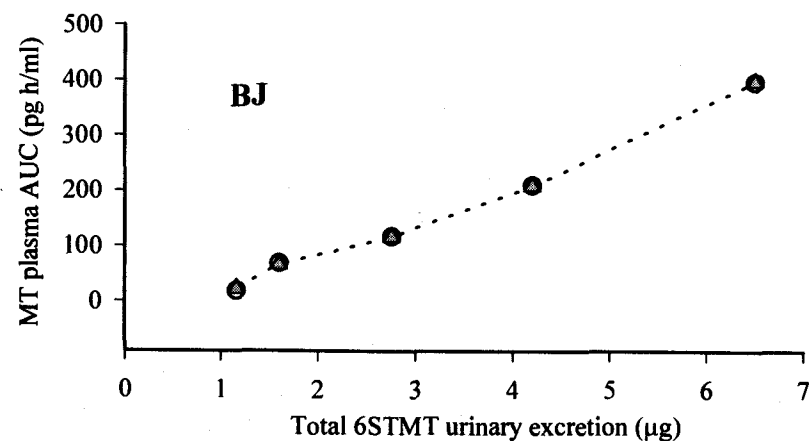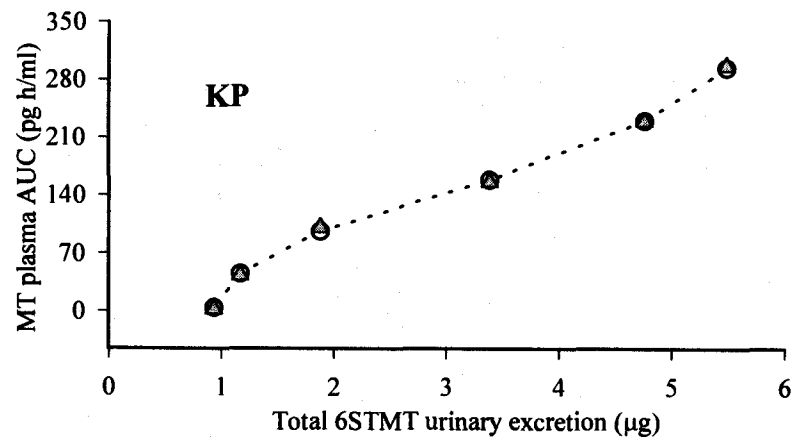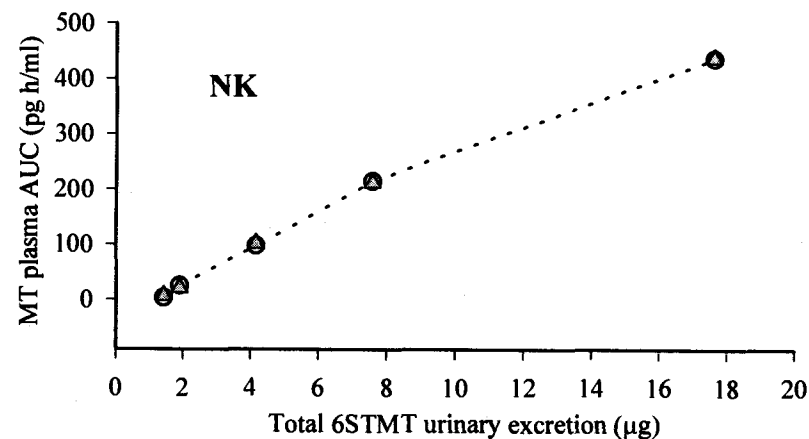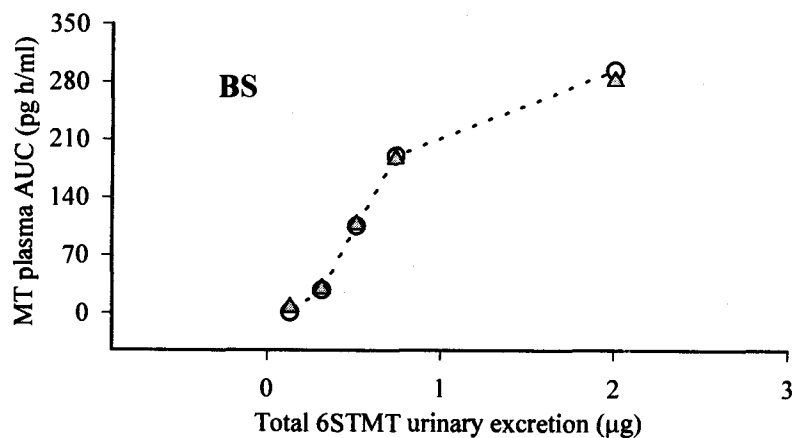
O Observed data

- · △ · · Simulated data using polynomial equation

Figure 5.5 : Relationship between MT plasma AUC (0-t h, pg h/ml) and total 6STMT urinary excretion (0-t h, μg) following transdermal application of MT in subject BS, KP, NK, and BJ.
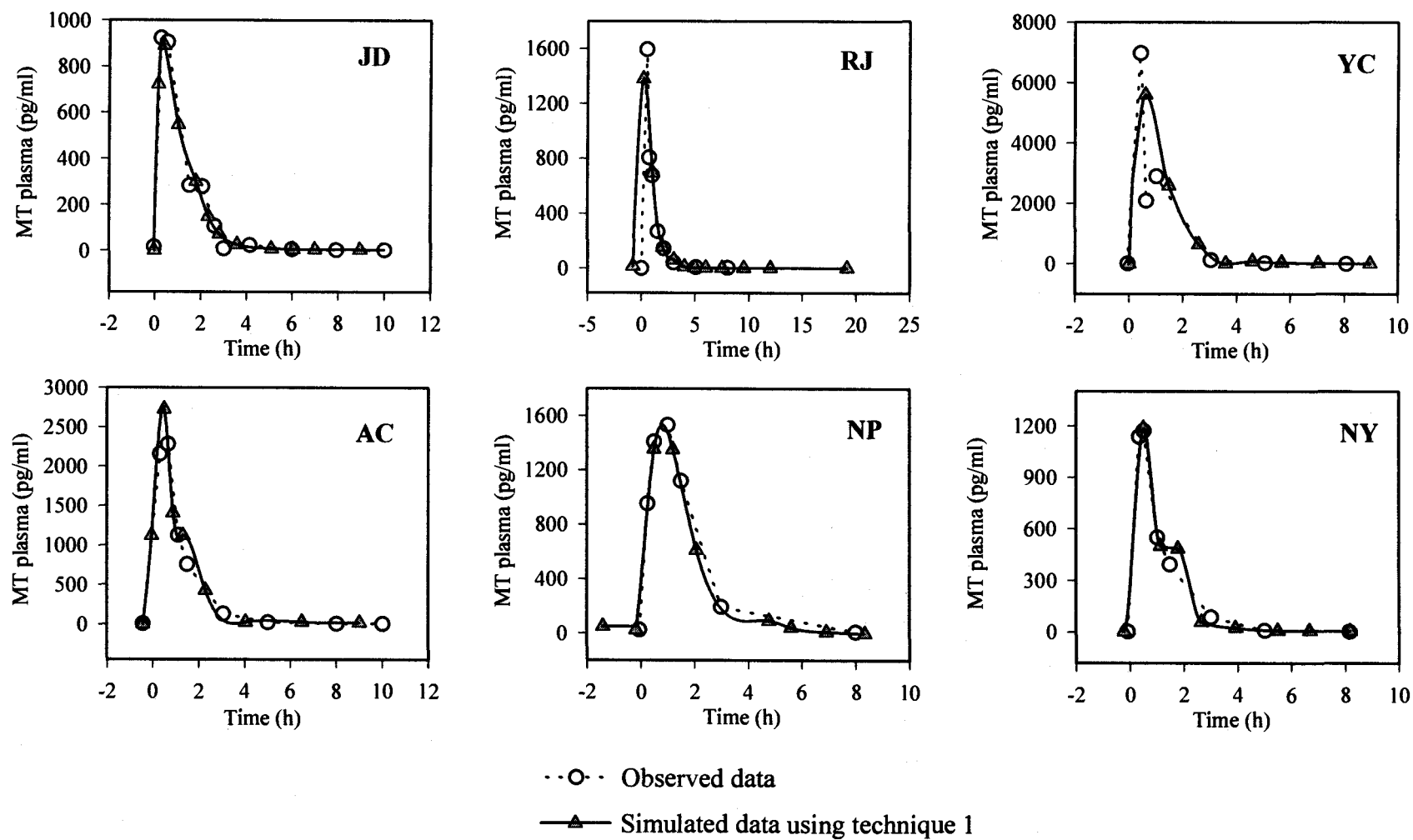
Figure 5.6 : Simulation of MT plasma profiles following oral administration of a solution of MT (750 µg) in subject JD, AC, RJ, NP, YC, and NY using technique 1.
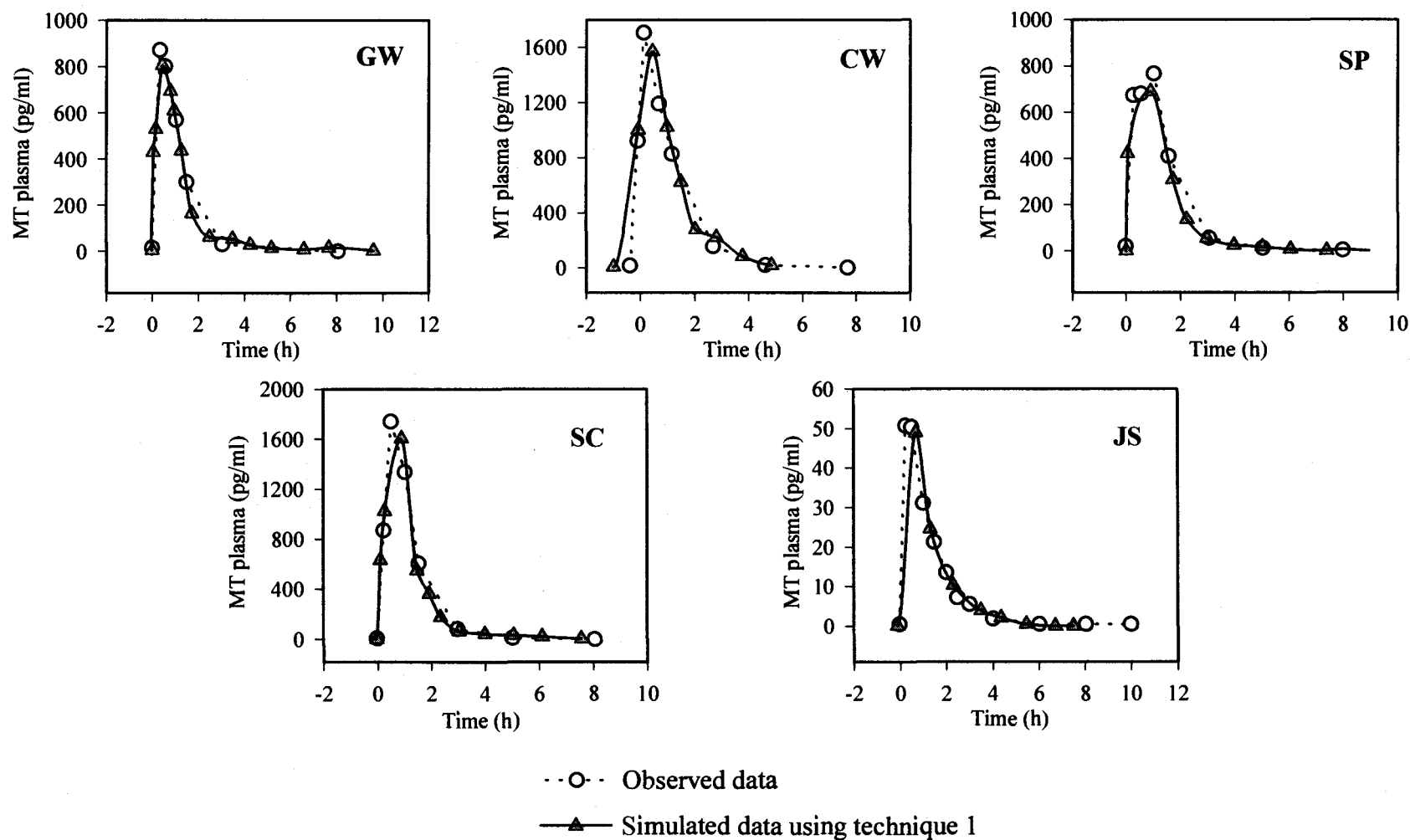
Figure 5.7 : Simulation of MT plasma profiles following oral administration of a solution of MT (750 μg) in subject GW, SC, CW, JS, and SP using technique 1.
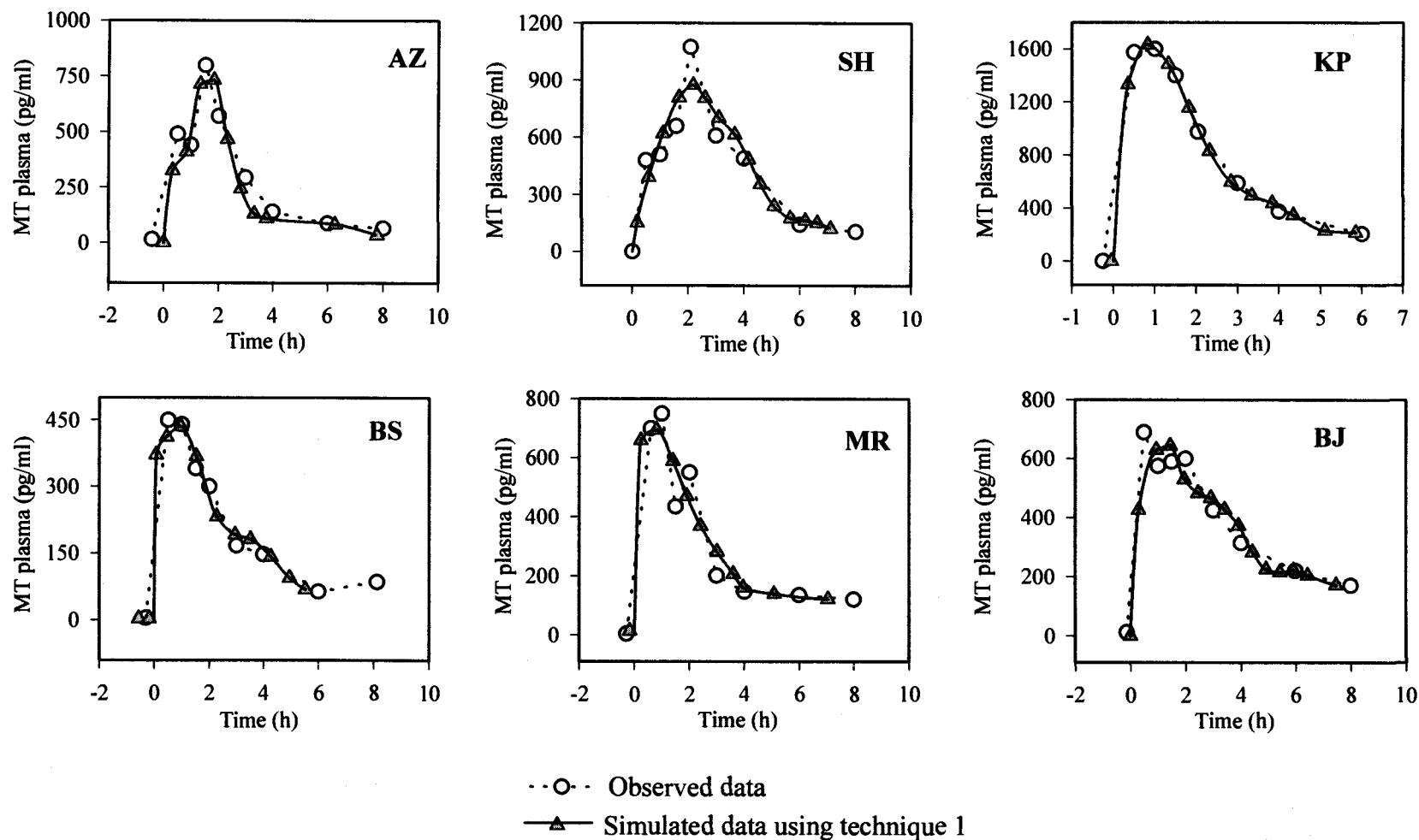
Figure 5.8 : Simulation of MT plasma profiles following oral administration of MT SR formulation, given at 500 μg (AZ, BS, SH, MR) and 1000 μg (KP, BJ), using technique 1.
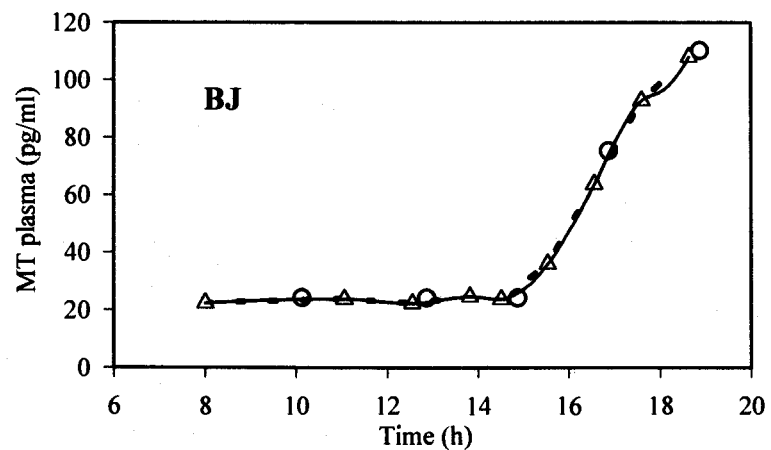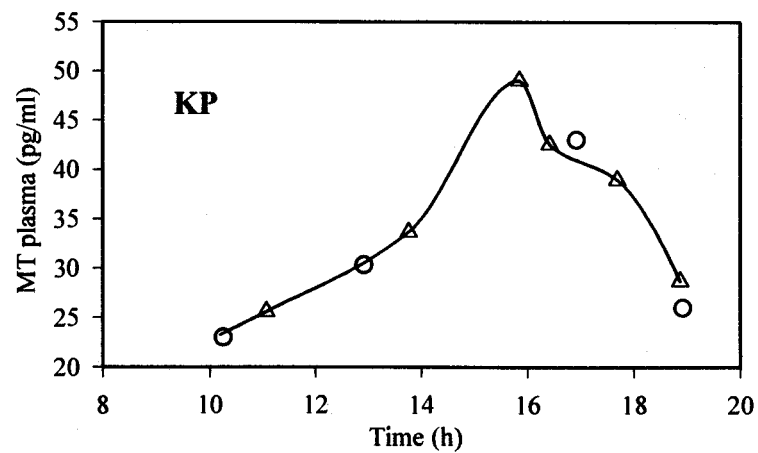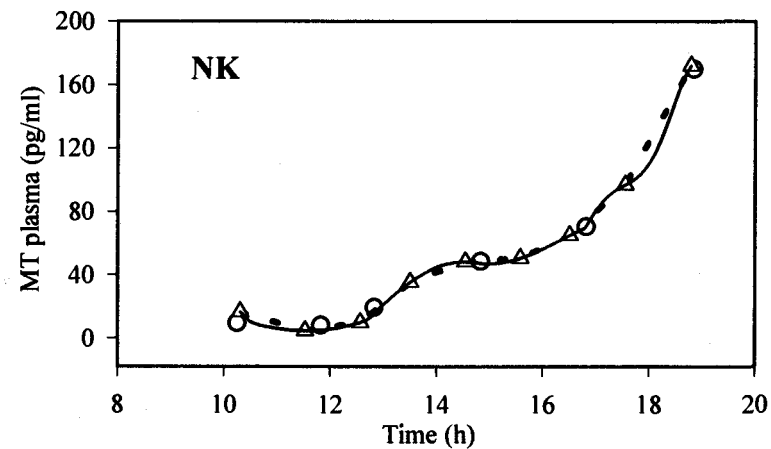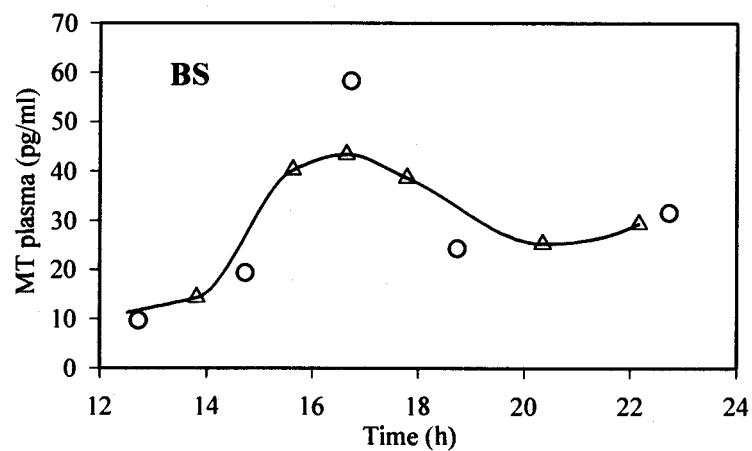
Figure 5.9 : Simulation of MT plasma profiles following transdermal application of MT in subject BS, KP, NK, and BJ using technique 1.

Modeling technique 2

Weighting function derived from deconvolution using PCDCON with different stepsize following administration of two formulations; oral solution, and oral SR formulation, are shown in Figure 5.10 to 5.12, respectively. Simulation of MT plasma profiles following administration of the two formulations are presented in Figure 5.13 to 5.15.

Weighting function for simulation of MT plasma profiles following transdermal application was not successfully ascertained due to unacceptable error which resulted in poor prediction.

In PCDCON, deconvolution strategies is explicit method which is based on curve fitting methods (polyexponentials and piecewise polynomial). The program fits input response and impulse response with a continuos function, e.g., polyexponential or piecewise polynomial before apply numerical deconvolution to fitted functions (18). It is suggested that the curve-fitting methods are relatively advantageous compared to direct methods (18). For examples, error sensitivity may reduce by compensating for error and variability. There is no absolute sampling restrictions, as well as sampling frequency affects only ability to accurately estimate the actual response time course (not the accuracy of the deconvolution algorithm itself). However, increased smoothing decreases sensitivity to random error and outliers but also decreases ability to detect rapid changes or fluctuations in input rate. Sampling frequency must be sufficiently high to adequately characterize input response and impulse function.
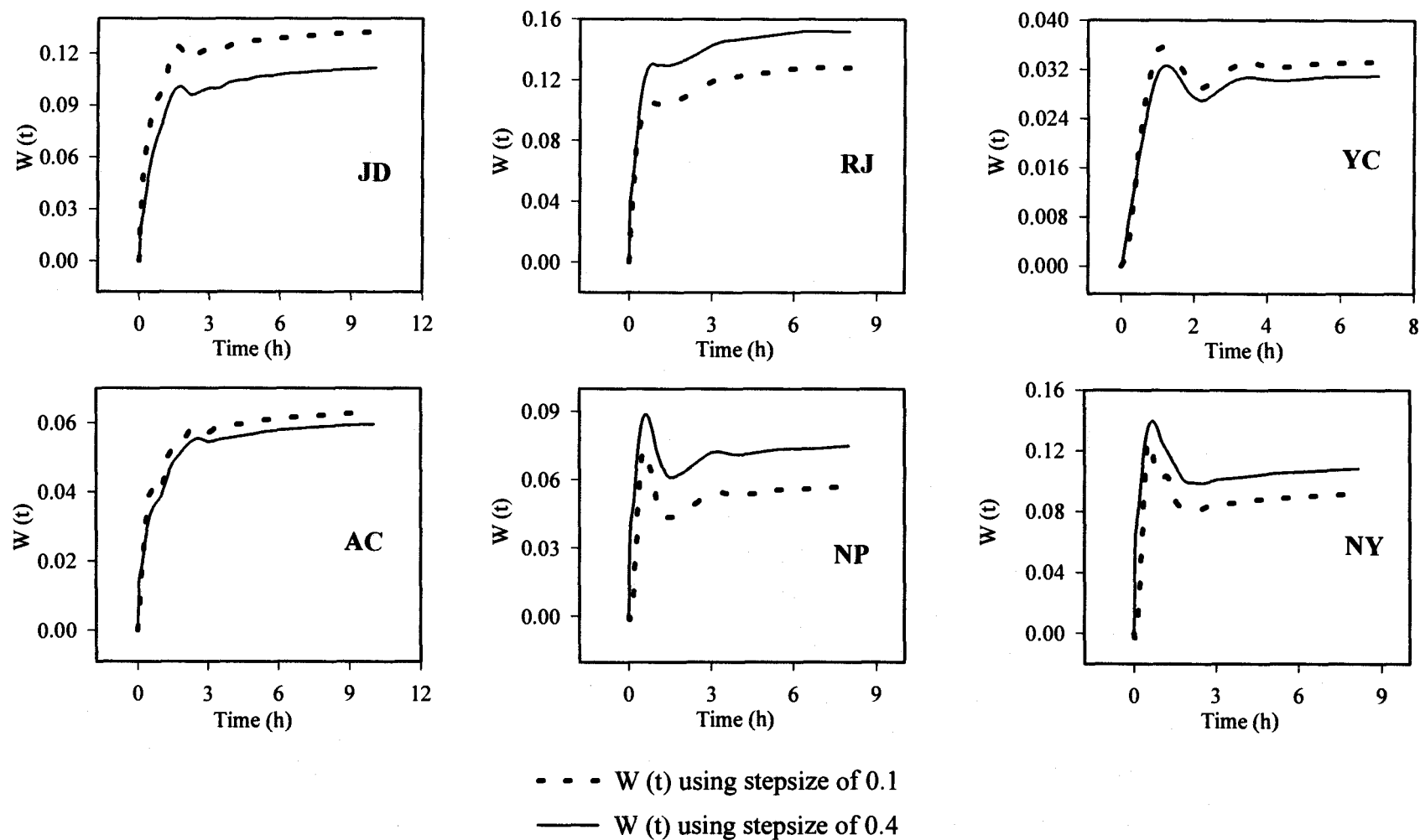
Figure 5.10 : Weighting function [W (t)] derived from deconvolution with different stepsize following oral administration of a solution of MT (750 μg).
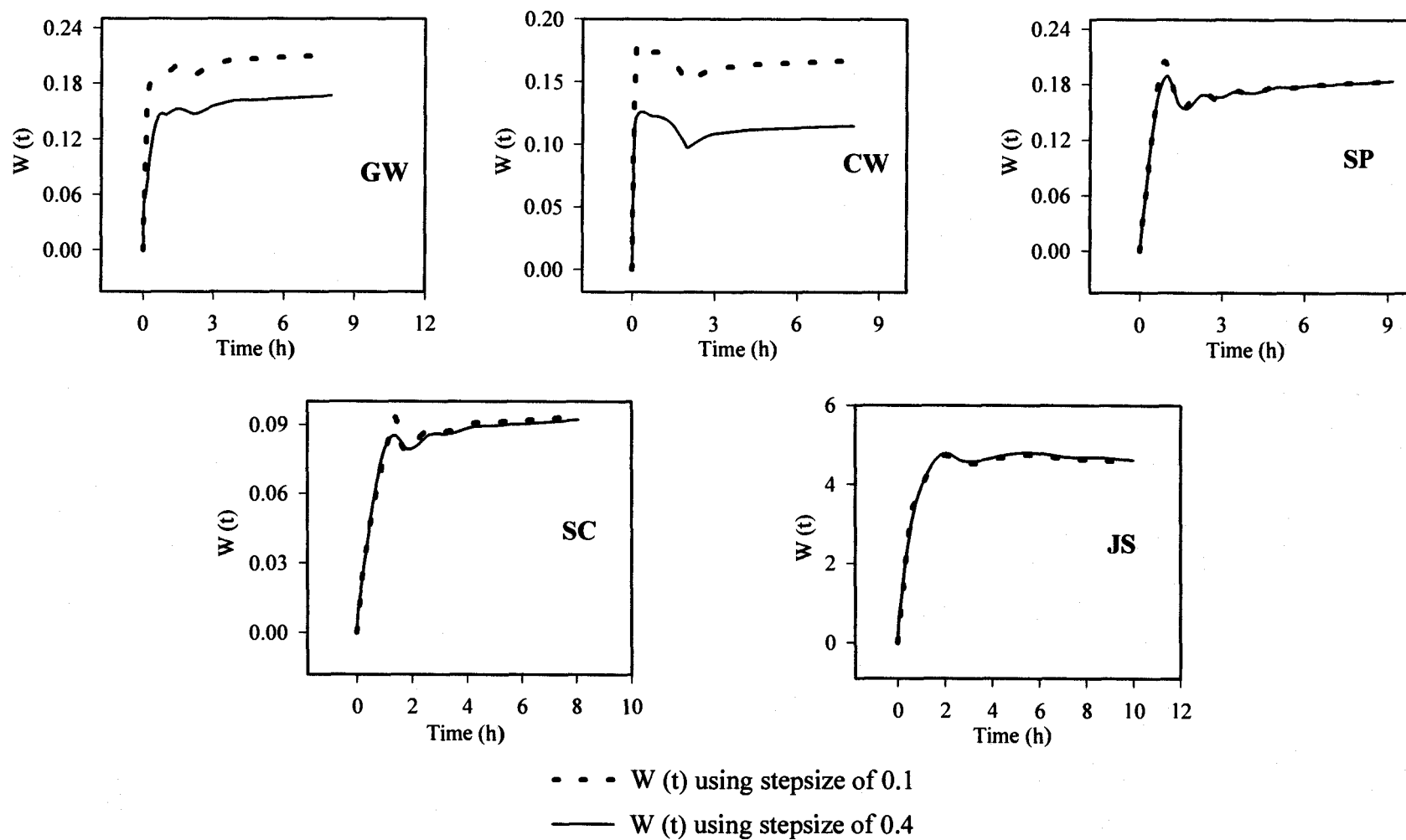
Figure 5.11 : Weighting function [W (t)] derived from deconvolution with different stepsize following oral administration of a solution of MT (750 μg).
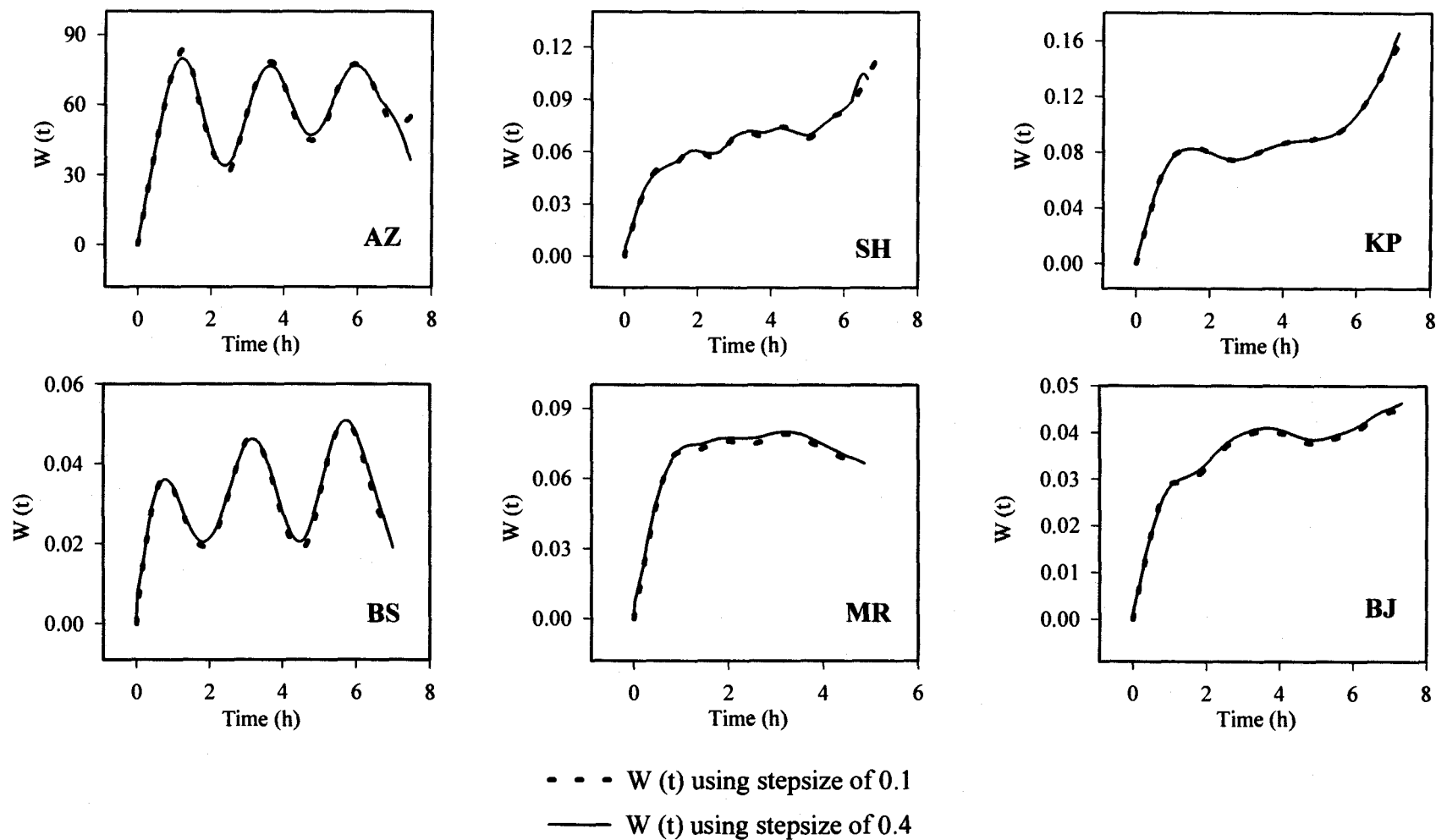
Figure 5.12 : Weighting function [W (t)] derived from deconvolution with different stepsize following oral administration of MT SR formulation at 500 µg (AZ, BS, SH, MR) and 1000 µg (KP, BJ).

○   Observed data

■ ■ ■ Simulated data using deconvolution at stepsize of 0.1

—— Simulated data using deconvolution st stepsize of 0.4
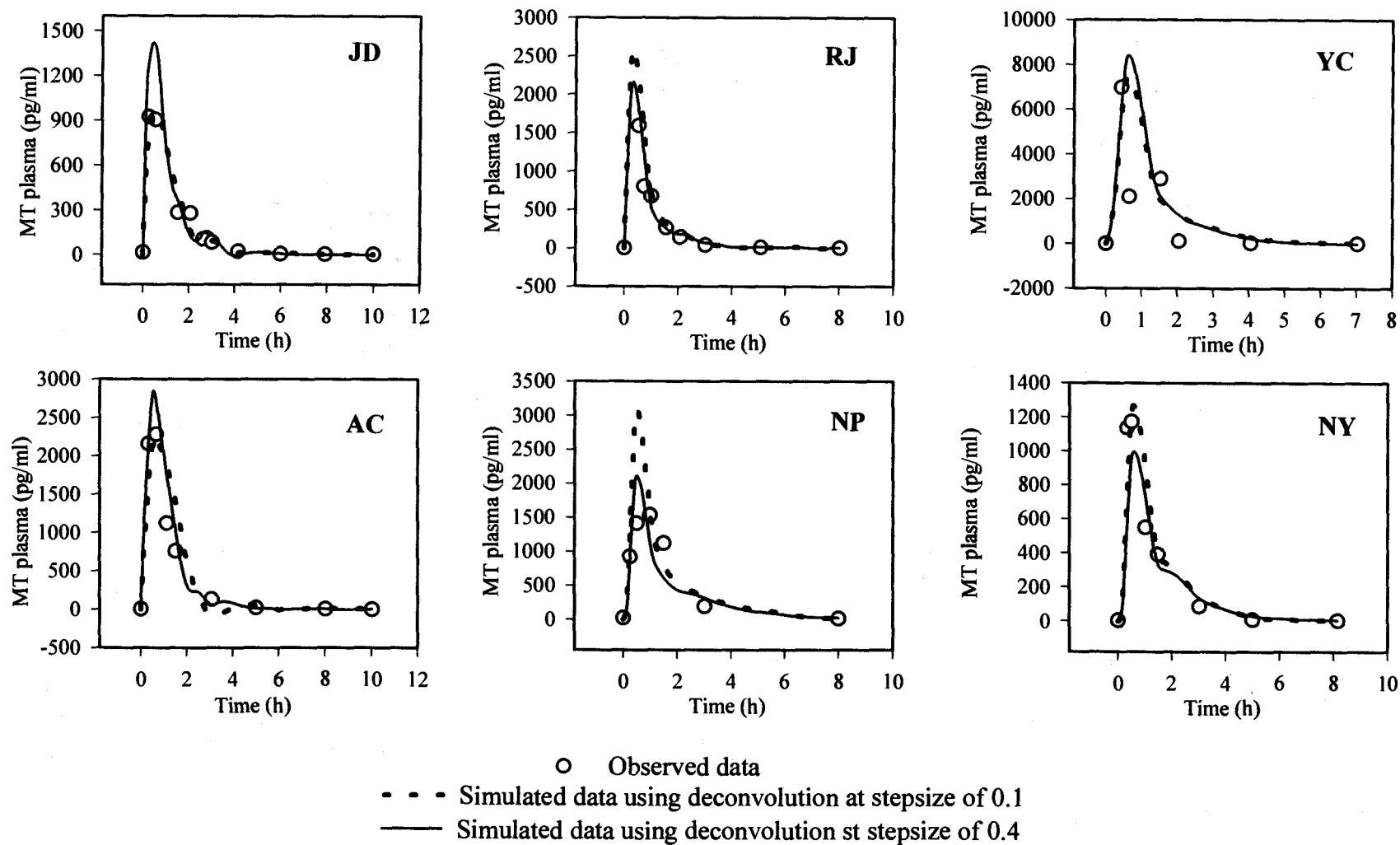
Figure 5.13 : Simulation of MT plasma profiles following oral administration of a solution of MT (750 µg) using deconvolution (technique 2) with different stepsize.
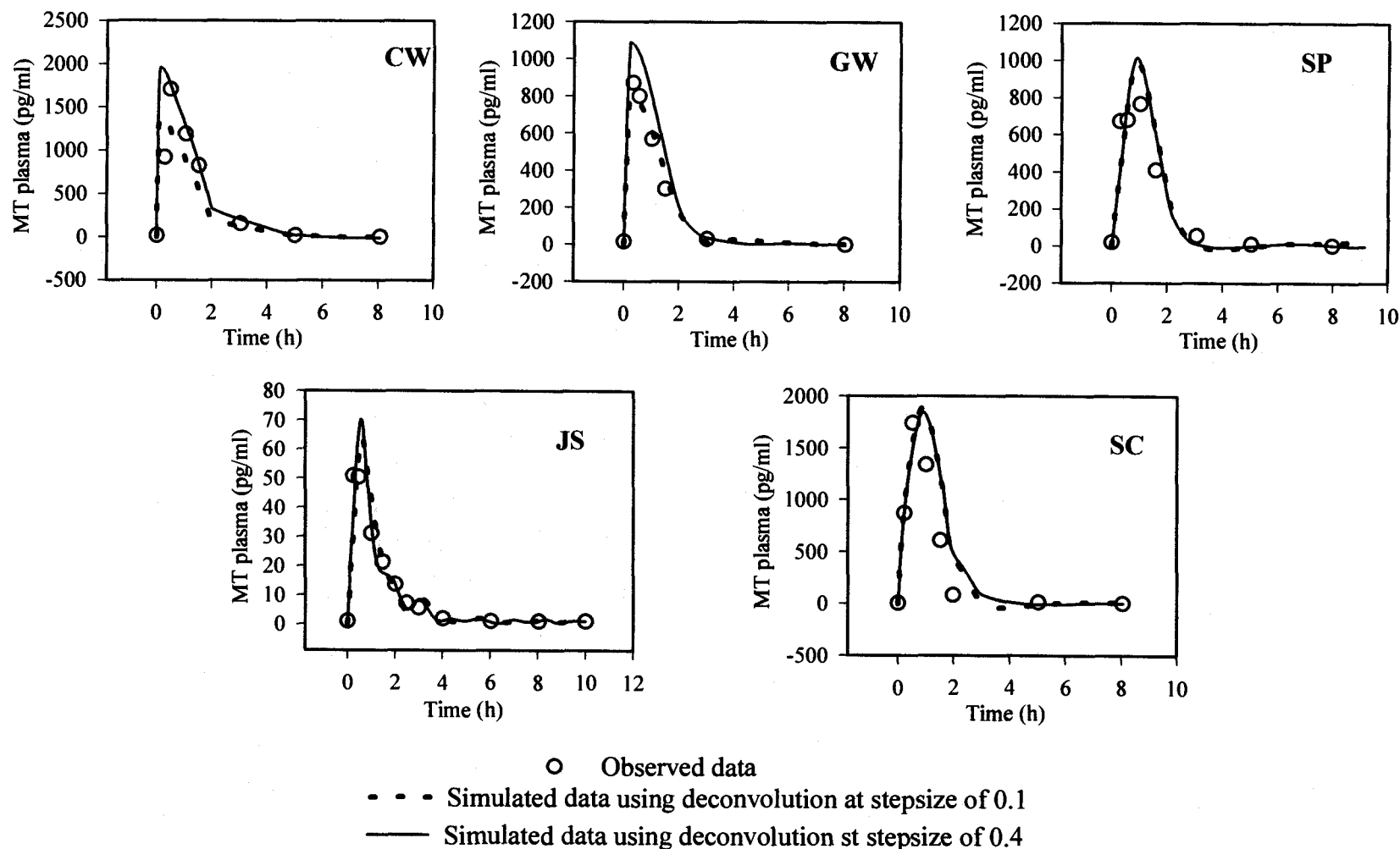
Figure 5.14 : Simulation of MT plasma profiles following oral administration of a solution
of MT (750 µg) using deconvolution (technique 2) with different stepsize.
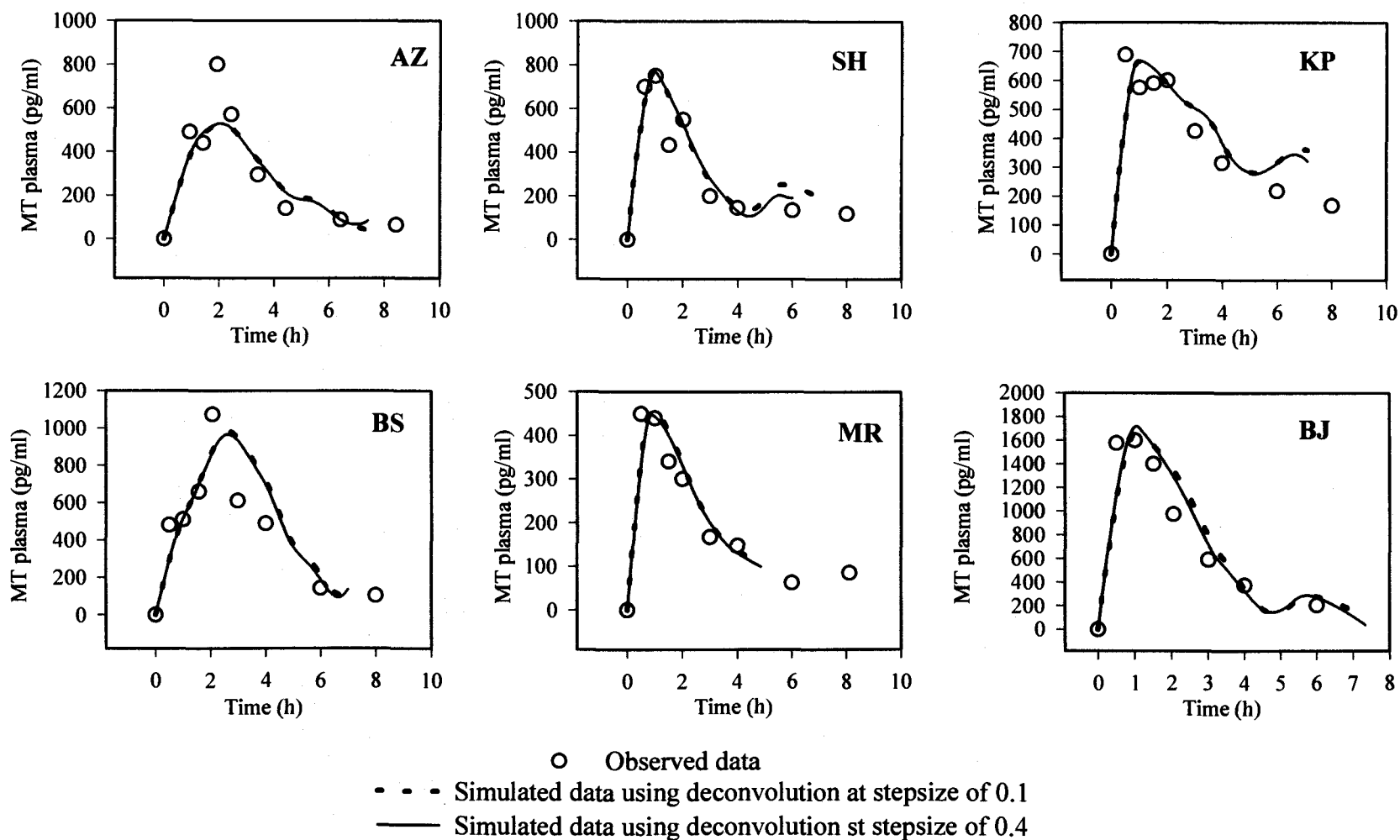
Figure 5.15 : Simulation of MT plasma profiles following oral administration of MT SR formulation, given at 500 µg (AZ, BS, SH, MR) and 1000 µg (KP, BJ), using deconvolution (technique 2) with different stepsize.

The first step in modeling technique 2 is to determine weighting function (W(t), see Equation 8). The obtained weighting function should be fairly precise. Since it would be later used in the second step to generate MT plasma profile (see Equation 9). An "ill-posed" problem in deconvolution technique is generally due to sensitiveness to errors/variability, and sampling frequency which is comparable to numerical differentiation problem. Therefore, accuracy of simulation of MT plasma profile is heavily based on good estimation of the weighting function as well as cumulative error occurring in both steps.

In this work, sampling frequency of impulse response employed in PCDCON greatly affected error sensitivity in some data set. This problem could sometimes be alleviated by refitting data using interpolating cubic spline, then selecting the fitted data (refine sampling frequency of impulse response). However, in some cases, deconvolution using PCDCON failed to give a reasonable time-course of weighting function in the first step as happened to data set from the study of MT transdermal application (15). To reduce error due to noise in data additional technique may be needed. Podczeck et al. were able to reduce error according to noise in data and flatten responses using information theory (maximum entropy approach (19, 20)).

Accuracy of prediction was also affected by stepsize chosen in deconvolution process. There is no specific criteria for optimum stepsize. Smaller stepsize does not always provide better prediction result.

It is important to realize that both techniques are based on assumption of linear pharmacokinetics and restricted to each individual subject and type of dosage forms.

Differences in metabolism (i.e. first pass effect) among subjects or different routes of administration can invalidate the assumption of the two proposed modeling techniques. In technique 1, application of the polynomial equation derived in Equation 1 for the future prediction of MT plasma concentrations resulting from different studies is appropriate only in the range of MT linear pharmacokinetics. Similarly, in technique 2, the function describing metabolite (6STMT) formation and excretion in urine is assumed to be identical between prediction. Modeling technique 1 may be less sensitive to error/noise in data and give better estimation of MT plasma profile compared to technique 2. However, simulation based on deconvolution (technique 2) can be performed directly using available pharmacokinetic and mathematical simulation software.

Thus, it is suggested that collection of drug concentration in blood and urinary excretion of metabolite data for a single dose of MT with specific type of dosage form (oral solution, oral controlled release, transdermal, etc.) allows prediction of drug concentration versus time data for parent drug following additional administration of different formulations of the same type of dosage form using only urinary excretion of metabolite information for the new formulation. The approach are anticipated to be of value in product formulation modification and be useful for long term evaluation of different MT dosage forms given to the same subject.

CONCLUSION

It is possible to simulate MT plasma profiles based on tracking urinary 6STMT data. In this work two modeling techniques were proposed based on MT linear pharmacokinetics assumption. Application the two techniques for future prediction is limited to each individual subject and type of dosage form. The proposed techniques may be useful for long term clinical evaluation of MT products and MT dose regimens where blood sampling is difficult.

REFERENCES

1. Arendt, J. In Melatonin and the mammalian pineal gland; Chapman & Hall, London, UK, 1995, pp. 40, 42, 207, 248.

2. Matthews, C.D.; Kennaway, D.J.; Fellenberg, A.J.G.; Phillipou, G.; Cox, L.W.; Seamark, R.F. Melatonin in man Adv. Biosci. 29, 371-81 (1981).

3. Arendt, J., Bojkowski, C., Franey, C., Wright, J., Marks, V. Immunoassay of 6-hydroxymelatonin sulfate in human plasma and urine: abolition of the urinary 24-hour rhythm with atenolo, J. Clin. Endocrinol. Metab. 60, 1166-73 (1985).

4. Bojkowski, C.J., Arendt, J., Shin, M.C. &Markey, S.P. Melatonin secretion in humans assessed by measuring its metabolite, 6-sulphatoxymelatonin. Clin. Chem. 33, 1343-1348 (1987).

5. Nowak, R., McMillen, I.C., Redman, J., Short, R.V. The correlation between serumand salivary melatonin concentration and urinary 6-hydroxymelatonin sulphate excretion rate: Two non-invasive techniques for monitoring human circadian rhythmicity. Clin. Endocrinol. 27, 445-452 (1987).

6. Waldhauser, F.; Waldhauser, M.; Lieberman, H. R.; Deng, M. H.; Lynch, H. J.; Wurtman, R. J. Bioavailability of oral melatonin in humans. Neuroendocrilnol. 39, 307-313 (1984).

7. Lee, B., Parrott, K. A., Ayres, J. W., Sack, R. L. Design and evaluation of an oral controlled release delivery system for melatonin in human subjects. Int. J. Pharm. 124, 119-127 (1995).

8. Lee, B., Parrott, K. A., Ayres, J. W., Sack, R. L. Preliminary evaluation of transdermal delivery of melatonin in human subjects. Res. Commun. Mol. Pathol. Pharmacol. 85, 337-346 (1994).

9. Balant, L.P., McAinsh, J. Use of metabolite data in the evaluation of pharmacokinetics and drug action. In: Jenner, P., Testa, B., eds. Concepts in drug metabolism. Part A Marcel Dekker, Inc. New York, 1980, pp. 311-371

10. Garfinkel, D., Laudon, M., Nof, D., Zisapel, N. Improvement of sleep quality in elderly people by controlled-release melatonin, Lancet 346 (1995) 541-544.

11. Fellenberg, A.J.; Phillipou, G.; Seamark, R.F. In Pineal Function; Matthew, C.D.; Seamark, R.F; Eds; Oxford, Elsevier, 1981, pp 143-149.

12. Lewy, A.J., Markey, S.P. Analysis of melatonin in plasma by gas chromatography negative chemical ionization mass spectroscopy, Science 201, 741-743 (1978).

13. Aldhous, M.E., Arendt, J. Radioimmunoassay for 6-sulphatoxymelatonin in urine using an iodinated trace, Ann. Clin. Biochem. 25, 298-303 (1988).

14. Lee, B., Parrott, K.A., Ayres, J.W., Sack, R.L. Development and characterization of an oral controlled release delivery system for melatonin Drug Dev. Ind. Pharm., 22(3), 269-274 (1996).

15. Lee, B., Parrott, K.A., Ayres, J.W., Sack, R.L. Preliminary evaluation of transdermal delivery of melatonin in human subjects, Res. Commun. Mol. Pathol. Pharmacol. 85, 337-346 (1994).

16. Langenbucher, F. Numerical convolution/deconvolution as a tool for correlation *in vitro/in vivo* drug availability. Pharm. Ind., 44, 11, 1166-1171 (1982).

17. Carstensen, J.T. In Modeling and data treatment in the pharmaceutical sciences,
Technomic Publishing Company, Inc., USA, 1996, pp. 177-180.

18. Gillespie, W.R. PCDCON: Deconvolution for pharmacokinetic applications. AAPS Short Course of Convolution, deconvolution and linear systems. Miami Beach, FL, November 5, 1995.

19. Shannon, C.E. Bell Syst. J. 27, 379 (1948).

20. Podczeck, F., Charter, M.K., Newton, J.M., Yuen, K.H. Eur. J. Pharm. Biopharm. 41, 254 (1995).

CHAPTER 6

DEVELOPMENT OF A TRANSDERMAL DELIVERY DEVICE FOR MELATONIN IN VITRO STUDY

ABSTRACT

The present study was undertaken to develop a transdermal delivery device for melatonin (MT) and to determine the effects of system design on the release of MT. MT diffusion characteristics from 2 solvents through a series of ethylene vinyl acetate membranes with 4.5%, 9%, 19%, 28% vinyl acetate were characterized using vertical Franz® diffusion cells. The solvent used were 40% (v/v) propylene glycol (PG) and 40%(v/v) propylene glycol with 30%(w/v) 2-hydroxypropyl-β-cytrodextrin. The best release rate ($Jss = 0.795$ $\mu g/h/cm^2$) was obtained from the 40% PG vehicle through the 28% vinyl acetate membrane. MT diffusion through this membrane with an acrylate pressure sensitive adhesive (PSA) with and without MT loading was also studied. The data revealed an interaction between MT and the PSA in the systems with MT-loaded adhesive. A MT transdermal delivery device was constructed based on the above data. Effect of storage time (1 day, 2 days, and 3 days) on the developed device was also investigated. Steady state flux values of MT did not vary significantly with storage time (p-value = 0.14). The steady state flux was 1.88 ± 0.6 $\mu g/hr/cm^2$(n=9). However, storage time did affect the burst effect of MT. Total amount of MT released in the first hour was 137.4 ± 25.7 μg after 3 days, 61.5 ± 8.9 μg after 2 days, and 43.8 ± 20.9 μg after 1 day.

INTRODUCTION

Melatonin (N-Acetyl-5-Methoxytryptamine,MT) is an indole neurohormone secreted by the pineal gland. Although the usefulness of administering MT to produce physiological or pharmacological plasma concentrations is still unknown (1), it appears that MT administration may be beneficial in patients with below normal MT blood concentrations. Therefore, it is desirable to develop drug delivery systems for MT which are able to mimic the physiological, endogenous plasma MT concentration in patients whose MT profile needs to be reestablished . Endogenous MT secretion is generally high during nighttime producing a bell-shaped plasma profile with a peak concentration of approximate 60 pg/ml. Daytime MT plasma concentrations are generally less than 20 pg/ml (2). Drug delivery systems for controlled release of MT such as transdermal, oral (3,4), and transmucosal (5) have been developed in order to deliver MT in a physiological pattern.

A previous study provided evidence that transdermal administration of MT was possible (4). The present study was undertaken to determine the effects of system design on the release of MT, using Franz® diffusion cells. Experiments were designed to (1) determine the flux of MT through a series of ethylene vinyl acetate (EVAc) membranes using a donor solution of either (a) 40% propylene glycol (PG) or (b) 40% PG with 30% (w/v) 2-hydroxypropyl-β-cyclodextrin (2-HPCD) (2) determine the flux of MT through an acrylate transfer adhesive with and without "MT loading" of the adhesive and (3) fabricate and evaluate, *in vitro*, a transdermal delivery device (TDD) based on the above.

MATERIALS AND METHODS

Materials

MT was purchased from Regis Chemical Co. (Morton Grove, IL). HPLC

grade, methanol, analytical grade, isopropanol, and ethyl acetate were obtained from

Mallinckrodt Specialty Chemicals Co. (Paris, KY). Methylparaben was purchased

from Sigma Chemical Co. (St. Louis, MO). Analytical grade propylene glycol (PG)

and heptane were obtained from J.T. Baker, Inc. (Phillisburg, NJ). 2-Hydroxypropyl-β

-cyclodextrin (2-HPCD) was provided courtesy of American Maize-Product Company

(Hammond, ID, USA). The 3M Company (St. Paul. MN) provided ethylene vinyl

acetate membranes (0.2 mm thickness) with 28%, 19%, 9%, and 4.5% vinyl acetate

content (3M CoTran™ controlled caliper film), neutral acrylate pressure sensitive

adhesive (3M CoTran™ PGTA #9871), backing film (heat sealable, tan polyester film

laminate, Scotchpak™ film #1006), and fluoropolymer coated release liner

(Scotchpak™ film #1022).

Equipment and Analytical Method

Vertical Franz® Diffusion cells (Crown Glass Co.) were used for all diffusion

studies. The cross sectional area and receptor volume for these cells were 3.14 cm^2

and 15 ml, respectively. MT concentration in non-biological fluids was determined

using an HPLC system with UV detection. The HPLC was equipped with an M-45

pump, WISP® 710B injector, reversed-phase C18 (4μ) radial compression column and

Model 441 detector with a 229-nm light source (all from Waters® Associates). Retention time and sensitivity for MT (mobile phase: methanol/water, 50:50) were 4 minutes and 10 ng/ml, respectively, at a flow rate of 1.2 ml/minute. Methylparaben was used as the internal standard. Its retention time was 6.5 minutes.

Data Analysis

The flux (μg/hr/cm^2) and lag time of MT released from each system were calculated from the slope and the intercept of the plot of the cumulative amount of MT in the receptor solution at steady state against time using linear regression analysis. After logarithm transformation, independent groups of calculated flux values were statistically analyzed by one-way analysis of variance as initial comparisons of means and by Tukey-Kramer intervals multiple comparison using STATGRAPHIC® version 5.0.

Membrane Studies

MT diffusion through four different ethylene vinyl acetate membranes was determined in triplicate. Two different donor solutions of MT were prepared as follows (4):

- 40%(v/v) propylene glycol vehicle

Melatonin	0.01438 g
Propylene Glycol (PG)	0.6 ml
Phosphate Buffer pH 6.1	0.9 ml

- 40%(v/v) propylene glycol with 30%(w/v) 2-hydroxypropyl-β-cyclodextrin (2-HPCD)

Melatonin	0.03061 g
Propylene Glycol (PG)	0.6 ml
2-hydroxypropyl-β-cyclodextrin[a] (2-HPCD)	0.45 g
Phosphate Buffer pH 6.1	0.9 ml

[a] Molecular weight, 1542, average degree of molar substitution, 6.5 moles of hydroxypropyl/mole of β-cyclodextrin, range of molar substitution, 5-8.

One and a half (1.5) ml of donor solution was placed in the donor cell. Normal saline was employed as the receptor solution and was maintained at 30°C throughout the study. Two hundred microliters were collected from the receptor chamber via a sampling port at 1,2,3,4,6,8 and 12 hours after adding the MT solution to the donor cell. An equal volume of saline was replaced through the sampling port after each sample collection. Samples were kept frozen until HPLC analysis.

Adhesive Studies

Ethylene vinyl acetate membrane, 28% vinyl acetate, (28%VAc), was used in these adhesive studies. Neutral acrylate adhesive was applied to a 2.5X2.5 cm area of the membrane by either using an air brush (spray method) or by a pressure transfer method. With the transfer method the adhesive with paper backing was pressed against the membrane. The backing was then carefully removed leaving the adhesive on the membrane. In the spraying method, adhesive was physically removed from the backing paper, weighed, and dissolved in either isopropanol or a 50%(v/v) mixture of ethyl acetate/heptane. The adhesive was then directly sprayed on the membrane under the hood. The sprayed surface was even and smooth with good tackiness. Details of each diffusion system are summarized in Table 6.1. Diffusion studies for each system were conducted using the method described in the Membrane Studies section. The 40% propylene glycol MT donor solution was used for these studies.

Table 6.1: Adhesive studies: Preparation of the studied diffusion systems.

System	Donor MT	Adhesive on the membrane	Solvent used
1	yes	spray method	isopropanol
2	yes	spray method	EtAc/heptane
3	yes	pressure transfer	none

Delivery Device Studies

A 3X3 cm device (TDD) was prepared by heat sealing 28% VAc membrane to a backing film (see Materials section). Adhesive was then applied using the spray method to the membrane surface. Ethyl acetate/heptane was used as the adhesive solvent. One, two or three days prior to the diffusion studies, 1.5 ml of the 40% propylene glycol vehicle with MT was placed in the device. A release liner was applied, the device was wrapped in foil and then stored at room temperature prior to the diffusion study. After 1, 2, or 3 days of storage, the device was evaluated using the method described in the Membrane Studies section. These studies were conducted in triplicate. The MT content of the device was determined after the conclusion of the diffusion study.

RESULTS AND DISCUSSION

Membrane Studies

Permeation profiles of MT through ethylene vinyl acetate (28%,19%, 9%, and 4.5% vinyl acetate) membranes from 40%PG vehicle and 40%PG with 30% 2-HPCD are shown in Figure 6.1. The associated physicochemical parameters are shown in Table 6.2. Flux increased with increasing VAc content of the membranes for both vehicles (Figure 6.2). ANOVA indicated significant differences among the resulting flux values (p-value=0). The flux rate obtained from the system of 40% PG vehicle through 28% VAc membrane was almost twice that of 40% PG with 30% 2-HPCD
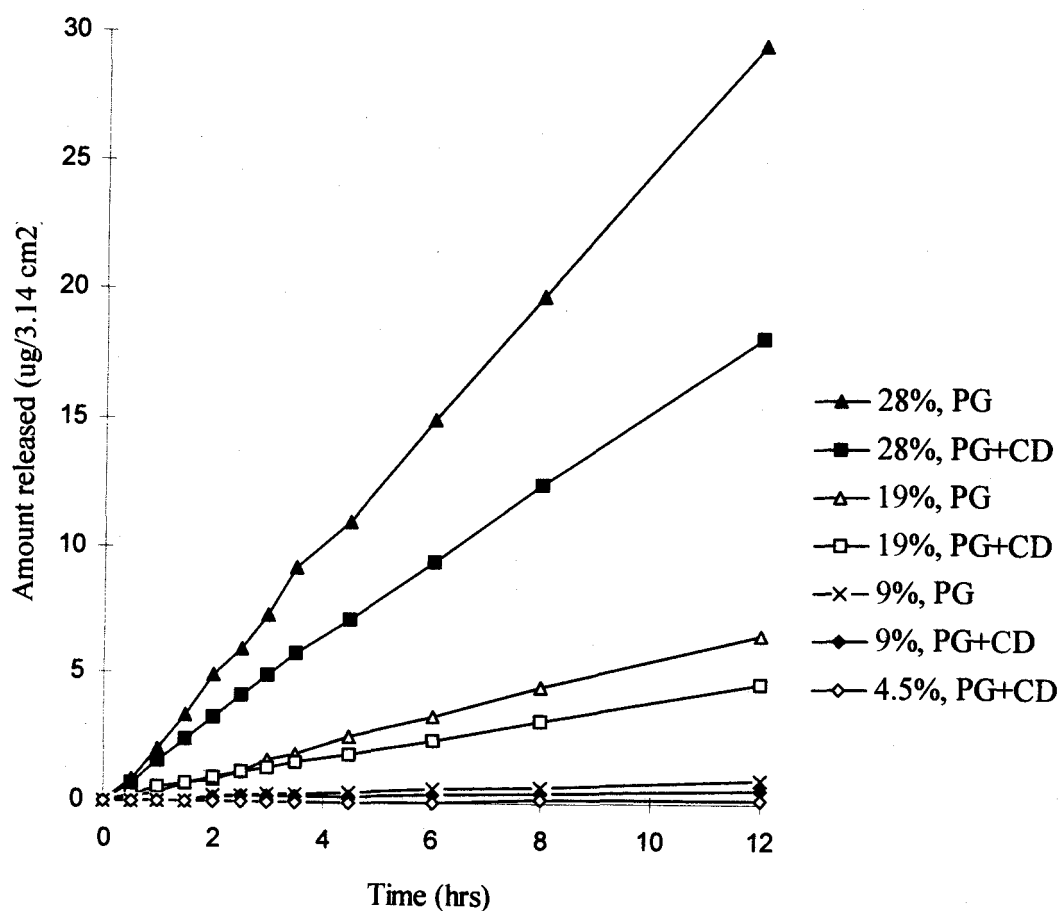
Figure 6.1 : MT diffusion profile through a series of ethylene vinyl acetate membranes with different vinyl acetate content (28%, 19%, 9%, and 4.5%) using a donor solution of (a) 40% propylene glycol(PG) or (b) 40% propylene glycol with 30% cyclodextrin (PG+CD).

Table 6.2: Flux (μg/hr/cm^2), permeability coefficient (cm/hr), and lag time of MT from vehicles through ethylene vinyl acetate membranes.

Vehicle: 40% PG (v/v) in Phosphate Buffer pH 6.1

VAc content	Flux(n=3) (μg/hr/cm^2)	MT Solubility (mg/ml)[b]	Permeability (cm/hrx10^{-5})[a]	Lag time
28 %	0.795 ± 0.14	9.587	8.292	none
19 %	0.183 ± 0.0041	9.587	1.909	15.7 ± 5.4min
9 %	0.023 ± 0.0032	9.587	0.240	1.5 hrs

Vehicle: 40% PG (v/v), 30% 2-HPCD (w/v) in Phosphate buffer pH 6.1

VAc content	Flux(n=3) (μg/hr/cm^2)	MT Solubility (mg/ml)[b]	P (cm/hrx10^{-5})[a]	Lag time
28 %	0.487 ± 0.026	20.408	2.386	none
19 %	0.123 ± 0.0032	20.408	0.603	none
9 %	0.011 ± 0.0041	20.408	0.054	1.5
4.5 %	_ c	20.408	-	_ c

[a]Permeability coefficient (P) = flux (μg/hr/cm^2) ÷ MT solubility (μg/ml).

[b]From reference 4.

[c]Not enough data points to calculate flux and lag time. MT released in the receptor phase was first detected at 8 and 12 hrs, respectively, in the triplicate samples.
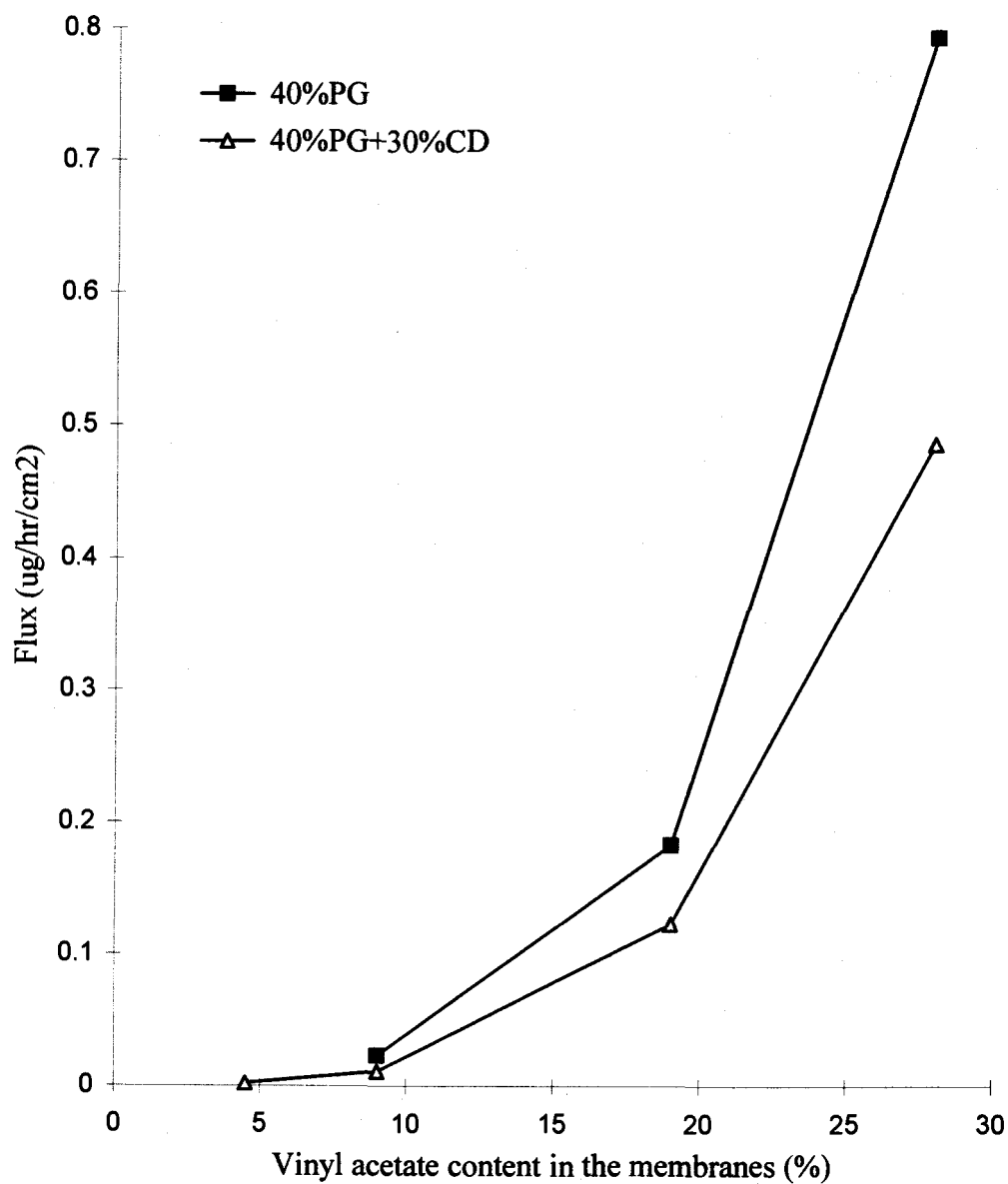
Figure 6.2: Relation between flux of MT through ethylene vinyl acetate copolymer membranes and percent content of vinyl acetate in the membranes using a donor solution of (a) 40% propylene glycol (40%PG) or (b) 40% propylene glycol with 30% cyclodextrin (40%PG+30%CD).

40% PG with 30% 2-HPCD vehicle, since 2-HPCD decreased the permeability coefficient through the membrane despite the higher drug solubility in this vehicle.

Diffusivity and solubility are the two key properties of membrane systems that influence diffusion and membrane substance selection for dosage form device. Diffusivity in polymer systems is affected by the size and shape of the active ingredient, the flexibility of the polymer chains, and the packing density or crystallinity of the polymer chains (6). Solubility of solutes in polymers involves many complex interactions between the solute and polymer such as polarity, hydrogen bonding, and steric effects. Solute solubility is low in polymer crystallites. Solubility decreases proportionately to increases in polymer crystallinity (7 and 8). In these experiments with MT, increasing vinyl acetate content of the EVAc membrane may reduce polymer crystallinity, and the polymer becomes rubbery and more permeable. This change in membrane property may facilitate the movement of MT through the membrane.

Adhesive Studies

The resulting flux from the three adhesive systems is displayed in Table 6.3. Flux through the three adhesive system was not significantly different (p-value=0.06) and did not differ from the flux through the 28% VAc membrane without adhesive. The pressure transfer method of adhesive application resulted in a lag time of approximately 2.5 hours, while the spray method of application resulted in no lag time. Using ethyl acetate/heptane (50/50) as a solvent in the spraying method provided the highest flux. This combination solvent was also convenient to use because it

evaporated quickly during spraying. Both solvents, isopropanol and EtOAc/heptane,

provided a smooth, even, and tacky adhesive layer. The pressure transfer technique

resulted in a rather rough adhesive layer, which separated from the membrane

overnight.

When both MT and adhesive were dissolved in the same solvent prior to

application to the membrane, there was very low MT flux (data not shown). The

HPLC chromatogram of the receptor solution showed an unidentified peak.

Table 6.3: Flux values and lag time of MT using a 28% vinyl acetate membrane with and without adhesive.

System[a]	Flux value (μg/hr/cm^2)[b]	Lag time (hrs)
1	0.927 ± 0.104	0
2	1.01 ± 0.082	0
3	0.743 ± 0.016	2.451 ± 0.021
No adhesive	0.795 ± 0.14	0

[a] See Table 6.1.

[b] The flux values were statistically compared to the flux of MT through an identical system without adhesive (0.795 ± 0.14 μg/hr/cm^2). They was no significant difference (p=0.06).

Delivery Device Studies

MT flux from aged TDD's is displayed in Table 6.4. Flux values from TDD's aged 1-day had a relatively high variation compared to those of the other two groups. There was no significant difference in flux (p-value=0.14) between the devices aged from one to three days. Mean steady-state flux was 1.88 ± 0.6 $\mu g/hr/cm^2$.

Table 6.4: Flux values of MT from transdermal delivery devices as a function of storage time.

Storage time	Flux ($\mu g/hr/cm^2 \pm$S.D.)[a]	Lag time (hrs)
1 day	2.53 ± 1.10	0
2 days	1.68 ± 0.27	0
3 days	1.55 ± 0.25	0

[a]There was no significant difference.

Although, the flux of MT was not significantly different, the cumulative amount of MT released over 12 hours was notably different (Figure 6.3). The highest burst effect was obtained from 3-day patches, following by that of 2-day patches and 1-day patches, respectively. This result is reasonable since a TDD aged by storage will have a membrane and adhesive saturated with MT, which will release at an initially high rate when placed in an desorbing environment (9). Thus, the longer storage time
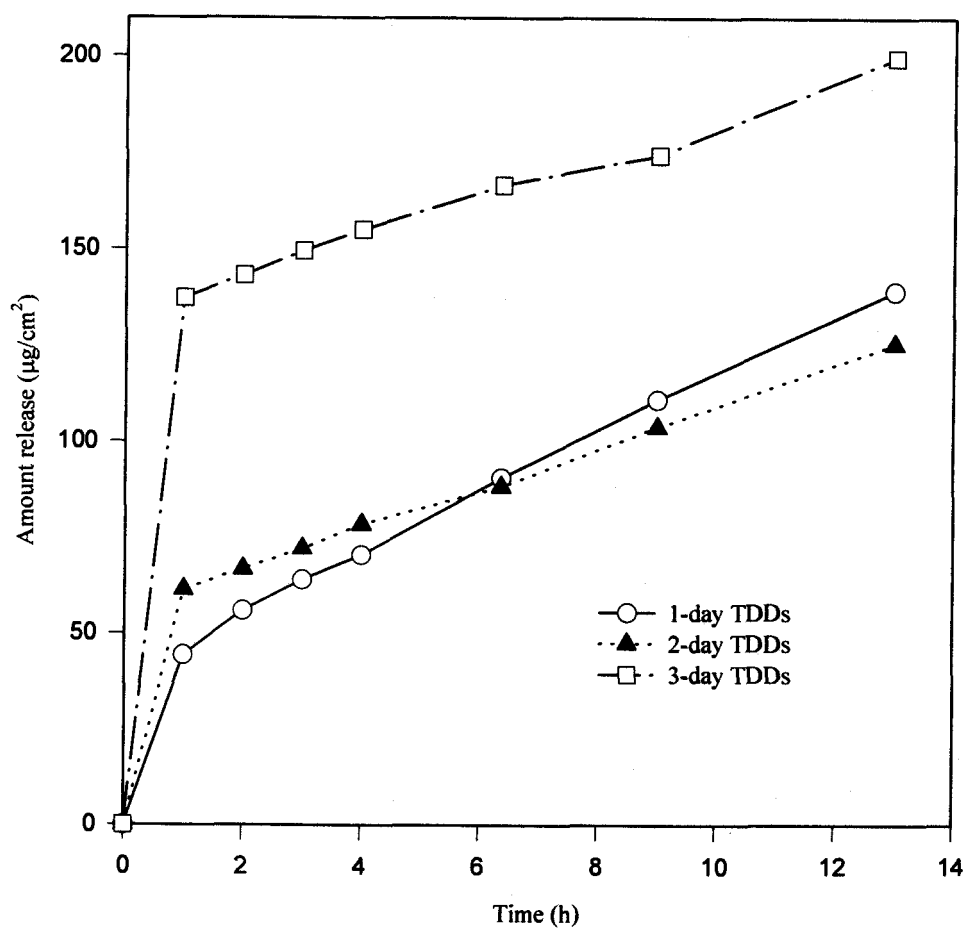
Figure 6.3: Cumulative amount ($\mu g/cm^2$) of MT released from transdermal delivery devices with storage. Values are expressed as mean (n=3).

resulted in more MT penetrating into the membrane and the adhesive. The changing of the burst effect with storage time resulted in a different overall release rate (total amount released/12 hours)as 3-day patches (4.89 ± 0.39 µg/hr/cm^2), followed by 1-day patches (3.40 ± 1.24 µg/hr/cm^2), 2-day patches (3.07 ± 0.29 µg/hr/cm^2), and freshly prepared patches (1.18 ± 0.10 µg/hr/cm^2).

Determination of the amount of MT remaining in the TDD reservoir showed that approximately 3.7 ± 0.8% of MT was probably trapped in the membrane and adhesive portion of the device as shown in Table 6.5.

Table 6.5: Mass balance of MT in transdermal delivery device. Values expressed as means plus standard deviation(n=3).

Storage time (day)	Applied MT (mg)	Recovered MT in reservoir (mg)	Recovered MT in receptor (mg)	Trapped MT in the membrane and adhesive (mg)[a]
1 day	13.11	12.47 ± 0.16	0.14 ± 0.052	0.50 ± 0.21
2 day	13.11	12.42 ± 0.06	0.12 ± 0.011	0.57 ± 0.052
3 day	13.11	12.54 ± 0.27	0.20 ± 0.021	0.37 ± 0.28

[a] Applied MT minus recovered MT in device reservoir and receptor solution.

MT flux value from the developed TDD is higher than the flux of the drug through human skin, which has been estimated to be about 0.83 µg/hr/cm^2 (4).

Therefore, patch size may be appropriately adjusted to deliver the drug to obtain desired plasma concentrations.

CONCLUSIONS

The study has provided information for a reservoir type of MT TDD. The membrane studies showed increased permeability coefficients with increasing VAc content of the membranes for both vehicles. The highest flux rate was obtained from the system of 40% PG vehicle through 28% VAc membrane. The 40% PG vehicle provided a greater flux compared to the 40% PG with 30% 2-HPCD vehicle, despite the higher MT solubility in the 40% PG with 30% 2-HPCD vehicle. The study of adhesive application onto the 28% vinyl acetate membrane either by the spray or pressure transfer method showed no significant difference in MT flux. However, the pressure transfer method was not acceptable. When MT was physically mixed with adhesive solution prior to the application, very low flux occurred, and the HPLC chromatogram had an unidentified peak. Delivery devices were constructed, and the effect of storage was studied. There was no significant difference in steady state flux among TDD's aged from one to three days. Nonetheless, the highest burst effect was obtained from 3-day patches, followed by that of 2-day patches and 1-day patches, respectively. MT flux values from the developed TDD were approximately twice the estimated MT steady state flux through human skin, which has been estimated to be 0.83 $\mu g/hr/cm^2$.

REFERENCES

1. Petterborg, L.J., Thalen, B.E., Kjellman, B.F., Wetterberg, L. Effect of melatonin replacement on serum hormone rhythms in a patient lacking endogenous melatonin. Brain. Res. Bull., 27, 2, 181, (1991).

2. Waldhauser, F., Dietzel, M. Daily and annual rhythms in human melatonin secretion: role in puberty control. Ann.,New York Acad. Sci., 453, 205, (1985).

3. Lee, Y. Development of transdermal delivery system for melatonin. M.S. Thesis, The College of Pharmacy, Oregon State University, (1989).

4. Lee, B. Development and evaluation of an oral controlled release and a transdermal delivery system for melatonin in human subjects. Ph.D. Thesis, The College of Pharmacy, Oregon State University, (1992).

5. Benes, L., Brun, J.,Claustrat, B., Degrande, G, Ducloux, N., Geoffriau, M., Horriere, F., Karsenty, H., Lagain, D. in Melatonin and the pineal gland from basic science to clinical application, Y. Touitou, J. Arendt, and P. Pe'vet, eds., Elsevier Science Publishers B.V., Amsterdam, the Netherlands, 347, (1993).

6. Smith, K.L., Herbig, S.M. in Membrane handbook, W. S. Winston, and K. K. Sirkar, eds., Van Nostrand Reinhold, NY, 915, (1992).

7. Crank, J., Park, G.S. Diffusion in polymers, J. Crank and G.S. Park, eds., Academic Press, NY, 1, (1968).

8. Grulke, E.A. in Polymer handbook, 3 rd ed., J. Brandrup and E. H. Immergut, eds., John Wiely and Sons, NY, 519, (1989).

9. Baker, R.W., Sanders, L. in Synthetic Membrane: Science, Engineering and Application, P.M. Bungray et al., eds., D. Reidel Publishing Company, Holland, 581, (1986).

10. Iguchi, H., Kato, K.I., Ibayashi, H. Melatonin serum levels and metabolic clearance rate in patients with liver cirrhosis. J. Clin. Endocrinol. Metab., 54, 5, 1025, (1982).

BIBLIOGRAPHY

Aldhous, M.E., Arendt, J. Radioimmunoassay for 6-sulphatoxymelatonin in urine using an iodinated trace, Ann. Clin. Biochem. 25, 298-303 (1988).

Anderson, J.H., Anderson, R.J., Iben, S. Hepatic uptake of propanolol. J. Pharmacol. Exp. Ther. 206, 172-180 (1978).

Arendt, J. In Melatonin and the mammalian pineal gland; Chapman & Hall, London, UK, 1995, pp. 40, 42, 207, 248.

Arendt, J., Bojkowski, C., Franey, C., Wright, J., Marks, V. Immunoassay of 6-hydroxymelatonin sulfate in human plasma and urine: abolition of the urinary 24-hour rhythm with atenolo, J. Clin. Endocrinol. Metab. 60, 1166-73 (1985).

Baker, R.W., Sanders, L. in Synthetic Membrane: Science, Engineering and Application, P.M. Bungray et al., eds., D. Reidel Publishing Company, Holland, 581, (1986).

Balant, L.P., McAinsh, J. Use of metabolite data in the evaluation of pharmacokinetics and drug action. In: Jenner, P., Testa, B., eds. Concepts in drug metabolism. Part A Marcel Dekker, Inc. New York, 1980, pp. 311-371

Bartsch, H., Bartsch, C. Effect of melatonin on experimental tumors under different photoperiods and times of administration. J. Neural Trans., 52, 269-279 (1981).

Bass, L., Keiding, S. Physiologically based models and strategic experiments in hepatic pharmacology. Biochem. Pharmacol. 37, 1425-1431 (1988).

Bass, L., Keiding, S., Winkler, K., Tygstrup, N. Enzyme elimination of substrates flowing through the intact liver. J. Theor. Biol. 61, 393-409 (1976).

Bass, L., Robert, M.S., Robinson, P.J. On the relation between extended forms of the sinusoidal perfusion and the convection-dispersion models of hepatic elimination. J. Theor. Biol. 126, 457-482 (1987).

Bass, L., Robinson, P.J., Bracken, A.J. Hepatic elimination of flowing substrates: the distributed model. J. Theor. Biol. 72, 161-184 (1978).

Bass, L., Winkler, K. A method of determining intrinsic hepatic clearance from the first-pass effect. Clin. Exp. Pharmacol. Physiol. 7, 339-343 (1980).

Benes, L.; Brun, J.; Claustrat, B.; Degrande, G.; Ducloux, N.; Geoffriau, M.; Horriere, F.; Karsenty, H.; Lagain, D. In Melatonin and the pineal gland from basic science to clinical application; Touitou, Y.; Arendt, J.; Pe'vet, P.; Eds.; Elsevier Science Publishers B.V., Amsterdam, the Netherlands, 1993; pp 347.

Benes, L.; Degrande, G.; Ducloux, N.; Horriere, F.; Karsenty, H.; Proceed Intern.Symp. Control. Rel. Bioact. Mater., Controlled Release Society, Inc., 21, 551-552 (1994).

Benet, L.Z., Massoud, N., Gambertoglio, J.G. Pharmacokinetic basis for drug treatment, Raven Press, New York, 1984.

Blask, D.E., Hill, S.M., Pelletier, D.B. Oncostatic signaling by the pineal gland and melatonin in the control of breast cancer In The pineal gland and cancer Gupta, D.; Attanasio, A.; Rieter, R.J., Ed; Muller & Bass, Tubingen, Germany, 1988, pp 195-206.

Bojkowski, C.J. 6-sulphatoxymelatonin as an index of pineal function in human physiology. Thesis, University of Surrey, UK.

Bojkowski, C.J., Arendt, J. Factors influencing urinary 6-sulphatoxymelatonin, a major melatonin metabolite, in normal human subjects. Clin. Endocrinol., 33, 435-444 (1990).

Bojkowski, C.J., Arendt, J., Shin, M.C. &Markey, S.P. Melatonin secretion in humans assessed by measuring its metabolite, 6-sulphatoxymelatonin. Clin. Chem. 33, 1343-1348 (1987).

Brockmeier, D. Acta Pharm. Technol. 1986, 32, 4, 164-167.

Budavari, S., Maryadele, J.O.N., Smith, A., Heckelman, P.E., Kinneary, J.F., eds. The Merck Index, an encyclopedia of chemicals, drugs, and biligicals. 12th ed. Merck Research Laboratories Division of Merck & Co., Inc. 1996 pp. 5860.

Cagnacci, A., Elliott, J.A., Yen, S. Amplification of pulsatile LH secretion by exogenous melatonin in women. J. Clin. Endocrinol. Metab. 73, 210-212 (1991).

Carstensen, J.T. In Modeling and data treatment in the pharmaceutical sciences, Technomic Publishing Company, Inc., USA, 1996, pp. 177-180.

Cochran WC, Cox GM. Experimental Designs, 2th ed. New York: John Wiley and Sons, 1957.

Crank, J., Park, G.S. Diffusion in polymers, J. Crank and G.S. Park, eds., Academic Press, NY, 1, (1968).

Dahlit, M., Alvarez, B, Vignau, J., English, J., Arendt, J., Parkes, J.D. Delayed sleep phase syndrome response to melatonin, Lancet 337, 1121-1124 (1991).

Dawson, D., Armstrong, S.M. Chronobiotics-Drugs that shift rhythms. Pharmacol. Ther. 69, 15-36 (1996).

Dawson, D., Encel, N. Melatonin and sleep in humans, J. Pineal Res. 15, 1-12 (1993).

Dement, W.C., Miles, L.E., Carskadon, M.A. "White Paper" on sleep and aging, JAGS 30, 25-50 (1982).

DiPiro JT, Talbert RL, Hayes PG, et al., eds. Pharmacotherapy, a pathophysiologic approach. 2th ed. Connecticut: Appleton & Lane Norwalk, 1993, pp. 37.

Dollins, A.B., Zhdanova, I.V., Wurtman, R.J., Lynch, H.J., Deng, M.H. Effect of inducing nocturnal serum melatonin concentrations in daytime on sleep, mood, body temperature, and performance, Proc. Natl. Acad. Sci. 91, 1824-1828 (1994).

Evans WE, Schentag JJ, Jusko WJ. Applied Pharmacokinetics, Applied Therapeutics, Inc. 1992.

Fellenberg, A.J., Phillipou, G., Seamark, R.F. Urinary 6-sulphatoxymelatonin excretion and melatonin production rate: studies in sheep and man. In Pineal function (C.D. Matthews and R.F. Seamark, Ed.), 1981, Elsevier/North Holland Biomedical Press, Amsterdam, pp. 143-50.

Fellenberg, A.J.; Phillipou, G.; Seamark, R.F. In Pineal Function; Matthew, C.D.; Seamark, R.F; Eds; Oxford, Elsevier, 1981, pp 143-149.

Garfinkel, D., Laudon, M., Nof, D., Zisapel, N. Improvement of sleep quality in elderly people by controlled-release melatonin, Lancet 346, 541-544 (1995).

Gilad, E., Zisapel, N. High-affinity binding of melatonin to hemoglobin Biochemical & Molecular Medicine 56(2), 115-120 (1995).

Gillespie, W.R. PCDCON: Deconvolution for pharmacokinetic applications. AAPS Short Course of Convolution, deconvolution and linear systems. Miami Beach, FL, November 5, 1995.

Gough, K., Hutchison, M., Keene, O., Byrom, B., Ellis, S., Lacey, L., McKellar, J. Assessment of dose proportionality: report from the statisticians in the pharmaceutical industry/pharmacokinetics UK joint working party. Drug Inform. J. 29, 1039-1048 (1995).

Groothius G.M.M., Hardonk, M.J., Keulemans, K.P.T., Niewenhuis, P., Meijer, D.K.F. Autoradiographic and kinetic demonstration of heterogeneity of taurocholate transport. American J. Physiol. 243, G455-G462 (1982).

Grulke, E.A. in Polymer handbook, 3 rd ed., J. Brandrup and E. H. Immergut, eds., John Wiely and Sons, NY, 519, (1989).

Haimov, I., Lavie, P., Laudon, M., Herer, P., Vigder, C., Zisapel, N. Melatonin replacement therapy of elderly insomniacs, Sleep 18, 598-603 (1995).

Hayashi, T.; Ogura, T.; Takagishi, Y. New evaluation method for *in vitro/in vivo* correlation of enteric-coated multiple unit dosage forms. Pharm. Res. 12(9), 1333-1337 (1995).

Iguchi, H., Kato, K.I., Ibayashi, H. Melatonin serum levels and metabolic clearance rate in patients with liver cirrhosis. J. Clin. Endocrinol. Metab., 54, 5, 1025, (1982).

James, S.P., Mendelson, W.B., Sack, D.A., Rosenthal, N.E., Wehr, T.A. The effect of melatonin on normal sleep. Neuropsychopharmacology, 1, 41-44, (1987).

James, S.P., Sack, D.A., Rosenthal, N.E., Mendelson, W.B. Melatonin administration in insomnia. Neuropsychopharmacology, 3,19-23, (1990).

Jones, A.L., Hradek, G.T., Renston R.H., Wong, K.Y., Karlaganis, G. et al. Autoradiographic evidence for hepatic lobular concentration gradient of bile acid derivative. American J. Physiol. 238, G233-G237 (1980).

Jones, R.L., Mc Geer, P.L., Greiner, A.C. Clin. Chim. Acta. 26, 281 (1969).

Jusko, W.J. Guidelines for collection and analysis of pharmacokinetic data. In: Evans, Schentag, Jusko, eds. Applied Pharmacokinetics, 2nd ed. Spokane, Washington: Applied Therapeutics, 1986.

Kalns, J. E. Pharmacokinetic and pharmacodynamics of 1) Oral sustained release acetaminophen suspension in children; 2) Potassium chloride in adults. Ph.D. Thesis, Oregon State University, 1993, pp. 64 -104.

Keiding S. Hepatic elimination kinetics: the influence of hepatic blood flow on clearance determinations. Scandinavian Journal of Clinical and Laboratory Medicine 36, 113-118 (1976).

Keiding S., Andreasen, P.B. Hepatic clearance measurements and pharmacokinetics. Pharmacology 19, 105-110 (1979).

Keller, F.; Kunzendorf, U.; Walz, G.; Haller, H.; Offermann, G. Saturable first-pass kinetics of propanolol J. Clin Pharmacol, 29, 240-245 (1989).

Konsil, J.; Parrott, K. A.; Ayres, J. W. Development of a transdermal delivery device for melatonin in vitro study. Drug Dev. Ind. Pharm. 21(12), 1377-1387 (1995).

Kopin, I.J., Pare, C.M.B., Axelrod, J., Weissbach, H. The fate of melatonin in animals, J. Bio. Chem. 236, 3072-3075 (1961).

Lagenbucher, F. Linearization of dissolution rate curves by the Weibull distribution. J. Pharm. Pharmacol. 24, 979-981 (1972).

Lanao, J.M.; Vincente, M.T.; Sayalero, M.L.; Dominguez-Gil, A. Computer program (DCN) for numerical convolution and deconvolution of pharmacokinetic function. J. Pharmacobio-Dyn., 15, 203-214 (1992).

Lane, E. A.; Moss, H. B. Pharmacokinetics of melatonin in man: first pass hepatic metabolism. J. Clin. Endocrinol. Metab. 61, 1214-1216 (1985).

Langenbucher, F. Numerical convolution/deconvolution as a tool for correlation in vitro/in vivo drug availability. Pharm. Ind., 44, 11, 1166-1171 (1982).

Langenbucher, F.; Moller, H. Correlation of *in vitro* drug release with *in vivo* response kinetics. Part I: Mathematical treatment of time functions, Phram. Ind., 45, 623-628 (1983).

Lee, B. Development and evaluation of an oral controlled release and a transdermal delivery system for melatonin in human subjects. Ph.D. Thesis, The College of Pharmacy, Oregon State University, (1992).

Lee, B., Parrott, K.A., Ayres, J.W., Sack, R.L. Design and evaluation of an oral controlled release delivery system for melatonin in human subjects, Int. J. Pharm. 124, 119-127 (1995).

Lee, B., Parrott, K.A., Ayres, J.W., Sack, R.L. Development and characterization of an oral controlled release delivery system for melatonin Drug Dev. Ind. Pharm., 22(3), 269-274 (1996).

Lee, B., Parrott, K.A., Ayres, J.W., Sack, R.L. Preliminary evaluation of transdermal delivery of melatonin in human subjects, Res. Commun. Mol. Pathol. Pharmacol. 85, 337-346 (1994).

Lee, P.I.D., Amidon, G.L. Influence of dosage on pharmacokinetics-Dose proportionality In Pharmacokinetic analysis Technomic Publishing Company, Inc., Pennsylvania, 1996, pp. 143-165.

Lee, P.I.D., Amidon, G.L. Pharmacokinetics of metabolites. In Pharmacokinetic analysis Technomic Publishing Company, Inc., Pennsylvania, 1996, pp. 237-272.

Lee, Y. Development of transdermal delivery system for melatonin. M.S. Thesis, The College of Pharmacy, Oregon State University, (1989).

Leeson, L. J.; Adair, D.; Clevenger, J.; Chiang, N. The in vitro development of extended-release solid oral dosage forms J. Pharm. and Biopharm. 13(5) 493-514 (1985).

Lerner, A.B., Case, J.D., Heinzelman, R.V. Structure of melatonin, J. Am. Chem. Soc. 81, 6084-6085 (1959).

Lewy, A.J., Markey, S.P. Analysis of melatonin in plasma by gas chromatography negative chemical ionization mass spectroscopy, Science 201, 741-743 (1978).

Lewy, A.J., Newsome, D.A. Different types of melatonin circadian secretory rhythms in some blind subjects, J. Clin. Endocrinol. Metab. 56, 1103-1107 (1983).

Lin, J.H. Dose-dependent pharmacokinetics: experimental observations and theoretical considerations. Biopharm. Drug Disposit. 15, 1-31 (1994).

Macfarlane, J.G., Cleghorn, J.M., Brown, G.M., Streiner, D.L. The effects of melatonin on the total sleep time and daytime alertness of chronic insomniacs: A primary study. Biol. Psych. 30, 371-376 (1991).

Maestroni, G.J.M., Conti, A., Pierpaoli, W. Melatonin stress and the immune system. Pineal. Res. Rev., 7, 268 (1989).

Mallo, C., Zaidan, R., Galy, G., Brun, J., Chazot, G., Claustrat, B. Pharmacokinetics of melatonin after intravenous infusion and bolus injection. Eur. J. Clin. Pharmacol. 38, 297-301 (1990).

Matthews, C.D., Kennaway, D.J., Fellenberg, A.J.G., Phillipou, G., Cox, L.W., Seamark, R.F. Melatonin in man, Adv. Biosci. 29, 371-81 (1981).

McArthur, A.J., Lewy, A.J., Sack, R.L. Non-24-hour sleep-wake syndrome in a sighted man: circadian rhythm studies and efficacy of melatonin treatment. Sleep, 19(7), 544-553 (1996).

Microsoft Fortran Power Station version 4.0 Standard Edition, Microsoft Corporation, 1995.

Morgan, D.J., Smallwood, R.A. Clinical significance of pharmacokinetic models of hepatic elimination Clin. Pharmacokinetic. 18(1), 61-76 (1990).

Nowak, R., McMillen, I.C., Redman, J., Short, R.V. Clin. Endocrinol. 27, 445-452 (1987).

Nowak, R., McMillen, I.C., Redman, J., Short, R.V. The correlation between serumand salivary melatonin concentration and urinary 6-hydroxymelatonin sulphate excretion rate: Two non-invasive techniques for monitoring human circadian rhythmicity. Clin. Endocrinol. 27, 445-452 (1987).

Ouslander JG. Drug therapy in the elderly Ann. Intern. Med. 95, 711-722 (1981).

P-PHARM, Population pharmacokinetic/pharmacodynamic data modeling program. Simed S.A., France.

Petrie, K., Conaglen, J.V., Thompson, L., Chamberlain, K. Effects of melatonin on jet lag after long haul flight, Br. Med. J. 298, 705-707 (1989).

Petterborg, L.J.; Thalen, B.E.; Kjellman, B.F.; Wetterberg, L. Effects of melatonin replacement on serum hormone rhythm in a patient lacking endogenous melatonin. Brain. Res. Bull. 27(2), 181-185 (1991).

Podczeck, F., Charter, M.K., Newton, J.M., Yuen, K.H. Eur. J. Pharm. Biopharm. 41, 254 (1995).

Prinz, P.N., Vitiello, M.V., Raskind, M.A., Theropy, M.J. Geriatrics: Sleep disorders and aging, NEJM 323, 520-526 (1990).

Rescigno, A.; Segre, G. Drug and tracer kinetics, Blaisdell Publishing Company. London, 1965.

Robert, S.L., Lewy, A.J., Hughes, R.J., McArthur, A.J., Blood, M.L. Melatonin as a Chronobiotic Drug. DN&P, 9(6), 325-332 (1996).

Robinson, J. R., Vincent, H. L., Ed, Controlled Drug Delivery Fundamentals and applications, Marcel Dekker, Inc.: New York, 1987; pp 24-25

Rosenthal, N.E., Sack, D.A., Gillin, J.C., Lewy, A.J., Goodwin, F.W., Davenport Y., Mueller, P.S. Seasonal effective disorder. A description of the syndrome and preliminary findings with light therapy, Arch. Gen. Psychiatry 4, 171-180 (1984).

Rosenthal, N.E., Sack, D.A., Gillin, J.C., Lewy, A.J., Goodwin, F.W., Davenport, Y., Mueller, P.S. Seasonal effective disorder. A description of the syndrome and preliminary findings with light therapy, Arch. Gen. Psychiatry 41, 71-80 (1984).

Rossi, S.; Ferri, F.; Bonferoni, M. C.; Caramella, C.; La Manna, A.; De Bernardi Di Valserra, M.; Feletti, F. A computer-aided simulation approach in the development of prolong release formulation. Boll. Chim. Farmaceutico. 130(11), 443-448 (1991).

RSTRIP II version 1.0 copyright 1992. Micromath Scientific Software Salt Lake City, UT.

Sack, R.L. Melatonin: advising patients about the use of melatonin ASDA News, 3(3), 15, 27 (1996).

Sanford, B. in: Pharmaceutical statistics, practical and clinical appliaction, third edition, 1997, Marcel Dekker, Inc., New York pp. 203-210.

Shannon, C.E. Bell Syst. J. 27, 379 (1948).

Shargel, L., Yu, A.B.C. In Applied biopharmaceutics and pharmacokinetics; Appleton&Lange, Connecticut,1993, pp. 200-201.

Simpson, H.W. Chronobiotics: Selected agents of potential value in jet lag and other desynchronisms. In: Chronobiology: principles and applications to shifts in schedules. L.E. Scheving and F. Halberg (Eds.), Sijthoff and Noordhoff, the Netherlands, 1980, pp. 443-446.

Singer, C., Jackson, J., Moffit, M., Blood, M., McArthur, A., Sack, R., Parrott, K.A., Lewy, A. Physiologic melatonin administration and sleep-wake cycle in Alzheimer's disease: a pilot study, Sleep Research 23, 84 (1994).

Singer, C., McArthur, A., Hughes, R., Sack, R., Kaye, J., Lewy, A. High dose melatonin administration and sleep in the elderly, Sleep Research 24, 151 (1995).

Singer, C., McArthur, A., Hughes, R., Sack, R., Kaye, J., Lewy, A. Physiologic melatonin administration and sleep in the elderly, Sleep Research 24, 152 (1995).

Singer, C., Wild, K., Sack, R., Lewy, A. High dose melatonin is well tolerated by the elderly, Sleep Research 23, 86 (1994).

Smith, K.L., Herbig, S.M. in Membrane handbook, W. S. Winston, and K. K. Sirkar, eds., Van Nostrand Reinhold, NY, 915, (1992).

Snedecor, G.W. and Cochran, W.G. Statistical methods, eight edition, 1991, Iowa State University Press, Ames, Iowa pp. 68-70.

STATGRAPHIC version 7.0, Portion copyright 1993 Manugistics, Inc. Statistical Graphics Corporation.

STATGRAPHICS Plus version 2.1 (for Windows), Portion copyright 1996 Manugistics, Inc. Statistical Graphics Corporation.

Swift CG, Homeida M., Halliwell M, et al. Antipyrine disposition and liver size in the elderly. Eur J Clin Pharmacol. 12, 149-152 (1978).

Vakkuri, O., Leppaluoto, J., Kauppila A. Oral administration and distribution of melatonin in human serum, saliva and urine. Life Sci. 37, 489-495 (1985).

Veng-Pedersen, P.; Karol, M.D.; Gillespie, W. AAPS short course: Convolution, deconvolution and linear systems, November 5, 1995, Miami Beach, Florida.

Vestal RE, Norris AH, Tobin JD, et al. Effect of age and cigarette smoking on propanolol disposition. Clin Pharmmacol Ther 26, 8-15 (1979).

Wagner, J.G. Comparison of nonlinear pharmacokinetic parameters estimated from the sinusoidal perfusion and venous equilibrium models. Biopharm. Drug Disposit. 6, 23-31 (1985).

Wagner, J.G., Antal, E.J., Elvin, A.T., Gillespie, W.R., Pratt, E.A., Albert, K.S. Theoretical decrease in systemic availability with decrease in input rate at steady-state for first-pass drugs Biopharm. Drug Disposit. 6, 341-343 (1985).

Waldhauser, F., Dietzel, M. Daily and annual rhythms in human melatonin secretion: role in puberty control. Ann.,New York Acad. Sci., 453, 205, (1985).

Waldhauser, F., Vierhapper, H., Oirich, K. Abnormal circadian melatonin secretion in night-shift workers, The New Eng. J. Med. 7, 441-446 (1986).

Waldhauser, F.; Waldhauser, M.; Lieberman, H. R.; Deng, M. H.; Lynch, H. J.; Wurtman, R. J. Bioavailability of oral melatonin in humans. Neuroendocrinol. 39, 307-313 (1984).

Weisiger, R.A., Mendel, C.M., Cavalieri, R.R. The hepatic sinusoid is not well-stirred: estimation of the degree of axial mixing by analysis of lobular concentration gradients formed during uptake of thyroxine by the perfused rat liver. J. Pharm Sci. 75, 233-237 (1986).

Wilson, C.G., Washington, N. The stomach: its role in oral drug delivery. In Physiological Pharmaceutics, biological barriers to drug absorption. John Wiley & Sons. New York, 1989, pp. 47-70.

Winkler, K., Bass, L., Keiding S., Tygstrup, N. The effect of hepatic perfusion on the assessment of kinetic constants. In Lundqvist & Tygstrup (Eds) Regulation of hepatic metabolism, pp. 797-807, Munksgaard, Copenhagen, 1974.

Winkler, K., Bass, L., Keiding S., Tygstrup, N. Clearance as a quantitative measurement of liver function. In Paumgartner & Preisig (Eds) The liver. Quantitative aspects of structure and function, pp. 144-155, Karger, Basel, 1973.

Winkler, K., Bass, L., Keiding S., Tygstrup, N. The physiological basis for clearance measurements in hepatology. Scandinavian Journal of Gastroenterology 14, 439-448 (1979).

Wynn, V.T., Arendt, J. The effect of melatonin on the human electrocardiogram and simple reaction time responses. J. Pineal Res., 5, 427-436 (1988).

Yeh, K.C., Kwan, K.C. A comparison of numerical integrating algorithms by trapezoidal, lagrange, and spline approximation. J. Pharm. Biopharm. 6(1), 79-98 (1978).

Yeleswaram, K., Mclaughlin, L.G., Knipe, J.O., Schabdach, D. Oral bioailability of melatonin in the rat, dog, and monkey J. Pineal. Res. in press (1997).

APPENDICES

APPENDIX A

Individual MT plasma concentrations, dissolution profile of SR MT formulation (10%

IR MT + 90% SR MT), and plots of CL/F and Vd/F versus age following

administration of 50 mg IR MT in young and old healthy subjects.

(Chapter 1)

Table A1: MT plasma concentrations (ng/ml) following administration of 50 mg IR MT in 12 healthy old and young volunteers.

Time	LA	SK	HF	AT	AK	AO	CB	SN	KT	VB	SL	JB
0	0	0	0	0	0	0	0	0	0	0	0	0
0.5	27.7	33.8	15.6	17.9	72.3	43.4	34.2	29.8	18.8	10.9	14.2	0.0
1	89.0	44.8	27.2	78.7	208.6	54.3	41.1	100.0	81.2	42.5	36.6	3.9
1.5	72.3	53.5	70.6	82.4	158.1	65.2	40.2	100.0	56.0	45.2	21.1	11.2
2	50.1	53.1	101.4	90.0	81.8	44.3	33.3	100.0	67.4	38.4	19.0	21.6
2.5	40.2	47.0	96.6	55.3	54.6	37.6	28.5	100.0	48.0	36.5	11.5	15.6
3	44.8	42.0	75.4	76.5	45.8	33.7	24.4	100.0	14.0	30.4	12.1	18.7
3.5	37.7	28.9	59.3	67.0	39.5	25.5	12.6	78.3	15.3	30.6	.	16.8
4	29.2	20.9	49.3	61.6	29.8	14.8	12.3	60.0	15.7	21.2	7.2	15.0
4.5	23.8	11.7	33.9	29.3	16.8	15.6	8.4	48.3	7.9	13.4	4.4	13.4
5	12.8	11.4	34.6	21.4	.	11.2	.	48.8	5.7	9.7	4.4	8.9
5.5	15.8	9.3	25.3	15.9	8.8	8.1	3.6	44.9	2.1	6.2	2.2	8.4
6	32.5	10.4	17.1	10.9	6.9	5.6	2.5	35.0	0.9	5.2	1.7	10.0
7	3.9	5.2	13.8	4.8	3.8	2.8	.	17.5	0.8	1.8	1.0	6.8
8	2.1	4.0	9.2	2.9	2.3	1.5	1.5	10.4	0.5	.	.	7.0
9	1.1	3.4	5.5	1.5	1.4	0.5	1.2	5.9	.	.	.	4.2
10	.	1.5	2.9	.	.	.	0.5	2.0	0.2	0.4	.	.
11	.	1.2	2.6	.	9.7	0.8	0.3	0.8	0.1	0.3	.	.
12	.	1.0	1.8	.	5.6	.	0.2	.	0.1	0.2	.	.

Table A2: MT plasma concentrations (pg/ml) following administration of MT SR formulation (10% IR MT + 90% SR MT) 0.2 mg in 13 healthy old and young volunteers.

Time	LA	SK	GL	HF	AT	AK	AO	CB	RC	SN	KT	VB	SL
0	8.7	10.7	8.5	2.5	2.5	2.5	2.5	2.5	2.5	21.8	22.5	2.5	2.5
0.5	139	67.4	129.1	39.5	95	168.5	59	9.7	44.7	222.9	91.3	29	2.5
1	85.3	65.5	225.7	114.3	121.8	186.7	117.3	91.1	60.4	314.2	79.6	75.2	53.3
1.5	142	36.2	175.4	96.5	119.6	140.4	144	74.6	61.7	232.6	77.9	66.3	24.8
2	115.5	37.8	209.4	62	75.4	102.8	130.7	65.1	57.9	179.5	93.6	67.2	22.8
2.5	119.9	44.8	138.3	53.7	107.1	91.8	90.1	58.9	54.6	189.2	74.2	41.8	23.5
3	115.1	31.7	129.4	69	94.4	95.4	124.2	54.2	55.1	162.3	70.1	51.7	16.7
3.5	116.8	28.5	124.5	64.4	88.3	69.8	72	46.9	44.3	148.6	74.7	31.4	11.5
4	70.3	20.6	128.3	49.5	89.7	66.1	100.2	54.7	35.1	180.6	76	24.9	14.8
4.5	109.7	15.4	90.9	35.1	80.5	61.4	100.5	37.3	43.3	201.5	71.2	25.9	15.5
5	117.5	20.8	84	22.7	64.6	49	104.2	57	31.5	93.8	61.9	30.1	11.5
5.5	94.2	15.4	105.1	27.8	94.6	33.6	99.7	48.7	37.7	146.8	58.4	35.4	14.4
6	70.8	12	77.7	22.6	78.6	33.1	66.2	35.4	21.8	126.2	55	32.8	9.7
7	56.2	10.9	70.3	16.2	53.2	31.5	68.8	25	25	107.7	57.8	19.3	6.1
8	61.2	10.5	33.9	9.7	38.1	25.5	41.5	15.1	19.1	71.2	52.9	12.8	4.6
9	42.2	8.6	37.4	8.8	32.6	23.7	41.5	14	12.2	78.9	62.1	9.8	2.5
10	37.4	8.2	32.7	14.4	30.8		34.4	11.6	10.8	50.8	33.2	8.1	2.5
11	41.5	28.3	23.1	9.4	23.2	22.9	25.6	20.3	11.7	53.7	24	5.5	2.5
12	46.1	4.7	26.2	8.6	26.3	15.4	20.2	31.2	20.6	88.9	19.7	12.1	2.5

Table A3: MT plasma concentrations (pg/ml) following administration of MT SR formulation (10% IR MT + 90% SR MT) 0.4 mg in 13 healthy old and young volunteers.

Time	LA	SK	GL	HF	AT	AK	AO	CB	RC	SN	KT	VB	SL
0	4.4	7.7	10.3	2.5	5.1	2.5	2.7	2.5	2.8	32.4	6	13.4	2.5
0.5	81.6	140.2	274.3	63	185	500	166.9	42.6	179.4	681.6	230.9	257	50.2
1	289.2	127.6	249.8	186.6	393.3	366.8	219.5	68.4	252	783.2	286.7	161.6	86.8
1.5	332.9	85.3	276.1	176.8	169.1	393.1	260.3	72.4	223.4	712	203.5	150.4	78.9
2	267.9	112.5	278.6	210.8	361.2	325.4	246.2	116.7	227.2	842	135.8	125.7	54.4
2.5	242.3	113.4	176.5	166.3	245.5	299.9	223.4	98.5	101.2	776	212.8	199.9	67.9
3	197.6	71.4	182.5	181.8	389	231.4	201.7	86.4	126.4	629.6	135.8	123.6	43.3
3.5	275.1	67.3	203.3	113.4	250.2	153.8	179.5	83.7	148.8	1051.2	112.9	126.4	41.3
4	197.9	63.4	167.2	137.2	264.4	136	173.8	83	122.7	743.6	134.3	131.8	37.8
4.5	224.4	65.3	186	128.9	283.6	155.6	173.4	80.6	127.3	565.6	172	122.2	31.2
5	207	52.1	156.6	123.2	280	137.8	192.2	72.9	87.4	433.2	173.6	207	22.4
5.5	211.6	64.8	174.4	104	220.9	137	176.6	67.1	105	450.4	159.4	87	29.9
6	145.8	33.1	137.2	80.6	200.3	112	192.9	55.7	87.9	277	170.4	81.8	22.4
7	80.7	35.3	116.1	53.1	158.8	137.5	142.2	40.5	95.8	241.8	86.2	60.9	18.1
8	121.9	27.5	97.9	50.4	168.1	101.4	156.1	27.7	64.3	166.3	74.8	43.6	26
9	100.7	27.9	89.7	32.5	142.2	99.8	128.2	22.6	44.1	149.1	55.9	34.7	18.3
10	97.8	24	71.3	32.1	95.2	89.3	121.6	26.5	29	132.4	59.1	34.9	26.3
11	66	13.5	68.2	27.3	87.4	113.1	105.1	36.6	50.7	147	48	24.6	14.8
12	67.7	16.4	53.1	18.7	94.1	119.8	84.2	18.8	79	149.1	77	26.7	12.5

Table A4: MT plasma concentrations (pg/ml) following administration of MT SR formulation (10% IR MT + 90% SR MT) 0.8 mg in 13 healthy old and young volunteers.

Time	LA	SK	GL	HF	AT	AK	AO	CB	RC	SN	KT	VB	SL
0	2.5	9.3	3.4	2.5	6	2.5	2.5	3.5	2.5	46.1	8	2.5	2.5
0.5	663.3	251.3	62.7	254.2	397.6	734	291.8	127.1	197.9	821	697.2	195.6	40.9
1	485.2	342.1	286	355.7	674.5	776.8	550	287.9	275	1317	536.8	302	185.7
1.5	416	365.1	387	.	772.9	801.2	588	276.8	256.6	1312	629.2	257.2	175.4
2	414	301.4	261.1	.	586.7	850.4	362.8	253.1	349.6	1657	399.2	246	133
2.5	424.8	277.3	321.4	.	578.1	711.2	582.8	262.5	220.6	1579	628.1	250	134.7
3	338.4	191.9	242.6	.	626.6	576.4	538.8	229.7	261.6	1126.8	398.1	197.6	109.5
3.5	392	209.8	279.1	444.9	649	440	414	261.9	190.7	1198	252.5	141.2	133.6
4	341.2	151.5	198.6	454	629.8	371.6	336.6	263.8	362.7	847.4	230.3	192	129.7
4.5	314	157.1	216.5	446.1	623.3	302.8	286.1	274	351.8	1040	293.3	101.2	107.2
5	264.8	124.8	221.4	358.7	590.4	234	291.6	250.7	415.3	759.4	241.2	119.2	99.4
5.5	222	116.6	210.8	386.1	657.6	271.6	221.6	198.7	349.2	722.7	218.3	88.1	80.3
6	187.6	96.8	191.6	171.5	471.6	176	203.6	182.8	316.5	666	223.4	.	59.5
7	184.4	75.4	155.5	186.7	302.3	115.2	144.8	148.2	190	451.9	226.2	74.3	42.2
8	174	80.1	108.1	119.9	235.8	216.4	124	108.5	134.3	375.3	155.6	47.9	43.4
9	155	73.1	82.5	110.9	184	298.4	134	77.5	82.8	311.2	209.8	62.3	59.8
10	105.2	80.6	72.8	101.5	185.3	230.4	172.8	54.5	52.2	310.1	256.5	33.2	37.4
11	96.4	56.4	59.4	104.2	162.9	196.4	133.2	53.9	69.1	253.4	213.1	30.2	32.3
12	97.1	53	53.7	91.1	149.5	148.8	150	54.2	90	299.9	278.7	35.9	34.3

Table A5: Dissolution profile of sustained release formulation (10% IR MT + 90% SR MT).

Time (h)	% dissolution
0	0
0.25	18.37
0.5	21.7
1	26.92
1.5	31.78
2	36.28
3	45.55
4	53.65
6	66.88
9	81.01
12	88.21
24	101.53
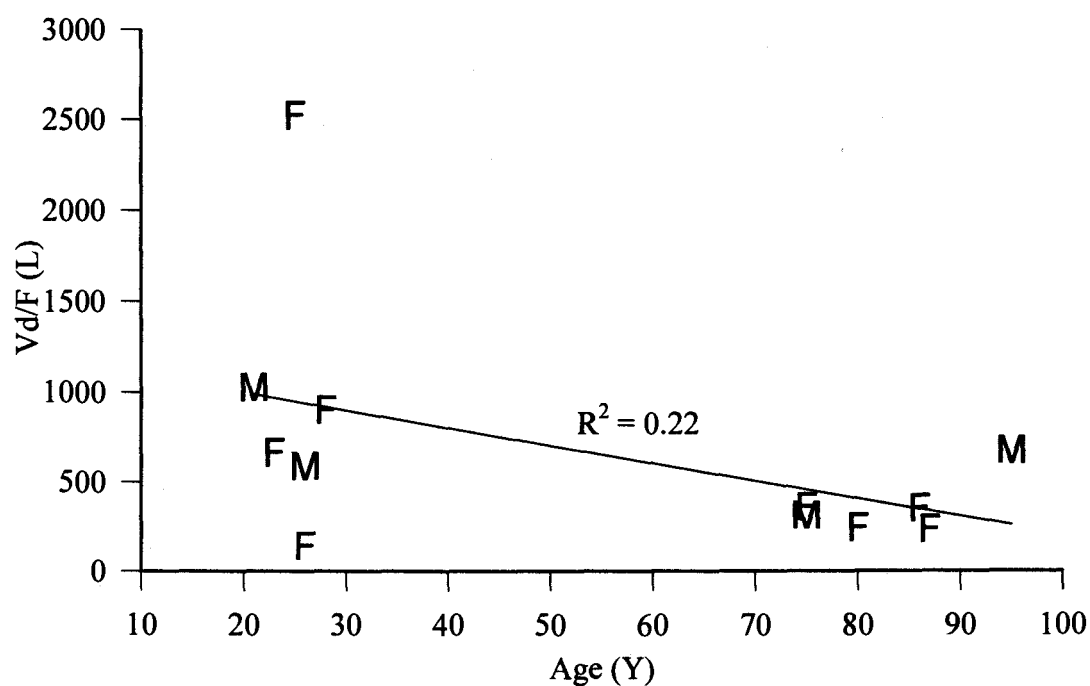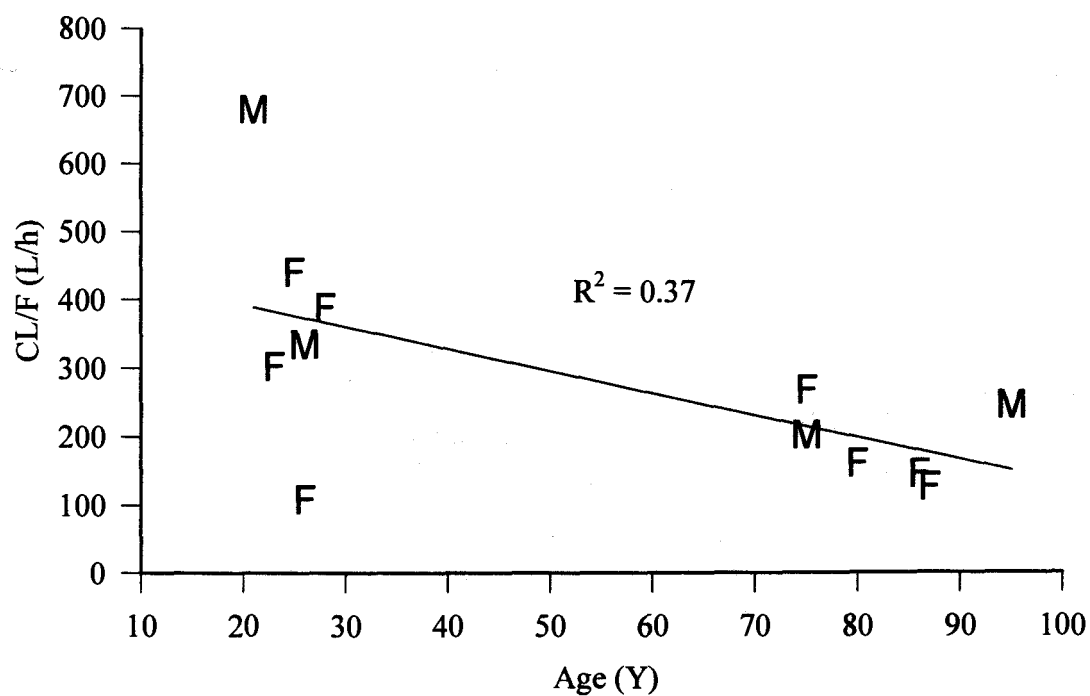
Figure A.1: Plots of CL/F and Vd/F versus age following administration of 50 mg IR MT in young and old healthy subjects. F = female M = male.
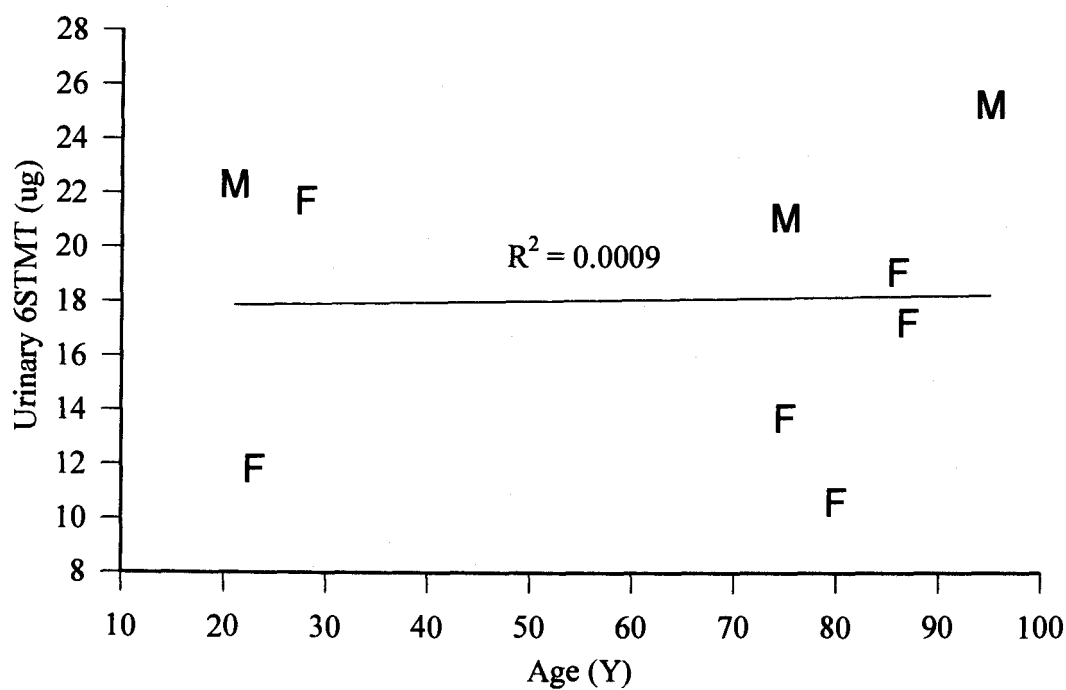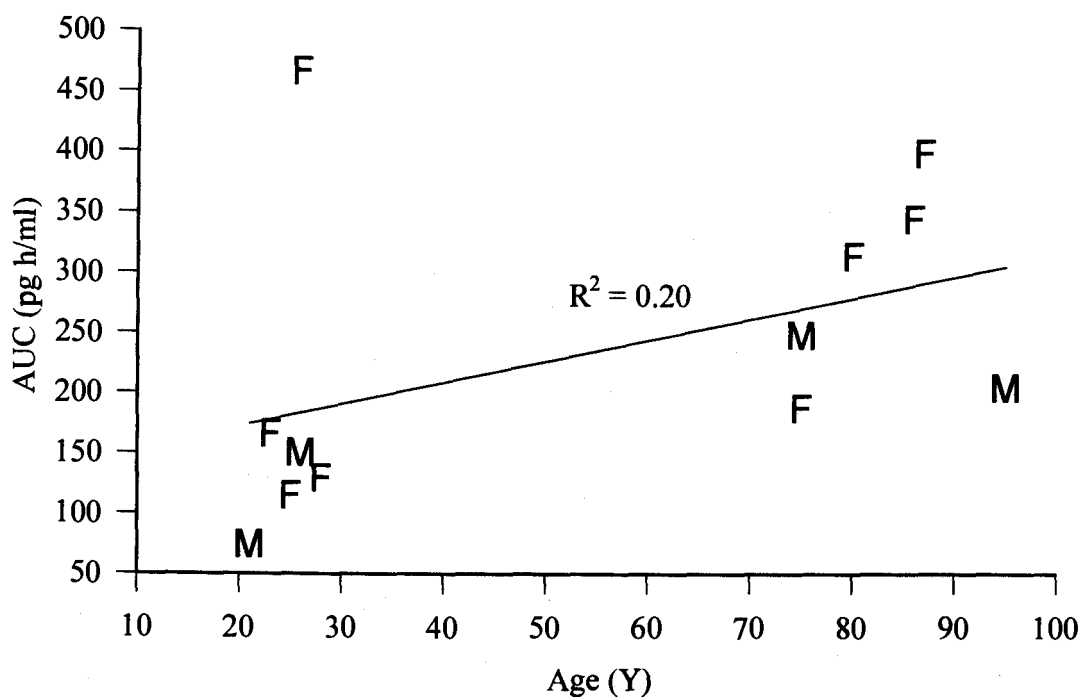
Figure A.2: Plots of AUC and urinary 6STMT versus age following administration of 50 mg IR MT in young and old healthy subjects. F = female M = male.

APPENDIX B

A plot of the normal nighttime MT plasma profile,

Individual MT plasma concentrations, urinary 6STMT data,

and dissolution profiles of SR MT formulations given to 12 healthy young volunteers

(Chapter 2)
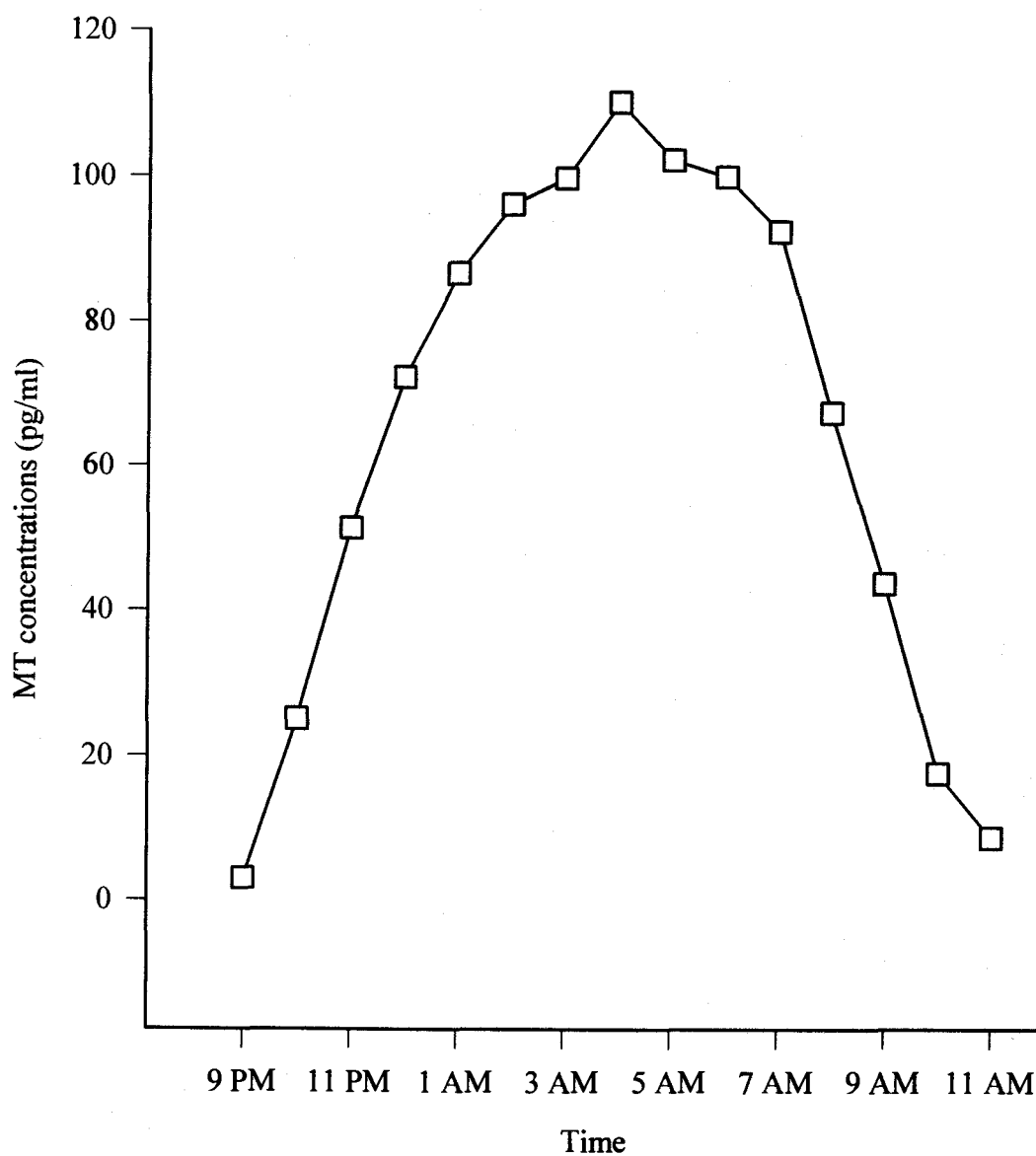
Figure B.1: The normal nighttime MT plasma concentration-time profile (unpublished data courtesy of Dr. Robert L. Sack, Department of Psychiatry School of Medicine, Oregon Health Sciences University)

Table B1: MT plasma concentrations (pg/ml) following administration of 750 µg formulation A (a solution of MT) in 11 young healthy volunteers.

Time (JD)	JD	Time (AC)	AC	Time (RJ)	RJ	Time (NP)	NP	Time (YC)	YC	Time (NY)	NY
0	15.2	0	3.8	0	1	0	22.5	0	11	0	3.6
0.25	922.5	0.33	2157	0.52	1595	0.25	925.5	0.42	6980	0.33	1138
0.533	906.2	0.67	2280	0.733	807.1	0.5	1410	0.65	2096	0.5	1173
1.52	282.8	1.12	1124	1	677.2	1	1532	1.53	2897	1.02	550.5
2.07	278.6	1.52	756	1.55	267	1.5	1118.5	2.05	121	1.48	392.8
2.62	105.6	3.08	128	2.07	143.5	3	191.4	4.05	26.8	3.02	87.2
3	83	5.03	20.4	3	40.8	8	8.1	7.03	5.3	5	8.7
4.15	22.7	8.03	3.1	5.08	7.1					8.15	3.7
6	6	10.02	1	8.02	2.6						
7.92	2.3										
10	2.3										

Time (GW)	GW	Time (SC)	SC	Time (CW)	CW	Time (JS)	JS	Time (SP)	SP
0	15.7	0	6.1	0	16.2	0	1	0	20.4
0.32	872.1	0.23	871	0.283	924	0.233	50.8	0.283	673
0.55	801.1	0.52	1743	0.5	1706	0.483	50.4	0.55	680
1.02	569.3	1.02	1337	1.05	1191	1	31.1	1.02	765.8
1.5	300.9	1.53	608.5	1.53	828	1.483	21.3	1.57	410.5
3.03	31.5	1.98	83.5	3.05	155.9	2	13.6	3.05	55.6
8.03	1	5.03	11.9	5	21.1	2.483	7.2	5.03	11.6
		8.05	1	8.067	3.8	3	5.5	7.98	2.9
						4.02	1.9		
						6.03	1		
						8.05	1		
						10	1		

Table B2.1: Mid time and base-line urinary 6STMT excretion rate (μg/h); control study in 12 young volunteers.

Time (JD)	JD	Time (AC)	AC	Time (MS)	MS	Time (RJ)	RJ	Time (NP)	NP	Time (YC)	YC
8.5	0.8	7.2	1.4	10.5	1.2	7.9	1.1	7.8	1.3	7.6	1.4
10.5	0.3	20.3	0.4	13.4	0.4	9.8	0.7	9.6	0.8	8.6	1.1
12.9	0.2	21.9	0.2	16.0	0.5	12.0	0.2	11.3	0.4	10.7	0.6
15.7	0.2	11.2	0.5	17.9	0.2	13.9	0.2	12.6	1.0	13.4	0.5
17.9	0.1	12.3	0.1	20.1	0.2	15.5	0.3	14.4	0.9	15.4	0.4
20.3	0.1	14.4	0.1	21.9	0.2	16.6	0.4	17.0	0.3	16.9	0.7
26.4	1.4	16.3	0.1	22.8	0.3	18.4	0.3	20.1	0.3	18.8	1.2
		17.4	0.1	27.1	1.4	21.2	0.1	22.2	1.1	25.8	0.9
		19.1	0.1			24.0	0.9	26.7	1.9	32.2	0.2
		20.8	0.9			28.6	1.9				
		21.9	1.3								
		24.0	1.4								
		26.7	2.2								
		28.8	1.9								
		30.2	1.2								

Table B2.2: Mid time and base-line urinary 6STMT excretion rate (μg/h); control study in 12 young volunteers.

Time (NY)	NY	Time (GW)	GW	Time (SC)	SC	Time (CW)	CW	Time (JS)	JS	Time (SP)	SP
		8.2	0.9	1.6	1.0			7.5	0.6	8.2	1.3
7.8	1.3	10.1	0.7	11.5	0.4	8.2	2.8	8.7	0.2	10.2	1.1
9.9	0.5	11.9	0.2	14.0	0.3	9.4	1.0	9.8	0.2	11.9	0.6
12.2	0.2	13.8	0.2	16.2	1.1	11.4	0.8	11.6	0.1	13.8	0.4
14.3	0.2	15.9	0.1	18.2	1.0	13.2	0.1	13.9	0.1	15.9	0.2
16.3	0.1	18.1	0.1	20.0	0.7	15.4	0.2	15.7	0.1	18.1	0.2
19.0	0.2	21.0	0.2	22.0	0.4	17.5	0.2	17.6	0.1	20.6	0.2
21.4	3.8	23.5	0.3	24.4	1.1	19.4	0.2	19.7	0.1	23.4	0.1
23.2	0.1	26.9	0.6			21.3	1.1	25.8	0.2	25.5	0.2
24.3	0.3	32.0	0.8			23.0	2.2			28.8	1.0
28.3	1.1					24.3	0.1			31.8	1.1
						24.9	11.8				
						27.5	1.2				

Table B3.1: Mid time and urinary 6STMT excretion rate (µg/h) following oral administration of 750 µg formulation A (a solution of MT) in 12 young volunteers.

Time (JD)	JD	Time (AC)	AC	Time (MS)	MS	Time (RJ)	RJ	Time (NP)	NP	Time (YC)	YC
-0.8	1.5	-1.2	0.3	-1.1	1.6	-0.5	1.0	-1.2	1.3	-1.2	0.7
0.2	45.2	0.2	38.1	0.2	6.5	0.3	239.1	0.1	3.3	0.1	28.2
0.7	80.1	0.6	87.3	0.6	1.5	1.1	86.0	0.5	157.4	0.6	271.0
1.5	64.1	1.1	76.4	1.6	110.3	2.0	30.5	1.2	58.7	1.5	65.2
2.5	25.1	1.7	59.8	2.6	37.8	3.0	25.9	2.1	23.1	2.6	18.9
3.9	10.4	2.4	44.1	3.3	20.9	4.0	10.5	2.8	29.5	3.6	8.0
5.0	6.2	3.2	17.4	4.3	12.3	5.0	7.1	3.7	15.2	4.6	4.2
6.1	3.9	4.1	9.9	5.5	3.3	6.0	6.3	4.8	9.1	5.7	2.8
7.5	2.4	4.8	6.4	6.4	9.8	7.5	0.8	5.6	6.9	7.0	2.1
9.5	1.5	5.5	5.7	8.0	2.1	9.5	1.4	6.9	3.7	9.0	1.9
11.2	1.3	6.5	3.5	9.9	1.1	12.0	0.7	8.3	3.4	11.2	11.9
14.7	1.4	8.6	1.9	11.6	0.4	19.1	1.3	10.6	1.6	15.2	1.7
12.7	2.5	9.7	1.2	18.2	1.8			13.2	1.5	20.4	1.6
18.8	1.4	10.3	0.9					18.3	2.2		
		10.9	0.6								
		12.1	0.9								
		13.7	4.2								
		17.0	1.4								
		21.9	0.8								
		25.4	0.7								

Table B3.2: Mid time and urinary 6STMT excretion rate (µg/h) following oral administration of 750 µg formulation A (a solution of MT) in 12 young volunteers.

Time (NY)	NY	Time (GW)	GW	Time (SC)	SC	Time (CW)	CW	Time (JS)	JS	Time (SP)	SP
-1.7	0.5	-1.3	0.9	-0.5	1.4	-0.2	1.2	-0.3	0.1	-0.6	1.3
0.1	1.3	0.2	156.8	0.3	77.2	0.1	255.5	0.2	41.7	0.2	28.3
0.5	145.9	1.3	190.1	0.9	138.3	0.8	183.3	0.7	174.6	0.9	52.9
1.2	174.6	2.4	19.8	1.3	149.7	1.3	115.1	1.8	122.8	1.7	82.8
1.8	171.5	2.9	14.0	1.6	86.2	1.8	46.5	2.8	37.9	2.2	38.4
1.6	21.2	3.9	12.4	1.9	41.4	2.0	21.9	4.0	18.1	3.0	14.9
2.3	8.3	4.6	7.0	2.4	28.4	2.9	1.6	4.9	14.7	4.0	7.8
5.5	3.0	5.5	3.6	3.0	11.7	3.4	45.0	6.0	7.7	5.0	7.4
6.7	2.5	6.9	2.4	4.0	10.1	4.1	11.6	7.3	1.1	6.1	5.4
8.2	2.0	8.5	2.0	5.1	5.5	5.2	6.7	8.0	2.5	7.4	3.3
10.8	1.5	9.7	1.0	6.1	2.6	6.2	8.8	8.4	3.7	9.2	2.4
15.3	0.9	12.1	0.9	7.6	2.8	7.4	3.3	8.9	2.2	11.8	1.3
20.9	1.3	15.3	0.7	9.7	1.3	9.3	2.6	9.9	1.6	15.2	0.6
		21.7	0.4	12.2	0.7	11.3	1.7	11.4	1.2	20.3	0.9
				14.9	1.0	12.3	1.3	13.8	0.8		
				20.2	1.4	17.6	1.1	16.5	1.7		

Table B4.1: Mid time and urinary 6STMT excretion rate (µg/h) following oral administration of 750 µg formulation B (10% Aquacoat® beads) in 12 young volunteers.

Time (JD)	JD	Time (AC)	AC	Time (MS)	MS	Time (RJ)	RJ	Time (NP)	NP	Time (YC)	YC
-0.9	4.9	-1.1	1.0	-1.1	2.3	-1.0	1.3	-1.0	1.4	-1.2	0.5
-0.6	2.9	0.4	8.7	0.1	9.6	0.4	10.0	0.2	6.3	0.3	25.7
1.3	16.2	1.1	42.5	1.1	50.4	1.4	36.6	0.8	47.2	1.3	75.8
2.5	49.9	1.8	32.8	2.3	89.0	2.5	48.4	1.6	51.4	2.4	60.6
3.4	81.6	2.9	35.9	3.3	51.8	3.5	30.2	3.0	39.0	3.3	39.7
4.2	37.5	4.2	17.5	4.4	42.2	4.7	14.9	4.4	33.0	4.1	24.3
5.2	17.8	5.3	12.5	5.9	27.7	5.7	0.0	5.4	0.0	5.1	11.1
6.1	15.7	6.3	10.9	7.4	11.8	6.6	9.8	6.2	12.7	6.3	9.5
7.1	10.4	7.2	8.1	8.4	14.7	7.5	10.3	7.0	12.6	7.3	5.5
8.2	10.7	8.1	7.6	9.4	7.4	8.6	8.4	7.9	11.2	9.0	4.6
9.1	11.2	9.3	6.4	10.6	6.5	9.7	7.3	8.8	8.5	10.6	6.6
10.1	10.4	10.9	6.9	12.2	5.6	11.4	5.9	10.0	7.3	11.7	5.7
12.7	6.1	13.0	6.1	18.4	4.2	14.8	3.7	11.6	5.1	14.0	5.2
17.0	2.5	17.3	2.5			19.8	3.9	12.7	6.8	16.1	5.0
		21.1	8.7					18.0	2.3	19.6	3.2

Table B4.2: Mid time and urinary 6STMT excretion rate (μg/h) following oral administration of 750 μg formulation B (10% Aquacoat® beads) in 12 young volunteers.

Time (NY)	NY	Time (GW)	GW	Time (SC)	SC	Time (CW)	CW	Time (JS)	JS	Time (SP)	SP
-1.1	1.1	-1.0	0.8	-1.0	1.4	-1.4	2.7	-1.0	0.2	-1.0	1.6
0.4	16.3	0.5	16.9	0.5	18.4	-0.1	9.1	0.2	1.1	0.5	6.7
1.3	69.1	1.5	68.1	1.5	60.5	0.9	51.7	0.6	21.6	1.5	62.9
2.4	53.4	3.0	35.8	2.5	49.7	1.5	60.8	0.9	68.2	2.5	65.9
3.4	45.3	4.7	32.2	3.9	32.7	2.3	79.6	1.4	51.1	3.4	48.8
4.5	22.3	5.7	30.0	5.5	18.3	3.2	46.1	2.0	90.4	4.4	37.2
5.7	14.5	6.4	7.9	6.6	13.9	4.0	28.0	2.5	44.6	5.4	23.4
6.5	19.7	7.5	11.9	7.4	9.6	5.0	17.6	4.2	28.2	6.5	14.6
7.0	27.4	9.0	7.0	8.4	10.6	6.0	16.5	4.8	23.2	7.5	10.9
7.7	12.4	10.5	5.7	9.4	10.6	6.8	14.0	5.6	23.3	8.4	12.0
8.5	7.6	11.6	6.1	11.4	8.6	11.1	8.1	6.6	17.6	9.5	10.9
9.8	4.1	12.2	5.9	14.0	7.6	13.8	6.6	7.7	13.8	12.0	5.5
11.1	3.6	12.8	5.7	18.9	4.5	18.7	4.9	8.8	10.9	14.5	3.3
12.1	2.4	13.9	3.1					9.9	7.6	17.6	2.7
13.1	3.2	15.3	2.8					11.9	6.1	21.8	3.7
14.2	2.2	16.3	2.6					17.3	3.4		
18.5	2.0	20.6	2.0								

Table B5.1: Mid time and urinary 6STMT excretion rate (μg/h) following oral administration of 750 μg formulation C (9%

Table B5.1: Mid time and urinary 6STMT excretion rate (µg/h) following oral administration of 750 µg formulation C (9% Eudragit® L30D coated on 20% Aquacoat® beads) in 11 young volunteers.

Time (JD)	JD	Time (AC)	AC	Time (MS)	MS	Time (RJ)	RJ	Time (NP)	NP	Time (YC)	YC
-0.9	2.2	-1.3	0.4	-1.6	14.1	-1.0	1.5	-1.5	1.9	-0.7	1.4
0.5	1.0	0.0	1.2	0.3	14.8	0.4	7.6	-0.1	1.6	0.1	1.6
1.8	1.6	0.7	2.2	2.2	20.1	1.5	27.2	1.1	31.2	0.7	55.9
3.0	15.5	1.5	52.2	3.2	39.8	2.5	30.9	1.7	49.2	1.3	83.6
4.4	15.5	2.3	18.8	4.3	31.7	3.5	17.7	2.6	34.9	2.2	55.4
5.8	8.1	3.3	16.7	5.2	30.9	4.7	16.8	4.0	27.7	3.3	28.3
6.9	8.5	4.4	15.9	6.2	34.5	5.8	9.7	5.4	42.9	4.3	33.1
7.8	8.4	5.2	12.9	7.3	24.9	6.6	17.7	6.5	27.4	5.7	32.6
8.8	7.2	5.9	15.0	8.3	28.8	7.6	21.0	7.5	12.2	7.1	30.3
10.2	10.2	6.8	15.3	9.3	22.0	8.6	17.9	8.5	29.5	8.1	23.5
12.4	11.0	7.4	17.0	11.2	18.8	9.5	17.4	9.5	8.5	9.3	24.6
		8.1	14.0	13.3	13.7	10.4	27.7	10.3	20.5	11.4	19.8
		8.8	14.4	18.6	11.9	12.0	16.9	10.8	11.9	17.2	14.6
		10.2	15.0			13.4	19.2	11.6	8.5		
		12.1	9.8			15.3	15.7	12.6	8.1		
		14.5	9.1			20.0	9.9	13.6	13.1		
		18.7	6.3					14.9	3.7		
								19.1	4.3		

Table B5.2: Mid time and urinary 6STMT excretion rate (μg/h) following oral administration of 750 μg formulation C (9% Eudragit® L30D coated on 20% Aquacoat® beads) in 11 young volunteers.

Time (NY)	NY	Time (SC)	SC	Time (CW)	CW	Time (JS)	JS	Time (SP)	SP
-1.1	2.8	-1.5	6.4	-0.7	0.7	-1.1	0.4	-1.0	1.5
0.4	1.2	-0.5	2.9	0.8	0.9	0.3	0.3	0.5	7.6
1.4	6.2	0.5	2.1	1.5	1.3	1.1	6.7	1.6	0.0
2.3	8.9	1.5	49.8	2.2	43.7	1.5	36.3	2.6	17.3
3.3	39.2	2.5	26.6	2.7	60.1	2.1	51.6	3.4	25.8
4.3	32.1	3.5	27.9	3.4	40.2	2.6	40.0	4.4	20.1
5.4	18.0	4.5	18.1	4.2	28.9	3.4	26.5	5.4	17.9
7.0	14.7	5.6	13.8	5.1	22.8	4.2	25.6	6.5	15.5
8.5	16.2	6.5	12.2	6.2	20.8	5.1	23.0	7.6	13.3
9.5	38.8	7.3	10.0	7.1	15.6	6.2	22.0	8.4	14.3
10.4	36.7	8.4	12.4	7.7	12.0	7.1	20.3	9.4	13.2
11.4	37.1	10.2	6.2	8.9	14.7	7.8	23.3	10.8	9.9
12.8	17.0	11.7	29.6	10.3	16.1	8.5	25.4	12.3	10.4
14.0	19.7	13.0	7.5	10.9	12.3	9.5	16.0	13.5	12.7
18.7	11.8	15.3	4.5	12.3	10.7	10.2	17.0	14.3	9.7
		18.8	3.1	14.0	14.4	11.0	10.2	14.8	10.8
				15.7	13.0	12.0	6.8	16.3	11.5
				20.3	1.7	12.7	7.9	20.3	6.0
						13.7	5.7		
						18.1	5.8		

Table B6: Dissolution profile of formulation B (10% Aquacoat® coated beads)

Time (h)	B
0	0
0.5	15.40
1	29.30
2	49.80
3	65.66
4	77.86
6	90.30
9	99.37
12	100.68
24	100.87

Table B7: Dissolution profiles of 3%, 6%, 9% (formulation C) , 12%, and 15% Eudragit® L30D coated on 20% Aquacoat® coated beads.

Time (h)	3% Eudragit® L30D	6% Eudragit® L30D	9% Eudragit® L30D	12% Eudragit® L30D	15% Eudragit® L30D
0	0	0	0	0	0
0.25	6.87	6.77	0	0	0
0.5	9.63	9.33	0	0	0
1	14.47	13.17	0	0	0
1.5	18.32	16.47	0	0	0
2	21.66	21.75	0	0	0
3	26.33	28.33	23.46	23.65	21.16
6	42.12	42.48	37.66	39.57	38.27
12	64.85	62.85	63.24	62.24	62.59
24	83.77	82.10	87.87	85.01	84.15

APPENDIX C

Convolution technique, MT plasma concentrations in 4 healthy subjects receiving SR

MT formulation C (20% Aquacoat® coated beads),

and dissolution profile of formulation C (chapter 3)

Area-area point convolution technique

Convolution and deconvolution operations can be solved algebraically by different procedures, the one most commonly employed being Laplace transforms (1, 2, 3, 4). It is usually more interesting to perform convolution and deconvolution operations numerically in experimental pharmacokinetics (1). The instructive explanation of numerical convolution/deconvolution concept can be found in the article by Langenbucher (5). In this work, an "area-area-points" convolution is applied to generate the interest response time curve i.e. plasma concentration-time profile. In "area-area-points" approach, only the response function is taken as points of the true curve, whereas input and weighting functions are interpreted as "staircase" curves. The single stairs are defined by their rectangle area or by the midpoint of the curve (5, 6). Summary of mathematical functions describing convolution and deconvolution are presented in Table 1. To illustrate application of convolution, examples of numerical convolution are presented below.

Let   R(t) = response function

I(t) = input function

W(t) = weighting function

In a formal notation, convolution is symbolized as

R(t) = I(t) * W(t)

The inverse operation of deconvolution calculates either input or weighting function by

I(t) = R(t) // W(t) or W(t) = R(t) // I(t)

Table C1: General numerical algorithm for convolution and deconvolution. The time interval is here denoted by T. For the area-area-point technique, only the Ri are curve points whereas the Ii and Wi represent areas or midpoint values (5).

Convolution R(t)=I(t) * W(t)

$R1 = I1\ W1\ T$

$R2 = (I1\ W2 + I2\ W1)\ T$

$R3 = (I1\ W3 + I2\ W2 + I3\ W1)\ T$

$Ri = (I1\ Wi + I2\ Wi\text{-}1 + ... + Ii\ W1)\ T$

For i = 1 to n (time interval) : $Ri = \sum_{j=1}^{j=i} I(j)\ W(i - j + 1)\ T$ Equation 1.

Deconvolution I(t) = R(t) // W(t)

$I1 = (R1\ /\ T)\ /\ W1$

$I2 = (R2\ /\ T - I1\ W2)\ /\ W1$

$I3 = (R3\ /\ T - I1\ W3 - I2\ W2)\ /\ W1$

$Ii = (Ri\ /\ T - I1\ Wi - I2\ Wi\text{-}1 - ... - Ii\text{-}1\ W2)\ /\ W1$

For i = 1 : $I1 = (R1\ /\ T)\ /\ W1$

For i = 2 to n : $Ii = \dfrac{1}{W1}\ (\dfrac{Ri}{T} - \sum_{j=1}^{j=i-1} I(j)\ W(i\text{-}j+1))$ Equation 2.

Deconvolution W(t) = R(t) // I(t)

$W1 = (R1\ /\ T)\ /\ I1$

$W2 = (R2\ /\ T - I2\ W1)\ /\ I1$

$W3 = (R3\ /\ T - I2\ W2 - I3\ W1)\ /\ I1$

$Wi = (Ri\ /\ T - I2\ Wi\text{-}1 - I3\ Wi\text{-}2 - ... - Ii\ W1)\ /\ I1$

For i = 1 : $W1 = (R1\ /\ T)\ /\ I1$

For i = 2 to n : $Ii = (Ri\ T - \sum_{j=2}^{j=i} I(j)\ W(i\text{-}j+1))\ /\ I1$ Equation 3.

For simplicity in computer programming, it is wise to rewrite mathematical functions in forms of Equation 1 (6), 2, and 3, respectively. The algorithm requires all raw data points to be supplied with the same time module (5). For experimental data, there are many times, this condition is not met. In this case, interpolation or extrapolation techniques should be used to generate the missing data. Unlike deconvolution that its accuracy is highly sensitive to the consistency of the supplied data, convolution is more stable in that reasonable results are obtained for any given raw data (5).

Steps involved in convolution using FORTRAN 90 on a personal computer (7)

Simulated response function R(t) is a convolution product of input function I(t) and weighting function W(t) or R(t) = I(t) * W(t). Practically, convolution can be carried out using Equation 1 ($Ri = \sum_{j=1}^{j=i} I(j) \, W(i - j + 1) \, T$; T = time interval).

1. Conversion data of both I(t) × T and W(t) to the same common time module. This process can be done using either interpolation or extrapolation technique. PCDCON (8) also provides cubic splines interpolation of any data set.

2. Save input data file named "CONV.txt" (formatted as ascii files). Data in this file must be arranged in consecutive columns as time, I(t) × T, and W(t), respectively, with no variable names in the first row. The result of convolution is written in the file named "COUT.txt" which can be used by most spreadsheet programs.

A program used for the loop calculation of equation 1 are presented below.

FORTRAN 90 (on a PC) Code used in loop calculation of Equation 1.

```
! Program CONVOL.f90
! Julraht (June) Konsil, Oregon State University
! Originated in October, 1996
! Modified for FORTRAN 90 on Feb. 14, 1997
! This program reads data from a file named 'CONV.txt' and calculate for
! convolution of input function and weighting function.
! Convolution result is written in an output file named 'COUT.txt'.
! One needs to change/or delete the file name when working with different
! file names.  The output file must not exist prior to program compiling
! since the status of the output file is specified as 'NEW'.
!****************************************************************************

       PARAMETER(N=200)

! N is total numbers of time modules of input function and weighting
! function.  Data in the file 'CONV.txt' must have the same total numbers of
! time modules.

       DOUBLE PRECISION TIME(N), INP(N), W(N), CONV(N)

! TIME(N), INP(N), W(N) are variables used in convolution process.
! TIME(N)= time, INP(N)=input response, W(N)=weighting response
! and CONV(N)=result of convolution initially set to be equal to zero for
! convenience in calculation.  'DOUBLE PRECISION' is type of data with
! high accuracy (accurate to 14 or 15 decimal digits).

       INTEGER INDEX, I, J, K, L, M

! INDEX, I, J, K, L, M are integers used as index for loop calculation

       DO 1 M=1,N
       CONV(M)=0
1      CONTINUE

! As mentioned earlier,
! initial values of CONV is set to zero (CONV = result of convolution)

    OPEN(UNIT=3,FILE='CONV.txt',STATUS='OLD')
    DO 5 INDEX=1,N
     READ(3,*) TIME(INDEX),INP(INDEX),W(INDEX)
5   CONTINUE
    CLOSE(UNIT=3)
```

! This is a specific statement in FORTRAN to read data from file named
! 'CONV.txt'. 'CLOSE' statement is essential in FORTRAN to make sure that
! the opened file is closed after open (make sure that the program is bug-free).

```
      DO 15 I=1,N
       DO 10 J=1,I
         CONV(I) = CONV(I) + INP(J)*W(I-J+1)
10    END DO
15    END DO
```

! This loop is to calculate convolution result from input function and
! weighting function. This calculation is exactly the same as Equation 1.

```
      PRINT*,'       TIME          CONVOLUTION_RESULT'
      DO 20 K=1,N,10
       PRINT*,TIME(K),CONV(K)
20    CONTINUE
```

! This print statement presents convolution result on the screen so
! that one can roughly see the result.

```
      OPEN (UNIT=4,FILE='COUT.txt',STATUS='NEW')
      DO 25 L=1,N
       WRITE (4,*) TIME(L), CONV(L)
25    CONTINUE
      CLOSE(UNIT=4)
```

! This statement is to write out the result on the new file named 'COUT.txt'.
! One can transfer the result to another application such as spreadsheet programs.

```
      END
```

Example 1.

For the first example data of I(t) × T, W(t), and R(t) are generated using polyexponential equations (5). The application of the generated data is useful for examining the accuracy of convolution technique with the selected time modules/time interval as well as whether there is error in the written FORTRAN 90 code or not. From the article by Langenbucher (5).

Weighting function: $W(t) = 12.37 \exp(-0.684\ t) + 7.857 \exp(-0.0725\ t)$ Equation 4.

Input function: $I(t) = 0.41 \exp(-0.41\ t)$ Equation 5.

Integration of input function: $\hat{I}(t) = \int_0^t I(t)dt = 1 - \exp(-0.41\ t)$ Equation 6.

Response function:

$R(t) = 8.965 \exp(-0.41\ t) - 18.51 \exp(-0.684\ t) + 9.545 \exp(-0.0725\ t)$ Equation 7.

Generated data is showed in Table C2

Table C2: Generated data from polyexponential equations for convolution

Time (h)	Midpoint time[@]	I(t) Eq. 5	W(t) Eq.4	R(t) Eq.7	I(t)*0.04 [@] or $\hat{I}_{(ti+1)} - \hat{I}_{(ti)}$ [a]	W(t) [@]
0		0.41	20.227		-	-
0.04	0.02	0.403331	19.87039	0.326101	0.016266	20.04755
0.08	0.06	0.39677	19.52286	0.641171	0.016002	19.69551
0.12	0.10	0.390316	19.18416	0.945536	0.015741	19.35242
.	.	.	.	.	.	.
7.92	7.90	0.015942	4.479623	5.641732	0.000643	4.4868
7.96	7.96	0.015683	4.465328	5.622714	0.000632	4.472466
8	7.98	0.015428	4.45111	5.603773	0.000622	4.45821

[@] Data was used in convolution process.
[a] Input function used in convolution is (amount) input between ti and ti+1 ($I(t)*0.04$ or $\hat{I}_{(ti+1)} - \hat{I}_{(ti)}$). Table C2 shows only the results of $\hat{I}_{(ti+1)} - \hat{I}_{(ti)}$.

Thus, the file "CONV.txt" is composed of three columns arranged as:

0.02	0.016266	20.04755
0.06	0.016002	19.69551
0.10	0.015741	19.35242
.	.	.
7.90	0.000643	4.4868
7.94	0.000632	4.472466
7.98	0.000622	4.45821

The first column is the midpoint time modules. The second column is either $I(t) \times T$ or $\hat{I}(t_{i}+1) - \hat{I}(t_i)$. Finally, the last column is $W(t_{midpoint})$.

Details of calculation of $I(t) \times T$ (Equation 1) applied for convolution are described below.

1. From input function ($I(t)$, usually in unit of mass/time)

   $I(t) \times T$ used in convolution is equal to $I(t)$ (mass/time) $\times$ time increment. Input function is such as rate of *in vivo* absorption as a function of time. Thus, multiplication of rate with time increment results in amount absorbed in that time interval.

2. From integration of input function ($\hat{I}(t)$)

   $I(t) \times T$ used in convolution can also obtained from difference between $\hat{I}(t_{i}+1)$ and $\hat{I}(t_i)$. Integration of input function is such as cumulative amount absorbed into the body. Thus, the difference between cumulative amount absorbed between t_i+1 and t_i is actually amount absorbed in that time interval. Convolution result is shown in Figure C1.

Figure C.1 graph: Response function (R(t)) vs Time (h)
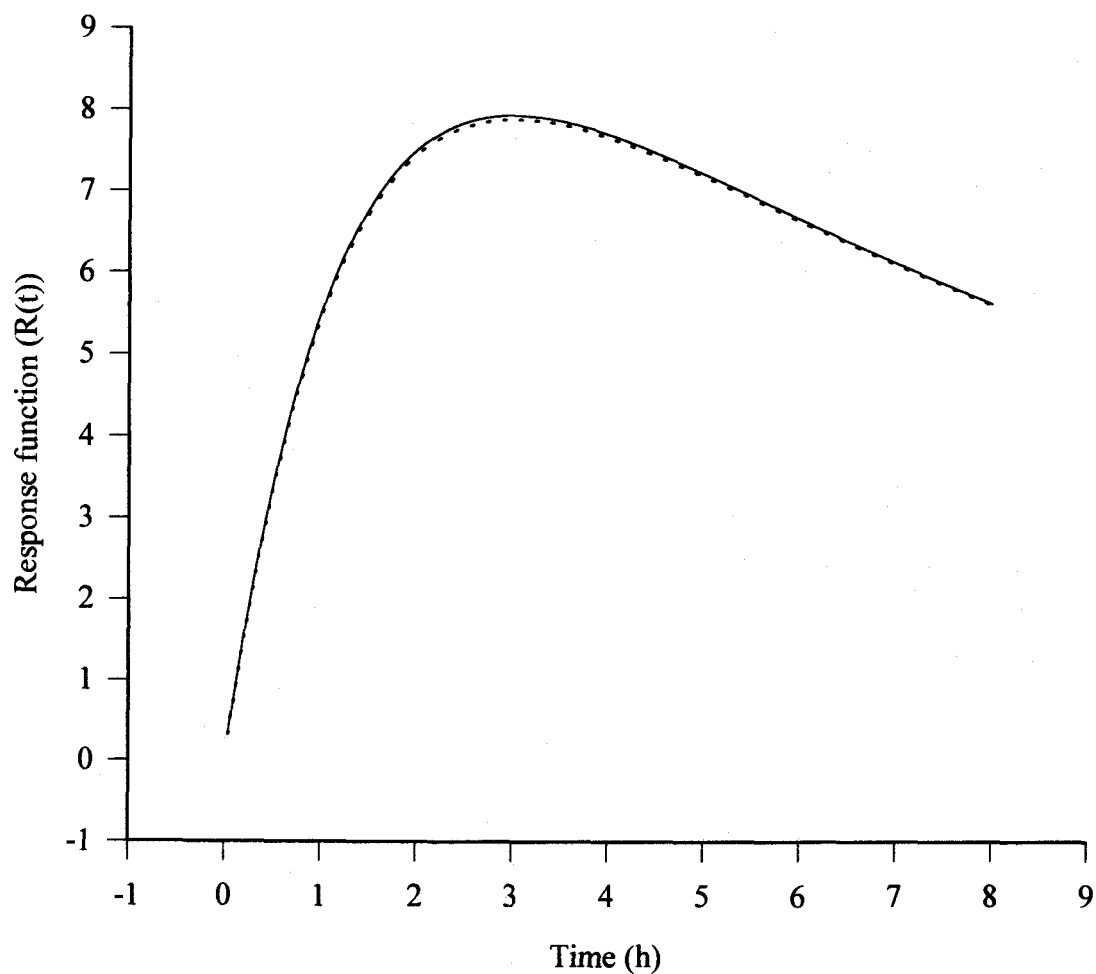
Legend:
——— Data generated from the polyexponential equations
· · · · · Convolution result

Polynomial Equations

Weighting function: $W(t) = 12.37 \exp(-0.684\ t) + 7.857 \exp(-0.0725\ t)$

Input function: $I(t) = 0.41 \exp(-0.41\ t)$

Integration of input function: $\hat{I}(t) = 1 - \exp(-0.41\ t)$

Response function:

$R(t) = 8.965 \exp(-0.041\ t) - 18.51 \exp(-0.684\ t) + 9.545 \exp(-0.0725\ t)$

Figure C.1 Comparison between generated data and convolution result (Example1).

Example 2.

In the second example, experimental data from pilot study of melatonin (MT) oral sustained release (SR) formulation (8) was employed to demonstrate how prediction of plasma concentration-time profile can be obtained using known *in vivo (in vitro)* dissolution (absorption) data and convolution technique. Convolution was performed using estimated *in vivo* absorption data derived from deconvolution of MT plasma concentration-time curves and literature data of MT plasma profiles following intravenous administration of MT given at 10 µg (9). *In vivo* absorption data and iv plasma concentration data was employed as $I(t) \times T$ and $W(t)$, respectively. Response function is MT plasma profile following MT oral SR beads. This is a good practice to perform convolution using data obtained from deconvolution to confirm that all computer programs work as expected.

Deconvolution:

$I(t) = R(t) // W(t)$ where

$I(t) = $ *in vivo* absorption of MT

$R(t) = $ MT plasma concentration-time profile following administration of

SR formulation given at 500 µg (20% immediate release (IR) MT + 80% SR MT) (8)

$W(t) = $ MT plasma profiles following intravenous administration of MT given at 10 µg (9)

Data involved in deconvolution process using PCDCON are presented in Table C3.

Table C3: Data used in deconvolution (PCDCON).

Input response (8)		Impulse response (9)		Deconvolution Results			
				Cumulative amount absorbed (ng)		Absorption rate (ng/h)	
Time (h)	Conc. (ng/ml)	Time (h)	Conc. (ng/ml)	Time (h)	Amount (ng)	Time (h)	Rate (ng/h)
0.5	0.5236	0.0333	0.611	0.04	6879.977	0.04	66319.39
1	0.5286	0.0833	0.321	0.08	8500.496	0.08	64075.36
1.5	0.5526	0.167	0.236	0.12	10121.02	0.12	61831.32
2	0.6176	0.5	0.128	.	.	.	.
3	0.3116	1	0.078	.	.	.	.
4	0.2246	2	0.036	7.92	100392.8	7.92	3686.401
6	0.1006	3	0.013	7.96	100541.8	7.96	3682.693
8	0.0876	8	0	8	100690.8	8	3678.986

Convolution:

Similarly,

$$R(t) = I(t) * W(t) \quad \text{where}$$

R(t) = Predicted MT plasma concentration-time profile following administration of SR formulation given at 500 µg (20% IR MT + 80% SR MT)

I(t) = *in vivo* absorption of MT obtained from deconvolution

W(t) = MT plasma profiles following intravenous administration of MT given at 10 µg or 10000 ng (9).

I(t) × T used in convolution process can be calculated from either I(t) * 0.04 h or difference between $\hat{I}$ (ti+1) and $\hat{I}$ (ti) like in Example 1. Data employed in convolution process are presented in Table C4.

Table C4: . Data employed in convolution process.

Time (midpoint) (h)	I(t) * 0.04 (ng)	$\hat{I}$ (ti+1)- $\hat{I}$ (ti) (ng)	W($t_{midpint}$)/dose (ml^{-1})
0.02	2742.537	6879.977	6.87E-05
0.06	2652.776	1620.519	4.49E-05
0.1	2563.014	1620.524	2.99E-05
.	.	.	.
7.9	147.456	149	4.44E-10
7.94	147.3077	149	1.7E-10
7.98	147.1594	149	3.41E-11

It is important to match units involved in calculation of convolution (see Equation 1). As a result, W(t) needs to be dose normalized. However, some times literature iv plasma concentration-time data is not available to be used as weighting function. It is possible to apply plasma concentrations measured in terminal phase (after absorption process is completed) receiving from other routes of administration as an estimation of weighting function. If data following oral administration is used, the actual dose involved in deconvolution/convolution process will be F × DOSE. One may apply only DOSE, or estimated F × DOSE in the calculation. For one-way calculation (only

either deconvolution or convolution), result may not be accurate unless the true F is known. On the other hand, for two-way calculation (i.e. deconvolution firstly done, followed by convolution, or vice versa), it may be reasonable to ignore F since it should be canceled after the two processes are employed. Therefore, it is wise to perform convolution on deconvoluted data of the original data set before applying the deconvoluted data and the weighting function the future prediction using convolution. Thus, the file "CONV.txt" is composed of three columns arranged as either:

0.02	2742.537	6.87E-05
0.06	2652.776	4.49E-05
0.1	2563.014	2.99E-05
.	.	.
7.9	147.456	4.44E-10
7.94	147.3077	1.7E-10
7.98	147.1594	3.41E-11

or

0.02	6879.977	6.87E-05
0.06	1620.519	4.49E-05
0.1	1620.524	2.99E-05
.	.	.
7.9	149	4.44E-10
7.94	149	1.7E-10
7.98	149	3.41E-11

Accuracy of convolution using deconvoluted data is dependent upon accuracy of the applied functions. Since deconvolution gives a different result depending on stepsize chosen during deconvolution process (i.e. using PCDCON), convolution could result

in different calculation. Additionally, either I(t) × T or $\hat{I}$ (ti+1) - $\hat{I}$ (ti) resulting from

PCDCON is usually not equal even with the same employed stepsize. Small stepsize

does not always give less error in convolution result. Figure C2, C3 and C4 are results

of convolution using data from deconvolution of the same data set but with different

stepsize or different calculation of input function (I(t) × T or $\hat{I}$ (ti+1) - $\hat{I}$ (ti)). A larger

stepsize (in deconvolution process) seems to give less error in prediction by

convolution. Stepsize and method of input function calculation should be carefully

selected to minimize error in prediction by convolution technique using data from

deconvolution.
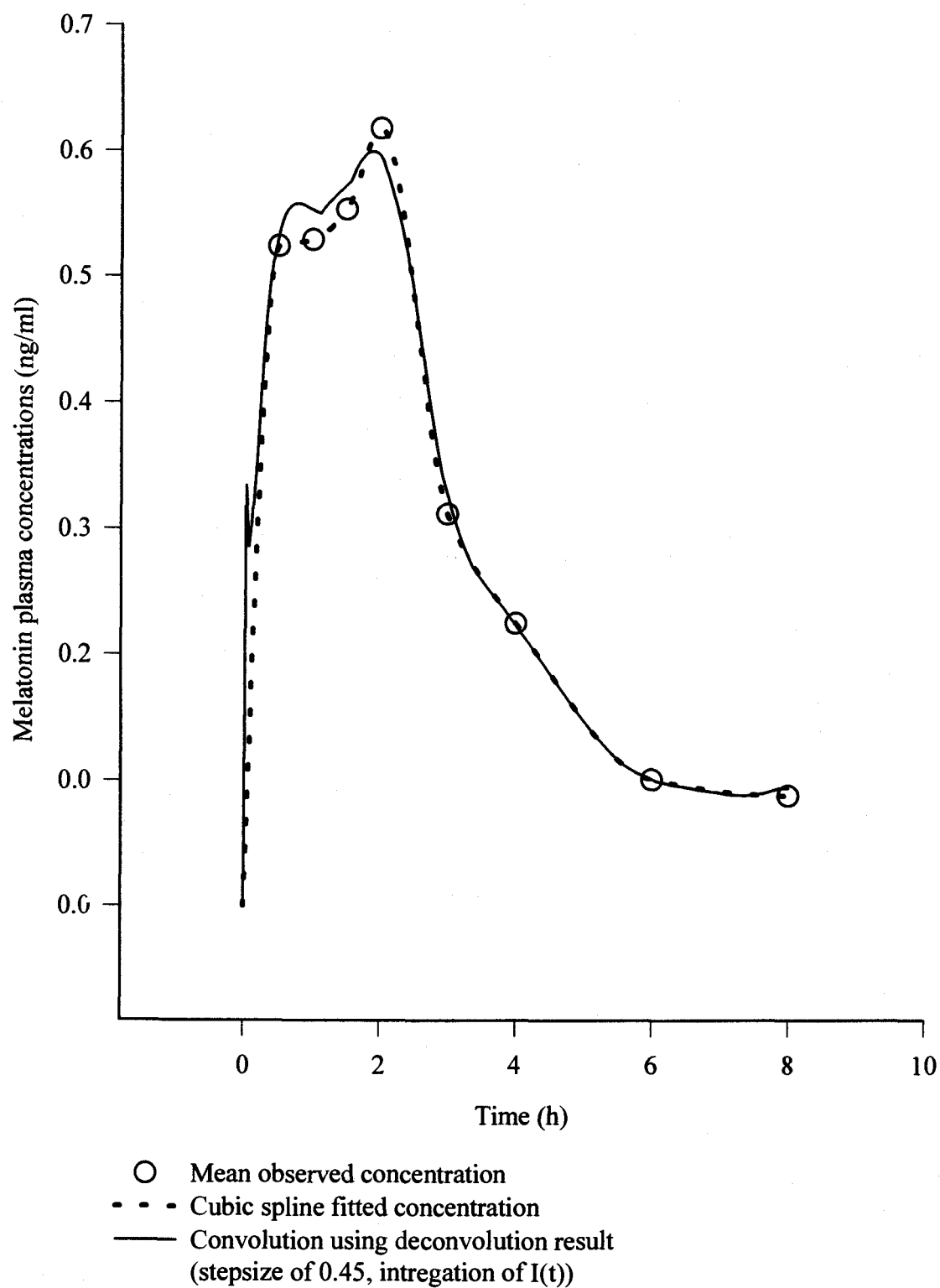
Figure C2: Convolution of MT plasma profile following oral administration of 500 µg SR formulation (n=4)
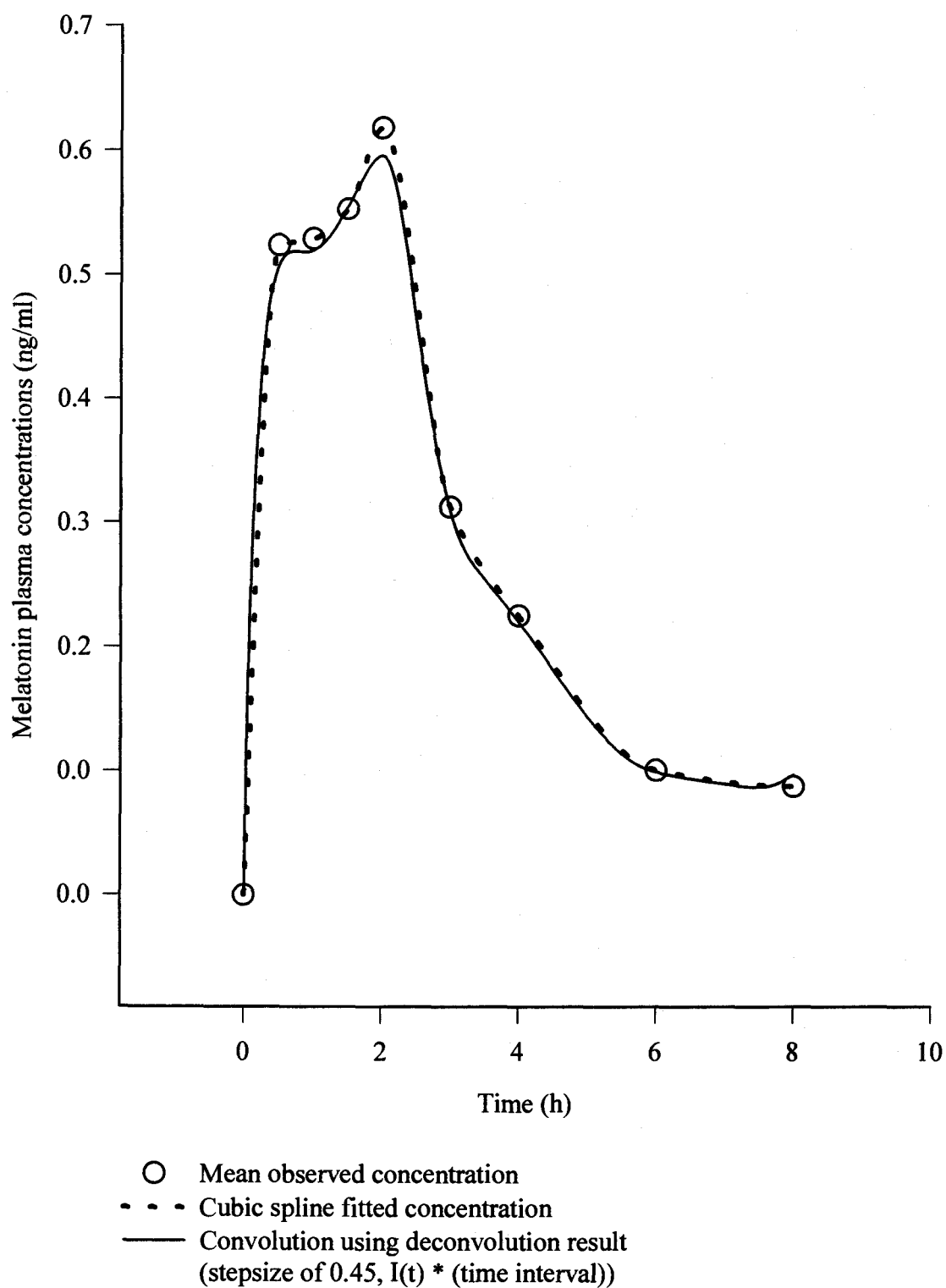
Figure C3: Convolution of MT plasma profile following oral administration of 500 µg SR formulation (n=4)
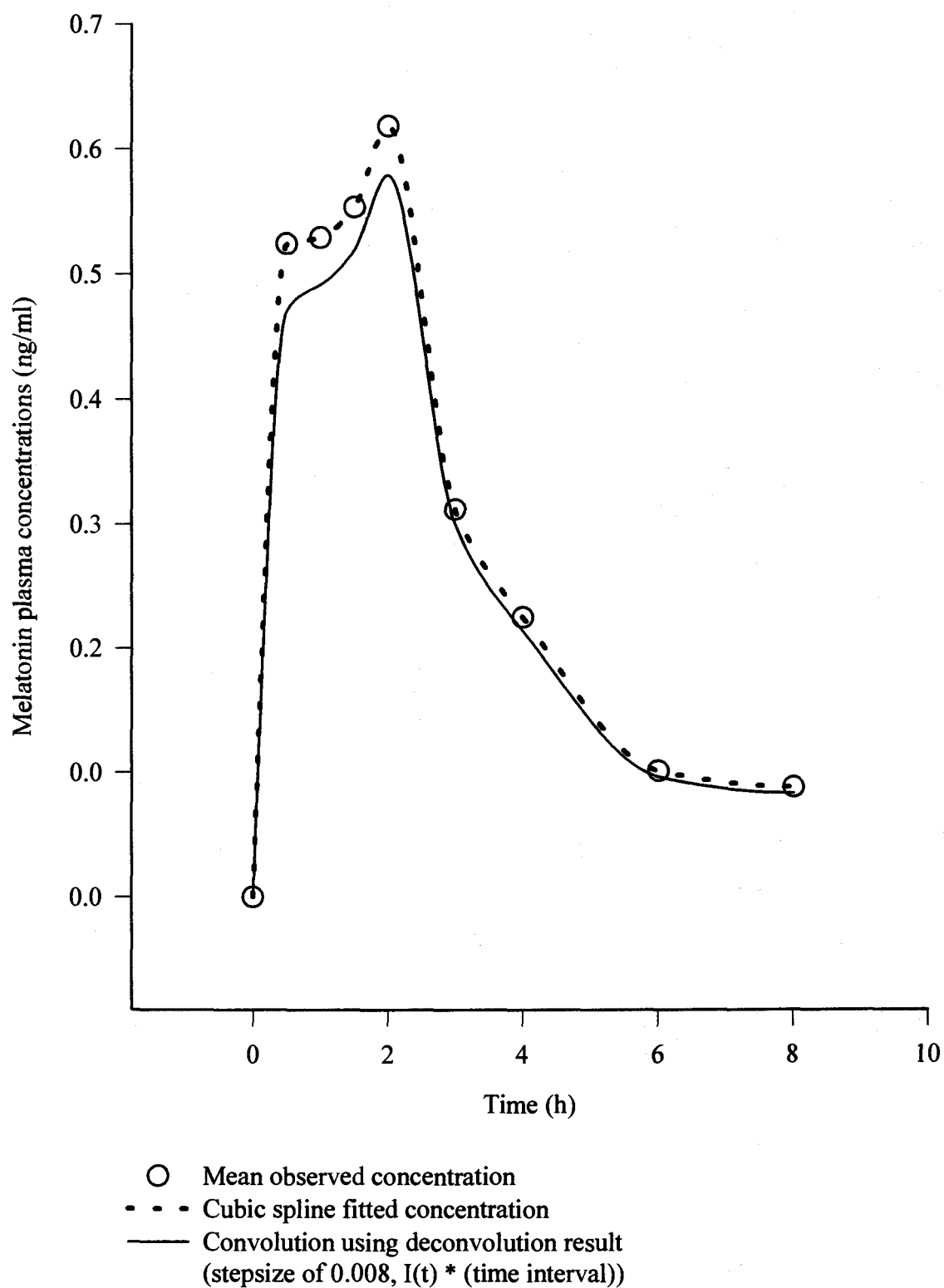
Figure C4: Convolution of MT plasma profile following oral administration of 500 μg SR formulation (n=4)

REFERENCES:

1. Lanao, J.M.; Vincente, M.T.; Sayalero, M.L.; Dominguez-Gil, A. Computer program (DCN) for numerical convolution and deconvolution of pharmacokinetic function. J. Pharmacobio-Dyn., 15, 203-214 (1992).

2. Veng-Pedersen, P.; Karol, M.D.; Gillespie, W. AAPS short course: Convolution, deconvolution and linear systems, November 5, 1995, Miami Beach, Florida.

3. Langenbucher, F.; Moller, H. Correlation of *in vitro* drug release with *in vivo* response kinetics. Part I: Mathematical treatment of time functions, Phram. Ind., 45, 623-628 (1983).

4. Rescigno, A.; Segre, G. Drug and tracer kinetics, Blaisdell Publishing Company. London, 1965.

5. Langenbucher, F. Numerical convolution/deconvolution as a tool for correlation in vitro/in vivo drug availability. Pharm. Ind., 44, 11, 1166-1171 (1982).

6. Hayashi, T.; Ogura, T.; Takagishi, Y. New evaluation method for *in vitro/in vivo* correlation of enteric-coated multiple unit dosage forms. Pharm. Res. 12(9), 1333-1337 (1995).

7. Microsoft Fortran Power Station version 4.0 Standard Edition, Microsoft Corporation, 1995.

8. Lee, B., Parrott, K.A., Ayres, J.W., Sack, R.L. Design and evaluation of an oral controlled release delivery system for melatonin in human subjects Int. J. Pharm. 124, 119-127 (1995).

9. Iguchi, H., Kato, K.I., Ibayashi., H. Melatonin serum levels and metabolic clearance rate in patients with liver cirrhosis., J. Clin. Endocrinol. Metab. 54, 1025-1027 (1982).

Table C5: Dissolution profile of formulation C (20% Aquacoat® coated beads)

Time (h)	3M
0	0
0.5	9.10
1	12.49
2	18.91
3	26.87
4	33.75
6	45.30
9	60.98
12	74.65
24	96.54

Table C6: MT plasma concentrations following administration of formulation C given at 760 µg (n=2) and 380 µg (n=2).

	Dose = 760 µg				Dose = 380 µg		
Time	subject 1	Time	subject 2	Time	subject 3	Time	subject 4
0	0	0	0	0	0	0	0
0.97	320.1	0.97	250.1	0.92	27.3	1	42.9
2.48	197.3	1.93	168.7	2.47	19.3	2.133	34.8
4.03	139.4	4	179.3	3.88	9.6	4.083	24.3
5.9	113.4	6.03	127.8	6.07	10.1	6.083	12.2

APPENDIX D

Cumulative amount of MT released ($\mu g/cm^2$) from

transdermal delivery devices with storage (chapter 6).

Table D1: Cumulative amount of MT released ($\mu g/cm^2$) from transdermal delivery devices with storage. Values are expressed as mean (n=3).

Time	1-day TDDs	2-day TDDs	3-day TDDs
0	0	0	0
1	44.48	61.52067	137.4013
2	56.04967	66.86717	143.2913
3	64.13383	72.17967	149.5202
4	70.5092	78.44011	154.9844
6.37	90.54734	88.22263	166.3122
9	110.9392	103.7845	174.0012
13	138.8975	125.1978	199.7069